

ABSTRACT

Title of Document: **DELINEATING THE ROLES OF *C. ELEGANS* HEME RESPONSIVE GENES HRG-2 AND HRG-3 IN HEME HOMEOSTASIS**

Caiyong Chen, Doctor of Philosophy, 2009

Directed By: **Associate Professor Dr. Iqbal Hamza,
Department of Animal and Avian sciences**

Heme is an essential cofactor for diverse biological processes such as oxygen transport, xenobiotic detoxification, and circadian clock control. Since free heme is hydrophobic and cytotoxic, we hypothesize that within eukaryotic cells, specific trafficking pathways exist for the delivery of heme to different subcellular destinations where hemoproteins reside. To identify molecules that may be involved in heme homeostasis, we conducted a *C. elegans* microarray experiment on RNA extracted from worms grown at different concentrations of heme in axenic liquid medium. Analysis of the microarrays revealed that the mRNA levels of *heme-responsive gene-2* (*hrg-2*) and *hrg-3* increased more than 70 fold when worms were grown at 4 μ M compared to 20 μ M heme. *hrg-2* is expressed in hypodermal tissues in the worm, and the protein localizes to the endoplasmic reticulum and the apical plasma membrane. *In vitro* hemin agarose pull-down experiments indicate that HRG-2 binds heme. Deletion of *hrg-2* in *C. elegans* leads to reduced growth rate at low heme. Moreover, expression of HRG-2 in *hem1 Δ* , a heme-deficient yeast strain,

results in growth rescue at submicromolar concentrations of exogenous heme. These results indicate that HRG-2 may either directly participate in heme uptake or facilitate heme delivery to another protein. Unlike *hrg-2*, *hrg-3* is exclusively expressed in the worm intestine under heme deficiency. Following its synthesis, HRG-3 is secreted into the body cavity pseudocoelom. Deletion of *hrg-3* results in increased heme levels in the worm intestine, suggesting that HRG-3 may function in intercellular heme transport in *C. elegans*. To identify the functional network or pathways for HRG-2 and HRG-3, we performed a genome-wide microarray analysis using RNA samples prepared from the worms grown at different concentrations of heme and oxygen. The results showed that a total of 446 genes were transcriptionally altered by heme and/or oxygen. Among them, 41 and 29 genes exhibited similar expression profiles to *hrg-2* and *hrg-3*, respectively. We postulate that these genes may function in conjunction with *hrg-2* and *hrg-3*. Taken together, we have identified two novel heme-responsive genes in metazoa that may play critical roles in modulating organismal heme homeostasis in *C. elegans*.

DELINEATING THE ROLES OF C. ELEGANS HEME RESPONSIVE GENES
HRG-2 AND HRG-3 IN HEME HOMEOSTASIS

By

Caiyong Chen

Dissertation submitted to the Faculty of the Graduate School of the
University of Maryland, College Park, in partial fulfillment
of the requirements for the degree of
Doctor of Philosophy
2009

Advisory Committee:

Dr. Iqbal Hamza, Chair

Dr. Eric Haag

Dr. Ian Mather

Dr. Michael Krause

Dr. Tom Porter

Dr. Caren Chang, Dean's Representative

© Copyright by
Caiyong Chen
2009

Acknowledgements

This dissertation would not have been written without the guidance of my committee members, the help from all members in our lab, and the support from my friends and family. I am very grateful to all the people who have generously provided help, directly or indirectly, in my research during the last six years.

I am especially thankful to my PhD advisor, Dr. Iqbal Hamza, for his thoughtful supervision and consistent support. I was lucky to have the opportunity to study and perform research in the Hamza lab. I would like to thank Iqbal for helping me develop my background in molecular biology and improve my presentation and writing skills, as well as for influencing me with his passion and excitement for science.

I am grateful to the members of my advisory committee, Dr. Caren Chang, Dr. Eric Haag, Dr. Ian Mather, Dr. Michael Krause, and Dr. Tom Porter, for their inspiring ideas, encouraging words, thoughtful criticism, and precious time. Their corrections and suggestions greatly improved this dissertation.

I would like to take this opportunity to thank all the members in our lab for their support and help. It was the first three lab members, Anita, Melissa, and Abbhi, who paved the way for my research project by standardizing numerous protocols for worm studies. Scott is always willing to help and give his wonderful suggestions. I want to thank him and Tamika for correcting my dissertation manuscripts and thank Jason and Tammy for proofreading my dissertation. I appreciate Xiaojing's help with the yeast experiments. In addition, many thanks are owed to Carine, Caitlin, Jon, Diana, Yike, and Margaret Ellen for their suggestions, help, and friendship.

As a student, I would like to thank my professors for passing their knowledge on to me. I thank Dr. Mather for clearly presenting an overwhelming amount of information in the Membrane Traffic class. Even now, I still need to search my notes from his class every so often for details that help me understand and plan experiments. I am grateful to Dr. Dennis Westhoff, Manju and Cherri for their instruction and encouragement in the first seminar class I took on this campus. I also want to thank Dr. Charles Delwiche for the bioinformatics, Dr. Bahram Momen for the biostatistics, and Dr. Barbara Gerratana for the enzymology.

It is also a pleasure to thank those who made my PhD study possible. I owe my deepest gratitude to the previous graduate director Dr. Inder Vijay for all the time he spent on me before I was even in the USA. His effort was well-reflected in the 25 emails he wrote to me during my application period. I also thank Edith, Sheryl, Gary, and Kim for their instruction and help on everything.

I could not have completed my PhD studies without the support of many close friends. Thanks also go to my teachers and friends in China for always caring about me and having confidence in me. I thank them for having asked me the question “when are you going to graduate” over 50 times.

Finally, I would like to express my sincere gratitude and thanks to my parents, my wife, my elder brother, and my two sisters for their love, understanding and encouragement during this long journey. I want to thank my parents for letting me go so far away from home and for missing me all the time. I thank my wife Jing for giving up her graduate study in China, being with me here, and sharing all the happy and unhappy moments together.

Table of Contents

Acknowledgements	ii
Table of Contents	iv
List of Tables	vii
List of Figures.....	viii
Abbreviations	ix
Chapter 1: Introduction	1
Uptake and intracellular transport of heme	4
Heme uptake in bacteria.....	4
Heme uptake in yeast	9
Heme transport and detoxification in insects	10
Cellular heme transport in mammals	13
Heme binding proteins	17
Cytoplasmic heme binding proteins.....	17
Extracellular heme binding proteins	19
Transcription factors and genes regulated by heme	21
Bach1	21
Rev-erbs	22
Hap1	25
Parasitic worms and heme.....	29
Chapter 2: Materials and Methods	31
Worm experiments	31
Worm culture	31
Deletion worm strains	32
Transgenic worm lines	32
Bombardment.....	33
RNA extraction and Northern blotting.....	34
cDNA synthesis and quantitative Real-Time PCR	34
Rapid Amplification of cDNA ends.....	35
RNA interference	35
GFP quantitation and zinc mesoporphyrin IX uptake assay	36
Worm lysis for immunoblotting.....	37
Iron and protoporphyrin IX response assays.....	37
Mammalian cells	38
Cell culture, plasmids and transfection	38
DNA cloning.....	38
Immunofluorescence	39
Protein preparation for immunoblotting.....	39

Fluorescence protease protection assay.....	40
Heme depletion in HEK293 cells.....	40
Hemin-agarose chromatography	40
Yeast experiments	41
Strains and growth	41
Cloning and yeast transformation	42
Heme rescue assay	42
β -Galactosidase assay	43
Yeast immunofluorescence	43
Microarray analysis	44
Microarray design and worm growth.....	44
RNA preparation and hybridization	44
Data analysis and model fitting.....	45
Gene ontology, protein domain, and protein interaction analyses	48
Clustering of genes with similar expression profiles to <i>hrg-2</i> and <i>hrg-3</i>	48
General procedures.....	48
Immunoblotting.....	48
Confocal microscopy	49
<i>In vitro</i> transcription and translation	49
Protein expression in bacteria	49
Purification of His-tagged HRGs	50
Bioinformatics.....	51
Statistics	51
Chapter 3: Delineating the role of <i>C. elegans</i> <i>hrg-2</i> in heme homeostasis	52
Summary	52
Results	53
Identification of <i>hrg-2</i> as a heme-responsive gene in <i>C. elegans</i>	53
Differential regulation of <i>hrg-2</i> and <i>cdrs</i>	63
HRG-2 is required for worm growth at low heme	63
<i>hrg-2</i> is expressed in hypodermal cells.....	66
HRG-2 is a type Ib membrane protein	75
HRG-2 binds heme.....	78
HRG-2 rescues the growth of a heme-deficient yeast strain.....	84
Discussion	87
<i>hrg-2</i> is induced by heme deficiency in <i>C. elegans</i>	87
HRG-2 is conserved in the <i>Rhabditidae</i> family	88
Potential functions of HRG-2 in heme transport.....	89
Implications of GST-like domains in HRG-2 and CDRs.....	91
Chapter 4: Identification and characterization of <i>hrg-3</i> in <i>C. elegans</i>.....	95
Summary	95
Results	96
Heme deficiency induces <i>hrg-3</i> expression in <i>C. elegans</i>	96
Sequence analysis of <i>hrg-3</i>	99
<i>hrg-3</i> is expressed in the intestine	99
Regulation of <i>hrg-3</i> is specific to heme	105
Analysis of <i>hrg-3</i> promoter	105
HRG-3 is a secreted protein	113
Examination of HRG-3 protein in the secretory pathway.....	118

Characterization of a <i>hrg-3</i> deletion allele	119
Characterization of HRG-3 in a heme-deficient yeast strain	127
Discussion	132
Identification of <i>hrg-3</i> as a heme-regulated gene.....	132
Identification of a 43-bp heme-responsive sequence	132
HRG-3 is a secreted protein	133
Potential biological roles of HRG-3	134
Chapter 5: Global analysis of heme- and oxygen- regulated genes in <i>C. elegans</i>	140
Summary	140
Results	141
Identification of heme- and oxygen- responsive genes	142
Validation by quantitative real-time PCR	145
Enrichment of biological pathways.....	145
Gene annotation and protein families.....	153
Worm interactome analysis.....	155
Identification of genes with similar expression patterns to <i>hrg-2</i> and <i>hrg-3</i>	158
Discussion	159
<i>C. elegans</i> tolerates chronic moderate hypoxia.....	159
Oxygen-regulated genes play important roles in hyperoxia resistance	163
Heme uptake systems induced by heme deficiency	165
Biological connections between heme and oxygen in <i>C. elegans</i>	166
Chapter 6: Conclusions and future directions	168
Conclusions	168
<i>hrg-2</i>	168
<i>hrg-3</i>	169
Heme oxygen microarray	170
Significance and speculations	171
Future directions	173
Ectopic expression of HRG-2 in the worm intestine.....	173
Examination of the possible heme reductase activity for HRG-2.....	174
Identification of the possible target tissues for HRG-3	174
Heme binding assays for HRG-3	175
Detailed understanding of the role SKN-1 plays in <i>hrg-3</i> regulation	175
Knock-down of other genes in <i>hrg-2</i> and <i>hrg-3</i> deletion strains	176
Appendices.....	177
Appendix I. Deletion worm strains and genotyping primers	177
Appendix II. Worm reporter constructs	178
Appendix III. Primers for Northern blot, qRT-PCR, and RACE	179
Appendix IV. qRT-PCR primers for microarray experiment.....	180
Appendix V. Localization of putative human FAX in HEK293 cells.....	182
Appendix VI. Detection of <i>hrg-3</i> expression in male worms.	184
Appendix VII. Effects of heme on the metabolic rates of <i>C. elegans</i>	186
Appendix VIII. The expression profiles of <i>hrgs</i> and <i>orgs</i>	187
Bibliography	196

List of Tables

Table 1. Gene ontology analysis of <i>hrgs</i> and <i>orgs</i> ...	149
Table 2. Enrichment of KEGG pathways in <i>hrgs</i> and <i>orgs</i> ...	152
Table 3. Expression patterns of gene families ...	154
Table 4. Genes with similar expression profiles to <i>hrg-2</i> ...	160
Table 5. Genes with similar expression profiles to <i>hrg-3</i> ...	161

List of Figures

Chapter 1

Figure 1.1. A schematic model of the heme trafficking pathways in a eukaryotic cell.....	3
Figure 1.2. Heme uptake systems in bacteria	7
Figure 1.3. Heme-regulated transcription factors in mammals	24
Figure 1.4. Heme-dependent transcription factor Hap1... ..	28

Chapter 2

Figure 2.1. Design and procedure of microarray experiments	47
--	----

Chapter 3

Figure 3.1. <i>hrg-2</i> is induced by heme deficiency	56
Figure 3.2. Regulation of <i>hrg-2</i> is specific to heme	58
Figure 3.3. Protein domains and conservation of HRG-2.....	61
Figure 3.4. Differential regulations of <i>hrg-2</i> and <i>cdrs</i>	65
Figure 3.5. Analysis of <i>hrg-2</i> deletion worm	69
Figure 3.6. Expression and localization patterns of HRG-2 in <i>C. elegans</i>	71
Figure 3.7. Ectopic expression of <i>hrg-2</i> in the intestine	74
Figure 3.8. Expression of HRG-2 in mammalian cells	77
Figure 3.9. Topology mapping of HRG-2 in mammalian cells	81
Figure 10. HRG-2 proteins bind heme	83
Figure 3.11. Characterization of HRG-2 in heme deficient <i>S. cerevisiae</i>	86
Figure 3.12. Proposed model of HRG-2 in heme homeostasis in <i>C. elegans</i>	94

Chapter 4

Figure 4.1. <i>hrg-3</i> is induced by heme deficiency in <i>C. elegans</i>	98
Figure 4.2. Genomic structure and conservation of <i>hrg-3</i> in <i>Caenorhabditis</i> species	101
Figure 4.3. <i>hrg-3</i> is specifically regulated by heme	103
Figure 4.4. Deletion analysis of <i>hrg-3</i> promoter	108
Figure 4.5. A 43-bp conserved region is critical for heme-regulated expression of <i>hrg-3</i>	110
Figure 4.6. SKN-1 binding site is required for <i>hrg-3</i> gene activation	115
Figure 4.7. HRG-3 proteins localize to coelomocytes and intestinal cells	117
Figure 4.8. Analysis of HRG-3 proteins in mammalian cells	121
Figure 4.9. Analysis of the <i>hrg-3</i> deletion worm	125
Figure 4.10. Characterization of HRG-3 in heme deficient <i>S. cerevisiae</i>	130
Figure 4.11. Proposed model of HRG-3 in heme homeostasis	139

Chapter 5

Figure 5.1. Overview of microarray results	144
Figure 5.2. Validation of gene expression by quantitative real-time PCR	147
Figure 5.3. Interactome network of heme- and oxygen- regulated genes	157

Abbreviations

ABC	ATP-binding cassette
acdh	Acyl-CoA dehydrogenase
ALA	δ -aminolevulinic acid
ALAS	δ -aminolevulinate synthase
APR	aspartic proteases
bZip	basic leucine zipper protein
CDD	conserved domain database
cds	cadmium-responsive gene
clec	C-type lectin
CLIC	chloride intracellular channel
CP	hemolymph carrier protein
CYP	cytochrome P450
DAVID	Database for Annotation, Visualization, and Integrated Discovery
Dcytb	duodenal cytochrome b
DMEM	Dulbecco's modified Eagle's medium
dsRNA	double-stranded RNA
ER	endoplasmic reticulum
FAX	failed axon connection
FBS	fetal bovine serum
fbxa	F-box A transcription factor
FDR	false discovery rate
FLVCR	receptor for feline leukemia virus subtype C
FPP	fluorescence protease protection
GaPP	gallium protoporphyrin IX
GFP	green fluorescent protein
GO	gene ontology
gpd	glyceraldehyde 3-phosphate dehydrogenase
GPI	glycosylphosphatidylinositol
GST	glutathione S-transferase
HA	hemagglutinin
HCP	heme carrier protein
HEK	human embryonic kidney
HeLp	heme lipoprotein
HIF	hypoxia-inducible factor
HO	heme oxygenase

hrg	heme-responsive gene
HRM	heme-responsive motifs
HSA	human serum albumin
ICP-MS	inductively coupled plasma-mass spectrometry
IPTG	isopropyl-beta-D-thiogalactopyranoside
Isd	iron-regulated surface determinants
KEGG	kyoto encyclopedia of genes and genomes
lbp	lipid binding protein
MARE	Maf recognition element
mCeHR	modified <i>C. elegans</i> Habitation and Reproduction
MEL	mouse erythroleukemia
mrp	multidrug resistance protein
ncx	Na/Ca exchanger
NGM	nematode growth medium
NLS	nuclear localization signal
O.D.	optical density
ORF	open reading frame
org	oxygen-responsive gene
PCR	polymerase chain reaction
pgp	P-glycoprotein
PPIX	protoporphyrin IX
PUG	protoporphyrin uptake gene
qRT-PCR	quantitative real-time polymerase chain reaction
RACE	rapid amplification of cDNA ends
RMA	Robust Multichip Average
ROS	reactive oxygen species
SC	synthetic complete
ssHRP	secretable form of horseradish peroxidase
Steap	six transmembrane epithelial antigen of the prostate
TM	transmembrane domain
UGT	UDP-glucuronosyl transferase
UTR	untranslated region
YFP	yellow fluorescent protein
YNB	yeast nitrogen base
YPD	yeast extract-peptone-dextrose
ZnMP	zinc mesoporphyrin IX

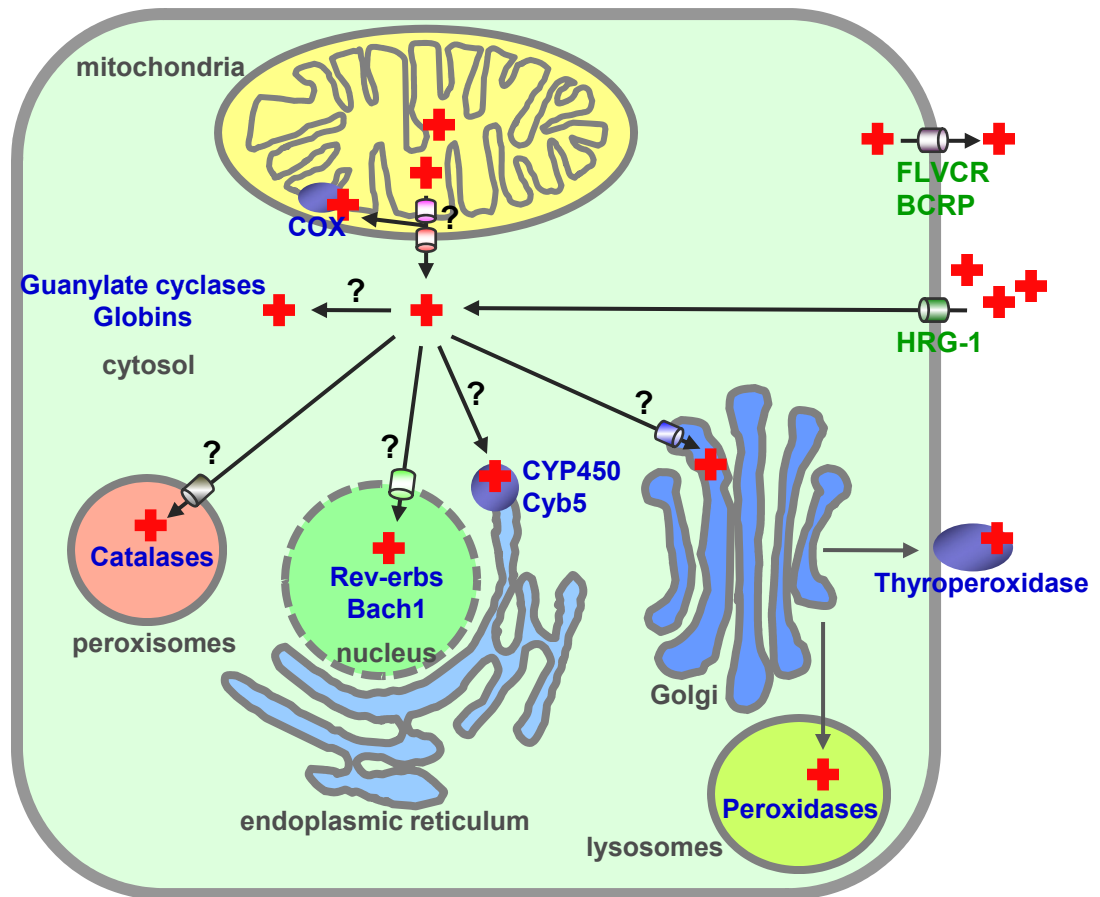
Chapter 1: Introduction

Iron deficiency is one of the most common nutritional disorders in humans. It is estimated that 60-80% of the world population may be iron deficient. Although there is an abundant amount of iron in the earth's crust, the absorption of inorganic iron in the intestine is limited because of its incomplete solubility at the pH of the duodenum. In addition, the presence of chelators such as phytates in the food further decreases the bioavailability of iron. Heme (iron protoporphyrin IX) is the major source of dietary iron for humans, because it can be absorbed more easily in the human intestine than inorganic iron (1,2). However, in drastic contrast to well-studied iron trafficking pathways, it is still unclear how heme is absorbed in the intestinal cells.

Heme is a critical cofactor for many proteins and plays critical roles in various biological processes such as oxygen transport, electron transport, gas sensing, xenobiotic detoxification, signal transduction, microRNA processing, and circadian clock control (3-6). Within eukaryotic cells, heme is synthesized via a conserved eight-step biosynthetic pathway. The last step of heme biosynthesis, the insertion of ferrous iron into the protoporphyrin IX (PPIX) ring, occurs inside the mitochondrial matrix (Figure 1.1). However, target proteins which require or bind heme such as guanylate cyclases, catalases, cytochrome P450 and certain transcription factors are present in extra-mitochondrial compartments including the cytoplasm, peroxisomes, the secretory pathway and the nucleus. Since free heme is hydrophobic and cytotoxic (7), it is highly possible that specific heme trafficking pathways exist for delivering heme to different subcellular destinations within eukaryotic cells (Figure 1.1).

Figure 1.1. A schematic model of the heme trafficking pathways in a eukaryotic cell.

In eukaryotic cells, the last step of heme biosynthesis occurs inside the mitochondrial matrix. Heme must be translocated across membranes to multiple subcellular compartments where target hemoproteins reside. Heme transporters that have been identified are highlighted in green. The question marks “?” represent the pathways that are currently unknown. COX: cytochrome c oxidase. CYP450: cytochrome P450. Cyb5: cytochrome b5.



Although heme biosynthesis and its regulation have been well-characterized, little is known about heme trafficking pathways in eukaryotes (8). In contrast, the heme uptake systems have been well characterized in many bacteria. The mechanistic findings in prokaryotes have provided a framework that may contribute to the understanding of heme transport in higher organisms.

Uptake and intracellular transport of heme

Heme uptake in bacteria

In most cases, bacteria, pathogenic or non-pathogenic, live in iron-restricted environments. The iron in their natural habitat is predominantly in the form of insoluble Fe^{3+} . In the hosts, iron that can be readily utilized by pathogens is also limiting. For example, it was estimated that free iron in the plasma of human hosts is at the order of $\sim 10^{-18}$ M (9). To satisfy their iron demands, bacteria have developed several distinct and functionally redundant pathways for iron acquisition such as direct uptake through receptors for iron and heme, or sequestering iron and heme by secreting small extracellular proteins called siderophores and hemophores.

Gram-negative bacteria

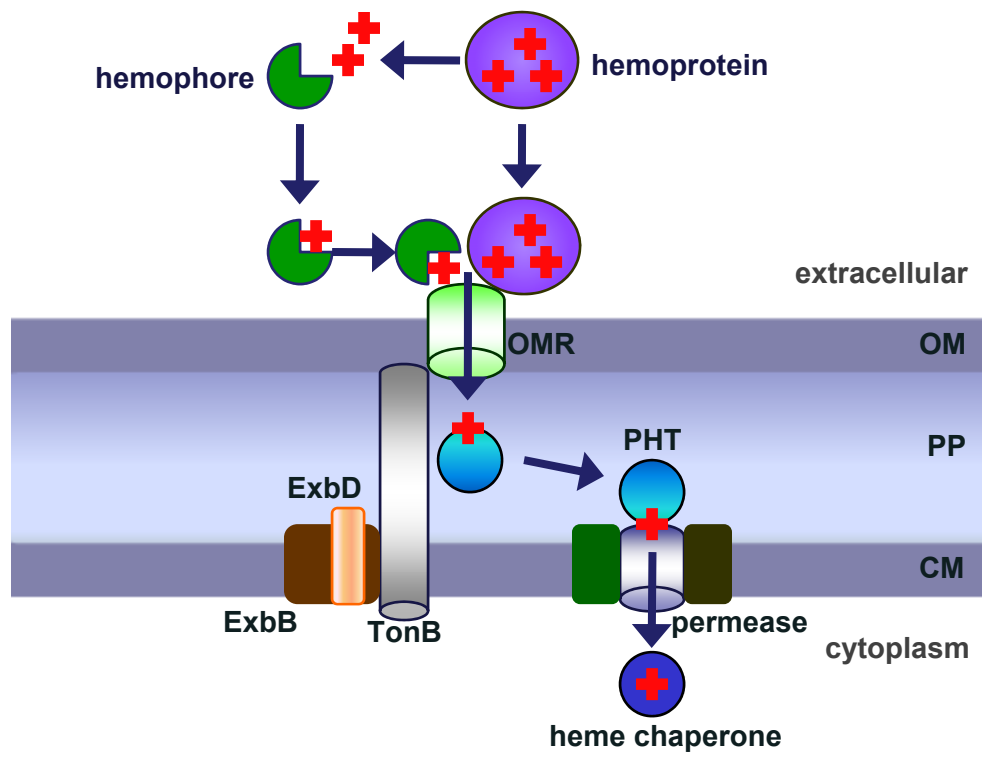
The first well-characterized heme uptake system in pathogenic Gram-negative bacteria comprises a specific outer membrane receptor that can directly bind heme or hemoproteins and ATP-binding cassette (ABC) transporters that can translocate heme into the cell (10) (Figure 1.2A). A number of Gram-negative bacteria have been shown to have this set of direct heme uptake pathways, including hemR-hemSTUV in *Yersinia enterocolitica*, hmuRSTUV in *Yersinia pestis*, shuASTUV in *Shigella dysenteriae*, and

phuRSTUVW in *Pseudomonas aeruginosa* (11). In general, the outer membrane receptors (e.g. HemR) first bind heme or hemoproteins and transport them into the periplasm using energy provided by the TonB-ExbB-ExbD complex. Once across the outer membrane, heme is bound by periplasmic heme transport proteins (e.g. HemT) and then delivered to specific ABC transporters on the cytoplasmic membrane (e.g. HemU and HemV). When the periplasmic heme transporter associates with the ABC transporter, they form heme permeases that can actively transport heme across the cytoplasmic membrane. In the cytoplasm, heme is catabolized by either heme oxygenase (HO)-like enzymes (e.g. HemS and HemO) or non-HO like enzymes (e.g. YfeX) to release iron (12). HemS may also function as a cytoplasmic heme chaperone to prevent heme toxicity.

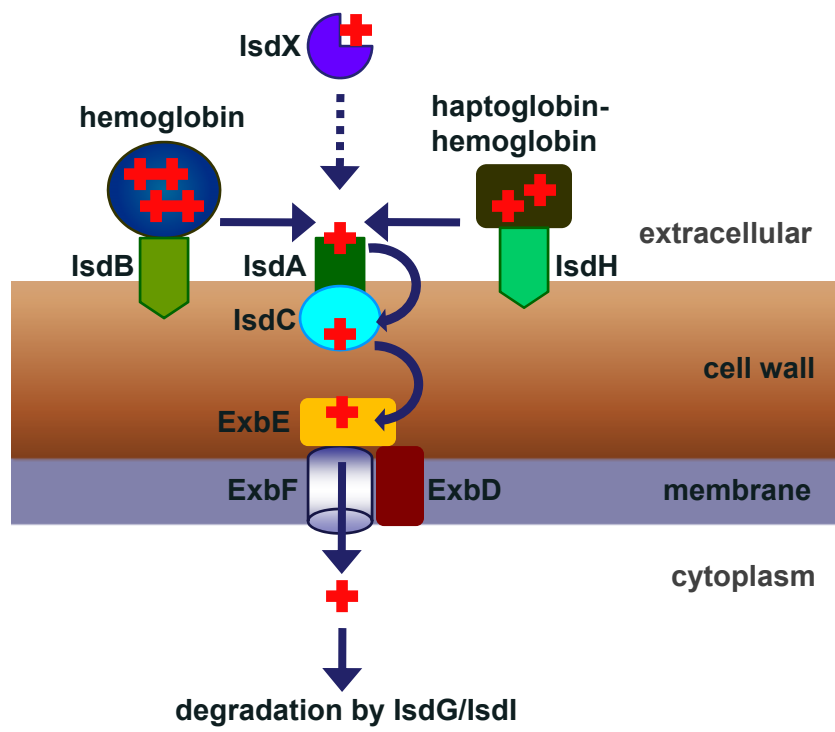
The second heme uptake system in Gram-negative bacteria is a hemophore combined with outer membrane transporters. The hemophore HasA has been identified in *Serratia marcescens*, *Pseudomonas fluorescens*, *P. aeruginosa*, *Y. pestis*, and *Y. enterocolitica* and HxuA has been reported in *Haemophilus influenzae* (11). HasA is secreted by ABC exporter machinery that includes an ABC protein HasD, a membrane fusion protein HasE, and an outer membrane protein HasF (13,14). It can sequester heme with high affinity, and the bound heme is then delivered to the outer membrane receptor HasR for internalization. Similar to other TonB-dependent heme receptors, HasR has been shown to transport both free heme and heme non-covalently bound to proteins (15,16). However, HasR only has low binding affinity for heme. The efficiency of heme uptake is dramatically increased in the presence of HasA. HasA can form exergonic complexes with HasR and heme is transferred to HasR (17,18).

Figure 1.2. Heme uptake systems in bacteria. (A) Gram-negative bacteria. The outer membrane receptors bind heme or hemoprotein and transport it into periplasm using energy provided by TonB-ExbB-ExbD complex. Some bacteria secrete hemophores to sequester heme and to deliver it to an outer membrane receptor. The periplasmic heme transporter relays heme to the ABC transporter on the cytoplasmic membrane. They form permeases that translocate heme into the cytoplasm where chaperones and heme degrading enzymes reside. OMR: outer membrane receptor; OM: outer membrane; PP: periplasm; CM: cytoplasmic membrane; PHT: periplasmic heme transporter. (B) Isd system in Gram-positive bacteria *S. aureus*. The surface receptors IsdB and IsdH bind hemoproteins and transfer heme to IsdA. IsdC accepts heme from IsdA and delivers it to IsdE. Heme is then transported by the cell membrane transporter complex into the cytoplasm where heme is degraded by IsdG and IsdI to release iron. *B. anthracis* secretes hemophore-like molecules, IsdX1 and IsdX2, to retrieve heme from hemoproteins. The figures are modified from Tong and Guo (11).

A



B



The bacterium *Neisseria meningitidis* has a unique heme acquisition system HpuAB in which both components reside on the outer membrane. HpuB is a TonB-dependent outer membrane receptor, whereas HpuA is an accessory lipoprotein. Both HpuA and HpuB are required for the transport of heme from hemoglobin and haptoglobin-hemoglobin complexes (19).

In addition to transporters and chaperones, cysteine proteases such as the gingipains Rgp and Kgp are essential for heme acquisition from hemoglobin, hemopexin and haptoglobin in *Porphyromonas gingivalis* (20,21). These two gingipains share identical hemoglobin binding domains but the catalytic domains are divergent (22). Smalley *et al.* (2007) found that Rgp converted hemoglobin (Fe^{2+}) into methemoglobin (Fe^{3+}), which was subsequently degraded by Kgp (23).

Gram-positive bacteria

Recently, significant progress has been made in identifying heme uptake pathways in Gram-positive bacteria. Gram-positive bacteria have thick, multilayered cell walls, which provide additional barriers for nutrient uptake. In addition to utilizing ABC transporters, these bacteria have evolved more complex surface proteins to bind and transfer heme or hemoproteins.

The iron-regulated surface determinants (Isd) comprise heme acquisition machinery in the human pathogen *Staphylococcus aureus* (24) (Figure 1.2B). The Isd system includes surface proteins IsdABC and IsdH/HarA, membrane transporters IsdDEF, and heme-degrading enzymes IsdGI. The surface receptors have different binding affinities for distinct heme sources. For example, IsdB is a hemoglobin receptor, whereas IsdH binds haptoglobin-hemoglobin (25,26). IsdA accepts heme from IsdB or IsdH and

transfers it to IsdC (27,28). Subsequently, heme is delivered to the lipoprotein IsdE and translocated by the cell membrane transporter complex into the cytoplasm, in which heme is degraded by IsdG and IsdI to release iron (11,28).

Instead of presenting heme receptors on the cell surface, the spore-forming bacteria *Bacillus anthracis* secretes two heme-binding molecules, IsdX1 and IsdX2, to retrieve heme from hemoglobin (29). This mechanism is homologous to the hemophore systems in Gram-negative bacteria.

The heme uptake pathway in another human pathogen, *Streptococcus pyogenes*, consists of the cell wall proteins Shr and Shp, as well as ABC transporters HtsABC. In this system, Shr interacts with host hemoproteins and relays heme to Shp (30). Heme then is delivered to HtsA and subsequently transported into the cytoplasm (31,32). Similarly, the heme binding proteins HtaAB on the cell wall and ABC transporters HmuTUV constitute a heme uptake system in *Corynebacterium diphtheria* (33).

Heme uptake in yeast

In contrast to our knowledge of bacterial heme uptake, the trafficking pathways in eukaryotes are much less well understood.

Heme uptake molecules have been identified in the pathogenic yeast *Candida albicans*. Weissman *et al.* (2002) first revealed that *C. albicans* can utilize heme and hemoglobin through a pathway that is distinct from iron uptake pathways (34). Heme uptake in *C. albicans* exhibits a rapid initial binding phase followed by a slower uptake phase (35). It was subsequently discovered by a genome-wide screen that Rbt51 and Rbt5 are involved in heme uptake in *C. albicans* (36). *RBT5* is highly induced by iron limitation and its deletion in *C. albicans* impairs the utilization of heme. Both Rbt51 and

Rbt5 are glycosylphosphatidylinositol (GPI)-anchored proteins mainly localized to the plasma membrane, suggesting that they might function as receptors for heme and hemoglobin (37). After being taken up by Rbt5/Rbt51, heme and hemoglobin are delivered to the vacuole through an endocytosis-mediated pathway (37). Heme is then degraded by HO. The heme oxygenase enzyme CaHMX1 was identified and characterized both in *C. albicans* and *in vitro* (35,38). The expression of *CaHMX1* is positively regulated by heme and hemoglobin (39).

In contrast to fungal pathogens, the budding yeast *Saccharomyces cerevisiae* utilizes exogenous heme very poorly. This indicates that *S. cerevisiae* lacks high-affinity heme transport systems. However, under conditions of heme starvation or hypoxia, an energy-dependent pathway for heme uptake has been detected (40). *Protoporphyrin uptake gene 1 (PUG1)* was identified by microarray analysis on *S. cerevisiae* grown under heme starvation conditions. Overexpression of PUG1 resulted in decreased cellular heme levels and increased PPIX content in both wild type and heme-deficient strains. However, heme uptake was not affected in *PUG1Δ* strain. Taken together, these data suggest that Pug1 is involved in PPIX influx and heme efflux.

Heme transport and detoxification in insects

Adult hematophagous arthropods ingest enormous amount of blood in a single meal (41). Accordingly, hemoglobin is undoubtedly the sole major source of iron for blood-feeding insects. In the mosquito *Aedes aegypti*, >98% of iron in the insect body and the eggs come from heme (42). On the other hand, free heme is toxic to cells because it can cause lipid peroxidation. To minimize the toxicity of the heme released by hemoglobin

digestion, these insects have evolved efficient strategies to excrete, transport, and sequester heme.

The first defense against free heme occurs in the gut. According to an inductively coupled plasma-mass spectrometry (ICP-MS) study in *A. aegypti*, 87% of total ingested heme iron was excreted by the end of the first gonotrophic cycle (42). In addition, insects have specialized structures in the gut to sequester and detoxify heme. In the lumen of the intestine, ferrous heme can be converted into ferric heme and aggregate into an insoluble structure called hemozoin (43). Hemozoin has been identified in the malarial parasite, *Plasmodium falciparum*, the parasitic worm, *Schistosoma mansoni*, the parasitic protozoan, *Haemoproteus columbae*, and the kissing bug, *Rhodnius prolixus* (43,44). In *R. prolixus*, the hemozoin in the lumen of midgut is the first defense against toxicity from free heme (45). Inhibition of hemozoin formation by chloroquine led to increased levels of free heme and therefore, increased lipid peroxidation (46). *In vitro* studies further confirmed that, compared with free heme, hemozoin generated fewer free radicals, caused less lipid peroxidation, and did not lead to the lysis of red blood cells (47).

Instead of forming hemozoin, the mosquito *A. aegypti* has a layer of peritrophic matrix covering the intestinal epithelium. This structure separates intestinal cells from the food and it has been shown to be associated with high levels of heme after feeding (48). Devenport *et al.* (2006) identified a heme-binding protein, *A. aegypti* intestinal mucin 1, in peritrophic matrix that might be one of the major molecules required for heme sequestration (49).

Heme uptake has been characterized at the cellular level by following fluorescent hemoglobin conjugates or heme analogs in *Boophilus microplus*. In contrast to most

eukaryotes and even the kissing bug *R. prolixus*, the cattle tick *B. microplus* lacks the heme biosynthetic pathway (50). Hemoglobin is taken up by the specialized digestive cells in the midgut through receptor-mediated endocytosis (51). After the endosomes fuse with primary lysosomes, hemoglobin is degraded (52). The released heme is sequestered in specialized intracellular membrane-bound organelles called hemosomes (41,51). Hemosomes provide a sequestration mechanism for heme and prevent it from forming free radicals.

After absorption, a fraction of heme in the digestive cells is translocated into the open circulatory system hemocoel. It has been shown that several heme-binding lipoproteins may play a role in the transport and sequestration of heme in the hemolymph. The major hemolymph protein in *B. microplus* has been characterized as a heme lipoprotein (HeLp). The gene encoding HeLp is expressed in both male and female ticks after host-attachment and blood feeding (53). The protein contains two molecules of heme and has the capacity to bind six more heme molecules (54). By injecting HeLp labeled with ^{55}Fe -heme into the hemocoel, a quick drop of the radioactivity in hemolymph and a simultaneous increase in oocytes were observed, suggesting that HeLp might play a role in delivering heme across tissues (54). In the American dog tick, *Dermacentor variabilis*, the homolog of HeLp, hemolymph carrier protein (CP), is also the major hemolymph protein and has been suggested to play a role in sequestering heme (53,55,56). *In vitro* assays indicated that HeLp/CP-bound heme induced less oxidative damage to phospholipids than free heme (57). These data suggest that HeLp/CP may be involved in the sequestration and transport of heme.

In ticks and other insects, the major yolk protein vitellogenin has heme-binding activity. Binding by vitellogenin strongly inhibited heme-induced lipid peroxidation (58). After blood feeding, vitellogenin is primarily produced in the fat body and midgut of female ticks and is then transferred to developing oocytes (59,60). Therefore, insect vitellogenin may play a role in transferring heme and other nutrients to eggs (56,58,59). In the eggs, heme is released when vitellogenin is degraded by endopeptidases such as vitellin-degrading cysteine endopeptidase, *Boophilus* yolk cathepsin and tick heme-binding aspartic proteinase (61,62).

Besides HeLp/CP and vitellogenin, other proteins such as *Rhodnius* heme-binding protein may bind heme and decrease toxicity of free heme in insect hemolymph (63,64).

Cellular heme transport in mammals

So far, only a small number of molecules that may play a role in heme uptake, delivery, and export have been characterized in mammals.

Heme uptake

It has been long thought that duodenal enterocytes internalize heme through a receptor-mediated endocytic pathway. Existence of heme receptors or heme uptake proteins has been shown in the microvilli of upper small intestine, cultured enterocytes and non-intestinal cells (65). Heme carrier protein (HCP1) and heme-responsive gene (HRG-1) are two newly identified molecules that may function to import heme into the cells (Figure 1.1).

Hcp-1 was initially identified from a suppression subtractive hybridization screen using hypotransferrinaemic mice (66). It encodes the protein HCP1 (also named as SLC46A1) that has nine transmembrane domains with a molecular size of ~50 kDa.

Expression of HCP1 in *Xenopus* oocytes and HeLa cells resulted in a 2-3 fold increase in heme uptake with an apparent K_m of 125 μ M. Furthermore, blocking with HCP1 antibodies significantly reduced the uptake of radiolabeled heme by everted duodenal sacs. However, Qiu *et al.* (2006) have shown that SLC46A1 was in fact a high affinity folate/proton symporter and therefore was re-named as PCFT/HCP1 (67). Expression of SLC46A1 in *Xenopus* oocytes, HepG2 cells, and HeLa cells increased folate uptake by >200, >30, and >13 fold, respectively. Knock-down of *Pcft/ Hcp-1* in Caco-2 cells led to 60-80% reduction in pH-dependent folate uptake. The high-affinity folate transport activity ($K_m \sim 1.3 \mu$ M at pH 5.5) suggests that folate may be the physiological ligand for PCFT/ HCP-1. It is still unclear whether low affinity heme transporting activity of PCFT/HCP-1 has any physiological relevance.

HRG-1 (SLC48A1), the first *bona fide* heme importer, was initially identified by a *Caenorhabditis elegans* microarray experiment (68). RNAi of the *hrg-1* paralog, *hrg-4* significantly reduced the uptake of a fluorescent heme analog in worm intestine, while knocking down the zebrafish *hrg-1* ortholog resulted in severe anemia, hydrocephalus, and a curved body with shortened yolk tube. In addition, heme-dependent transport across the plasma membrane was observed in *Xenopus* oocytes expressing *hrg-1*. Only one *hrg-1* gene is present in the human genome, whereas worms have three *hrg-1* paralogs. This indicates that worms might have evolved redundant heme acquisition pathways since they lack the ability to synthesize heme.

Heme export

The existence of a heme exporter has been speculated for two reasons: 1) efflux may be one of the main mechanisms for heme detoxification, since the accumulation of

excess heme is highly toxic to the cells; 2) efflux may facilitate inter-cellular heme transfer and heme iron recycling. For example, when macrophages phagocytize senescent red blood cells and degrade hemoglobin to release heme, a portion of the iron is exported from macrophages as intact heme-iron (69).

The cell surface receptor for feline leukemia virus subtype C (FLVCR) belongs to the major facilitator superfamily (70). Suppression of FLVCR by the virus FLV-C in feline embryonic fibroblasts significantly increased the cellular heme content, while ectopic expression of FLVCR in renal epithelial cells reduced the intracellular heme levels (70). This result was further confirmed by heme export assays using a fluorescent heme analog and ⁵⁵Fe-heme in renal epithelial and K562 cells. FLVCR was highly expressed in hematopoietic cells, and heme efflux mediated by FLVCR was essential for erythroid differentiation (70,71). Cats infected with FLV-C developed pure red cell aplasia in which erythroid progenitor cells failed to mature from burst-forming units to the colony-forming-units erythroid cells. No erythropoiesis was observed in FLVCR knock-out mice, and these mice died at midgestation (72). Deletion of FLVCR also perturbed the heme efflux from macrophages and therefore blocked the recycling of heme and iron from senescent red blood cells (72).

The ABC transporter ABCG2, also named as BCRP, was originally identified as a drug resistance protein in breast cancer cells. Krishnamurthy *et al.* (2004) showed that heme interacts with ABCG2 by using hemin-agarose pull-down assays (73). PPIX levels in the erythrocytes of ABCG2-null mice were ten times higher than that in wild type mice (74), suggesting that ABCG2 might function as an exporter for porphyrin compounds. However, no evidence has directly confirmed that ABCG2 can export heme.

Intracellular heme transport

Whether synthesized within cells or taken up from the environment, heme in all eukaryotic cells has to be translocated across membrane barriers for either storage and sequestration, or utilization and incorporation into hemoproteins. The molecules and the mechanisms involved in intracellular heme trafficking remain poorly understood. One molecule, ABCB6, could play a role in heme transport between mitochondria and the cytoplasm.

ABCB6 was initially identified as a mammalian ortholog for yeast ATM1, a mitochondrial iron transporter important for Fe-S cluster biogenesis (75). However, Krishnamurthy *et al.* (2006) revealed that ABCB6 was more likely a porphyrin/heme transporter in mitochondria (76). In cells expressing ABCB6, ^{55}Fe -heme was readily transported into mitochondria from the cytoplasm in an energy-dependent manner. Another tetrapyrrole compound, coproporphyrin III, competed with ABCB6 for heme binding and inhibited heme uptake into mitochondria.

More recently, two molecular weight forms of ABCB6 of 79 kDa and 104 kDa were identified (77). Using specific ABCB6 antibodies, it was shown that while the light form localized to the mitochondrial outer membrane, the heavy form predominantly resided on the plasma membrane. Transfection of the plasma membrane form of ABCB6 reduced the cellular accumulation of another porphyrin compound pheophorbide A but not heme. It is possible that two ABCB6 forms have distinct functions at different subcellular locations, but further studies are required to pinpoint their physiological roles in the cell.

Heme binding proteins

Heme has peroxidase activity and the iron in heme can generate reactive oxygen species through Fenton reactions. In addition, as a small lipophilic molecule, free heme can easily intercalate with, and disrupt the lipid bilayers of cell membranes. Therefore, heme-binding proteins or heme chaperones may be required to prevent the toxicity associated with free heme. The heme-binding proteins may function to sequester or transport heme.

Cytoplasmic heme binding proteins

Glutathione S-transferases (GSTs) catalyze the conjugation of glutathione to various electrophilic substrates and play essential roles in xenobiotic detoxification. Besides their enzymatic functions, GSTs have also been known for their ability to bind a variety of ligands in the cytoplasm. In fact, GSTs were first identified in mammalian liver as “ligandins” that can selectively bind steroids, bilirubin and organic anions (78). Subsequent studies showed that GSTs interact with heme and porphyrins (79-81).

In malarial parasites and helminths, GSTs are highly abundant in the cytoplasm. A GST from *P. falciparum* (Pf-GST) is capable of interacting with heme (82). This Pf-GST was subsequently shown to contain both high- and low-affinity heme binding sites (83). In the rodent malarial parasite, *Plasmodium berghei*, heme but not PPIX can inhibit GST activities (84). Furthermore, an inverse correlation between heme levels and GST activities has been shown both in vitro and in *P. berghei* (84,85). van Rossum *et al.* (2005) discovered a novel GST from the blood-feeding helminth *Haemonchus contortus* (Hc-GST-1) that is able to interact with heme (86). The homologous protein in

Ancylostoma caninum, Ac-GST-1, also binds heme (87). These GSTs have been postulated to play critical roles in the detoxification and transport of heme (82,86,88).

A murine 22 kDa protein, p22HBP, was identified as a cytosolic heme-binding protein ubiquitously expressed in various tissues with high levels in the liver (89). In mouse erythroleukemia (MEL) cells, p22HBP was induced during erythroid differentiation and knock-down of the gene resulted in reduced heme content in MEL cells. In addition to heme, the protein binds other porphyrin compounds such as PPIX (89,90). It was revealed by a structural analysis that a hydrophobic cleft was responsible for tetrapyrrole binding in p22HBP (90). Two homologous proteins in *Arabidopsis thaliana*, cHBP1 and cHBP2, were also found to bind tetrapyrroles reversibly *in vitro* (91). These two HBPs may play similar roles in different plant tissues since cHBP1 is highly expressed in leaves whereas the highest level of cHBP2 is detected in roots (91).

The murine heme-binding protein SOUL has 27% sequence identity to p22HBP. In contrast to p22HBP, which is a monomer protein, SOUL forms dimers in the absence of heme and hexamers in the presence of heme (92,93). In addition, SOUL is specifically expressed in the retina and pineal gland and uses histidine as an axial ligand to coordinate the heme (92,93). Although p22HBP/SOUL proteins were proposed to be involved in intracellular heme trafficking or heme sequestration, the definite biological functions of this family remains undefined.

HBP23 belongs to the peroxiredoxin family of peroxidases and is also called mouse stress-inducible 23 kDa protein or proliferation-associated gene product. The protein was originally identified from rat liver using chromatography on hemin-agarose and was shown to have a high binding affinity for heme (94). On the protein surface, two

hydrophobic regions, both containing histidine residues, might be responsible for heme binding (95). The protein is highly expressed in the cytoplasm of the liver and also present in kidney, spleen, small intestine, and heart. Heme, PPIX, and other metalloporphyrins are able to stimulate HBP23 expression in rat primary hepatocytes (96). Furthermore, incubation of rat liver HBP23 with heme inhibited its antioxidant activity (97).

Fatty acid binding proteins have also been shown to bind heme (98,99). However, the cellular functions of heme-binding activities in these cytosolic proteins are still unclear.

Extracellular heme binding proteins

Heme and hemoglobin are released into the plasma during the destruction of senescent erythrocytes and enucleation of erythroblasts. Under pathological conditions such as hemoglobinopathies, trauma, and infections, more severe intravascular hemolysis is induced. To prevent tissues from experiencing heme toxicity and to increase the recycling of heme iron, mammalian cells secrete specific molecules to bind heme and hemoglobin in the circulation.

Haptoglobin (*hapto*- “bind to”), primarily synthesized by hepatocytes, is a plasma glycoprotein with hemoglobin-binding capacity. There are three major subtypes of haptoglobin (100), all of which can form soluble complexes in an equimolar ratio with hemoglobin dimers ($K_d \sim 10^{-12}$ M) (11,101,102). Haptoglobin-hemoglobin complexes bind to the CD163 receptor on the surface of monocytes and macrophages, and these complexes are subsequently endocytosed (103). Receptors for the haptoglobin-hemoglobin complex also exist in hepatocytes and hepatoma cell lines (104,105). After

entering the cells, iron is released by heme degradation, whereas the remaining protein complex is degraded by lysosomes (106-108). Physiologically, binding of haptoglobin reduces the loss of hemoglobin and heme iron (108,109).

Hemopexin is a heme-binding plasma protein that binds heme with high affinity ($K_d \sim 10^{-13}$ M) (110). Hemopexin-heme complexes are endocytosed in response to the binding with LRP/CD91 (LDL receptor-related protein, or CD91) in a variety of cells including hepatocytes, macrophages, and syncytiotrophoblasts (111). Unlike haptoglobin, hemopexin is recycled back into the circulation after the release of heme during endocytosis (111,112). In response to heme overload, hemopexin null mice exhibited increased oxidative stress and altered regulation of HO-1 as well as ferritin, suggesting critical roles of hemopexin in heme detoxification (113).

Human serum albumin (HSA), a 66 kDa protein, binds a wide variety of proteins as well as heme ($K_d \sim 10^{-8}$ M) (114,115). The crystal structure shows that a hydrophobic cleft in one of its three sub-domains binds heme. Three basic residues at the entrance to this cleft form charge pair interactions with the propionate side chains of heme, and the iron in heme is coordinated by a tyrosine residue (116).

Two additional serum proteins, high-density and low-density lipoproteins, bind heme faster than both hemopexin and HSA with an affinity that is higher than that of HSA for heme ($K_d \sim 10^{-11}$ M) (114,117). It is thought that this rapid binding is critical to prevent damage by heme during the initial release of heme and provides a buffer period for hemopexin and HSA to steadily but tightly bind heme. Eventually, hemopexin and HSA remove all but a residual amount of heme from the lipoproteins (117).

Transcription factors and genes regulated by heme

Heme regulates the expression of many genes that are involved in erythropoiesis, heme biosynthesis, oxidative stress, energy metabolism, and circadian rhythm control (4,118-120). It is capable of inducing and inhibiting gene expression at the levels of transcription, translation, and post-translation. The mammalian transcription repressor Bach1, the circadian clock gene *Rev-erba*, and the yeast transcriptional activator Hap1 are three well-studied transcription factors that are regulated by heme.

Bach1

Bach1, a basic leucine zipper protein (bZip), was the first mammalian transcription factor shown to bind heme (121). Bach1-Maf heterodimers bind to Maf recognition elements (MAREs) and repress the expression of target genes such as globins and HO-1(119,121,122) (Figure 1.3A). Heme can interact with Bach1 and de-repress transcription. Bach1 has six putative heme regulatory motifs, four of which surround the C-terminal bZip domain and are responsible for heme binding (123). The net effect of heme in this pathway is the activation of hemoglobin, myoglobin, neuroglobin genes as well as HOs (124-126).

Heme negatively regulates Bach1 activity through three major mechanisms (Figure 1.3A). First, heme displaces Bach1-Maf complexes from enhancers (123,127). The DNA-binding activity is almost completely lost in the presence of 1 μ M heme (123). In this case, the activators NF-E2 or Nrf2 can be recruited to MAREs with Mafs and induce gene transcription (121,127). Expectedly, when all HRMs are mutated, Bach1 can still attach to MAREs even when there is excess heme (123). Second, heme stimulates Bach1 export from the nucleus. Under basal growth conditions, Bach1 is localized to the nucleus

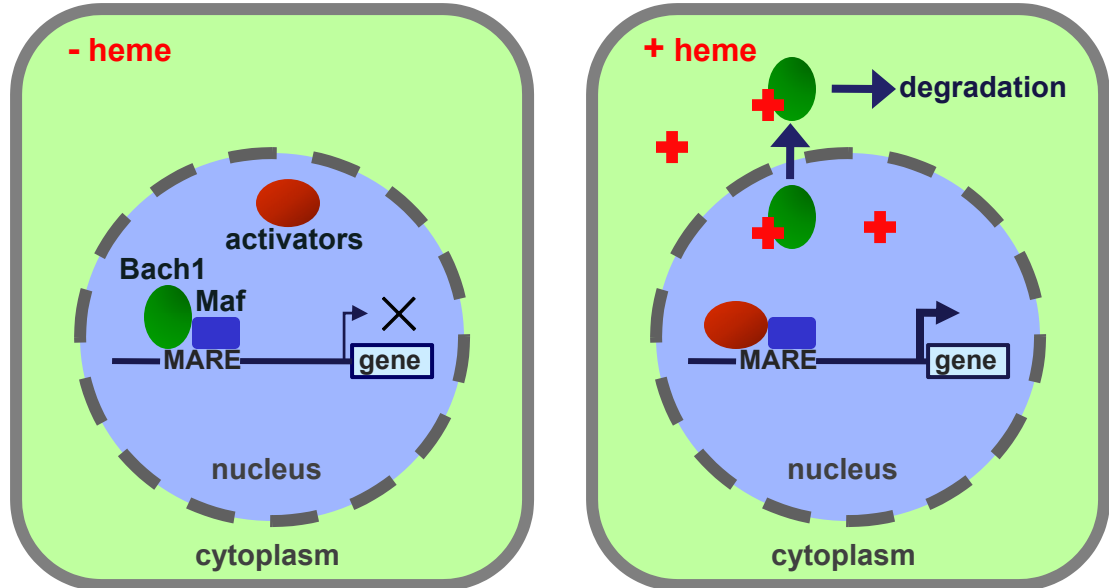
in the presence of MafK. Heme treatment triggers Bach1 translocation from the nucleus to the cytoplasm, whereas the majority of MafK is retained in the nucleus. A region with two HRMs is thought to be essential for Bach1 translocation and this process depends on the nuclear exporter Crm1 (128). Third, heme binding induces Bach1 degradation. Zenke-Kawasaki *et al.* (2007) showed that the levels of endogenous Bach1 protein were significantly decreased in the presence of heme (129). In contrast, succinylacetone, the inhibitor of heme biosynthesis, resulted in higher Bach1 levels in murine embryonic fibroblasts. Further analysis suggested that heme stimulates the polyubiquitination and degradation of Bach1 protein (129).

Rev-erbs

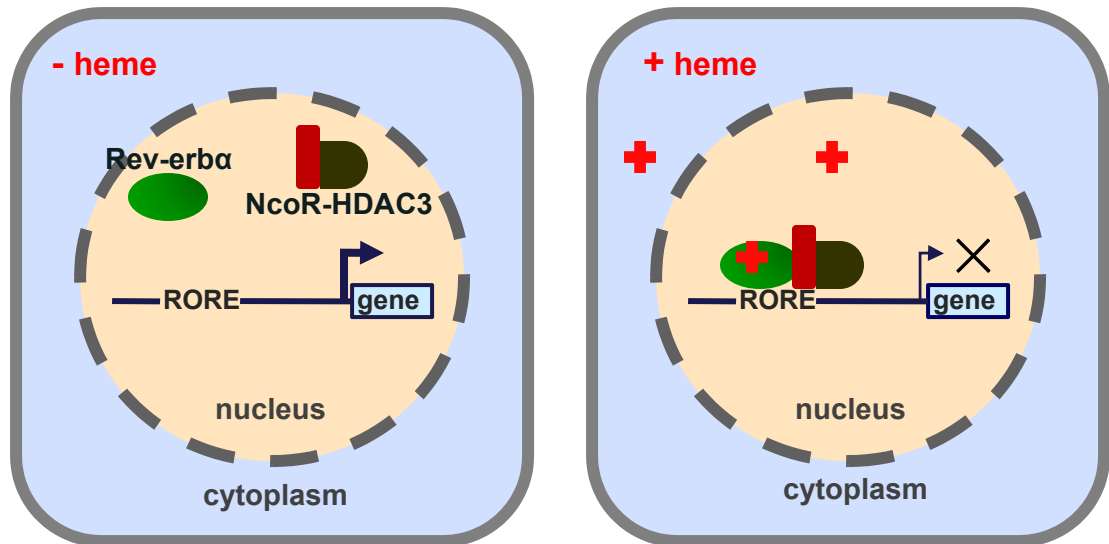
Rev-erb α and Rev-erb β were initially discovered as orphan members of the nuclear hormone receptor family twenty years ago (130,131). Rev-erbs can form monomers, homodimers, and heterodimers and recognize retinoic acid receptor-related orphan receptor response elements or Rev-erb response elements (132,133). Recently, heme has been identified as the physiological ligand for both Rev-erbs and it can reversibly associate with the ligand-binding domain in the proteins (4,134). In fact, Rev-erbs serve as intracellular heme sensors that regulate circadian rhythm, glucose homeostasis and heme biosynthesis. In the presence of the co-repressor NcoR-HDAC3 complex, Rev-erb α negatively regulates the expression of BMAL1, a key player in the mammalian circadian clock (4,135). Heme is required for the efficient recruitment of the NcoR-HDAC3 complex (Figure 1.3B). The interaction between Rev-erbs and NcoR significantly decreases in heme-depleted conditions, and the mutation of the heme binding site abolishes recruitment of both NcoR and HDAC3 (4,134). In a similar way, heme also

Figure 1.3. Heme-regulated transcription factors in mammals. (A) Bach1. At low heme, Bach1-Maf heterodimers bind to MAREs in the enhancer region and repress the expression of target genes such as globins and HO-1. In the presence of heme, Bach1 is displaced whereas the activator NF-E2 or Nrf2 is recruited to MAREs to induce the gene transcription. Heme also stimulates the nuclear export and degradation of Bach1. (B) Rev-erb α . In the presence of heme and co-repressor NcoR-HDAC3 complex, Rev-erb α binds to retinoic acid receptor-related orphan receptor response elements and negatively regulates the expression of downstream genes that are involved in circadian rhythm control, glucose homeostasis and heme biosynthesis.

A



B



represses the expression of gluconeogenic genes including phosphoenolpyruvate carboxykinase and glucose 6-phosphatase through Rev-erb α .

In addition to Rev-erbs, two other clock proteins NPAS2 and PER2 contain heme as a prosthetic group (136,137). NPAS2 activates the expression of ALAS1, the rate-limiting enzyme in the heme biosynthesis pathway. The presence of heme inhibits this transcriptional activity and heme synthesis (136).

Hap1

In biological systems, heme and oxygen are closely intertwined with each other in many respects. Oxygen is required as an electron acceptor in heme biosynthesis (138), whereas hemoproteins are responsible for the transport of oxygen molecules. In addition, heme participates in a variety of oxygen-related biological functions such as oxidative phosphorylation and oxidative stress control. In *S. cerevisiae*, heme also plays critical roles in oxygen-regulated gene expression through the transcription factor Hap1.

Aerobic genes and anaerobic or hypoxic genes are two general classes of oxygen-regulated genes (139). In response to changes in oxygen levels, Hap1 can activate aerobic genes and inhibit anaerobic genes in a heme-dependent manner (119) (Figure 1.4). Heme promotes the binding of Hap1 homodimers to the upstream activation sequences and increases the expression of the target genes (119). Hap1 contains a C6 zinc cluster motif and a dimerization element at the amino terminus. In addition, there is an activation domain at the carboxyl terminus, as well as three repression modules and seven heme-responsive motifs (HRM) dispersed in the protein (140,141). The HRMs and non-regulatory regions, as well as two molecular chaperones Hsp90 and Hsp70, are required for heme-dependent regulation of Hap1 activity (140,142). Under hypoxic conditions,

Hap1 recruits co-repressors Tup1/Ssn6 and directly inhibits the transcription of ergosterol biosynthesis genes (143). The presence of heme relieves this transcriptional repression (143). Taken together, these results suggest that heme is required for both activation and repression activities of Hap1, depending on the oxygen levels. However, Hap1 can bind to its promoter and repress its own expression, but this negative regulation is independent of heme concentrations (141).

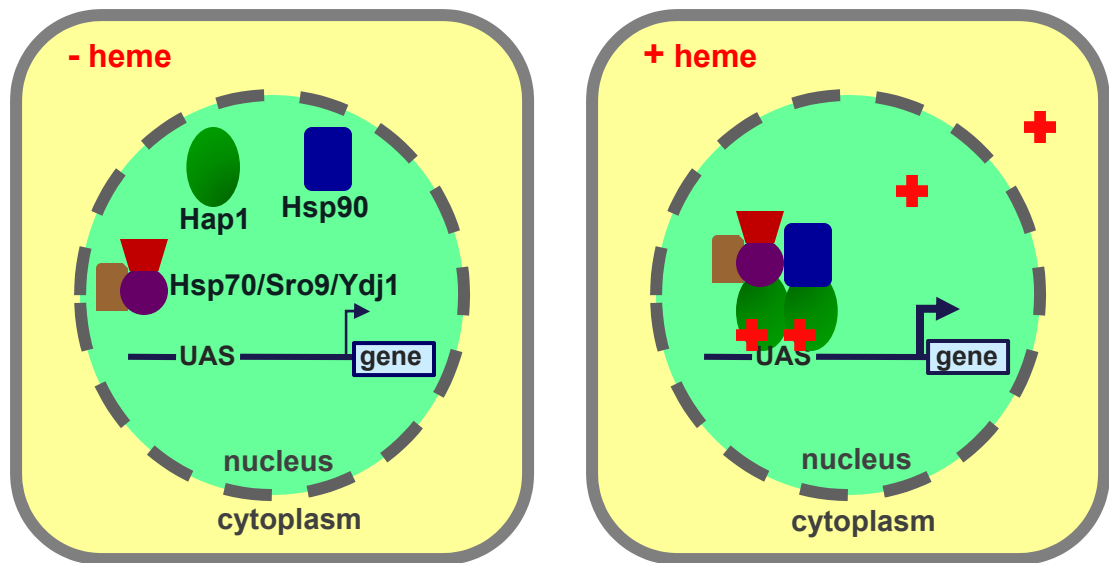
Heme also directly regulates the activities of other transcription factors such as the bacterial iron response regulator protein Irr (144), the CAAT box-binding factor NF-Y (145), and the heme-responsive Ku protein complex (146,147).

In addition to heme biosynthesis genes and heme-containing enzymes, heme transporters may also be regulated by heme levels in order to maintain heme homeostasis. For example, the heme uptake gene *hrg-1* is transcriptionally upregulated when *C. elegans* is grown at low concentrations of heme (68). This regulation is similar to that of transporters for other ligands. The transcription of the copper uptake molecule *ctr1B* in flies is induced in response to copper deficiency and repressed in response to copper repletion (148). In yeast, copper down-regulates *CTR1* through repressing the activation domain of the transcription factor Mac1p (149). In addition, the divalent metal ion transporter 1 is regulated post-transcriptionally through IRP-IRE machinery in response to changes in iron levels (150).

Figure 1.4. Heme-dependent transcription factor Hap1. (A) Under aerobic conditions, heme promotes the binding of Hap1 to the upstream activation sequences and the aerobic genes are induced. Small chaperones such as Hsp70 and Hsp90 are involved in this regulation. (B) Under hypoxic conditions, Hap1 recruits co-repressors Tup1/Ssn6 and inhibits the transcription of ergosterol biosynthesis genes. The presence of heme relieves this transcriptional repression.

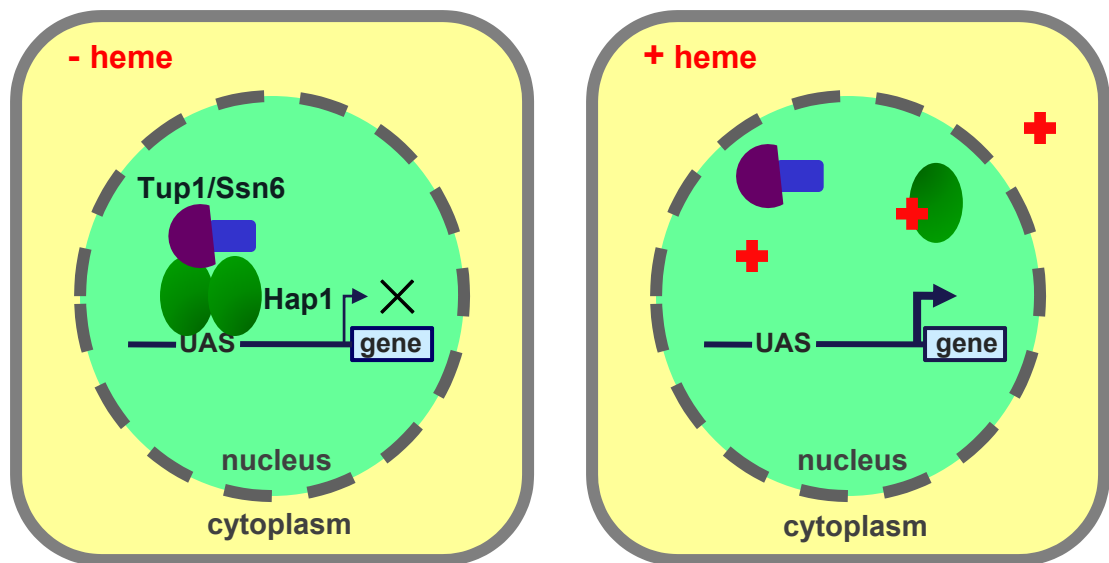
A

under aerobic conditions:



B

under hypoxic conditions:



Parasitic worms and heme

Parasitic worms are a major cause of chronic infections in humans, farm animals and plants. More than a quarter of the world's population is affected by one or more of the 20 most common parasites including *Ascaris*, *Ancylostoma*, *Trichuris* and *Schistosoma* (151,152). In addition, animal parasites and plant parasites cause enormous economic loss in agricultural production every year. Traditional drugs are becoming more and more ineffective in helminthic control as drug-resistant nematodes are already prevalent in humans and other animals (153,154).

Heme and iron play essential roles in development, reproduction and pathogenicity of parasitic worms. For example, iron supplement stimulates the growth of the fluke *S. mansoni* *in vitro* (155). Due to the fact that free iron is tightly controlled in animal hosts and *S. mansoni* ingests huge amount of blood, it is highly possible that these parasites acquire iron predominantly in the form of heme from the blood (156). In the hookworm, *Ancylostoma ceylanicum*, host iron status has been shown to be a key mediator of pathogenicity. Challenged animal hosts supplied with iron-restricted diet had a significant reduction in the intestinal load of worms (157).

In the intestine of the canine hookworm *A. caninum*, hemoglobin is degraded by a cascade of proteolytic reactions involving aspartic proteases (APR-1), cysteine proteases and metalloproteases (158). Vaccination of dogs with APR-1 dramatically reduced the hookworm burdens, fecal egg counts, as well as host blood loss, after challenging with *A. caninum* larvae (159).

Recently, Rao *et al.* discovered that parasitic worms including *Strongyloides*, *Ancylostoma*, *Haemonchus*, *Trichuris* and *Ascaris* are unable to synthesize heme *de novo*,

despite requiring this tetrapyrrole nutritionally (160). Analysis of the genomes for these nematodes indicates that they encode abundant hemoproteins such as globins, cytochrome P450s, catalases and guanylate cyclases. Therefore, worms must have developed an efficient heme uptake system to meet their nutritional requirement and a heme storage system to store essential but cytotoxic heme. In addition, since none of the cells have the ability to synthesize heme, an intercellular heme transport system is required to mobilize heme from intestinal cells – the site of absorption – to other cell types including neurons, muscles, hypodermis, and developing embryos. Thus, worm-specific molecules involved in heme homeostasis, especially in heme uptake, could be potential drug targets for helminthic control.

The free-living roundworm *C. elegans* is a unique animal model for interrogating heme trafficking pathways. *C. elegans* has been used as a model organism to study RNA interference, apoptosis, development, aging, toxicology, neurobiology, sex determination, and membrane trafficking. Similar to the parasitic worms, *C. elegans* lacks the ability to synthesize heme and acquires it from the diet (160). Thus, the organismal heme levels are dependent upon the heme concentration in the food. This “clean” genetic background, in combination with other advantages, such as a fully sequenced genome and a comprehensive map of all cell lineages, makes *C. elegans* a valuable model system for delineating the cellular pathways and biochemical mechanisms of heme homeostasis.

By using this genetic model, we have identified two heme-responsive genes, *hrg-2* and *hrg-3*, as candidate genes involved in heme homeostasis. At the molecular level, HRG-2 may play a role in heme uptake or intracellular heme allocation, whereas HRG-3 may be involved in heme-regulated signaling or intercellular heme transport.

Chapter 2: Materials and Methods

Worm experiments

Worm culture

Routine maintenance, synchronization, genetic crosses and microscopic observation were described by Epstein and Shakes (1995) (161). Wild type N2 Bristol strain, deletion strains and transgenic worms were maintained at 20°C either on nematode growth medium (NGM) agar plates or in axenic modified *C. elegans* Habitation and Reproduction (mCeHR-2) medium supplemented with hemin chloride (161,162). Continuous shaking was provided for all liquid worm cultures. Hemin chloride was prepared as a 10 mM stock by dissolving it in 0.3 M NH₄OH and adjusting the pH to 8.0 with HCl (160).

Worms for microarray experiments were prepared by Dr. Wayne Van Voorhies (New Mexico State University). All worms were maintained in mCeHR-2 medium in metabolic chambers at 20°C. Oxygen levels were controlled by pre-mixing oxygen and nitrogen at different ratios and directing the air mixture to individual chambers through Luer fittings (163).

In CdCl₂ induction assays, synchronized stage 1 (L1) larvae were grown at 1.5 and 20 µM hemin for 7 d. The worms were then treated with no or 100 µM CdCl₂ for 24 h before harvesting.

Deletion worm strains

The deletion strains *hrg-2* (*tm3798*) and *hrg-3* (*tm2468*) were isolated in mutagenesis screens by the Japanese deletion consortium (National Bioresource Project for the Experimental Animal Nematode *C. elegans*) (164). The allele *cdr-4* (*ok863*) was provided by *Caenorhabditis* Genetics Center, University of Minnesota, Minneapolis. All alleles were confirmed by sequencing and outcrossed eight times with the N2 Bristol strain. Progeny from genetic crosses were genotyped by single worm polymerase chain reaction (PCR). During the final outcross, both homozygous mutants and their wild type brood mates were saved for further analysis.

For single worm PCR, the individual worms were transferred to 200 μ L PCR tubes containing 5 μ L of lysis buffer (50 mM KCl, 10 mM Tris-HCl, 2.5 mM MgCl₂, 0.45% NP-40, 0.45% Tween-20, 0.01% gelatin, and 1mg/mL fresh proteinase K). Worms were lysed by freezing and heating (2 h at -80°C, 1 h at 65°C, and 30 min at 95°C) and the lysates were subjected to PCR reactions. Genotyping primers are shown in Appendix I.

Transgenic worm lines

Transcriptional reporter constructs were generated either by fusion PCR or by the multisite Gateway system (Invitrogen). The constructs utilized in this study are shown in Appendix II. For example, the transcriptional fusion *hrg-2::gfp* comprises the 1.5 kb promoter region upstream of the *hrg-2* start codon, a nuclear localization signal, a green fluorescent protein (GFP), and an *unc-54* 3'UTR or a *hrg-2* 3'UTR. Translational reporter constructs and ectopic expression constructs were generated by the multisite Gateway system (Appendix II). Worms with extra-chromosomal arrays or stable transgenic lines were obtained by microinjection (165) or by microparticle bombardment

(166). At least two lines were analyzed for each construct. A worm strain with the intestinal Golgi marker (*RT1315*, *vha-6::MANS-GFP*) was a gift from Dr. Barth Grant (Rutgers University).

Bombardment

One week before biolistic transformation, $\sim 10^6$ *unc-119* (*ed3*) worms were transferred to fresh mCeHR-2 medium with 20 μ M hemin. For bombardment, worms were harvested by centrifugation at 800 \times g for 2 min. The pellets were resuspended in M9 buffer (86 mM NaCl, 42 mM Na₂HPO₄, 22 mM KH₂PO₄, and 1 mM MgSO₄), and the adult worms were allowed to settle for 15 min on ice. The supernatant was aspirated, and the washing process was repeated 3 times or until the majority of the worms in the pellet were adult worms. The worms were then evenly plated on a dry, ice-chilled 10 cm NGM agar plate seeded with JM109 bacteria.

Biolistic transformation of *C. elegans* was carried out following the protocol described by Praitis *et al.* (166). Briefly, 8 μ g of reporter plasmid and 5 μ g of *unc-119* rescue plasmid were mixed with 6 mg of ~ 2.2 μ m gold particles (Degussa). The DNA-gold mixture was delivered into *unc-119* (*ed3*) worms by bombardment using the PDS-1000/He particle delivery system with the Hepta adaptor (Bio-Rad). Worms from each bombardment were grown at 25 °C in 20 10 cm NGM agar plates containing JM109 bacteria for two weeks. *unc-119* (*ed3*) mutants are immobile, and they can not survive dauer formation in the absence of food. Only those mutant worms transformed with a wild type *unc-119* gene can survive the starvation. The surviving worms with wild type movement were isolated and examined for the expression of reporter genes.

RNA extraction and Northern blotting

Synchronized worms were grown at different concentrations of hemin chloride in mCeHR-2 medium. After two generations, all F₂ worms were harvested at the late L4 stage. To analyze the expression of *hrg-3* at different developmental stages, synchronized F₁ worms were grown in the presence of 4 µM heme for one generation. An aliquot of the eggs from bleaching the F₁ gravids was saved for RNA extraction. Synchronized L1 worms at the F₂ generation were grown with 4 µM heme for another 84 h. Aliquots of worms were harvested every 12 h. L4 stage worms grown with 20 µM heme were used as control.

Total RNA was isolated with TRIzol reagent (Invitrogen), purified with RNeasy Midi kit (Qiagen), and DNase-treated with RQ1 DNase (Promega). RNA quality was assessed by gel electrophoresis and by measuring the absorbance at 260 nm and 280 nm using a UV-visible spectrophotometer (Shimadzu). Twenty micrograms of denatured RNA was electrophoresed on a 1% formaldehyde agarose gel and blotted onto a nylon membrane (Zeta Probe, Bio-Rad). The [³²P] α -dCTP (Amersham) labeled cDNA probes were generated using Prime-It II random primer labeling kits (Stratagene) with primers shown in Appendix III. The RNA membrane was incubated with probes in ULTRAHyb (Ambion) for 16 h. After washing the membrane, the signals were analyzed using a PhosphorImager (Storm 860, Molecular Dynamics).

cDNA synthesis and quantitative Real-Time PCR

After DNase digestion, 2 µg total RNA was used to synthesize cDNA using oligo (dT) primers and a SuperScript First-Strand Synthesis kit (Invitrogen). Quantitative real-time polymerase chain reaction (qRT-PCR) was performed in triplicate in an iCycler iQ

Multicolor Real-time PCR Detection System (Bio-Rad) with SYBR Green as the detection dye. Gene-specific PCR primers were designed by Beacon Designer version 4.0 (Appendix III and Appendix IV). Each 20 μ L PCR reaction contained 1 μ L template cDNA, 350 nM primers, 0.12 U/ μ L Taq polymerase, 40 nM fluorescein (Invitrogen), and a 1:10,000 dilution of SYBR Green I Nucleic Acid Gel Stain (Invitrogen). The PCR program was 30 sec at 94°C, 30 sec at 60°C and 15 sec at 72°C. The purity of PCR products was determined by melting curve analysis and gel electrophoresis. The relative gene expressions were calculated using the comparative cycle threshold (C_t) method or $\Delta\Delta C_t$ method by normalizing to glyceraldehyde 3-phosphate dehydrogenase-2 (*gpd-2*) (167).

Rapid Amplification of cDNA ends

To identify the full length mRNA of *hrg-2* and *hrg-3*, we performed both 5' rapid amplification of cDNA ends (RACE) and 3' RACE using the SMART RACE kit (Clontech). Total RNA isolated from worms grown at 4 μ M heme was reverse transcribed into first strand cDNA using modified oligo (dT) primers. RACE PCR was performed with one universal primer and one *hrg* specific primer. The PCR products were cloned into the PCR II plasmid using a TA cloning kit (Invitrogen) and sequenced. Each cDNA end was confirmed by sequencing at least three positive clones.

RNA interference

RNAi experiments were performed either by feeding the worms with bacteria expressing double-stranded RNA (dsRNA) or by directly soaking worms in dsRNA transcribed *in vitro*. For RNAi feeding, *hrg-2* and *hrg-3* open reading frames (ORFs) were first cloned into the L4440 plasmid (Fire Vector kit, Addgene) that contains the T7

promoter in both 5' and 3' flanking regions. RNase III-deficient bacteria *HT115(DE3)* transformed with either empty vector or *hrg* constructs were spotted onto NGM plates containing 50 µg/mL carbenicillin, 12 µg/mL tetracycline and 2 mM isopropyl-beta-D-thiogalactopyranoside (IPTG). L1 larvae were placed onto RNAi plates and incubated at 20°C. The phenotype was investigated in 3-4 d.

In preparation for soaking RNAi, dsRNA was transcribed from 2 µg of L4440-*hrg* plasmids using the MEGAscript RNAi kit (Ambion). The reaction was subsequently treated with DNase I and RNase to remove DNA and ssRNA. Free nucleotides and proteins were removed by column purification. RNA quality was determined by gel electrophoresis and by measuring the absorbance at 260 nm and 280 nm in a UV-visible spectrophotometer. Soaking RNAi was performed using the conditions described by Ahringer (168). Synchronized L1 larvae were placed into 50-200 ng/ µL dsRNA in the soaking buffer (21.5 mM NaCl, 10.5 mM Na₂HPO₄, 5.5 mM KH₂PO₄, 15 mM spermidine, and 0.25% gelatin). After 24-48 h, the worms were removed for examination of phenotypes or for subsequent growth assays at different heme concentrations.

GFP quantitation and zinc mesoporphyrin IX uptake assay

GFP-expressing strains were grown at varying heme concentrations in mCeHR-2 medium. After 4 d, worms were washed with M9 buffer and harvested for protein extraction. Total worm lysates were subjected to GFP fluorescence measurements using the Victor 1420 Multilabel counter (Perkin Elmer). Measurements were performed in triplicate and all fluorescence intensities were normalized to the protein concentrations (Bio-Rad).

For zinc mesoporphyrin IX (ZnMP, Frontier Scientific) uptake assays, synchronized L1 worms were grown at 2 μ M heme in mCeHR-2 medium. At the early L4 stage, they were washed with M9 buffer and incubated with 10 μ M ZnMP in the presence of 1.5 μ M heme. After 16 h, worms were washed twice with M9 buffer, paralyzed in 10 mM levamisole, and mounted on 1.2% agarose pads on glass slides. After placing a coverslip on the agar pad, the worm samples were analyzed with a Leica DMIRE2 epifluorescence/DIC microscope. Images were obtained using a Retiga 1300 cooled Mono 12-bit camera and quantitated using SimplePCI version 6.2.0 software (Compix Inc).

Worm lysis for immunoblotting

Transgenic worms were maintained at low heme (≤ 4 μ M) for at least one generation to ensure *hrg-2* or *hrg-3* expression. Worms were then harvested, washed once with M9 buffer, and resuspended in M9 buffer with protease inhibitor cocktail set III (Calbiochem). The samples were transferred to 2 mL tubes containing Lysing Matrix D beads and subjected to FastPrep-24 (MP Biomedicals) bead beater disruption (four pulses of 60 s at 6.5 m/s). The homogenates were centrifuged at 16,000 \times g for 30 min to remove worm debris and the total protein concentrations were measured using the Bradford reagent (Bio-Rad).

Iron and protoporphyrin IX response assays

An iron response experiment was performed in iron-depleted mCeHR2 medium. To make iron-depleted medium, all stock components except for $\text{Fe}(\text{NH}_4)_2(\text{SO}_4)_2 \cdot 6\text{H}_2\text{O}$ were assembled following mCeHR-2 protocol (162). The medium was incubated with 1 mM ferrozine (Sigma), a membrane impermeant iron chelator, for 3-5 d at 20°C in order to chelate any residual iron from the medium. To test whether iron regulates *hrg*

expression, transgenic worms were grown in iron-depleted medium supplemented with either 0.1 or 20 μ M ammonium ferric citrate ($C_6H_8O_7 \cdot Fe \cdot NH_3$) in combination with 1.5 or 20 μ M hemin chloride for 48 h.

PPIX (Frontier Scientific) was prepared as a 1 mM stock solution following the same procedure used for preparing the hemin stock (160). Transgenic worms were treated with 20 μ M PPIX in mCeHR-2 medium in the presence of 1.5 μ M hemin. After 48 h, the animals from these two experiments were analyzed for GFP fluorescence by confocal microscopy.

Mammalian cells

Cell culture, plasmids and transfection

Mammalian cells were cultured at 37°C in a humidified incubator with 5% CO₂. Human embryonic kidney (HEK) 293 cells were maintained in Dulbecco's modified Eagle's medium (DMEM, GIBCO/BRL) supplemented with 10% fetal bovine serum (FBS) and penicillin/streptomycin/glutamine. DNA constructs were transiently transfected into HEK293 cells using Lipofectamine 2000 (Invitrogen) for western blotting studies and FuGENE 6 (Roche) for immunofluorescence assays.

DNA cloning

Total worm RNA was first reverse transcribed into cDNA using oligo (dT) primers. *hrg-2* and *hrg-3* ORFs were amplified with primers flanked by *Bam*HI and *Xho*I restriction sites. Sequences for hemagglutinin (HA) or FLAG epitope tags were included in the primers to generate tagged HRG proteins. Following restriction digestion and DNA purification, the PCR products were cloned into the pcDNA3.1(+) zeo vector (Invitrogen)

and the pEGFP-N1 vector as well as its equivalent GFP variant living color vectors (Clontech). Truncated constructs, including HRG-2N, HRG-2Δ1, HRG-2Δ2, HRG-2ΔN, HRG-3N, and HRG-3ΔN were introduced into mammalian expression plasmids in a similar way.

Immunofluorescence

Transfected HEK293 cells grown on coverslips were fixed with 4% paraformaldehyde for 20 min. After permeabilization with 0.2% Triton X-100 for 10 min, the cells were blocked in 3% bovine serum albumin and 50% SuperBlock solution (Pierce). Samples were incubated in a primary polyclonal anti-HA antibody (Sigma) at 1:2,000 dilution for 1 h at room temperature, followed by goat anti-rabbit IgG secondary antibodies conjugated to either Alexa 488 or Alexa 568 at 1:6,000 dilution for 30 min. Coverslips were mounted onto slides using ProLong Antifade (Invitrogen). For GFP fluorescence studies, cells were directly mounted onto slides after fixation. The specimens were examined and photographed on a laser scanning confocal microscope LSM 510 (Zeiss).

Protein preparation for immunoblotting

For western blotting, transiently transfected cells were lysed with cell lysis buffer (150 mM NaCl, 0.5% Triton X-100, 20 mM HEPES, pH 7.4) for 5 min on ice. Cell lysates were collected after centrifugation at 10,000×g for 10 min at 4°C. The total protein concentration was quantified with the Bradford reagent (Bio-Rad).

Fluorescence protease protection assay

The procedure for fluorescence protease protection (FPP) assay was modified from the protocol by Lorenz *et al.* (169). HRG-2-GFP, HRG-3-GFP, and control plasmid pCFP-CD3δ-YFP (a gift from Dr. Jennifer Lippincott-Schwartz, NIH) were transfected into HEK293 cells growing in Lab-Tek chambered coverglass (Nunc). After 24 h, the cells were washed with KHM buffer (110 mM potassium acetate, 2 mM MgCl₂, and 20 mM HEPES, pH 7.3) and the cell chambers were moved to a DMIRE2 epifluorescence microscope (Leica) connected with a Retiga 1300 cooled Mono 12-bit camera. The plasma membrane was permeabilized with 30 μM digitonin for 2 min and the cells were immediately incubated in 50 μg/ml proteinase K for 2 min. Images were taken before digitonin treatment, after digitonin treatment, and after proteinase K digestion.

Heme depletion in HEK293 cells

To deplete heme, HEK293 cells were grown in heme-depleted growth medium supplemented with 0.5 mM succinylacetone for 24 h. The FBS (10%) for this medium was depleted of endogenous heme by incubating with 10 mM ascorbic acid for 7 h at 37°C, followed by dialysis for 3 times in phosphate buffered saline (PBS) (170).

Hemin-agarose chromatography

Hemin-agarose pull-down assays were performed according to the procedure outlined by Rajagopal *et al.* (68). Briefly, transfected HEK293 cells were lysed in MS buffer (210 mM mannitol, 70 mM sucrose, 10 mM HEPES, pH 6.4 or 7.4), in the presence of Protease Inhibitor Cocktail III (Calbiochem) on ice for 30 min. Following centrifugation at 100×g for 5 min, the post-nuclear supernatant was subjected to SDS-PAGE and immunoblotting with a rabbit anti HA antibody (Sigma). The expression level

of each HA-tagged protein was quantified using Image Quant software version 5.1. Hemin-agarose was prepared following methods described by Tsutsui (171). Each binding reaction contained 300 nmol hemin-agarose, as well as 500 µg HRG-2 cell lysate or the equivalent amount of target proteins from other cell lysates. Cell lysates from untransfected HEK293 were added to bring the total protein content of all samples to 500 µg. The binding reactions were incubated with gentle rocking at room temperature for 30 min and then centrifuged at 800×g for 3 min. The pellets were washed three times with 1 ml wash buffer (150 mM NaCl, 1% NP-40, and 50 mM Tris-HCl, pH 8.0) and three times with RIPA buffer (150 mM NaCl, 1% NP-40, 0.5% sodium deoxycholate, 0.1% SDS, and 50 mM Tris-HCl, pH 7.9). The bound proteins were eluted by incubating in 8 M urea and Laemmli sample-loading buffer containing 100 mM DTT for 5 min at room temperature and boiling for 3 min. Equivalent amounts of input protein, the flow-through after RIPA washes, and the eluted protein were subjected to electrophoresis in 4-10% polyacrylamide gels and immunoblotting with HA antibodies. Each hemin-binding assay was done in ≥ 2 replicates.

Yeast experiments

Strains and growth

The heme-deficient *S. cerevisiae* strain, DY1457 *hem1Δ(6D)*, was provided by Dr. Caroline Philpott (NIH). This *hem1Δ* strain lacks the gene encoding δ -aminolevulinic acid synthase, which is the rate-limiting enzyme in the heme biosynthesis pathway (172). Yeast were maintained on enriched yeast extract-peptone-dextrose (YPD) plates or YPD liquid medium at 30°C. Solid and liquid synthetic complete (SC) media comprised 0.17% yeast nitrogen base (YNB, BIO 101), 2% dextrose, 0.5% (NH₄)₂SO₄, and amino acids, as

described by Sherman (173). The regular growth medium was supplemented with 250 μ M δ -aminolevulinic acid (ALA).

Cloning and yeast transformation

Untagged or tagged versions of *hrg-2* and *hrg-3* ORFs were cloned into either the 2 micron plasmid pYES-DEST52 (Invitrogen) by Gateway cloning or a modified plasmid pJBS7 (provided by Dr. Caroline Philpott, NIH) using primers engineered with *Bam*HI and *Xba*I restriction sites. *cdr-1* and truncated *hrg* constructs were cloned into the pJBS7 vector. HA-tagged *hrg-4* was cloned into pYES-DEST52 using the Gateway system and pRS423Gal plasmid (a gift from Dr. Daniel Kosman, University at Buffalo) by using *Sal*I and *Not*I restriction sites. The reporter construct pRS314m-CYC1-lacZ was generated by homologous recombination using the PCR product of CYC1::LacZ and the plasmid pRS314m-CYC1-HIS (gifts from Dr. Caroline Philpott). These expression plasmids were transformed into yeast using polyethylene glycol and lithium acetate at 42°C for 20 min. Positive clones were isolated by plating the transformants onto the selective SC medium. In this SC medium, uracil was dropped out for single transformation with pYES-DEST52 constructs. For co-transformation with pRS423Gal constructs or pRS314m-CYC1-lacZ, the selective medium lacks uracil plus histidine or uracil plus tryptophan, respectively. ALA was supplemented to all of the transformations.

Heme rescue assay

Expression plasmids containing vector only or HRG constructs were transformed into *hem1 Δ* yeast. After 3 d, individual yeast colonies were transferred onto selective SC agar plates containing raffinose instead of glucose. Residual ALA was removed by incubating the transformants in SC liquid medium without ALA for 16 h. Equal numbers

of transformed yeast were inoculated onto growth assay plates containing 4% galactose for gene induction as well as different concentrations of hemin chloride or ALA. Yeast growth was analyzed after incubation at 30°C for 3-5 d.

β-Galactosidase assay

β-Galactosidase was assayed as described (174). The transformed yeast was grown in 10 mL selective SC medium containing 2% galactose for 7-8 h or until an optical density (O.D.) of 0.5 at 600 nm had been reached. Cells were harvested and resuspended in 250 μL breaking buffer (1 mM dithiothreitol, 20% glycerol, and 100 mM Tris-HCl, pH 8.0) with 2.5% protease inhibitor cocktail set III. Cells were then disrupted using a FastPrep-24 (MP Biomedicals) Bead Beater (three 30 s pulses at 6.5 m/s) in the presence of acid-washed glass beads. Yeast lysates were centrifuged at 16,000×g for 10 min and the supernatant used immediately to determine the enzyme activity. β-Galactosidase activity was measured by incubating an equal volume of yeast lysate at 30°C with 0.4 mg/mL o-nitrophenyl-β-D-galactopyraniside in Z buffer (60 mM Na₂HPO₄·7H₂O, 40 mM NaH₂PO₄·H₂O, 10 mM KCl, 1 mM MgSO₄·7H₂O, and 40 mM β-mercaptoethanol with pH adjusted to 7.0). After 5 min, 0.2 M Na₂CO₃ was added to stop the reaction. The O.D.₄₂₀ of the assay solutions were measured in a UV-visible spectrophotometer and normalized to total protein measured by the Bradford assay. Enzyme activity was expressed as nmol/min/mg protein.

Yeast immunofluorescence

Transformed yeast cells were grown under inducing conditions in liquid SC medium to mid-log phase. After fixing with 4% formaldehyde for 1 h, cells were harvested by centrifugation and washed twice with PBS. Cells were subsequently

resuspended in 500 μ L of 1.2 M sorbitol with 1 mM dithiothreitol, and were then treated with 3 μ L of 10 mg/mL zymolyase-100T (US biological) at 30°C for 30 min. The resulting spheroplasts were washed twice with sorbitol buffer and finally resuspended in 100 μ L sorbitol buffer. Ten microliter aliquots of the spheroplasts were added to poly-L-lysine-coated 8-well slides and incubated for 10 min to allow attachment. Spheroplasts were incubated with rabbit polyclonal anti-HA antibody at a 1:2,000 dilution (Sigma) for 1 h and then Alexa 488-conjugated polyclonal goat anti-rabbit IgG antibody at a 1:5,000 dilution for 30 min. ProLong Antifade solution (Invitrogen) and a coverslip were applied to each slide.

Microarray analysis

Microarray design and worm growth

The microarray experiment used a 3 \times 3 full factorial arrangement with triplicates for each treatment (Figure 2.1A). Heme levels were 1.5, 20, and 500 μ M, and oxygen concentrations were 4%, 21%, and 100%. N2 worms maintained at 20 μ M heme, 21% O₂ were bleached to obtain F₁ larvae (Figure 2.1B). Equal numbers (3,000 worms/mL) of L1 larvae were inoculated into mCeHR-2 medium for all of the nine treatments. After one generation, the worms were synchronized again and the F₂ larvae received the same treatment as their mothers. When the F₂ worms reached late L4 stage, they were washed once with M9 buffer and flash frozen in liquid nitrogen followed by storage at -80°C.

RNA preparation and hybridization

Frozen worm pellets were ground into a fine powder using a mortar and pestle and subsequently homogenized using a Dounce homogenizer. Total RNA was isolated using

TRIzol reagent (Invitrogen), purified with an RNeasy Midi kit (Qiagen), and DNase-treated by RQ1 DNase (Promega).

The RNA samples were subjected to cRNA synthesis and hybridization to Affymetrix *C. elegans* whole genome arrays (Figure 2.1B). RNA quality assessment, RNA labeling, hybridization, and signal quantitation were carried out in the Genomics Core Facility at the National Institute of Diabetes and Digestive and Kidney Diseases, NIH.

Data analysis and model fitting

The raw data were background-adjusted and normalized using a Robust Multichip Average (RMA) algorithm in R statistical environment (175). ANOVA analyses and estimations of contrasts and false discovery rates (FDR) were conducted using the statistical package MAANOVA version 1.4.1 in R environment version 2.8.0 (175,176). Each probe set was first fitted against the full two-way ANOVA model including the main effects of heme (H) and oxygen (O) as well as the interaction (H*O). If no interaction was observed, only main effects were examined for the probe set. Otherwise, simple effects in each treatment were tested. The cut-off value for differential expression was fold change ≥ 2.0 and FDR q value < 0.05 . Since FDR was estimated based on the subset of genes with significant P values (< 0.05), we used it to reduce the type I error. Differentially expressed genes were clustered into groups based on whether the gene was up- or down- regulated at different heme or O₂ concentrations in comparison to the control level. Fold changes were converted into heat maps using Multiexperiment viewer version 4.3 (177).

Figure 2.1. Design and procedure of microarray experiments. (A) Experimental design. The microarray experiment used a 3×3 full factorial arrangement with triplicates for each treatment. Heme levels were 1.5, 20, and 500 μ M and oxygen concentrations were 4%, 21%, and 100%. (B) Procedure of worm growth, RNA preparation and microarray.

A

		Heme (μ M)		
		1.5	20	500
O ₂ (%)	4			
	21			
	100			

B

worm growth

P₀: N2 worms at 20 μ M heme in mCeHR-2 medium
 ↓ synchronize
 F₁: 3000 L1/ml in 90 ml mCeHR-2 medium per treatment
 ↓ synchronize
 F₂: 3000 L1/ml in 90 ml mCeHR-2 medium per treatment
 ↓
 Harvest worms at late L4 stage

RNA
preparation

Extract total RNA
 ↓
 RNA purification and DNase treatment

microarray

cRNA synthesis
 ↓
 Hybridization to Affymetrix arrays
 ↓
 Scan, quantitate and analyze data

Gene ontology, protein domain, and protein interaction analyses

Enrichment for gene ontology (GO) terms and Kyoto Encyclopedia of Genes and Genomes (KEGG) pathways were determined using the Database for Annotation, Visualization and Integrated Discovery (DAVID program) (178-180). The genes regulated by 1.5 μ M heme (189), 500 μ M heme (289), 4% oxygen (4), and 100% oxygen (94) were analyzed separately. The list of 22,625 probe sets in the Affymetrix *C. elegans* whole genome array was used as the background dataset for the calculation of the statistical significance and the fold enrichment. GO terms and protein families were considered significantly over-represented in the gene lists if they had >2.0 fold enrichment and a *P* value of <0.05. Protein-protein interactions were identified for the products of significantly changed genes by mapping them to Worm Interactome version 8 using Cytoscape version 2.6 (181,182).

Clustering of genes with similar expression profiles to *hrg-2* and *hrg-3*

The normalized microarray data were subjected to analysis with Genespring software version 7.3 (Agilent). Distinct sets of genes with expression patterns similar to *hrg-2* or *hrg-3* were identified based on the correlation coefficient (*r*) calculated for the pairwise comparisons between their signals and those of *hrg-2* or *hrg-3* across all 27 chips. Genes with *r* >0.8 were included in the gene clusters.

General procedures

Immunoblotting

Protein samples were separated by SDS-PAGE on 4-20% Tris-HCl criterion gels and transferred to nitrocellulose membrane (Bio-Rad). After blocking in 5% non-fat dried

milk, the membranes were incubated in rabbit anti-HA (Sigma) at a 1:2,000 dilution or mouse anti-GFP at a 1:5,000 dilution for 16 h at 4°C. HRP-conjugated secondary antibodies diluted to 1:20,000 were applied to the membrane for 30 min at room temperature. Signal was detected by SuperSignal chemiluminescence reagents (Thermo Scientific) in the Gel documentation system (Bio-Rad). The molecular weights of protein bands in the blots were determined with Precision Plus Protein Kaleidoscope Standards (Bio-Rad) using Quantity One software (Bio-Rad).

Confocal microscopy

GFP, mCherry and Alexa fluorophores were examined in a laser-scanning confocal microscope LSM 510 with Ar (458 nm and 488 nm) and HeNe (543 nm and 633 nm) lasers (Zeiss). Samples of mammalian cells, worms and yeast were examined using 63× and 100× oil immersion objective lenses. Images with a *z* resolution of 1 μm were acquired and processed in the LSM image browser (Zeiss).

***In vitro* transcription and translation**

HA-tagged *hrgs* in the pcDNA3.1(+) Zeo vector were transcribed and translated *in vitro* using the TNT Coupled Wheat Germ Extract System (Promega). One microgram of each plasmid DNA was added to wheat germ lysates in the presence of amino acids and TNT RNA polymerase. The reactions were incubated at 30°C for 2 h. The samples were subjected to SDS-PAGE and immunoblotting.

Protein expression in bacteria

Amino terminus-deleted HRG-2 and HRG-3 constructs were cloned into the expression vector pET14b (Invitrogen) between *Nde*I and *Bam*HI restriction sites. DNA

constructs were transformed into the *E. coli* strain *BL21(DE3)* or *C43(DE3)* for protein expression. The cells were grown aerobically in liquid Luria-Bertani medium until a $\text{O.D.}_{600} \sim 0.5$ had been reached. Gene expression was induced by the addition of 1 mM IPTG and the cells were incubated at 18°C for 16 h. The cells were harvested, washed with binding buffer (20 mM Tris-HCl, pH 7.9, 5 mM imidazole, and 500 mM NaCl) and stored at -80°C. Samples in 1 mL aliquots of bacteria before and after induction were lysed by heating for 5 min in Laemmli sample buffer with 2% SDS. Lysates were separated by SDS-PAGE and the proteins detected by either Coomassie blue staining or immunoblotting.

Purification of His-tagged HRGs

The frozen cell pellets were resuspended in binding buffer containing protease inhibitor cocktail set III (Calbiochem). Immediately after adding 1 mM phenylmethylsulphonyl fluoride, cells were homogenized by three passages through a French pressure cell (SLM Aminco) at an internal pressure of up to 15,000 psi (1 psi = 6.89 kPa). Bacterial supernatants were obtained by centrifugation at 14,000×g for 20 min at 4°C followed by filtration through a 0.45 µm filter. Lysates were applied to the His-Bind columns preloaded with charged His bind Resin (Novagen). After washing with binding buffer and washing buffer (20 mM Tris-HCl, pH 7.9, 60 mM imidazole, and 500 mM NaCl), the bound proteins were eluted with 1.0 M imidazole. Fractions of eluates were analyzed by Bradford assay for total protein concentration and by Coomassie blue staining following SDS-PAGE.

Bioinformatics

BLAST searches were applied to identify homologous genes of *hrg-2* and *hrg-3*. A putative ortholog was assigned when it had a significant E value ($< 10^{-4}$) and met the criterion of reciprocal best BLAST hit. Putative *hrg-3* homologs in *C. briggsae* and *C. remanei* were predicted by the GeneMark.hmm program (183). Binding sites for transcription factors in *hrg-3* promoter were predicted using the TFSEARCH program (<http://www.cbrc.jp/research/db/TFSEARCH.html>). Molecular weights and isoelectric points were calculated in the Compute pI/Mw program (184). Transmembrane domains, signal peptides, protein motifs, and protein secondary structures were predicted using the Transmembrane prediction with Hidden Markov Model (TMHMM) program (www.cbs.dtu.dk/services/TMHMM/), the eukaryotic linear motif (185), the conserved domain database (CDD, www.ncbi.nlm.nih.gov/Structure/cdd/cdd.shtml), and the Jpred3 (186), respectively. Multiple sequence alignment was performed using the ClustalW (187) and was visualized with the BoxShade program (www.ch.embnet.org/software/BOX_form.html). Following the multiple sequence alignment of HRG-2 and CDR-1 proteins, a phylogenetic tree was constructed using the neighbor-joining method in MEGA 4 (Molecular Evolutionary Genetics Analysis, Version 4.0) with 1000 pseudoreplicates (188,189).

Statistics

All data are presented as mean \pm S.E. Statistical significance was tested using one-way ANOVA followed by the Tukey-Kramer Multiple Comparisons Test in GraphPad INSTAT version 3.01 (GraphPad, San Diego). A *P* value of <0.05 was considered as statistically significant.

Chapter 3: Delineating the role of *C. elegans hrg-2* in heme homeostasis

Summary

Heme is an essential cofactor for diverse biological processes such as oxygen transport, xenobiotic detoxification, microRNA processing, circadian clock control and gene regulation. Since free heme is hydrophobic and cytotoxic, we hypothesize that within eukaryotic cells, specific intracellular trafficking pathways exist for the delivery of heme to different subcellular destinations where hemoproteins reside. To identify molecules that may be involved in heme homeostasis, an Affymetrix *C. elegans* genome array experiment was performed using RNA extracted from worms that were grown at low (4 μ M), optimal (20 μ M) and high (500 μ M) heme in axenic liquid growth medium. From the 288 genes that showed significant changes in gene expression, the mRNA levels of *heme-responsive gene-2* increased more than 70 fold when worms were grown at 4 μ M compared to 20 μ M heme. Results from quantitative real-time PCR and Northern blot confirmed the expression profile. In *C. elegans*, *hrp-2* shows high sequence similarity to a group of genes previously named *cadmium-responsive genes (cdrs)*. However, these *cdrs* are not heme responsive. Deletion of *hrp-2* in *C. elegans* resulted in reduced growth rate at low heme. Using reporter constructs, we found that *hrp-2* is expressed in hypodermal tissues and the protein localizes to the endoplasmic reticulum and apical plasma membrane. In addition to studies in the worm, fluorescence protease protection assays performed using transiently transfected mammalian cells confirmed that

HRG-2 is a type I membrane protein. *In vitro* hemin agarose pull-down experiments indicated that HRG-2 binds heme. Furthermore, expression of HRG-2 in *hem1Δ* yeast resulted in growth rescue of the heme-deficient strain at submicromolar concentrations of heme. Taken together, these results suggest that HRG-2 may play a critical role in the uptake or intracellular trafficking of heme in the hypodermal tissues of *C. elegans*.

Results

Identification of *hrg-2* as a heme-responsive gene in *C. elegans*

Within eukaryotic cells, proteins that require or bind heme are present in various compartments including the cytoplasm, the nucleus, lysosomes, peroxisomes, and the secretory pathway. Since free heme is hydrophobic and cytotoxic (7), it is highly possible that specific heme trafficking pathways exist for delivering heme to different subcellular destinations within eukaryotic cells. The free-living roundworm *C. elegans* is a unique genetic model for interrogating heme trafficking pathways because this animal lacks the ability to synthesize heme and thus acquires heme from the diet (160).

To identify molecules that may be involved in heme homeostasis, an Affymetrix genome-wide microarray experiment was performed using the RNA extracted from *C. elegans* grown at 4, 20 or 500 μ M heme in axenic mCeHR-2 liquid culture (68). The microarray result revealed that *heme-responsive gene-2* (*hrg-2*¹) (WormBase accession number K01D12.14) was significantly induced by heme deficiency in *C. elegans* (72.08 fold induction). To confirm this regulation, we performed RNA blotting analysis and found that *hrg-2* mRNA (~0.9 kb transcript) was highly expressed at 4 μ M heme, whereas no *hrg-2* message was detected at 20 and 500 μ M heme (Figure 3.1A).

¹ Worm gene names are shown in lower case italics, and protein names are shown in capital letters.

Quantitative real-time PCR showed that the *hrg-2* gene was upregulated more than 200 fold at 1.5 μ M heme but was almost completely repressed at 8 μ M heme (Figure 3.1B).

Heme consists of a PPIX ring and an iron atom. To test whether iron regulates *hrg-2* expression, we generated a translational fusion construct that contained the 1.5-kb promoter region of *hrg-2*, *hrg-2* gene, yellow fluorescent protein (YFP) coding region and *hrg-2* 3' untranslated region (UTR) (Figure 3.2A). This *hrg-2::HRG-2-YFP*² construct was predominantly expressed in hypodermal tissues when the transgenic worms were maintained at 1.5 μ M heme (Figure 3.2B). However, no YFP expression was observed at 20 μ M heme. This regulation pattern is consistent with the results from Northern blot analysis and qRT-PCR. The transgenic worms were grown in iron-depleted liquid medium supplemented with 0.1 or 20 μ M ammonium ferric citrate for 2 d. We found that different iron concentrations did not exhibit any effect on the expression of *hrg-2::HRG-2-YFP* (Figure 3.2B). This experiment was performed at both low (1.5 μ M) and optimal (20 μ M) concentrations of heme. Under both conditions, there was no difference in HRG-2-YFP expression when worms were treated with either 0.1 or 20 μ M iron. We next grew this transgenic strain in 1.5 μ M heme plus 20 μ M PPIX. No decrease in *hrg-2* expression was observed in this treatment compared to 1.5 μ M heme (Figure 3.2C). These results suggest that the regulation of *hrg-2* is specific to heme.

² The transcriptional constructs are shown in the format *promoter::gfp*, and the translational constructs are shown as *promoter::GENE-YFP*.

Figure 3.1. *hrg-2* is induced by heme deficiency. (A) Northern blot analysis of *hrg-2* expression in response to different heme concentrations. *gpd-2* was used as a loading control. (B) Quantitation of *hrg-2* mRNA by qRT-PCR. Relative fold changes were derived by normalizing the cycle threshold values to *gpd-2* and then to the control heme level of 20 μ M using $\Delta\Delta$ CT methods. The experiment was performed in triplicate, and the data were represented as the mean \pm S.E.

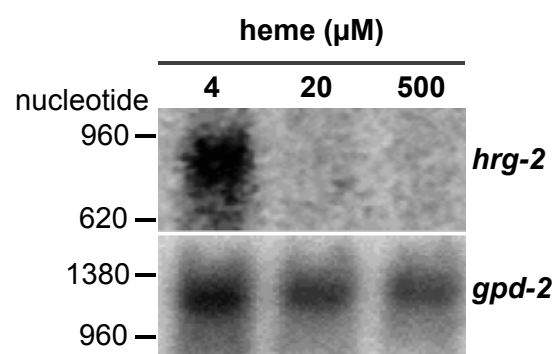
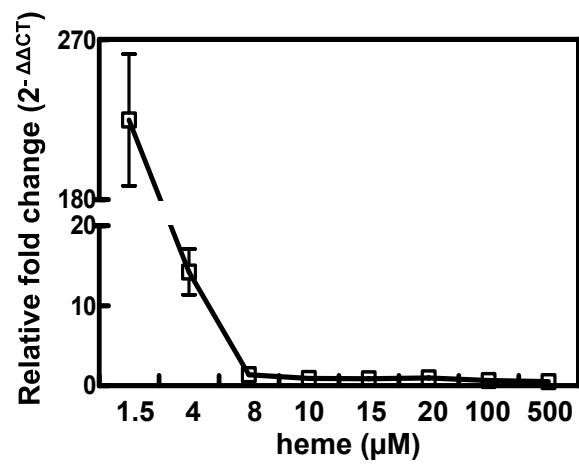
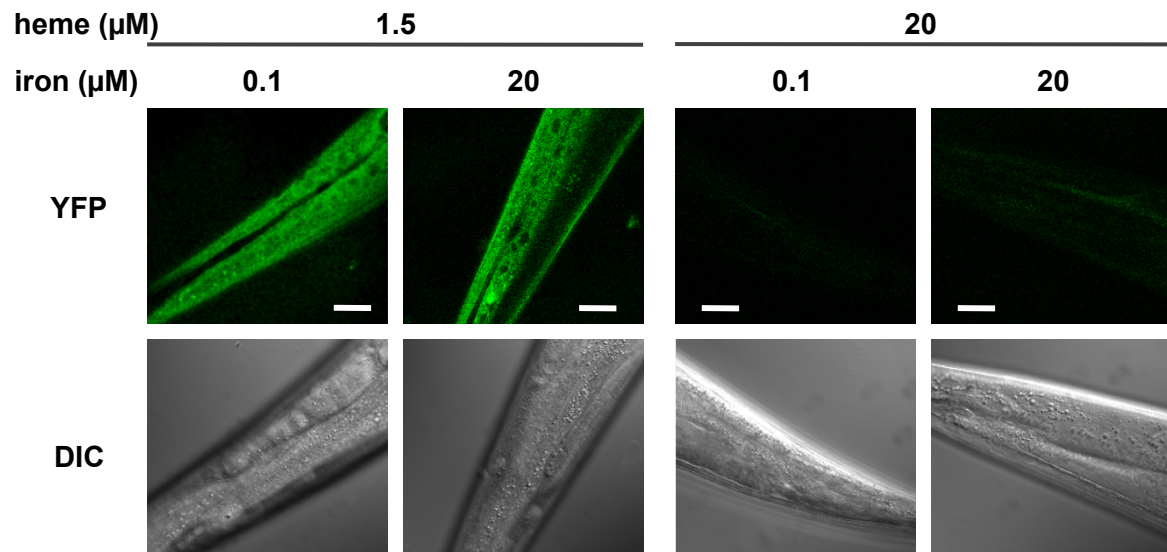
A**B**

Figure 3.2. Regulation of *hrg-2* is specific to heme. (A) Schematic representation of the *hrg-2* translational construct. UTR: untranslated region. (B) *hrg-2* expression at different concentrations of iron. The transgenic worms with the *hrg-2::HRG-2-YFP* construct were treated with 0.1 and 20 μ M ammonium ferric citrate in iron-depleted medium for 48 h. YFP signal was examined as a direct reporter for the activity of the *hrg-2* promoter. This experiment was performed at both 1.5 and 20 μ M heme. Representative images of the tail region in adult worms are shown. (C) Response of *hrg-2* expression to PPIX. *hrg2::HRG-2-YFP* transgenic worms were grown at 1.5 μ M heme with or without 20 μ M PPIX in mCeHR-2 medium. The expression levels were analyzed by confocal microscopy in 48 h. Representative images of the worm body in larvae are shown. DIC: differential interference contrast. (scale bar = 20 μ m)

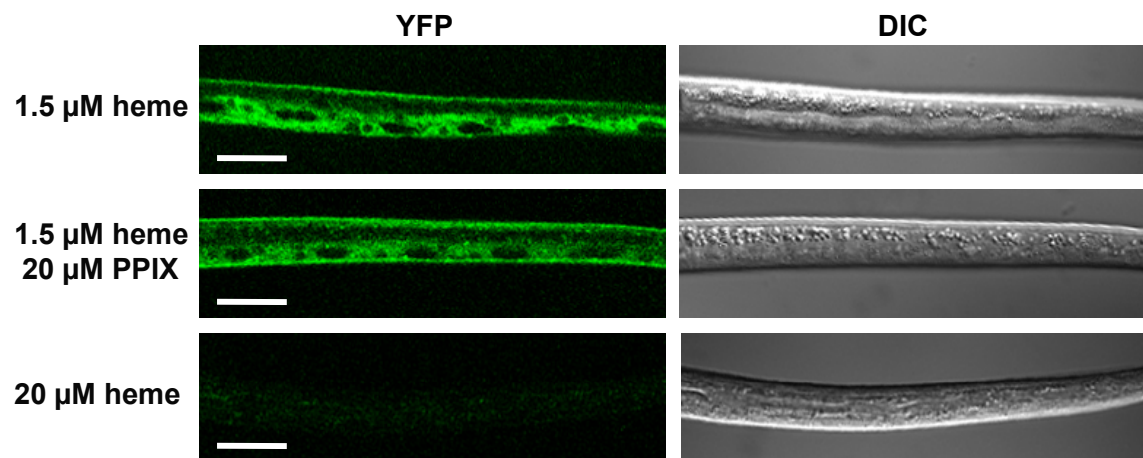
A



B



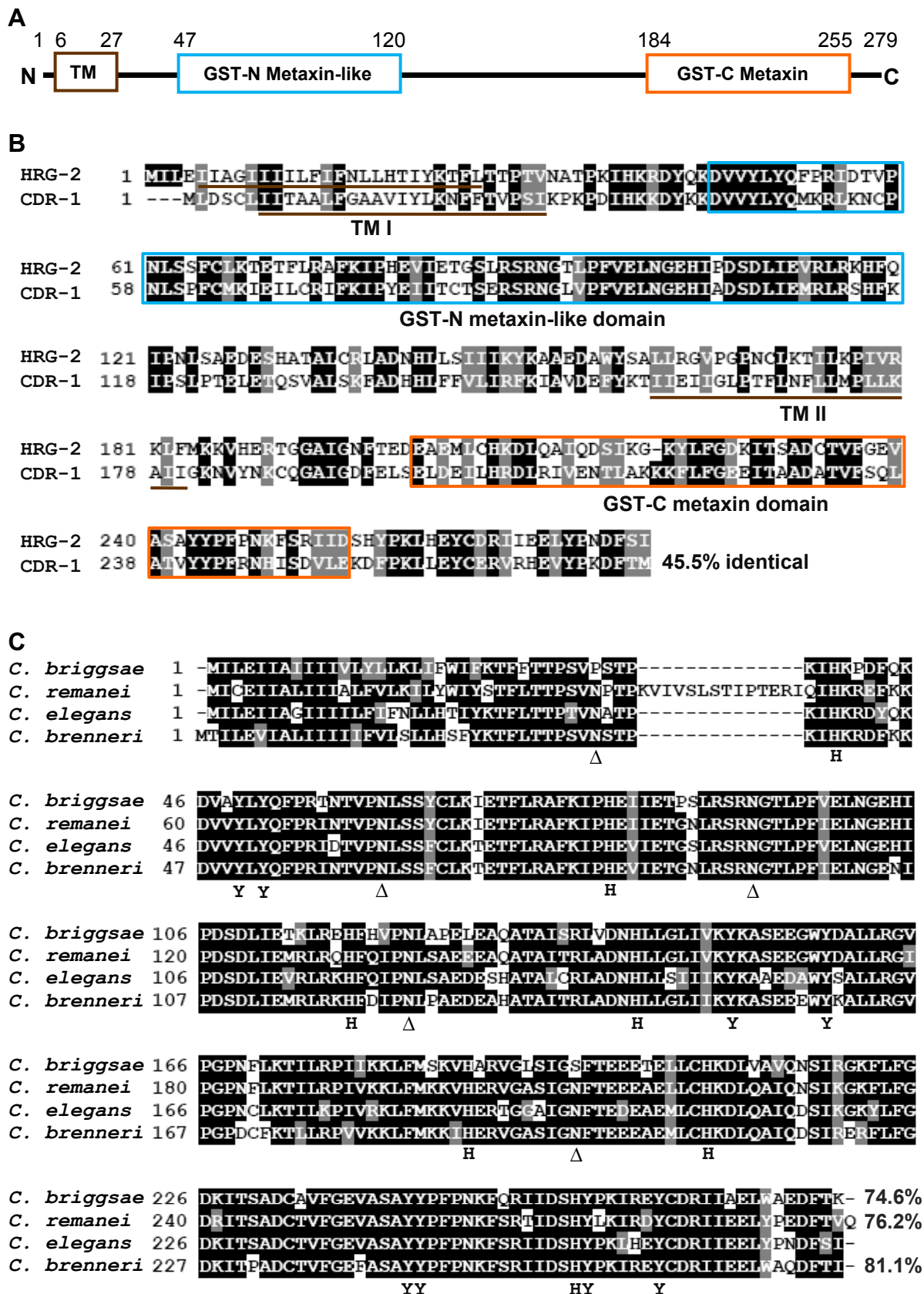
C



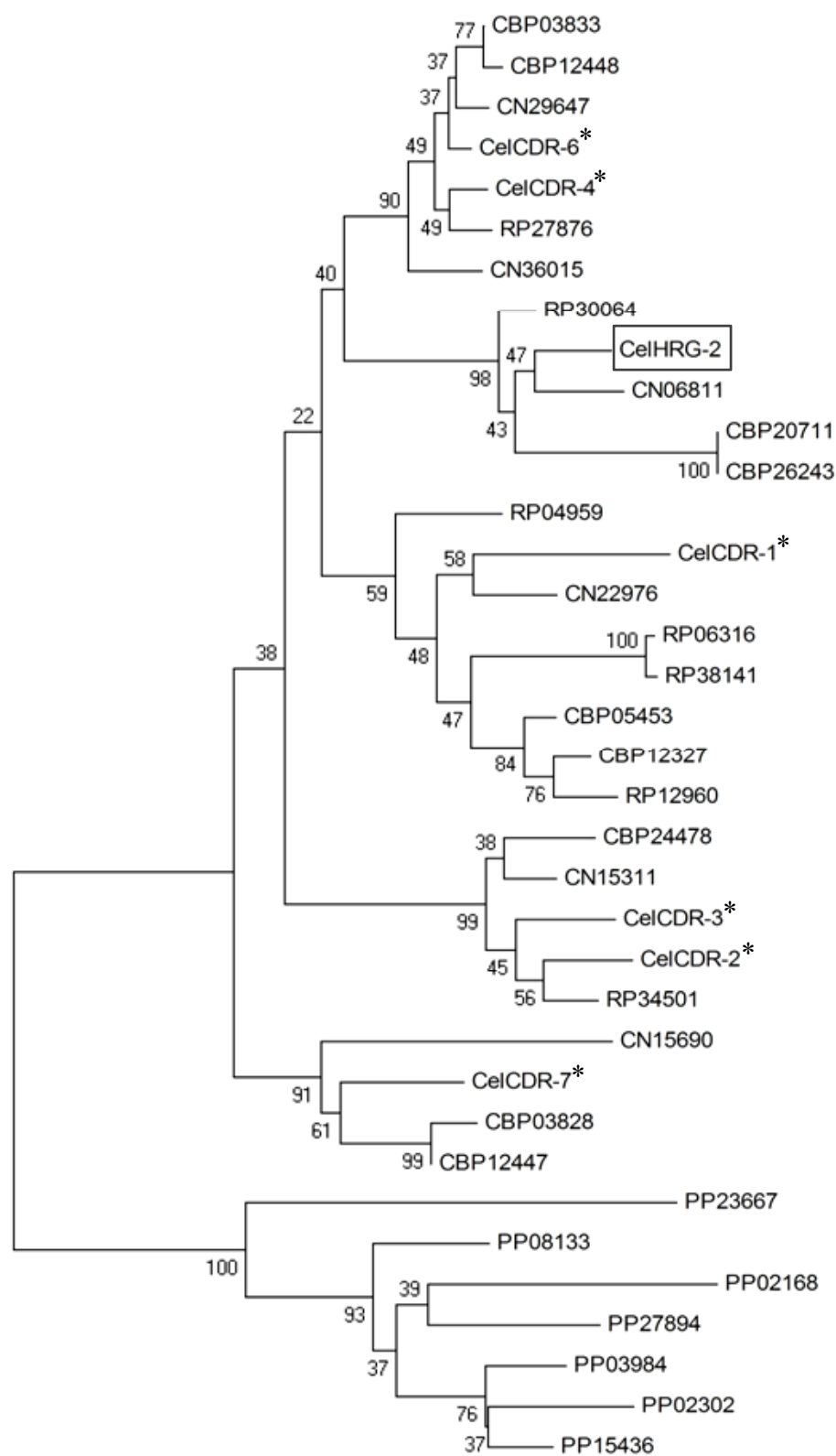
The *hrg-2* gene encodes a protein of 279 amino acids with a predicted molecular mass of 31.9 kDa and an isoelectric point of 6.83, as calculated using the Compute pI/Mw program (184). The TMHMM algorithm and the CDD program predicted that HRG-2 has an amino (N)-terminal transmembrane domain (TM), a GST-N metaxin-like domain and a GST-C metaxin domain (Figure 3.3A and 3.3B). In addition, HRG-2 protein has five putative N-linked glycosylation sites after the N-terminal transmembrane domain (Figure 3.3C).

In WormBase, *hrg-2* has been named *cadmium-responsive gene-5 (cdr-5)* because it has sequence homology to the *cdr-1* gene (WormBase accession number F35E8.11). This putative *cdr* family contains seven gene members in *C. elegans*. HRG-2 shares ~45% identity with each of the other CDR proteins, and the homology is throughout the peptide sequence (Figure 3.3B). Based on the prediction by CDD, all seven proteins have a GST-N metaxin-like domain and a GST-C metaxin domain, suggesting they may be involved in similar biological processes. Two proteins in *C. briggsae* (CBP20711 and CBP26243) show the highest homology to HRG-2 in *C. elegans*, suggesting that the *hrg-2* gene was duplicated in the *C. briggsae* genome (Figure 3.3C and 3.3D). Putative HRG-2 orthologs were also identified in *C. remanei* (RP30064) and *C. brenneri* (CN06811). They share >70% identity with HRG-2 at the protein level. No HRG-2 orthologs have been found in non-nematode species based on BLAST searches and homology comparison. Using BLAST, we found that *C. briggsae*, *C. remanei*, *C. brenneri*, and *Pristionchus pacificus* all have multiple *cdrs*, but it is difficult to assign all the *cdr* gene names solely based on the protein sequences (Figure 3.3D).

Figure 3.3. Protein domains and conservation of HRG-2. **(A)** Putative domains in HRG-2. The TM domain was predicted by the TMHMM program and GST-like domains were predicted using Conserved Domain Database. Numbers above the schematic indicate the positions of amino acids in HRG-2. **(B)** Comparison of HRG-2 and CDR-1. TMs and GST-like regions are indicated in both proteins. TM II is only present in CDR-1 but not in HRG-2. GST-like domains were drawn based on the amino acid positions in HRG-2 and are boxed. **(C)** Multiple sequence alignment of HRG-2 proteins among *Caenorhabditis* species. *C. briggsae* has two putative HRG-2 orthologs, of which the most similar one (WormBase protein ID CBP20711) is shown in the alignment. The protein IDs for HRG-2 in *C. remanei* and *C. brenneri* are RP30064 and CN06811, respectively. Sequences were aligned by the ClustalW program and visualized with BoxShade program. Conserved histidines and tyrosines are marked as H or Y. Δ indicates putative N-linked glycosylation sites. The numbers at the end of the alignment indicate percentage identities, which were derived from the pairwise alignment between *C. elegans* HRG-2 and its putative orthologs. **(D)** Evolutionary relationships of HRG-2, CDRs, and their homologs in nematodes. Protein sequences were aligned using the ClustalW program, and the phylogenetic tree was constructed with neighbor-joining method in MEGA 4. The branch lengths of the tree reflect the evolutionary distances, which are in the units of the number of amino acid substitutions. The scale bar represents 10% sequence divergence. HRG-2 and CDRs in *C. elegans* are marked with a box or asterisks. Cel: *C. elegans*. CBP: *C. briggsae*. CN: *C. brenneri*. RP: *C. remanei*. PP: *P. pacificus*.



D



0.1

Differential regulation of *hrg-2* and *cdrs*

In *C. elegans*, all *cdrs* except for *cdr-1* are clustered together on chromosome V. This suggests that these genes might be regulated by an operon, which has been shown to regulate ~15% of the genes in *C. elegans* (190). However, a previous study has suggested that *cdr* genes were not within an operon because none of the mRNAs were trans-spliced with the SL2 splice leader sequence (191), which is a hallmark for downstream mRNAs within an operon. Besides *hrg-2*, no significant changes were observed for any of the *cdrs* in response to heme (Figure 3.4A). qRT-PCR results confirmed that the expression of *cdr-4* (WormBase accession number K01D12.11) and *cdr-7* (WormBase accession number K01D12.13), the two *cdrs* that flank *hrg-2* gene in the genome, did not show any response to heme (Figure 3.4B). Furthermore, the genomic structure of *hrg-2* was confirmed by 5' and 3' rapid amplification of cDNA ends, indicating that the gene is not trans-spliced (Figure 3.4C). These results indicated that *hrg-2* is not transcribed as part of an operon.

To further understand the differential regulation of *cdrs* by cadmium and heme, we grew N2 worms at 1.5 or 20 μ M heme in the presence or absence of 100 μ M CdCl₂. qRT-PCR result indicated that *cdr-1* was induced only by cadmium whereas *hrg-2* responded only to heme (Figure 3.4D). These results suggest that the transcriptional regulation of both *hrg-2* and *cdr-1* is specific to distinct environmental cues despite the fact that these two genes are highly similar by sequence.

HRG-2 is required for worm growth at low heme

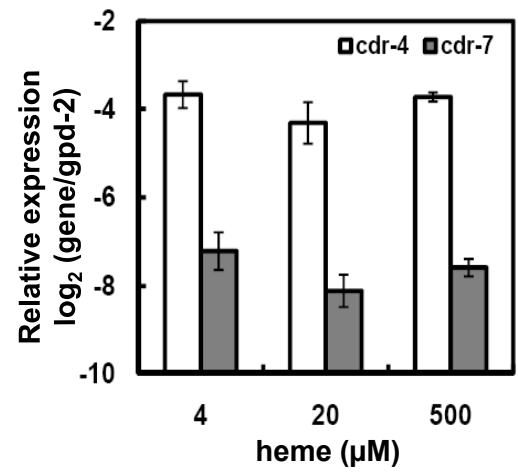
To characterize the functions of *hrg-2* in *C. elegans*, we examined the phenotype of the *hrg-2* (*tm3798*) deletion allele (164). This allele has a 502-base pair deletion that

Figure 3.4. Differential regulations of *hrg-2* and *cdrs*. (A) Expression profiles of *hrg-2* and *cdrs* by microarray analysis. All data are presented as mean \pm S.E. (B) Quantitation of *cdr-4* and *cdr-7* expression by quantitative RT-PCR. *cdr-4* and *cdr-7* genes are adjacent to the *hrg-2* gene in the worm genome. qRT-PCR was performed using RNA from worms grown at different heme concentrations. The gene expression was normalized to the internal control *gpd-2*. No significant difference was observed across heme levels ($P > 0.05$). (C) Genomic structure of *hrg-2* revealed by RACE analysis. Exons are depicted as empty boxes, and untranslated regions are shown as gray boxes. The number indicates the size of each region in nucleotides. (D) Transcriptional responses of *hrg-2* and *cdr-1* to heme and CdCl₂. N2 worms grown at 1.5 and 20 μ M heme were treated with 0 or 100 μ M CdCl₂ for 24 h. Total RNA was extracted and subjected to qRT-PCR analysis. Data above the dotted line are significantly different from those below the line for *hrg-2* and *cdr-1*, respectively ($P < 0.001$).

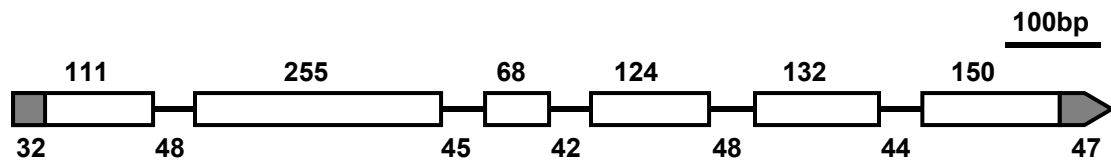
A

	heme (μM)		
	4	20	500
<i>cdr-1</i>	1.3 ± 0.1	1	1.2 ± 0.1
<i>cdr-2</i>	1.7 ± 0.4	1	1.5 ± 0.2
<i>cdr-3</i>	1.6 ± 0.4	1	-5.7 ± 5.3
<i>cdr-4</i>	1.3 ± 0.1	1	0.7 ± 0.9
<i>hrg-2</i>	72.1 ± 12.4	1	3.8 ± 1.0
<i>cdr-6</i>	1.2 ± 0.1	1	1.1 ± 0.1
<i>cdr-7</i>	1.2 ± 0.1	1	0.4 ± 0.8

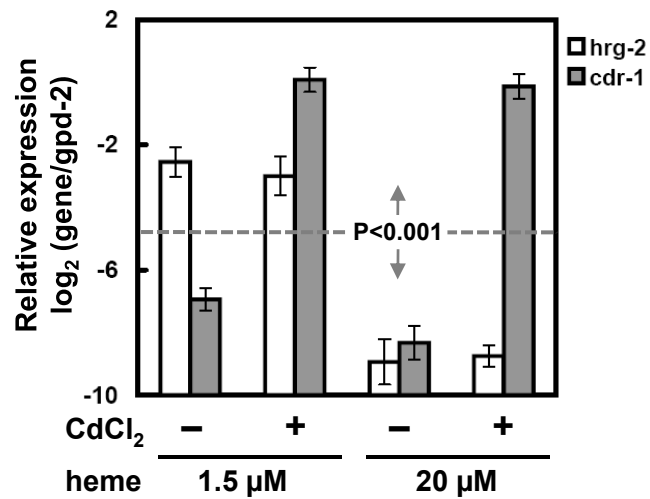
B



C



D



includes the putative TATA box, the transcription start site and first two exons (Figure 3.5A). The mutant worm was outcrossed with the N2 Bristol strain eight times to remove possible mutations in other genomic locus. During the final outcross, both homozygous mutants and their wild type brood mates were saved. At low concentrations of heme, *hrg-2* (*tm3798*) worms tended to grow slower than both wild-type N2 worms and the wild-type brood mate controls (Figure 3.5B). Only marginal difference was observed when these worms were maintained at 20 μ M heme. Furthermore, deletion of the homologous gene *cdr-4* did not lead to any developmental delay under the same conditions.

***hrg-2* is expressed in hypodermal cells**

The cell-specific expression of *hrg-2* was investigated in *C. elegans* using *gfp* reporters. We generated transcriptional fusion constructs that contain the 1.5-kb promoter region of *hrg-2*, a nuclear localization signal (NLS), GFP and either the *unc-54* 3' UTR or the *hrg-2* 3' UTR (Figure 3.6A). These *hrg-2::gfp* constructs predominantly expressed in the worm hypodermis (Figure 3.6B). The hypodermal cells in the head body, and tail all had GFP expression when the transgenic worms were maintained at low heme conditions. In contrast, when the worms were grown at 20 μ M or higher concentrations of heme, these transcriptional reporters were inactive (Figure 3.6C). No difference in expression pattern or heme response was observed between the two tested UTRs.

As is shown in Figure 3.6A, the putative 1.5-kb promoter contains a *cdr-7* gene and a 0.5-kb intergenic region. To exclude the possibility that the transgene expression was driven by introns of the *cdr-7* gene, we fused only the intergenic sequence with *NLS-gfp*. The expression pattern is similar to those observed using the 1.5-kb promoter (Figure

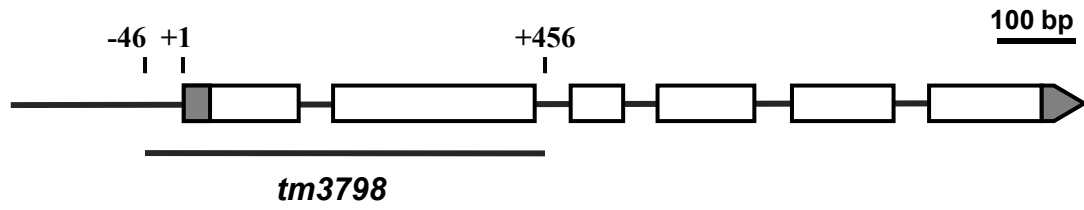
3.6D). These data suggest that the heme response was conferred by the 0.5-kb region upstream of *hrg-2*.

To understand the subcellular distribution of HRG-2 in *C. elegans*, we analyzed the *IQ8122* strain, which has the translational reporter *hrg-2::HRG-2-YFP*. Similar to the transcriptional reporter, this transgene is active only when the worms are grown at low heme. Confocal studies revealed that within hypodermal cells, HRG-2 is localized to the hemi-adherens junction structures fibrous organelles, endoplasmic reticulum (ER), and apical plasma membrane (Figure 3.6E). Fibrous organelles are composed of intermediate filament arrays that associate with cuticle, muscle, and neurons (192). The ER localization has been confirmed by analyzing another transgenic strain, *IQ8123*, which expresses both *hrg-2::HRG-2-YFP* and an ER marker in hypodermal cells *dpy-7::mCherry-TRAM* (Figure 3.6F). Additionally, HRG-2 localizes to the apical surface of the plasma membrane in the hypodermis.

Our previous study with HRG-1 and HRG-4 has permitted us to develop several reporter constructs and heme analog assays to interrogate intestinal heme homeostasis in *C. elegans* (68). To test whether heme exerts any effect on HRG-2, we ectopically expressed *hrg-2* in the intestine by using the intestine-specific promoter of *vha-6*. In the intestine, the majority of HRG-2 resided in the apical plasma membrane, whereas a small portion localized to cytoplasmic membrane structures (Figure 3.7A). These structures could be ER, considering the localization patterns of HRG-2 in hypodermal tissues. These transgenic worms were exposed to 0 and 20 μ M heme for either 3 h or 2 d, but the presence or absence of heme did not evoke any apparent changes in the subcellular localization patterns of HRG-2 (Figure 3.7B).

Figure 3.5. Analysis of a *hrg-2* deletion worm. **(A)** Location of *tm3798* deletion in *hrg-2* gene. In the *tm3798* allele, part of the promoter region and the first two exons of *hrg-2* gene are deleted. Exons are depicted as empty boxes and untranslated regions are shown as gray boxes. “+1” is the confirmed transcription start site. **(B)** Growth rate of *hrg-2* deletion worm. The worms were first grown at 2 μ M heme for one generation in mCeHR-2 medium. Synchronized L1 larvae were inoculated into the liquid medium containing 0, 4, and 20 μ M heme. After 9 d of growth, worms in all treatments were counted, and the numbers were normalized to the actual input (0 μ M). The experiment was done in duplicate. Brood mate is the wild-type worm saved from the final outcross of the mutant. No statistical difference was observed ($P > 0.05$).

A



B

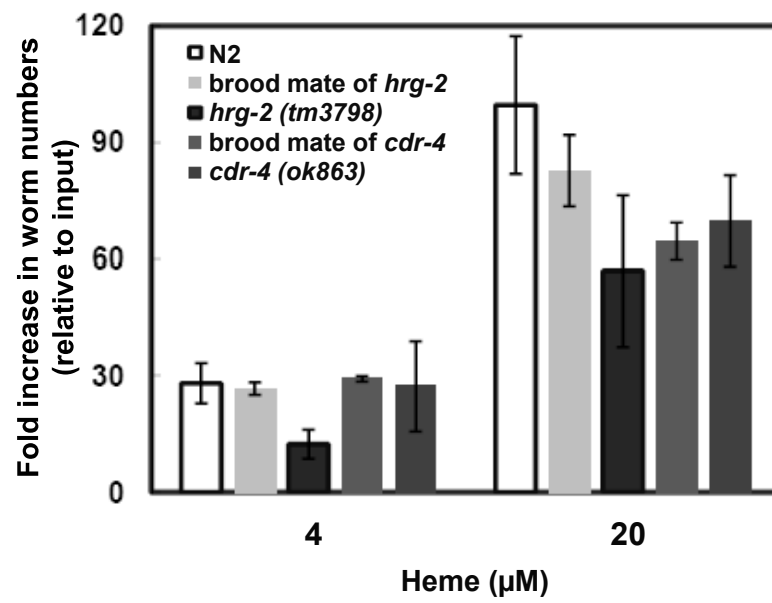
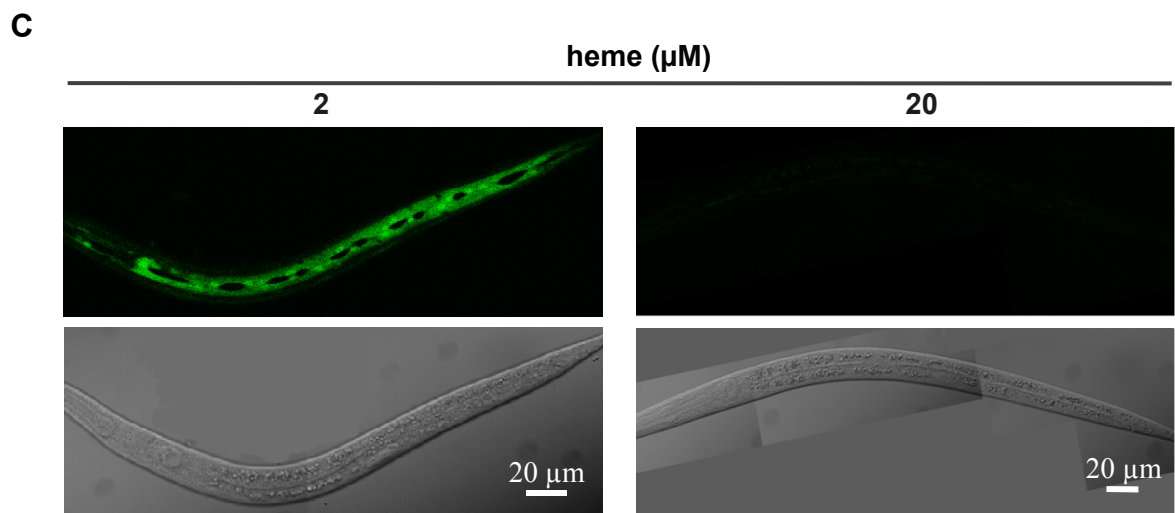
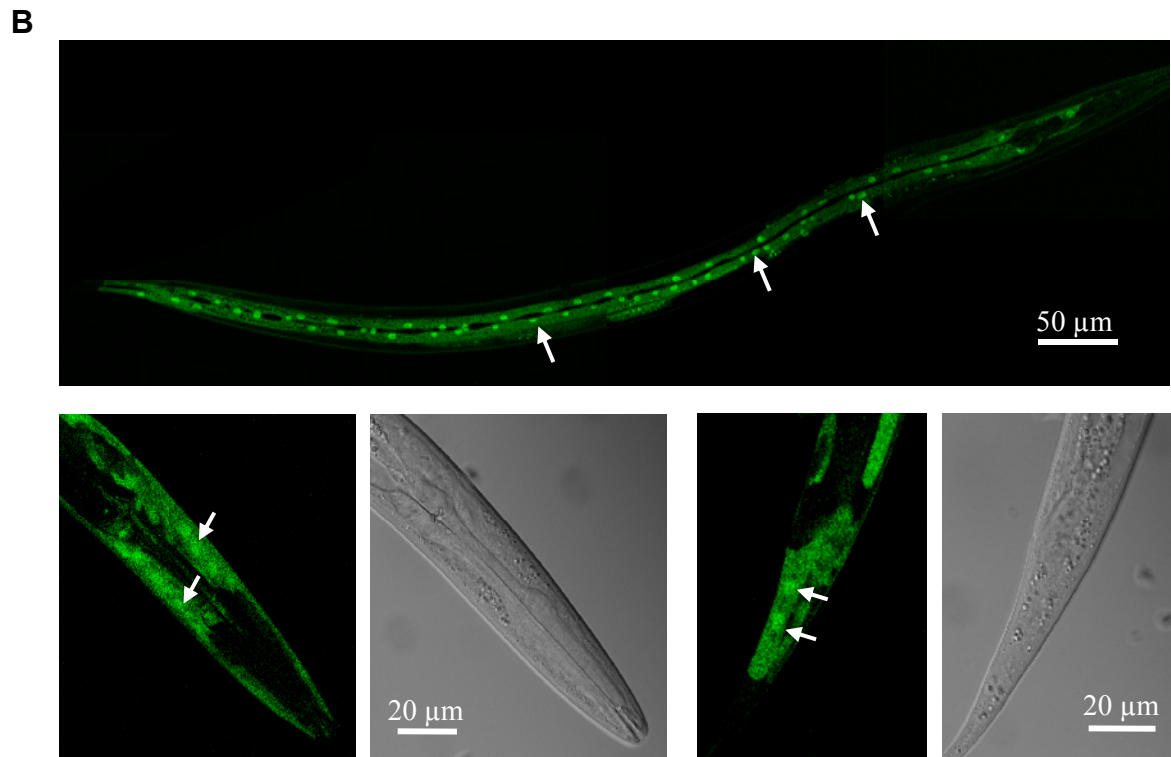
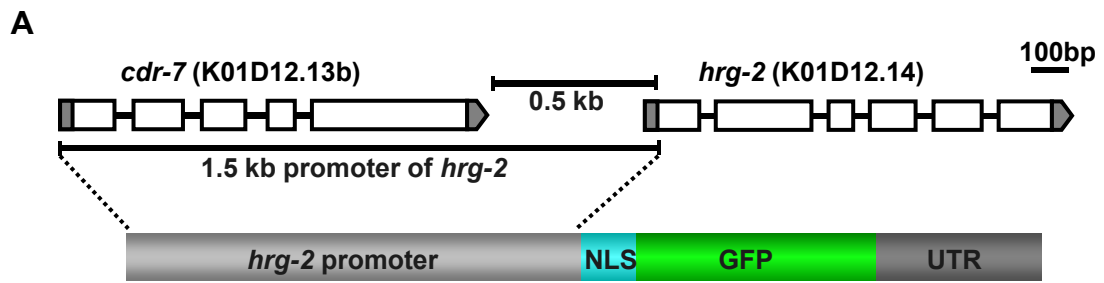
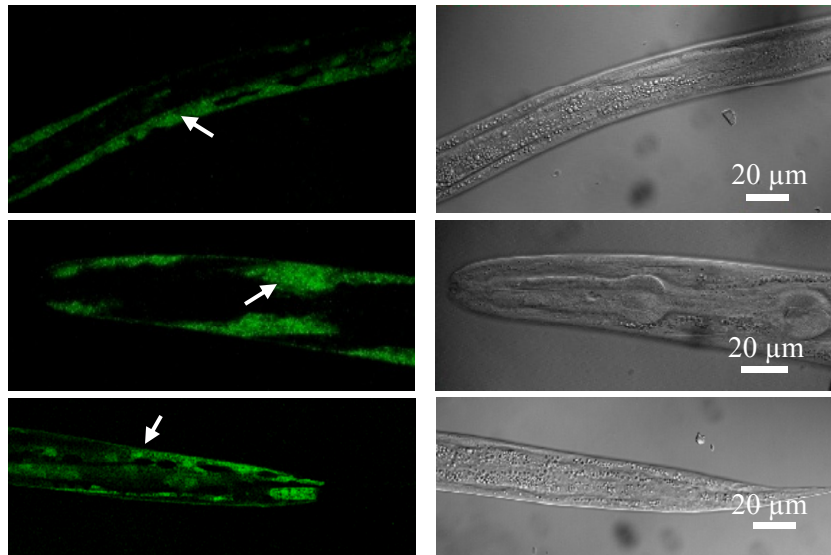


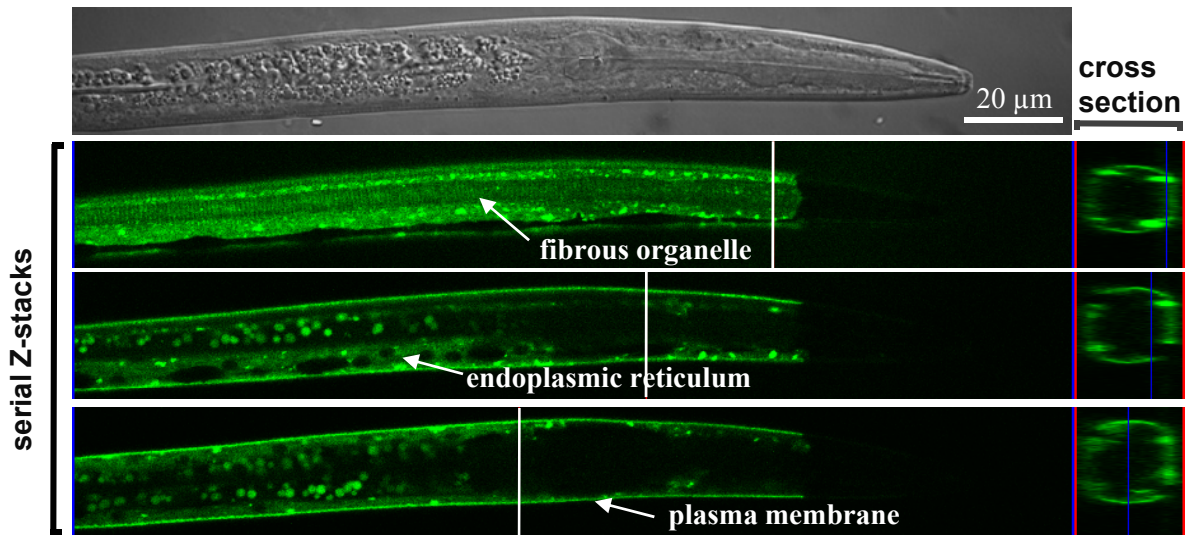
Figure 3.6. Expression and localization patterns of HRG-2 in *C. elegans*. (A) Schematic representation of the *hrg-2::gfp* reporter constructs. Genomic structures of *hrg-2* and *cdr-7* are shown on the top. NLS: nuclear localization signal. (B) *hrg-2::gfp* is predominantly expressed in hypodermal cells in *C. elegans*. This *IQ8021* worm strain contains the construct that has the 1.5-kb promoter region of *hrg-2* fused with NLS-*gfp*. Arrow: hypodermal cells. (C) Responses of *hrg-2::gfp* reporter to heme levels. GFP can be detected only when the transgenic worms are maintained at low concentrations of heme, while 20 μ M heme fully turns off the gene expression within 48 h. (D) Expression pattern of GFP in *IQ8023* strain. The construct in this strain is identical to that in *IQ8021* worms except that it contains the 0.5-kb promoter region of *hrg-2*. Arrow: hypodermal cells. (E) Subcellular localization of HRG-2 in hypodermal cells. Three representative fluorescence images from a confocal z-stack are displayed. HRG-2-YFP presents in fibrous organelles, apical plasma membrane and ER. White vertical lines indicate the positions for cross-section images, which are shown to the right. (F) Co-localization of HRG-2 with the ER marker mCherry-TRAM. The translational reporter *hrg-2::HRG-2-YFP* and the hypodermal ER marker construct *dpy-7::mCherry-TRAM* were introduced into worms together by bombardment. Localization patterns of YFP and mCherry were analyzed after incubating the worms at 2 μ M heme for 4 d. mCherry-TRAM is not present in fibrous organelles or plasma membrane. TRAM: translocating-chain associated membrane protein. (G) Schematic representation of the hypodermal cell (hyp7) in a cross-section of worm body. The schematic was modified from Labouesse (193).



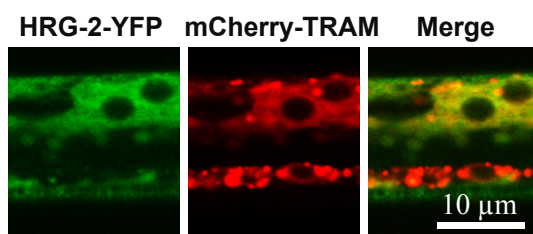
D



E



F



G

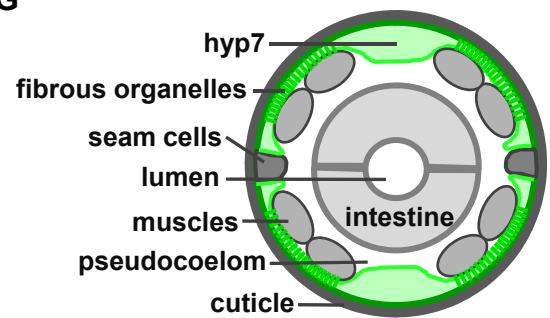
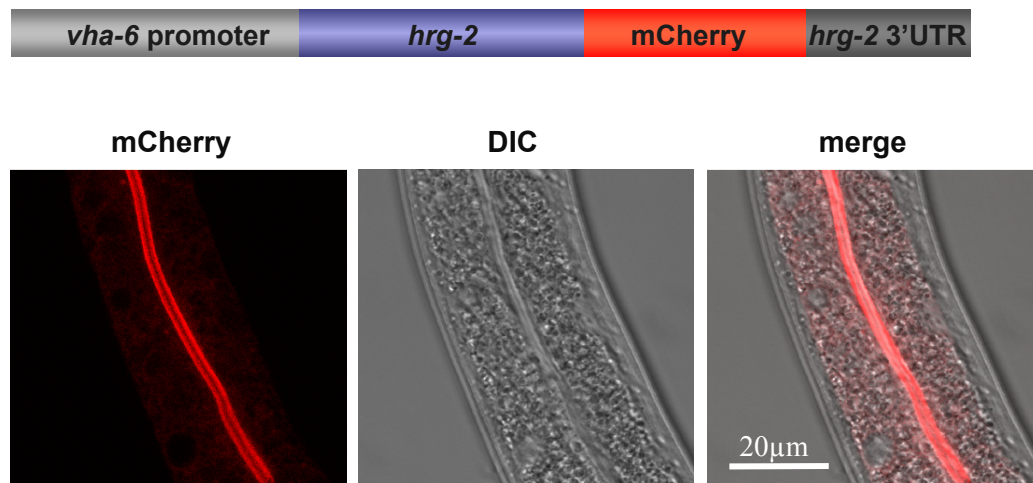
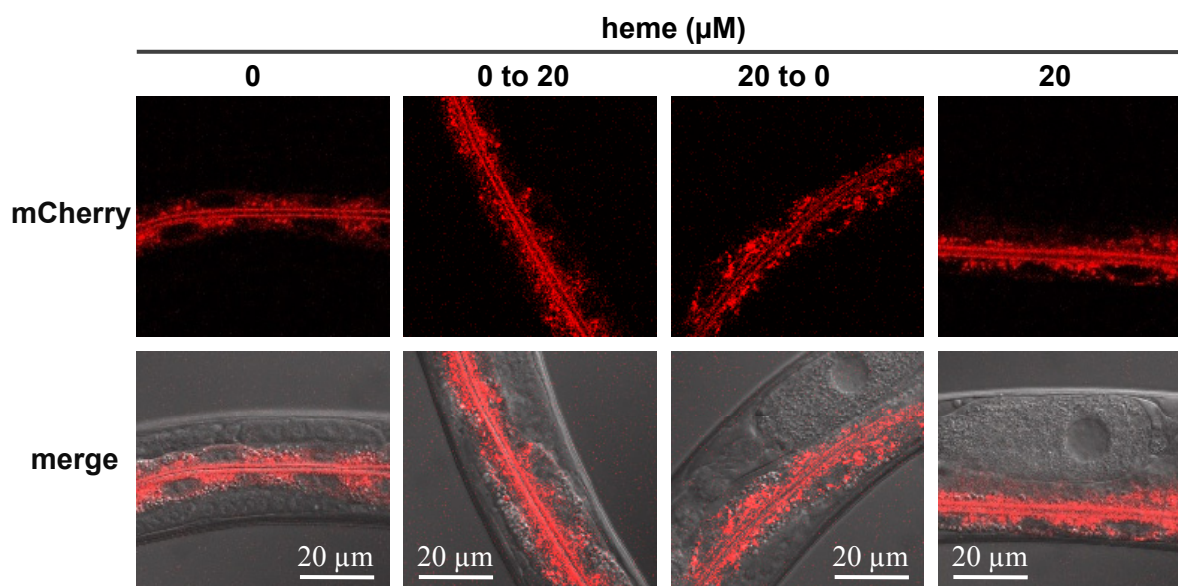


Figure 3.7. Ectopic expression of *hrg-2* in the intestine. (A) *hrg-2-mCherry* was placed after *vha-6* promoter. This construct was introduced into worms by bombardment. Examination using confocal microscope revealed that the majority of HRG-2-mCherry presents on the apical plasma membrane, while some localizes to cytoplasmic structures, possibly ER. (B) Transgenic worms with *vha-6::HRG-2-mCherry* construct were subjected to the following treatments in mCeHR-2 medium: 1) 0 μ M heme for 48 h; 2) 0 μ M heme for 45 h and then 20 μ M heme for 3 h; 3) 20 μ M heme for 45 h and then 0 μ M heme for 3 h; or 4) 20 μ M heme for 48 h. Subcellular localizations of mCherry were analyzed by confocal microscopy.

A



B



HRG-2 is a type Ib membrane protein

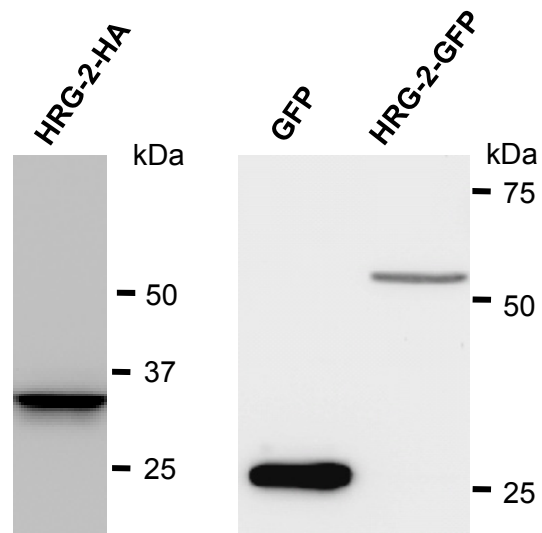
To explore the subcellular localization in more detail, we expressed HRG-2 with HA epitope or GFP variants at the C-terminus in HEK293 cells. SDS-PAGE and immunoblotting analyses revealed that the tagged proteins were readily expressed in mammalian cells and they migrated as monomers with the predicted sizes (Figure 3.8A). Confocal microscopy showed that HRG-2 co-localized with the ER marker CD3 δ -GFP, whereas no plasma membrane localization was observed (Figure 3.8B). The absence of HRG-2 at the plasma membrane of HEK293 cells could plausibly be due to the fact that HEK293 cells are nonpolarized, unlike the polarized hypodermal cells in *C. elegans*.

As a first step toward understanding the signal for ER localization of HRG-2, a series of truncated constructs were generated and analyzed in HEK293 cells (Figure 3.8B). When the GST-C domain was removed, the resultant N-terminal protein (HRG-2 Δ 2) still localized to ER. However, deletion of the N-terminal transmembrane portion of HRG-2 resulted in an unstable protein that was undetectable by immunofluorescence (Figure 3.8B) and western blotting (not shown). Further results indicated that the first 27 amino acids were able to target YFP to ER (Figure 3.8B). These results revealed that the N-terminal portion of HRG-2 is sufficient and necessary for ER targeting.

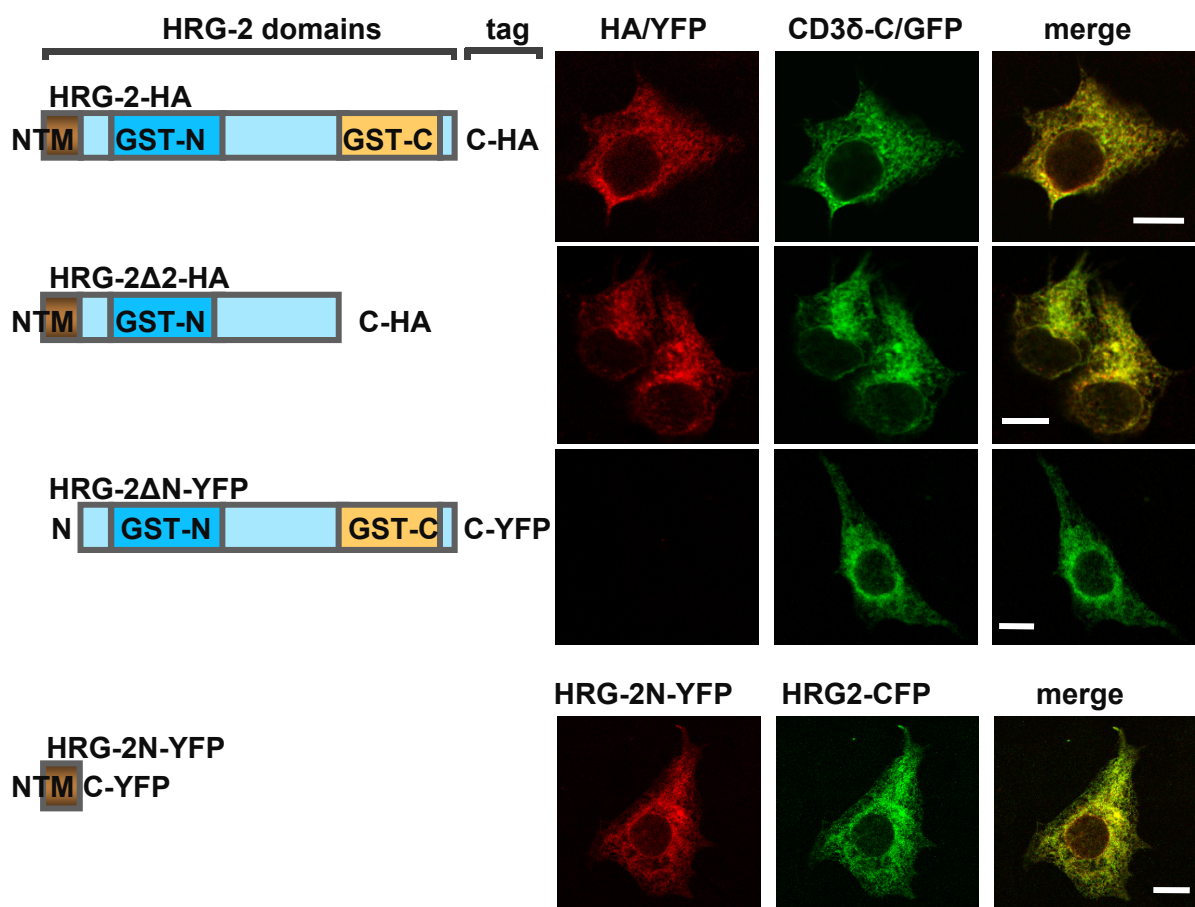
As described earlier, *in silico* hydropathy analysis predicted that HRG-2 has an N-terminal transmembrane domain. To confirm this prediction and to determine the topology of HRG-2, FPP assays were performed on HRG-2 tagged with GFP at the C-terminus. In this assay, the plasma membrane was first permeabilized with digitonin, which forms complexes with hydroxysterols in cholesterol-rich membranes (169). Then the cells were treated with protease to digest any peptide that is exposed to the cytoplasm.

Figure 3.8. Expression of HRG-2 in mammalian cells. (A) Western blot of HRG-2 transiently expressed in HEK 293 cells. The lysates of transfected cells were subjected to SDS-PAGE and western blotting using anti-HA or anti-GFP antibodies. (B) Immunofluorescence analysis of HRG-2 constructs in HEK293 cells. HA-tagged HRG-2 was detected using anti-HA and fluorophore-conjugated anti-rabbit IgG antibodies in the fixed cells. Images were acquired using a confocal microscope. HRG-2 co-localizes with the ER markers CD3 δ -CFP or CD3 δ -YFP. In the HRG-2 Δ 2 construct, the GST-C like domain was removed. (scale bar = 10 μ m)

A



B



When the FPP assay was performed on the control construct pCFP-CD3 δ -YFP that contains both ER luminal CFP and cytoplasmic YFP, CFP was resistant to the protease, whereas YFP was degraded (Figure 3.9A). After digitonin and protease treatment, the fluorescent tag in HRG-2-GFP was degraded, indicating that the C-terminus of HRG-2 is cytoplasmic (Figure 3.9B). The same pattern was observed in HRG-2N-YFP construct, which has only the N-terminal 27 amino acids of HRG-2 fused with YFP.

When produced using an *in vitro* transcription and translation system, HRG-2-HA exhibited identical molecular size to the same construct expressed in mammalian cells (Figure 3.9C). Accordingly, HRG-2 protein does not undergo such modifications as signal peptide cleavage or N-linked glycosylation during or after translation. We concluded that HRG-2 contains a single transmembrane domain with a cytoplasmic C-terminus facing the cytoplasm. Since the N-terminal transmembrane domain is not processed, it belongs to the class of type Ib membrane proteins.

HRG-2 binds heme

Heme has been shown to interact with amino acid residues such as histidines, tyrosines, cysteines, aspartates and glutamates in heme-containing proteins. HRG-2 has 7 histidines and 8 tyrosines, as well as many cysteines, aspartates and glutamates, that are conserved among *Caenorhabditis* species (Figure 3.3C). To test whether HRG-2 can bind heme, hemin-agarose pull-down assays were performed using the cell lysates from HEK293 cells transiently transfected with HRG-2 constructs. The eight TM protein human zinc transporter hZIP-4 was used as negative control for nonspecific hydrophobic interactions, and the newly identified heme transporter HRG-4 was used as the positive control (68,194). At both pH 6.4 and pH 7.4, HRG-2 showed higher affinities to hemin

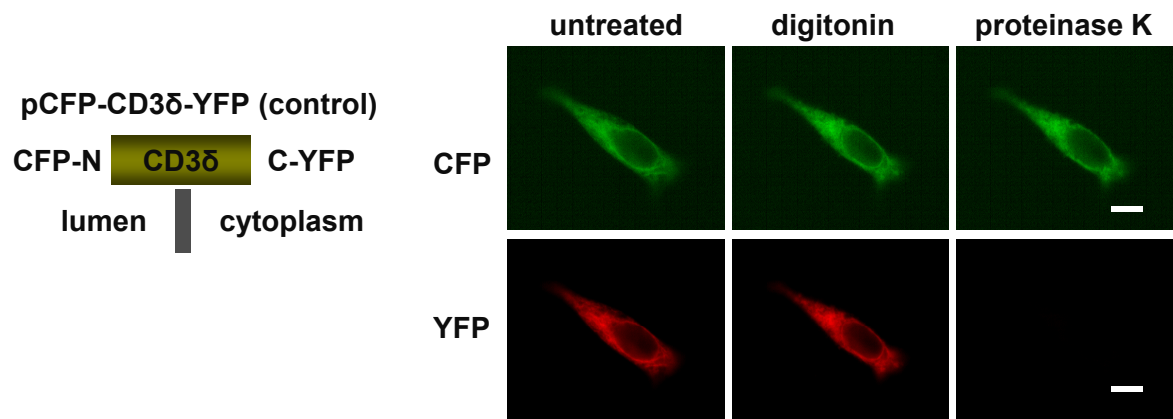
agarose than hZip-4 (Figure 3.10A). In comparison to pH 6.4, pH 7.4 tends to increase the association of HRG-2 to hemin agarose. This result is in agreement with the subcellular localization pattern of HRG-2, as we would expect an optimum pH for the function of HRG-2 around the cytoplasmic pH or pH 7.3~7.4 (195).

Ligands and proteins can have either stable covalent conjugations or more transient non-covalent interactions. The binding of ligands to transporters and chaperones is commonly transient and dynamic. To explore the possible binding kinetics of HRG-2 for heme, the effects of cellular heme status on the heme-binding activity were studied by growing the transfected cells in heme-depleted medium with 0.5 mM succinylacetone, the inhibitor of heme synthesis pathway, or with 10 μ M added heme. Heme-depletion was confirmed using a heme-sensor construct containing horseradish peroxidase attached to the signal sequence of human growth hormone (ssHRP). Heme binding was observed for HRG-2 in both heme depletion and heme repletion at comparable levels (Figure 3.10A). This indicated that the heme binding by HRG-2 is not affected by the heme status in the cell.

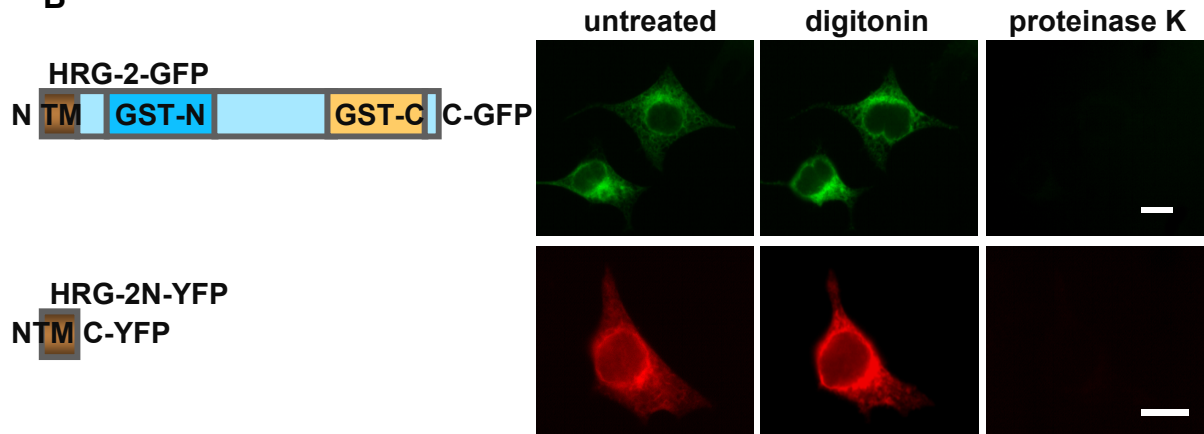
We next performed heme binding experiments on the truncation constructs of HRG-2 and its homologous protein CDR-1. HRG-2 proteins were still able to bind heme when the GST-C domain was removed, although the truncated proteins tended to have decreased binding (Figure 3.10B). Interestingly, the homologous protein CDR-1 also exhibited moderate heme binding activity although its gene is not regulated by heme.

Figure 3.9. Topology mapping of HRG-2 in mammalian cells. (A) Fluorescence protease protection assays on the cells expressing pCFP-CD3 δ -YFP. In this assay, the transfected cells were treated with 30 μ M digitonin for 2 min followed by 50 μ g/ml proteinase K for 2 min. Images were acquired throughout the process by epifluorescence microscopy. (B) FPP assays on HRG-2 constructs. (C) Western blot of HRG-2 proteins produced by *in vitro* transcription and translation system (IVT) or by expression in HEK293 cells. There is no difference in the sizes of HRG-2 proteins (arrow). (scale bar = 10 μ m)

A



B



C

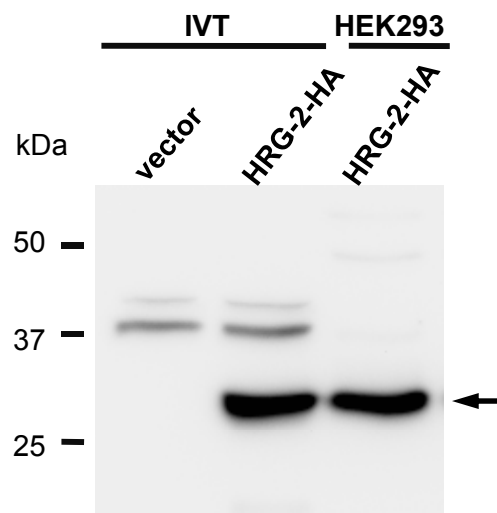
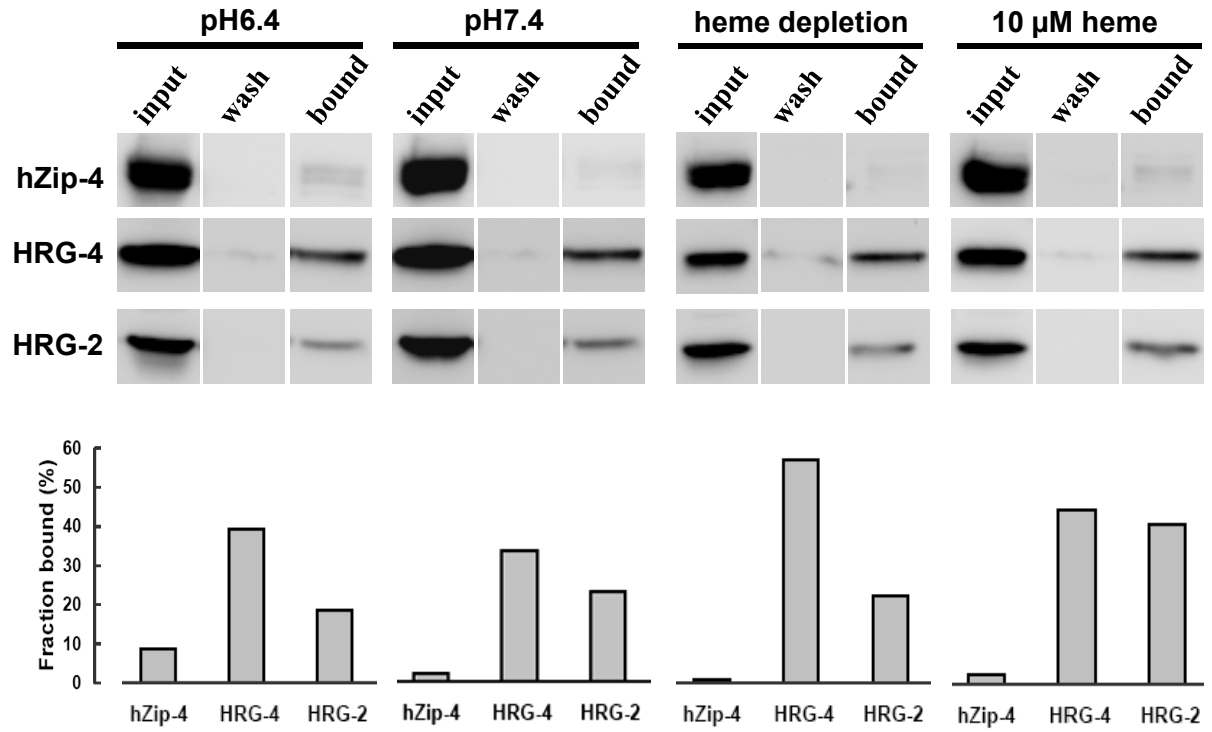
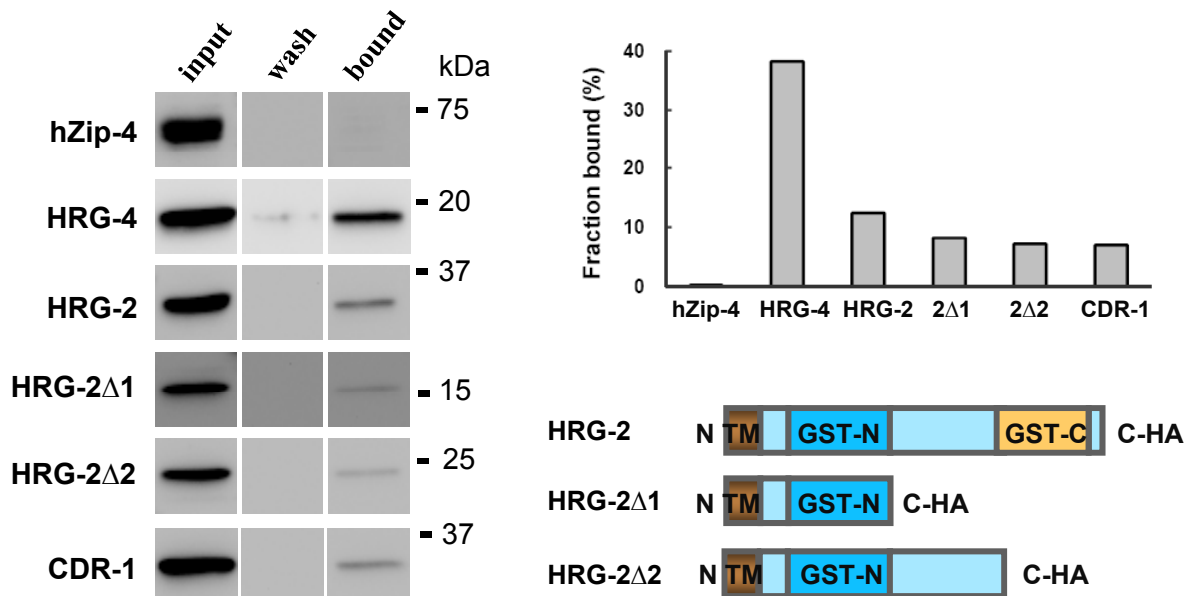


Figure 3.10. HRG-2 proteins bind heme. (A) Hemin agarose pull-down assays on full-length HRG-2. Heme binding assays were performed by incubating the lysates of HEK293 cells expressing HRG-2-HA or control plasmids with hemin agarose. Equivalent amounts of input lysates (input), the final washes before elution (wash), and the eluates (bound) were subjected to SDS-PAGE and western blotting using anti-HA antibodies. Each hemin-binding assay was done in duplicate and one representative binding result is shown. Human zinc transporter hZip-4 and *C. elegans* heme transporter HRG-4 were used as negative and positive controls, respectively. The panel below the western blots shows the quantification results of the signals as bound fraction relative to the input for each protein. **(B)** Heme binding assays on HRG-2 deletion constructs and CDR-1. This assay was performed at pH 7.4. Images on the left are the western blot results. Quantitation is shown in the right top panel and the architectures of the deletion constructs are in the right bottom. HRG-2 Δ 1 and HRG-2 Δ 2 are two HRG-2 truncation constructs in which the GST-C like domain was deleted. No statistical difference was observed among the binding conditions or among HRG-2 constructs ($P > 0.05$). All data were represented as mean \pm S.E.

A



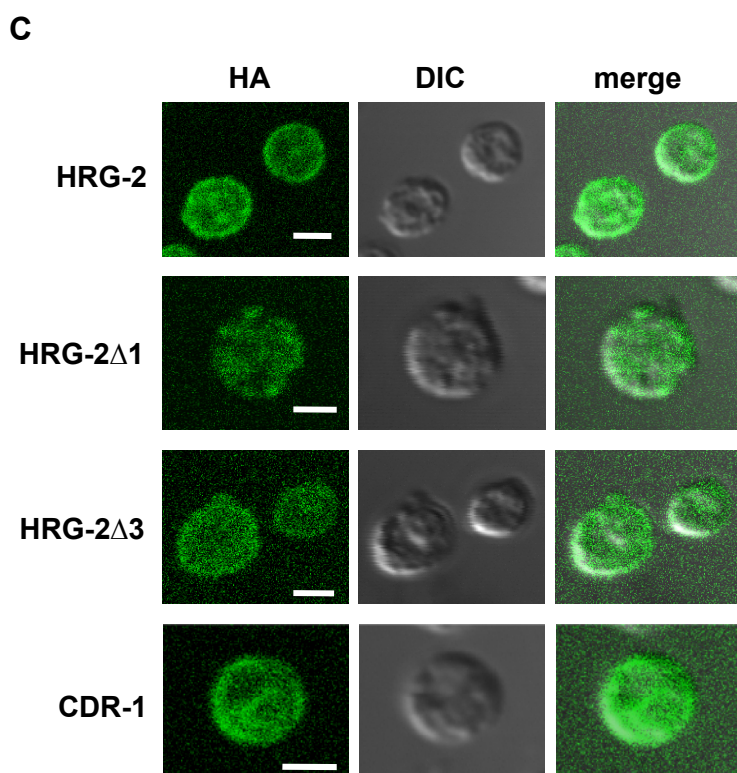
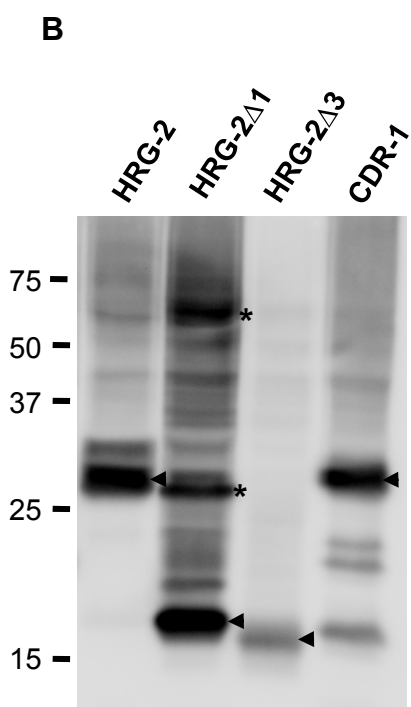
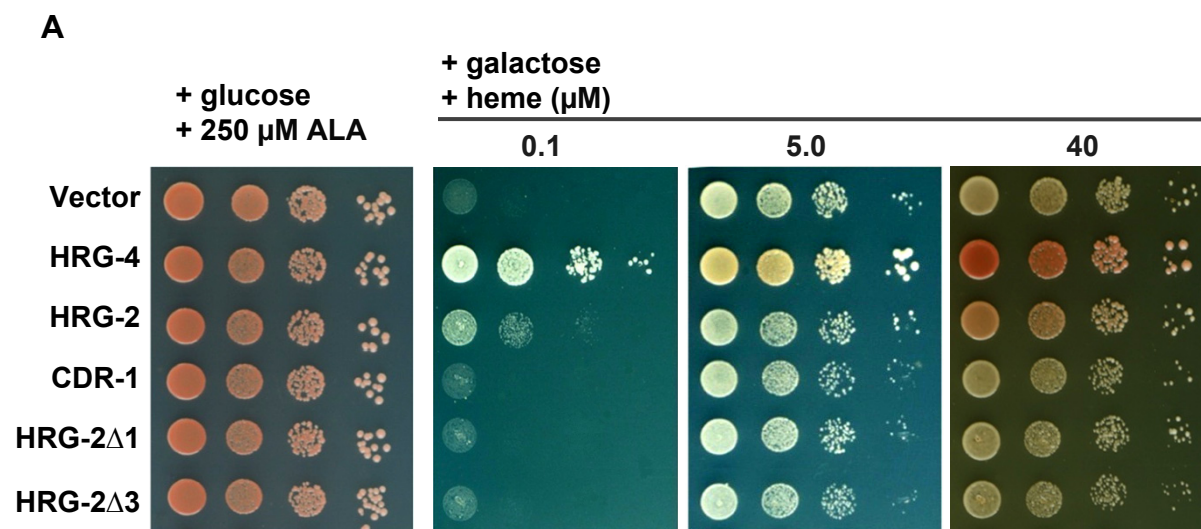
B



HRG-2 rescues the growth of a heme-deficient yeast strain

A heme-deficient *S. cerevisiae* strain, DY1457 *hem1Δ(6D)*, was utilized to further probe the molecular function of HRG-2 (172). This *hem1Δ* yeast strain lacks the rate-limiting enzyme in the heme biosynthetic pathway and therefore requires external heme for growth (172). In comparison to the vector control, the expression of HRG-2 significantly increased the growth of *hem1Δ* yeast at low concentrations of heme (Figure 3.11A). This result was highly reproducible and was consistent among untagged, HA-tagged, and HIS-tagged HRG-2. The maximum rescuing activity by HRG-2 was observed at 0.1 μ M heme. As heme concentration increased, the difference between yeast transformed with *hrg-2* and the vector control diminished. At 5.0 μ M heme, no noticeable effect of HRG-2 expression was observed. However, when grown at 40 μ M heme, yeast transformed with *hrg-2* displayed darker pink color than the negative control. This *hem1Δ* strain inherited the mutation in *ADE2* from the parent strain W303 (172,196). Mutations in the *ADE2* locus lead to the accumulation of P-ribosylaminoimidazole, an intermediate product in adenine biosynthesis pathway, which is converted into a red pigment in the presence of oxidative phosphorylation or mitochondrial respiration (197,198). Yeast transformed with *hrg-2* and grown at higher heme concentration (40 μ M) revealed more pigment accumulation than the control, indicating that the cells were able to utilize exogenous heme for mitochondria respiration. As a positive control, the heme importer HRG-4 dramatically increased the growth of *hem1Δ* at all tested concentrations of heme and showed greater accumulation of red pigment than HRG-2. In contrast, the rescue effects by HRG-2 were mostly seen at low heme.

Figure 3.11. Characterization of HRG-2 in heme deficient *S. cerevisiae*. (A) HRG-2 rescues the growth of *hem1Δ* yeast at low heme. The DY1457 *hem1Δ(6D)* yeast strain transformed with indicated constructs was spotted in 10-fold serial dilutions on synthetic complete medium plates lacking uracil. The empty vector pYES-DEST52 and the heme transporter HRG-4 were used as controls. The plate with glucose and 250 μ M δ -aminolevulinic acid was used as positive control for yeast growth. Plates with different concentrations of heme supplemented with 2% galactose to induce expression of transformed genes. Yeast grown on the positive control plate and the plate with 40 μ M heme displayed red pigment accumulation due to mutation in the *ADE2* locus. HRG-2 Δ 1 and HRG-2 Δ 3 are two HRG-2 truncation constructs in which the GST-C like domain and the GST-N like domain were deleted, respectively. (B) Western blot of HRG-2 proteins and CDR-1 expressed in the yeast. Arrowhead indicates the band of predicted molecular weight for each protein. Two asterisks show putative dimers and tetramers for HRG-2 Δ 1. The lower bands on the last lane are degradation products of CDR-1 in yeast cells. (C) Immunofluorescence assays of HRG-2 proteins and CDR-1 in yeast. The transformed yeast was fixed and spheroplasted. Anti-HA and fluorophore-conjugated anti-rabbit IgG antibodies were applied to detect the proteins. Images were acquired with different settings of laser power and detection gain on confocal microscope. (scale bar = 2 μ m)



Interestingly, when the GST-C like domain (HRG-2 Δ 1) or the GST-N like domain (HRG-2 Δ 3) was deleted, the truncated HRG-2 did not have any detectable effects on the growth of *hem1 Δ* yeast (Figure 3.11A). Furthermore, the expression of CDR-1 in *hem1 Δ* strain did not increase the yeast growth at any heme concentrations, although CDR-1 is highly homologous to HRG-2.

Western blot and immunofluorescence assays were performed using yeast transformed with HA-tagged constructs. All constructs except for HRG-2 Δ 3 were robustly expressed in the yeast (Figure 3.11B). In HRG-2 Δ 1 samples, we also detected bands with higher molecular sizes, which could be dimers or tetramers. Immunofluorescence results showed that the majority of HRG-2 was detected at the periphery of yeast, while only a small portion resided inside the cells (Figure 3.11C). This indicated that, when ectopically expressed in yeast, HRG-2 predominantly localized to the plasma membrane. HRG-2 Δ 3 and CDR-1 exhibited similar localization patterns to HRG-2, whereas HRG-2 Δ 1 presented as puncta. Taken together, these results suggest that expression of HRG-2 in the yeast may help facilitate the uptake or sequestration of heme.

Discussion

hrg-2* is induced by heme deficiency in *C. elegans

The nematode *C. elegans* lacks the heme biosynthetic pathway, but it requires heme for various biological functions and growth (160). Therefore, worms must have a robust system to acquire heme from food and the environment. The efficiency of heme uptake in *C. elegans* is significantly increased in response to low heme (68). Here we have identified *hrg-2* as a nematode-specific gene that is highly inducible by heme deficiency,

suggesting it might play a role in the uptake or sequestration of heme. It has been shown indirectly that *C. elegans* possesses a heme degradation system, and heme can be used for iron nutrition (160). However, the repression of *hrg-2* expression is not due to PPIX or iron, the structural components of heme.

HRG-2 is conserved in the *Rhabditidae* family

HRG-2 is 45.5% identical to CDR-1 at the amino acid level. In *C. elegans*, these two proteins are also homologous to five other proteins (191). These seven homologous genes may respond to distinct environmental cues and function in developmental-stage or tissue-specific manners. For example, cadmium induces *cdr-1* expression whereas heme represses *hrg-2* gene activity. *cdr-1* and *cdr-4* are expressed in the intestine (199,200), while *hrg-2* is expressed in hypodermal tissues. Although CDRs have been proposed to play roles in cadmium detoxification, their relevant biological functions are still largely unknown (199).

Using reciprocal BLAST, we have identified putative *hrg-2* orthologs in *C. briggsae*, *C. remanei*, and *C. brenneri*, which belong to the *Rhabditidae* family. In addition, CDR homologs were also found in *P. pacificus*, one species in *Diplogasterida* family. These two families also contain parasitic nematodes such as the human thread worm *Strongyloides stercoralis* and the common insect parasite *Heterorhabditis bacteriophora*. It will be interesting to see whether these parasitic species have a *hrg-2* gene. The genome of *Brugia malayi*, a parasitic nematode in another order *Spirurida*, was annotated to contain *cdr-5*, or *hrg-2* (201). However, the BLAST search of this gene against *C. elegans* database did not retrieve *hrg-2* as the best hit. It still remains to be determined whether *hrg-2* is conserved in *B. malayi* and other helminths.

HRG-2 also displayed ~25% identity to failed axon connection (FAX) protein in *D. melanogaster*. FAX was identified as an enhancer of the tyrosine kinase *abl* in a forward genetic screen (202). Flies with mutations in both *fax* and *abl* displayed severe disruptions in axon connections. However, FAX proteins may not be HRG-2 orthologs for three reasons. First, a non-CDR protein, CE22631, was identified as the best hit when these insect or vertebrate FAX proteins were used to BLAST against the *C. elegans* database. Second, in contrast to HRG-2, none of the FAX proteins contain putative transmembrane domains. Third, when expressed in mammalian cells, putative human FAX protein is associated with mitochondria, which is distinct from the ER localization of *C. elegans* HRG-2 (Appendix V).

Potential functions of HRG-2 in heme transport

The *S. cerevisiae* strain *hem1Δ* lacks the first enzyme in the heme biosynthetic pathway and, therefore, its growth is solely dependent on the heme levels in the environment (172). This provides a quick way to assay for heme transport activities of protein molecules (203). We found that HRG-2 can rescue the growth of *hem1Δ* yeast at low concentrations of heme, indicating that the presence of HRG-2 enhances the availability of exogenously-supplied heme to this yeast. However, no rescuing effect was detected for CDR-1, which was due to either the difference in the protein topologies or different biological functions of HRG-2 and CDR-1. The presence of HRG-2 on the membrane of yeast cells suggested that the growth rescue may be due to increased heme uptake through HRG-2 at low heme. Deletion of *hrg-2* in *C. elegans* resulted in reduced growth rates at low concentrations of heme. This further demonstrated the involvement of

HRG-2 in heme homeostasis, possibly in heme acquisition into hypodermal cells (Figure 3.12).

Since the GST-N metaxin-like domain belongs to thioredoxin superfamily, it is possible that HRG-2 functions as a membrane-associated hemin reductase (Figure 3.12). Reductases have been shown to be essential for the uptake of metals. For example, duodenal cytochrome b (Dcytb) and six transmembrane epithelial antigen of the prostate 3 (Steap3) were identified as ferric reductases that were associated with efficient iron uptake into cells (204,205). Subsequent studies found that Dcytb and proteins in the Steap family also function as cupric reductases (206,207). Studies have indicated that hemin (heme with an oxidized iron molecule) has to be reduced for its covalent attachment to such hemoproteins as cytochrome c (208,209). In Gram-negative bacteria, cytochrome c synthetase CcmF was recently proposed to function as a quinol:heme oxidoreductase (209). In addition, the lipocalin α 1-microglobulin also has the ability to reduce hemin in cytochrome c and methemoglobin (210). However, plasma membrane-associated hemin reductases that might play a role in hemin uptake remain elusive. HRG-2 could be one of the candidates for these hemin reductases.

In addition, HRG-2 could play a role in intracellular heme trafficking by contributing to the redistribution of heme among cellular compartments (Figure 3.12). HRG-2 presents on the ER membrane as a type Ib protein, a topology identical to that of microsomal cytochrome P450s. HRG-2 could be involved in heme delivery to cytochrome P450s or even to the secretory pathway. It has been shown recently that the heme-binding protein Dap1p in yeast and its human ortholog PGRMC1 can interact with cytochrome P450s and increase their activities (211,212). We have standardized a

protocol for ssHRP construct, in which the signal sequence from human growth hormone was fused with horseradish peroxidase (213). The activity of secreted ssHRP enzymes was solely controlled by the heme in the medium. The expression of HRG-2 in the ER of mammalian cells increased the activity of the ssHRP, suggesting an increased amount of heme was loaded into the secretory pathway.

Implications of GST-like domains in HRG-2 and CDRs

All HRG-2, CDR, FAX, CE22631, and CE02505 proteins contain GST-N metaxin-like and GST-C metaxin domains, suggesting that they may function in similar biological processes. Metaxin was originally identified as a gene essential for normal embryonic development in mice (214). Subsequent study showed that it resided on the outer mitochondria membrane and was involved in the import of proteins into mitochondria (215).

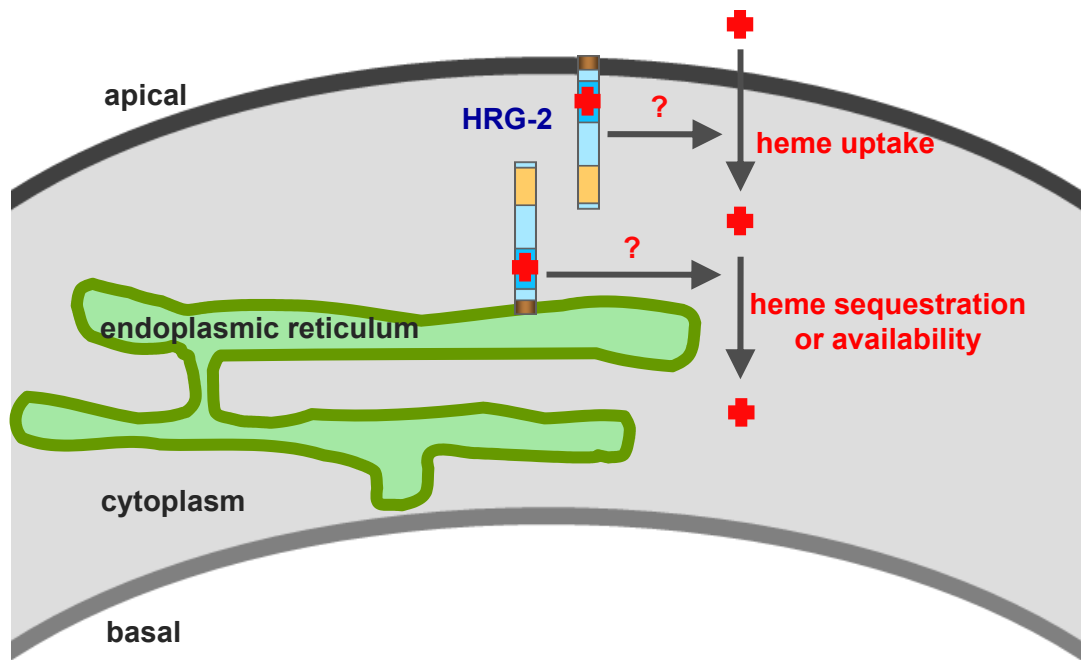
GSTs catalyze the conjugation of glutathione to various electrophilic substrates and play essential roles in xenobiotic detoxification. Besides their enzymatic functions, GSTs are also able to bind a variety of ligands such as steroids and porphyrins in the cytoplasm (78-80). A number of heme-binding GSTs have been identified in malarial parasites and nematodes, and they have been suggested to play a role in the detoxification and transport of heme (82,86,216). HRG-2 also has heme-binding activity. Since it is induced by heme deficiency rather than heme overload, HRG-2 may play a role in transport but not heme detoxification.

Proteins with GST-like structures can adopt diverse functions. The chloride intracellular channels (CLICs) are a newly-identified family in which all members contain GST-N CLIC and GST-C CLIC domains. As confirmed by crystal structures,

CLIC1, CLIC2, and CLIC4 all have thioredoxin folds and are structurally analogous to GSTs (217-219). Interestingly, these CLICs can either present as intracellular soluble proteins or as chloride channels on the membrane (217,220). *In vitro* studies indicated that CLICs significantly increased the chloride efflux from phospholipid vesicles (220-222). HRG-2 and CDRs all contain both GST-N metaxin-like and GST-C metaxin domains. The two domains and the GST-like domains in CLICs belong to the same thioredoxin-like and GST-C superfamilies. Furthermore, HRG-2 and most CDRs (except for CDR-7) are membrane proteins with at least one putative transmembrane domain, suggesting that they are more likely to be involved in transport or other membrane-associated activities.

In summary, we have identified *hrg-2* as a novel heme-responsive gene in *C. elegans*. Genetic, biochemical, and cell biological results suggest that HRG-2 may play a critical role in heme uptake or intracellular heme trafficking in *C. elegans*.

Figure 3.12. Proposed model of HRG-2 in heme homeostasis in *C. elegans*. HRG-2 localizes to the apical plasma membrane and ER in the hypodermal cells. On the plasma membrane, HRG-2 may function as a heme transporter or hemin reductase and play a role in heme uptake. On the ER membrane, HRG-2 may contribute to the sequestration or redistribution of intracellular heme.



Chapter 4: Identification and characterization of *hrg-3* in *C. elegans*

Summary

Heme regulates the expression of many genes that are involved in erythropoiesis, heme biosynthesis, oxidative stress, energy metabolism, and circadian rhythm control. The regulation can occur at the levels of transcription, translation, and protein stability. Here we identified a novel heme-responsive gene, *hrg-3*, that may play a critical role in heme homeostasis. Results from microarray, quantitative real-time PCR, and Northern blotting revealed that *hrg-3* is highly induced by heme deficiency in *C. elegans*. Analysis of the *hrg-3* promoter suggests that a 43-bp element is both necessary and sufficient for its intestinal expression and that the heme-dependent regulation is mediated by the stress-responsive transcription factor SKN-1. Following its synthesis in the intestine, HRG-3 is secreted into the body cavity pseudocoelom. Fluorescence protease protection assays and immunoblotting revealed that HRG-3 is specifically targeted to the Golgi via its amino terminal signal peptide which is then cleaved to generate a mature 45-amino acid protein. *hrg-3* mutant worms exhibit reduced growth rate independent of heme concentrations in axenic liquid culture. Additionally, deletion of *hrg-3* results in increased heme levels in the worm intestine. Furthermore, expression of epitope-tagged HRG-3 in *hem1Δ* yeast dramatically reduced cell viability at all tested heme concentrations. Based on our results we speculate that HRG-3 may function in intracellular heme transport or as a signaling molecule under heme deficiency.

Results

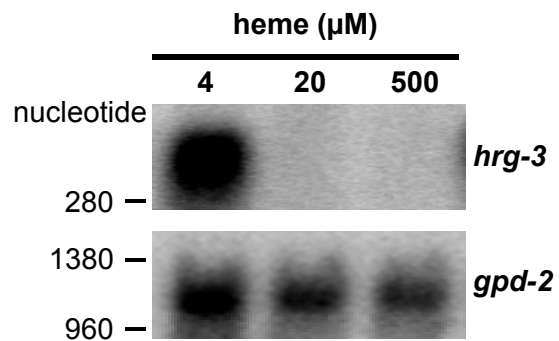
Heme deficiency induces *hrg-3* expression in *C. elegans*

Heme regulates the expression of many genes that are involved in erythropoiesis, heme biosynthesis, heme trafficking, oxidative stress, energy metabolism, and circadian rhythm control (4,68,118-120). To identify genes that are transcriptionally regulated by heme in *C. elegans*, total RNA extracted from worms that were grown at low (4 μ M), optimal (20 μ M), and high (500 μ M) heme in axenic liquid medium was hybridized to Affymetrix genome arrays (68). F58E6.7 was identified because it was greatly upregulated at low heme. In comparison to 20 μ M heme, low heme increased the F58E6.7 mRNA level by 71 fold. Results from Northern blotting further confirmed this expression pattern (Figure 4.1A). In contrast to the strong signal at 4 μ M heme, the *hrg-3* message was undetectable at 20 and 500 μ M heme. Therefore, we named this gene *heme-responsive gene-3* (*hrg-3*). qRT-PCR analysis on total RNA isolated from worms grown at different concentrations of heme revealed that compared to 20 μ M heme, 1.5 and 4 μ M increased the abundance of *hrg-3* mRNA by more than 900 fold and 400 fold, respectively (Figure 4.1B). At ≥ 10 μ M heme, the gene was not expressed. Thus, results from microarray, Northern blotting and qRT-PCR results consistently showed that heme deficiency induces *hrg-3* expression in *C. elegans*.

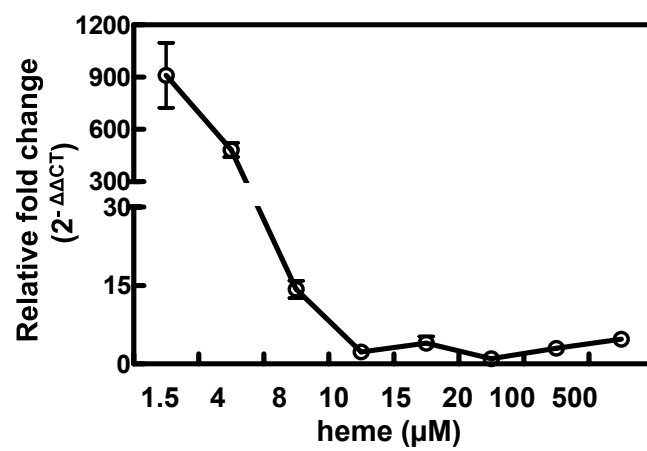
We analyzed the temporal expression pattern of *hrg-3* across all developmental stages by using qRT-PCR. In comparison to optimal heme level, 4 μ M heme increased *hrg-3* expression by at least 100 fold at all stages (Figure 4.1C). In addition, the highest expression level of *hrg-3* was detected in young adult worms, whereas the lowest level was detected in the larvae.

Figure 4.1. *hrg-3* is induced by heme deficiency in *C. elegans*. (A) Northern blot analysis of *hrg-3* expression in response to different heme concentrations. *gpd-2* was used as a loading control. The detected *hrg-3* mRNA is ~370 nucleotides. (B) Quantitation of *hrg-3* mRNA by qRT-PCR. Relative fold changes were derived by normalizing the cycle threshold values to *gpd-2* and then to the control heme level of 20 μ M using $\Delta\Delta$ CT methods. The experiment was performed in triplicate, and the data are presented as mean \pm S.E. (C) Expression of *hrg-3* at different developmental stages. Synchronized L1 worms were grown at 4 μ M heme and were harvested every 12 h for RNA extraction. Fold change was calculated by normalizing the Δ CT values to the control RNA sample, which was isolated from L4 worms grown at 20 μ M heme. Asterisk indicates $P < 0.05$ when compared to the expression value at LL3 stage. EL3: early L3; LL3: late L3; EL4: early L4; LL4: late L4; AD: young adult; GR: gravid.

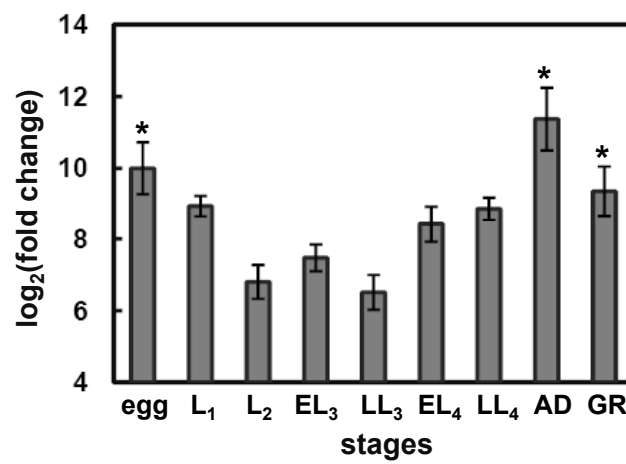
A



B



C



Sequence analysis of *hrg-3*

The sequence of full-length *hrg-3* cDNA was determined by the 5' and 3' RACE. The mature *hrg-3* mRNA is 375 nucleotides (Figure 4.2A), which is consistent with the observed size displayed on Northern blot (~370 nucleotides, Figure 4.1A). The *hrg-3* gene is comprised of a 7-nucleotide 5' UTR, three exons and a 155-nucleotide 3' UTR.

The *hrg-3* transcript encodes a 70-amino acid protein with predicted molecular mass of 8.1 kDa. The amino terminus of HRG-3 contains a stretch of hydrophobic amino acids, which could serve as either a transmembrane region or a signal peptide (Figure 4.2B). Based on the prediction using the program Jpred3 (186), HRG-3 has an α -helix in the N-terminal region and a β -sheet in the C-terminal region (Figure 4.2B). However, the majority of the protein was predicted to be random coils. Genomic sequences highly similar to *hrg-3* were identified in *C. briggsae*, *C. remanei*, *C. brenneri* and *C. japonica* using TBLASTN in NCBI (E values $<10^{-6}$). Putative HRG-3 orthologs in *C. briggsae* and *C. remanei* were predicted by using GeneMark.hmm program (183). These nematode HRG-3 proteins share >50% sequence identity at the amino acid level (Figure 4.2B).

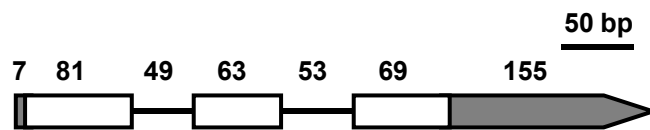
hrg-3 is expressed in the intestine

Transcriptional reporters were constructed using the 3.0-kb putative promoter region of *hrg-3* fused to a NLS, GFP, and either *unc-54* 3' UTR or *hrg-3* 3' UTR (Figure 4.3A). The constructs were introduced into worms by either microinjection (165) or bombardment (166). These *hrg-3::gfp* reporters were exclusively expressed in the intestine, as illustrated by the *IQ8031* transgenic worms (Figure 4.3B). The highest level of GFP was present in the mid anterior (int2 and int3) and middle intestinal cells (int4, 5, and 6). In contrast, the most anterior (int1) and the most posterior gut cells (int7-int9)

Figure 4.2. Genomic structure and conservation of *hrg-3* in *Caenorhabditis* species.

(A) Genomic structure of *hrg-3* revealed by RACE analysis. The full-length *hrg-3* mRNA is 375 nucleotides in length. Exons are depicted as empty boxes and untranslated regions are shown as gray boxes. The number indicates the size of each region. **(B)** Multiple sequence alignment of HRG-3 proteins among *C. elegans*, *C. briggsae* and *C. remanei*. Putative HRG-3 orthologs were predicted in the GeneMark.hmm program using homologous genomic sequences. Sequences were aligned by ClustalW and visualized with BoxShade. The secondary structure of HRG-3 was predicted using Jpred3. Arrowhead marks the putative signal peptidase cleavage site predicted by the Eukaryotic Linear Motif database. The gray underline depicts the transmembrane region predicted by the TMHMM program. The secondary structures are marked with the underlines. The numbers indicate the identity to CelHRG-3.

A



B

CelHRG-3 1 MVNFTTRSCSLLIILLFIIFLIS-NVELRPVMKSGYSKNHHLFRPKNL-QTDS--EEGFWN
 CbrHRG-3 1 MVNYSKHVLFSLILILVHLSIVESVPVIKSGYTKNHRLLFRPRQG-TSNSNETENGFWT
 CreHRG-3 1 MVTNMQHFVLFVTLILFLVI-PLAAPVMKSGYTKNHHMFRQRQSNLSSTKTETEDGFWS

α-helix

CelHRG-3	56	NVYFVITASDSFFGG	identity
CbrHRG-3	60	NVYFVITASDSFFGG	56.8%
CreHRG-3	60	NVYFVLTAIDDSFFGG	55.4%

β-sheet

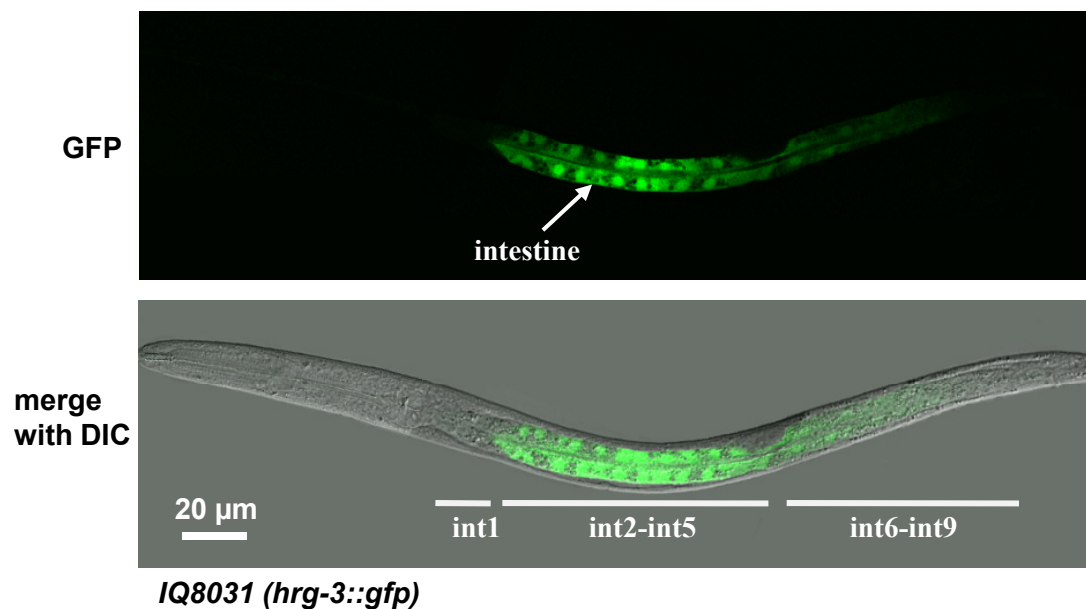
Figure 4.3. *hrg-3* is expressed in the intestine and specifically regulated by heme. (A)

Schematic representation of the *hrg-3::gfp* construct. NLS: nuclear localization signal. UTR: untranslated region. Both the *unc-54* 3'UTR and *hrg-3* 3'UTR were tested in the constructs. **(B)** Expression of the *hrg-3* transcriptional reporter in *C. elegans*. The *IQ8031* strain containing the transcriptional construct was maintained at 2 μ M heme. GFP expression was analyzed in 3~4 d. **(C)** Expression of *hrg-3* at low and normal concentrations of iron. The *IQ8031* transgenic worms were treated with 0.1 or 20 μ M ammonium ferric citrate in iron-depleted medium for 48 h. The GFP signal was examined as a direct reporter for the activity of the *hrg-3* promoter. This experiment was performed at both 1.5 and 20 μ M heme. All images were taken using same confocal settings. **(D)** Response of the *hrg-3* reporter to PPIX. The *IQ8031* worms were grown at 1.5 μ M heme with or without 20 μ M PPIX in mCeHR-2 medium. The expression levels were analyzed by confocal microscopy after 48 h and representative images of anterior and middle regions of the worms are shown. Same regions are shown for all the following figures of transcriptional reporters. (scale bar = 20 μ m)

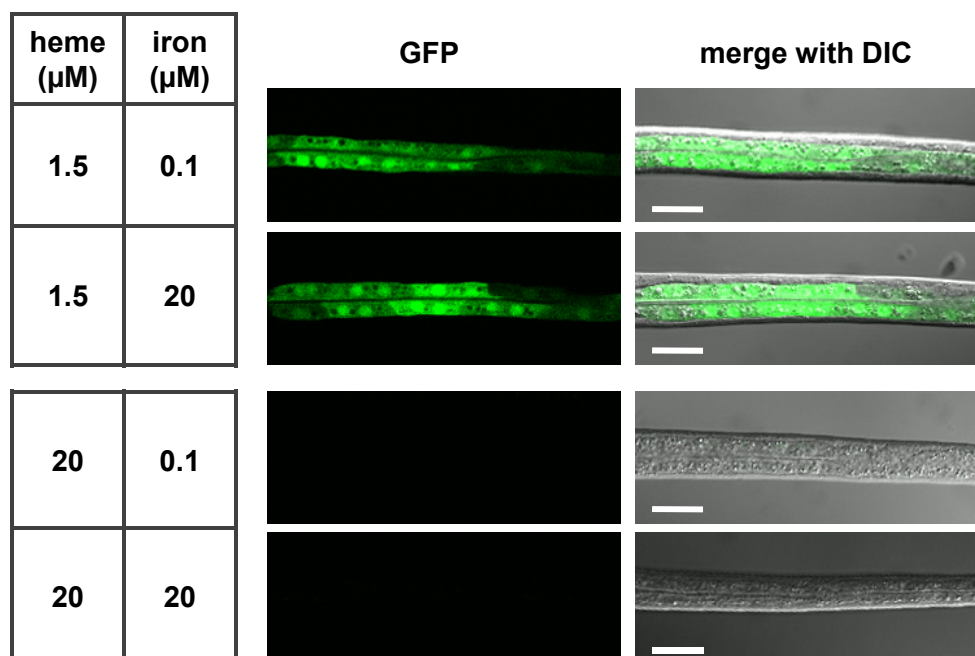
A



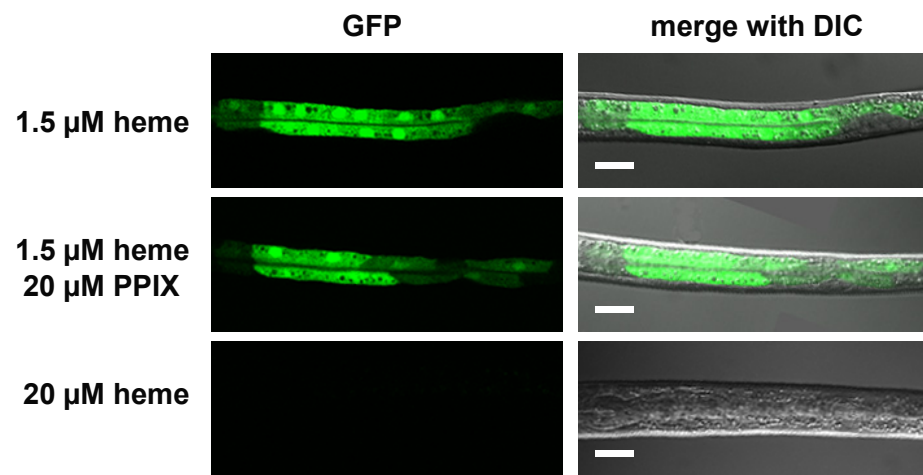
B



C



D



only weakly expressed this construct (Figure 4.3B). GFP signal could be observed only when the transgenic worms were maintained at ≤ 6 μM heme. When the worms were grown at 20 μM or higher concentrations of heme, no GFP expression was detected. No difference in expression pattern or heme response was observed between the two 3' UTRs tested. These results suggested that heme-dependent *hrg-3* expression is mediated by *cis*-acting elements within the 3-kb upstream flanking region.

Regulation of *hrg-3* is specific to heme

We examined the effects of PPIX and iron, two structural components of heme, on the activity of the *hrg-3* promoter. *IQ8031* worms were treated with either 0.1 or 20 μM ammonium ferric citrate in combination with 1.5 or 20 μM heme for 2 d in iron-depleted liquid medium. Results showed that the GFP intensity was solely dependent on heme concentrations (Figure 4.3C). Twenty micromolar iron did not inhibit the promoter activity at low heme, and even 0.1 μM iron could not turn on GFP expression in the presence of 20 μM heme. In addition, the transgenic worms grown at 1.5 μM heme and with 20 μM PPIX for 2 d retained robust GFP expression (Figure 4.3D). These data indicated that heme, rather than heme substrates, regulates *hrg-3* promoter activity.

Analysis of *hrg-3* promoter

We have shown that the 3.0-kb upstream flanking region is sufficient for heme response in *hrg-3* reporters. To narrow down the heme-responsive region, we constructed a series of *gfp* reporters that contained truncated sequences of the *hrg-3* promoter region. Removal of the region -2992 to -133 bp upstream of *hrg-3* did not affect the expression

pattern. The transgenic worm lines with *hrg-3Δ732³::gfp*, *hrg-3Δ295::gfp*, *hrg-3Δ194::gfp*, and *hrg-3Δ132::gfp* all had GFP expression in the mid anterior intestine at low heme (Figure 4.4), which is similar to the GFP pattern observed in worms transformed with constructs containing up to 3.0-kb upstream sequences. The expression of each of these constructs was repressed by high heme. The transgene *hrg3Δ112::gfp* also showed intestinal expression of GFP and an obvious response to heme levels, although there was a ~30% decrease in total GFP intensity at lower heme concentrations in comparison to the reporters with longer 5' sequences.

Among these reporter constructs, the 112-bp upstream sequence of *hrg-3* was the shortest functional promoter that directed intestine-specific expression and responses to heme. When an additional 20 bp was deleted, as in the line *hrg-3Δ92::gfp*, we found that <5% of worms had the GFP signal in one or two intestinal cells. The majority of the worms did not have any GFP expression even at 2 μM heme (Figure 4.4).

Heme regulation of the *hrg-3* promoter is conserved in *Caenorhabditis* species. In the *hrg-3* transcriptional reporter construct, we replaced the *C. elegans* upstream sequence with the 300-bp sequence upstream of *C. briggsae hrg-3*. The *IQ8631* worm line with this construct exhibited GFP expression in the intestine and the expression was inhibited at 20 μM heme (Figure 4.5A). This expression pattern is similar to that of the transcriptional constructs with the *hrg-3* promoter. Through alignment of *hrg-3* promoters among *C. elegans*, *C. briggsae* and *C. remanei*, we found that the 112-bp *C. elegans* minimal promoter is highly conserved (Figure 4.5B). Out of 81 nucleotides upstream of the putative TATA element, 48 are identical across these three species. However, the sequence between -69 and -49 bp is not conserved in *C. remanei*. When

³ The number indicates the removal of sequence upstream of this position.

Figure 4.4. Deletion analysis of the *hrg-3* promoter. Different lengths of *hrg-3* upstream sequence were used for the transcriptional reporter constructs. At least two transgenic worm lines for each transgene were analyzed for GFP expression at 2 and 20 μ M heme. The confirmed transcription start site is marked as “+1”.








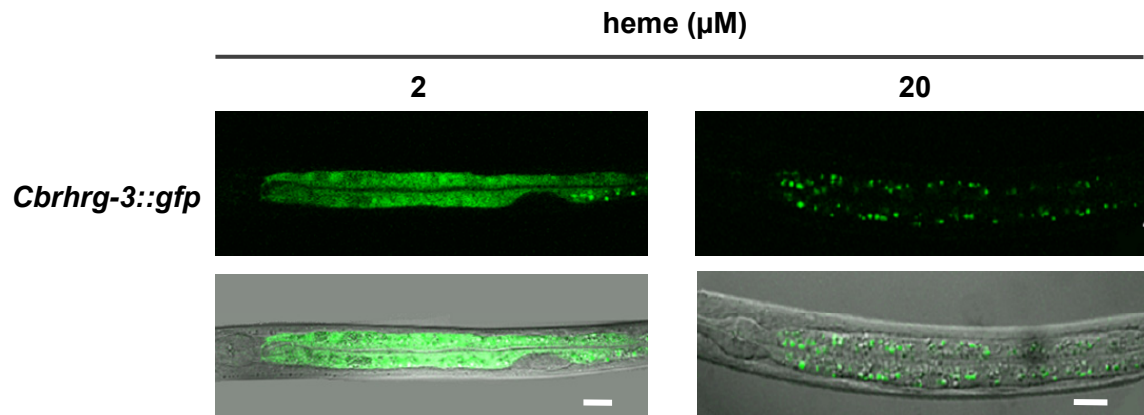
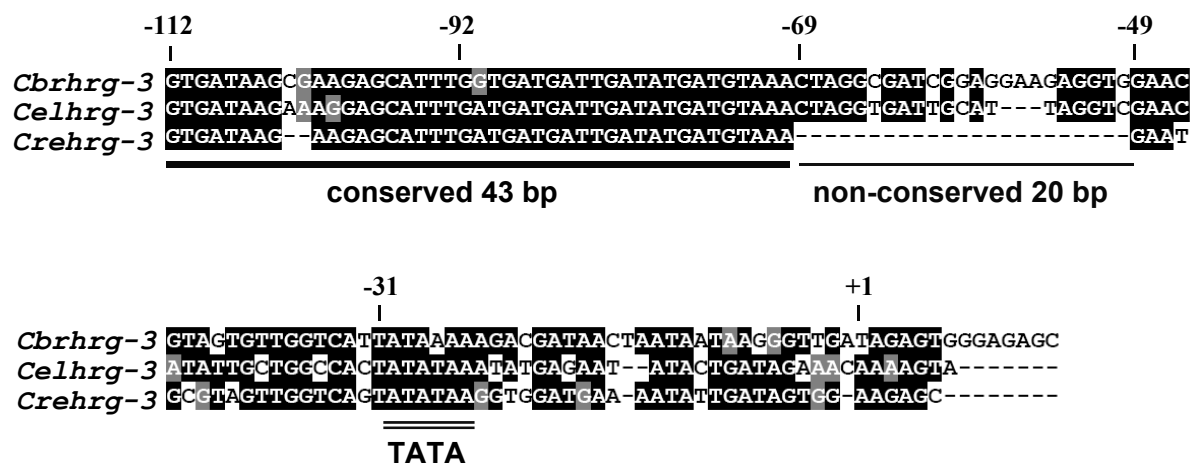
			heme (μ M)	
			2	20
<i>hrg-3-3kb::gfp</i>	-2992		+	-
<i>hrg-3Δ732::gfp</i>	-732		+	-
<i>hrg-3Δ295::gfp</i>	-295		+	-
<i>hrg-3Δ194::gfp</i>	-194		+	-
<i>hrg-3Δ132::gfp</i>	-132		+	-
<i>hrg-3Δ112::gfp</i>	-112		+	-
<i>hrg-3Δ92::gfp</i>	-92		-	-

Figure 4.5. A 43-bp conserved region is critical for heme-regulated expression of *hrg-3*. (A) The promoter of *C. briggsae hrg-3* is regulated by heme in *C. elegans*. The *IQ8631* transgenic worms containing 300-bp sequence upstream of *cbrhrg-3* fused with NLS-GFP were grown at 2 and 20 μ M heme, and GFP expression was analyzed at 4 d. Small green puncta in the image of 20 μ M heme are the autofluorescent gut granules in the intestine. (B) Multiple sequence alignment of ~112-bp upstream sequences of *hrg-3* among *C. elegans*, *C. briggsae* and *C. remanei*. Sequences were aligned by ClustalW and visualized with BoxShade. Numbers are the nucleotide positions relative to the *C. elegans* transcription start site, which is marked as “+1”. (C) Heme response by the *hrg-3 Δ 112 Δ 49::gfp* transgenic worms. In this construct, the non-conserved region between -69 and -49 bp was removed. (D) Analysis of enhancer activities using the *egl-18* basal promoter. The constructs contain *egl-18* basal promoter fused to either the *hrg-3 Δ 132* sequence or the concatemers of the 43-bp conserved region. The transgenic worms were analyzed for GFP expression at 2 and 20 μ M heme. The *egl-18* basal promoter is shown as control. (scale bar = 10 μ m)

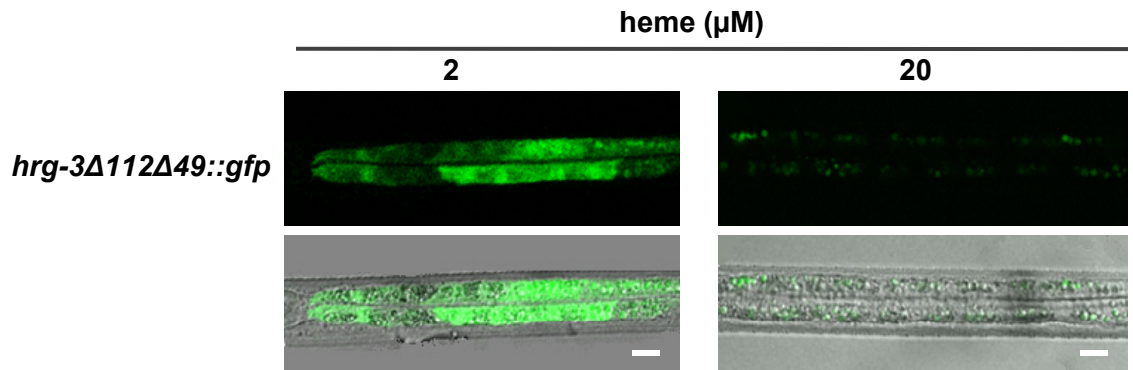
A



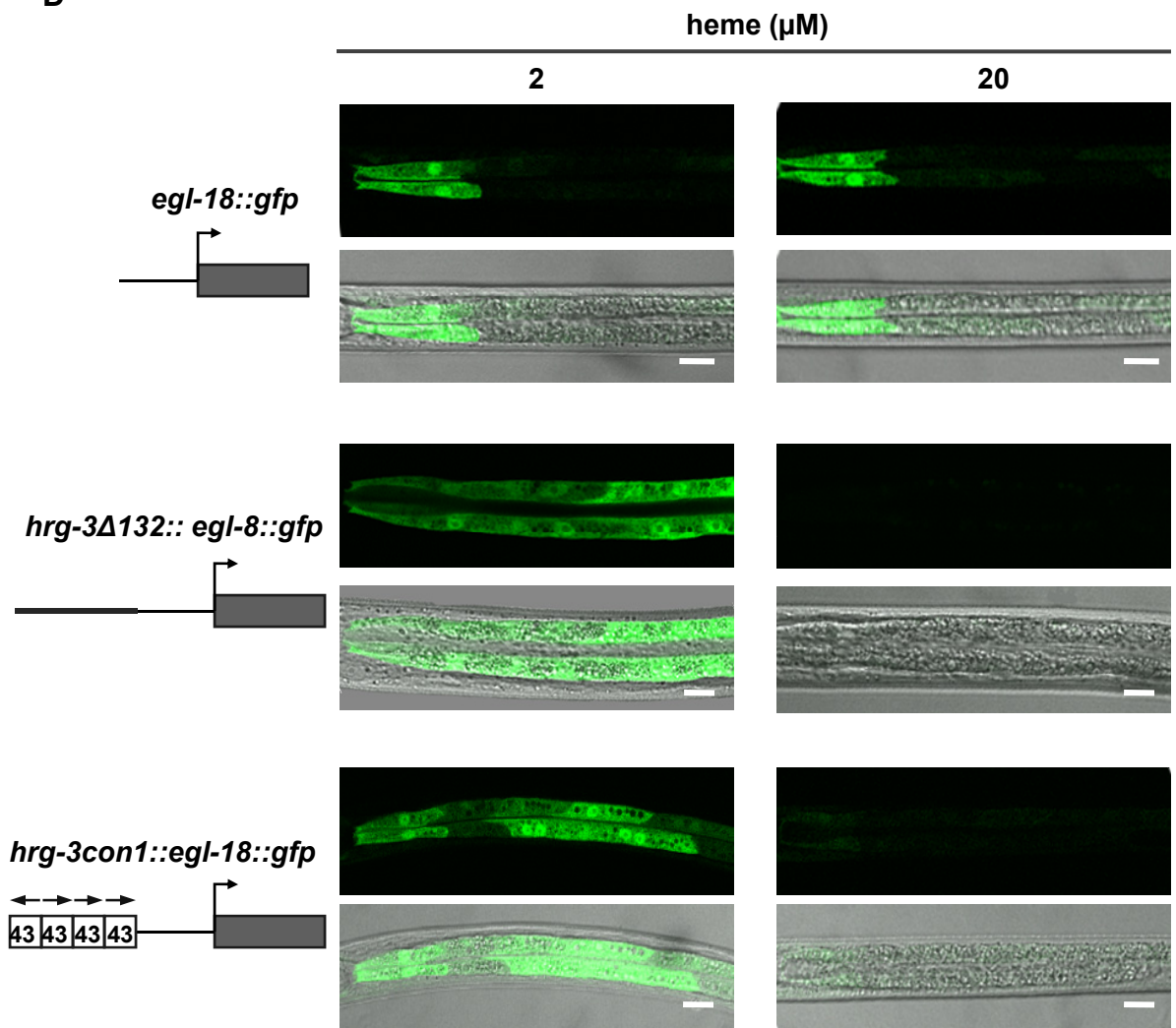
B



C



D



this 20-bp sequence was deleted in the *C. elegans* minimal promoter (*hrg-3Δ112Δ49::gfp*), the resultant construct was still responsive to changes in heme levels (Figure 4.5C).

We next examined whether the 43-bp conserved region (-112 to -69 bp) was sufficient for heme response by constructing a concatemer that has four repeats of this sequence. This concatemer was cloned upstream of the minimal promoter *egl-18* in the plasmid pKKMCS. The constructs *egl-18::gfp* and *hrg-3Δ132::egl-18::gfp* were used as negative and positive controls, respectively. These constructs were introduced into worms by bombardment transformation. In the worm with the *egl-18* minimal promoter alone, the first 4 and last 2 intestinal cells had moderate levels of GFP (Figure 4.5D), a pattern common to many *C. elegans* reporter genes that is unrelated to *hrg-3*. As expected, the expression was independent of heme levels. In contrast, the GFP expression in the transgenic worm with the concatemer construct *hrg-3con1::egl-18::gfp* was regulated by heme in the same pattern as the *hrg-3Δ132* promoter (Figure 4.5D). When the worms were maintained at 2 μM heme, strong GFP expression was observed in anterior and mid intestinal cells. At higher concentrations of heme, there was no GFP expression in the intestine. Furthermore, the minimal transcription due to the *egl-18* promoter alone was also inhibited in the intestine. These results suggested that the *cis*-elements in this 43-bp sequence were sufficient for heme-dependent gene regulation.

This 43-bp region is highly conserved across the three *Caenorhabditis* species; 39 bp out of 43 bp were identical (Figure 4.6A). This region contains one consensus ELT-2 GATA site (TGATAA) and a putative SKN-1 binding site (AATCATCATCA). The exclusive expression of *hrg-3* constructs in the intestine supports that this GATA motif is a functional binding site for ELT-2, the major intestinal-specific transcription factor

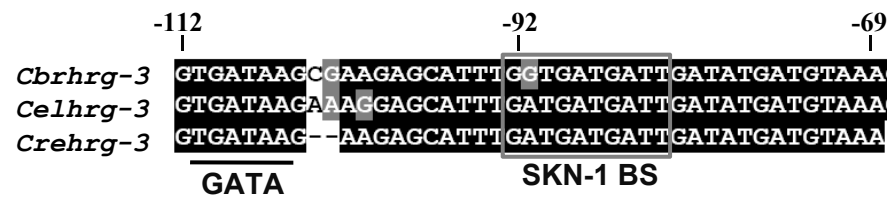
(223,224). To test whether *hrg-3* is regulated by SKN-1, the putative SKN-1 binding site was mutated in the context of the 139-bp promoter region. The resulting *IQ8531 (hrg-3mut1)* worms did not display any GFP expression even at low heme concentrations (Figure 4.6B). To confirm the requirement for SKN-1, we examined the effect of knocking down SKN-1 by the RNAi on the activity of the 3.0-kb *hrg-3* promoter in the *IQ8031* strain. Compared to the vector control, knockdown of *skn-1* significantly reduced the GFP expression when the worms were maintained on RNAi plates, which contain an equivalent of $\sim 5 \mu\text{M}$ heme (Figure 4.6C). These results suggested that SKN-1 was essential for the heme-dependent regulation of *hrg-3*.

HRG-3 is a secreted protein

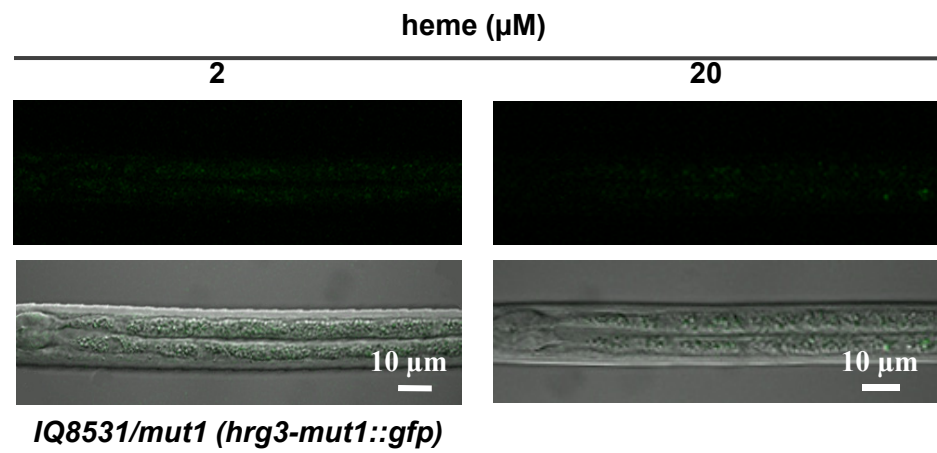
To identify the subcellular distribution of HRG-3 in *C. elegans*, we introduced the translational reporter *hrg-3::HRG-3-YFP* into the worm by bombardment. In this construct, the protein product is a HRG-3-YFP chimera. Similar to the transcriptional reporters, this transgene was active only when the worms were grown at $\leq 4 \mu\text{M}$ heme. However, even at $2 \mu\text{M}$ heme, the signals of HRG-3-YFP in the intestine were weaker than the autofluorescence of gut granules, which are lysosome-related organelles containing birefringent material (225). In the intestine cells, these weak HRG-3-YFP signals presented as small cytoplasmic puncta (Figure 4.7A, upper panel). This pattern is reminiscent of the *C. elegans* Golgi (226). In addition to intestinal localization, HRG-3-YFP also accumulated as vesicular structures in the coelomocytes (Figure 4.7A). In *C. elegans*, coelomocytes function as macrophage-like scavenger cells that nonspecifically endocytose various substances from the body cavity pseudocoelom (227). The fluorescence intensity of HRG-3-YFP was much brighter in coelomocytes than in the

Figure 4.6. A SKN-1 binding site is required for *hrg-3* gene activation. (A) The 43-bp conserved sequence contains a GATA motif and a putative SKN-1 binding site (BS). (B) Mutation of the SKN-1 binding site abolished the gene activation normally observed at low heme. The first 9 bp in the gray box were mutated into TCGTCGTCG in the *hrg-3Δ132* promoter. The *IQ8531* transgenic worms carrying this *hrg-3mut1* construct were subjected to gene expression analysis at both heme concentrations. (C) *skn-1* RNAi reduced *hrg-3* gene activity. The *IQ8031* worms were grown on *HT115(DE3)* bacteria expressing double-stranded RNA directed against L4440 vector or *skn-1*. The seeded RNAi plates contain an equivalent of ~5 μM heme. GFP levels were analyzed after 4 d.

A



B



C

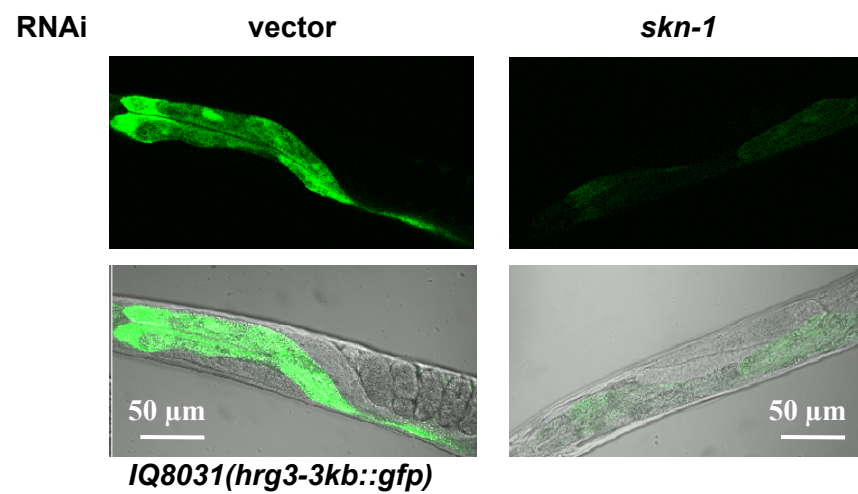
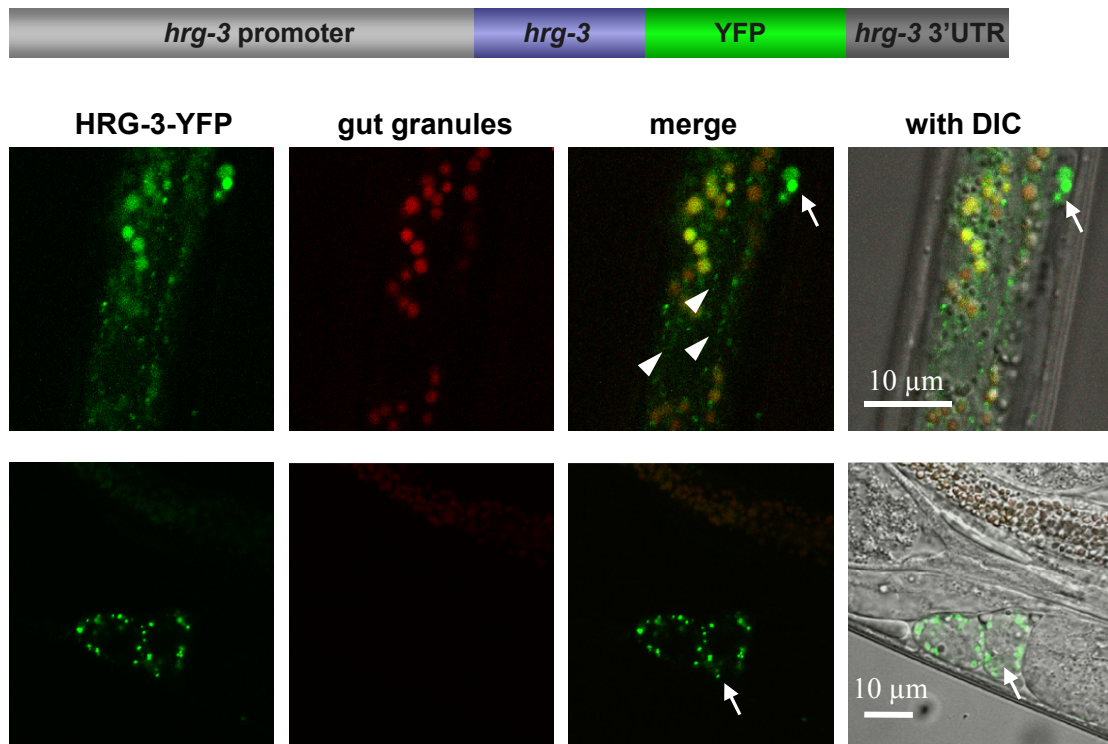
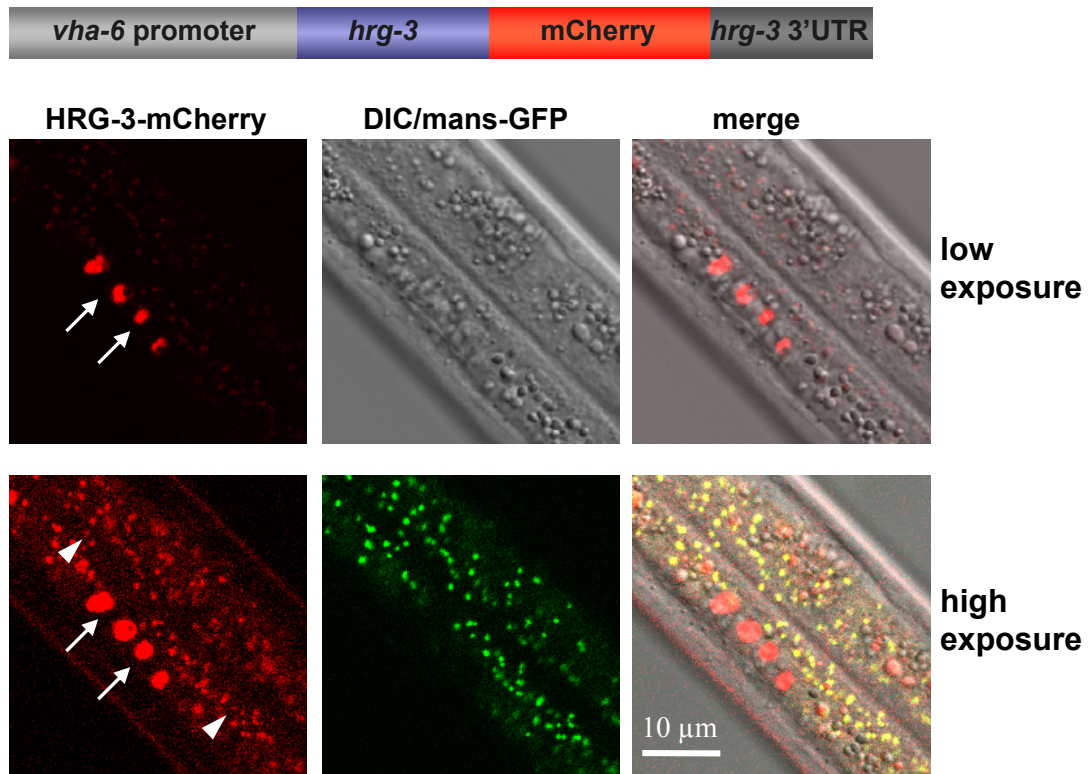


Figure 4.7. HRG-3 localizes to intestinal cells and coelomocytes. (A) The localization pattern of HRG-3-YFP translational constructs. The schematic representation of the construct is shown on the top of each image panel. The transgenic worms were grown at 2 μ M heme for 4 d prior to confocal analysis. Two representative images are shown. The green channel shows HRG-3-YFP and the red channel shows the nonspecific autofluorescence of gut granules. **(B)** Ectopic expression of HRG-3-mCherry using the intestinal-specific *vha-6* promoter. Part of a single worm containing the constructs HRG-3-mCherry and *vha-6::MANS-GFP* is shown. Images on the bottom panel were acquired using higher laser power and detector gain in the confocal microscope. Arrow: vesicular localization in coelomocytes. Arrowhead: Golgi localization in the intestine.

A



B



intestine. Since the *hrg-3* promoter is active only in the intestine, the most likely explanation is that HRG-3-YFP protein is translocated from the intestinal cells to the pseudocoelom for eventual uptake and accumulation in coelomocytes.

Examination of HRG-3 protein in the secretory pathway

HRG-3 contains a stretch of hydrophobic amino acids at its amino terminus (Figure 4.2B). To uncover the potential role of this region, we expressed either the full-length HRG-3, or the N-terminal 29 amino acids (HRG-3N), or HRG-3 without the 29 amino acids (HRG-3 Δ N). Each of these constructs was tagged with YFP and transfected into HEK293 cells (Figure 4.8A). Examination using confocal microscopy showed that the full-length HRG-3 co-localized with the Golgi marker CFP-Golgi. Interestingly, the 29-amino acid region at the N-terminus was sufficient to target YFP to the Golgi. When this segment was removed from HRG-3, the rest of the protein predominantly localized to the cytoplasm. These results indicated that the N-terminal hydrophobic region is essential for targeting HRG-3 to the Golgi in HEK293 cells.

To reveal the topology of HRG-3, we performed FPP assays in transfected HEK293 cells. In this assay, the cells were sequentially incubated with digitonin and protease (169). Peptides exposed to the cytoplasmic side are susceptible to protease digestion, whereas Golgi luminal proteins will be intact. In the FPP assays, the C-terminal YFP tags in both HRG-3 and HRG-3N were protected against protease digestion, indicating that the C-terminus of HRG-3 faces the lumen of the Golgi (Figure 4.8B).

To examine whether the N-terminal targeting region is retained or cleaved in HRG-3, full-length or deletion constructs of HRG-3-GFP were transfected into HEK293 cells and the lysates were subjected to analysis by SDS-PAGE and immunoblotting (Figure

4.8C). The full-length HRG-3 and the HRG-3 Δ N proteins were found to be equivalent in size; a difference of <400 Da was observed between these two proteins. By contrast, expression of HRG-3N-GFP resulted in a protein that was indistinguishable from GFP alone in size. These results indicated that the N-terminal hydrophobic region is cleaved to produce the mature HRG-3-GFP protein.

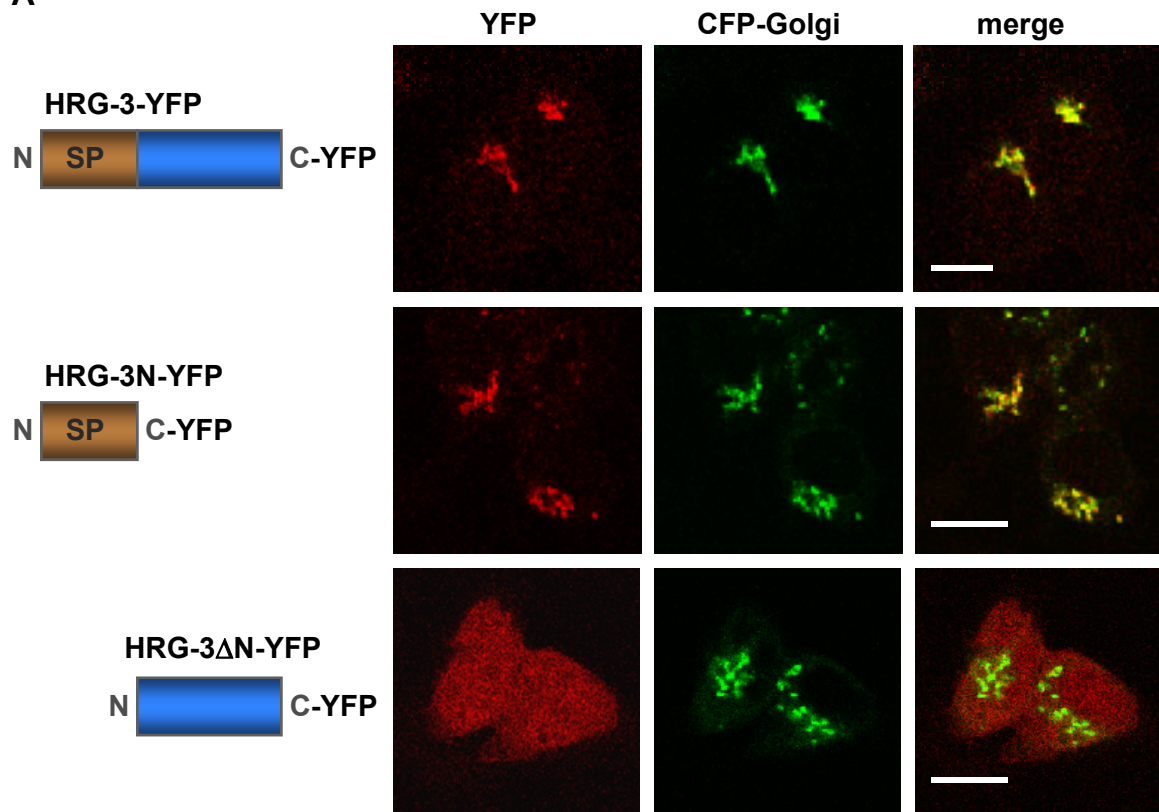
We expressed HA-tagged HRG-3 either by transfection into HEK293 cells or by *in vitro* transcription and translation. Western blot using anti-HA antibody showed that the HRG-3-HA protein had an apparent molecular weight of ~13.3 kDa when generated from an *in vitro* system (Figure 4.8D, lane 2). However, the protein product of the same construct expressed in mammalian cells was only ~10.1 kDa (Figure 4.8D, lane 1 and 3). This reduction of ~3.2 kDa correlates with the removal of N-terminal region. Interestingly, this N-terminal region was not cleaved when HRG-3-HA was expressed in *S. cerevisiae* (Figure 4.8D, lane 4). These results indicated that the N-terminal hydrophobic region acts as a signal peptide for HRG-3 targeting to the Golgi. Once the protein goes through the secretory pathway, this region is cleaved to give rise to the mature protein. In worms, the HRG-3 protein is secreted into the pseudocoelom. It still remains to be determined whether the secreted HRG-3-YFP protein expressed in *C. elegans* lacks the N-terminal region.

Characterization of a *hrg-3* deletion allele

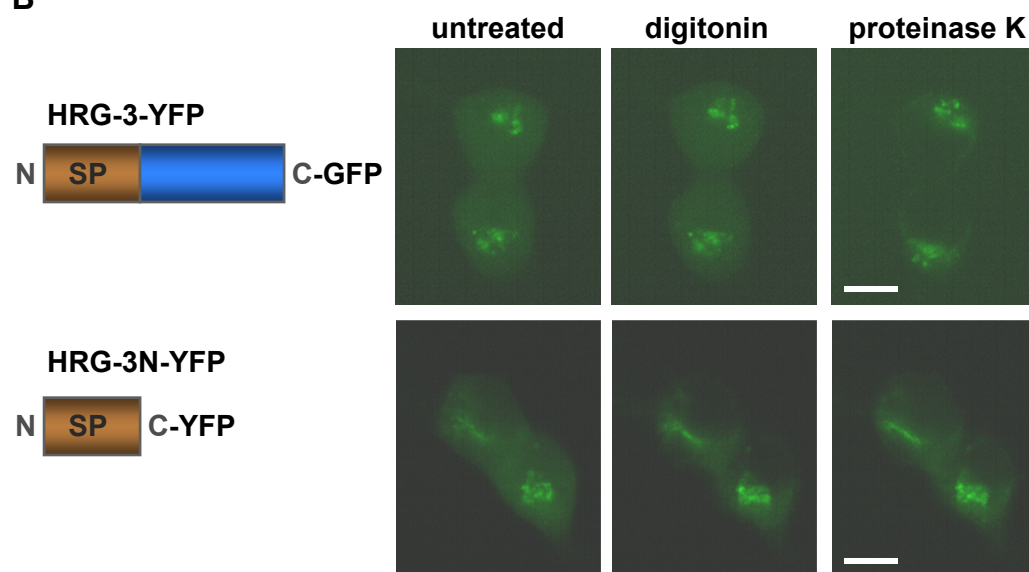
To understand the potential function of *hrg-3* in heme homeostasis, we analyzed the worms in which *hrg-3* was deleted (164). The *tm2468* allele results in a 218-bp deletion that comprises a 70-bp promoter sequence, the first exon, the first intron, and part of the second exon in *hrg-3* gene (Figure 4.9A). This mutant worm was outcrossed eight times

Figure 4.8. Analysis of *C. elegans* HRG-3 in mammalian cells. (A) Fluorescence analysis of HRG-3-YFP constructs in HEK293 cells. Schematics of the constructs are shown on the left and the confocal images are shown on the right. CFP-Golgi: Golgi marker. SP: signal peptide. (B) Fluorescence protease protection assays on HRG-3 constructs. In this assay, the transfected cells were treated with 30 μ M digitonin for 2 min followed by 50 μ g/ml proteinase K for 2 min. Images were acquired throughout the process by epifluorescence microscopy. Resistance to protease digestion after digitonin treatment indicates that the C-terminal GFP is in the lumen of the Golgi complex. (C) Western blot of HRG-3-GFP constructs expressed in HEK293 cells. The difference between HRG-3-GFP (lane 1) and the top band of HRG-3 Δ N-GFP (lane 2) is \sim 0.4 kDa. Lane 2 contains a second band which could be the degradation product of HRG-3 Δ N-GFP. The difference between HRG-3-GFP and GFP (lane 4), HRG-3N-GFP (lane 3), as well as the bottom band of HRG-3 Δ N-GFP is \sim 3.4 kDa. (D) Western blot of HRG-3-HA proteins generated in HEK293 cells, yeast, and an *in vitro* transcription and translation system (IVT). There is \sim 3.2 kDa difference in the sizes between HEK293-expressed species (lane 1 and 3) and HRG-3-HA generated by other systems (lane 2 and 4). (scale bar = 10 μ m)

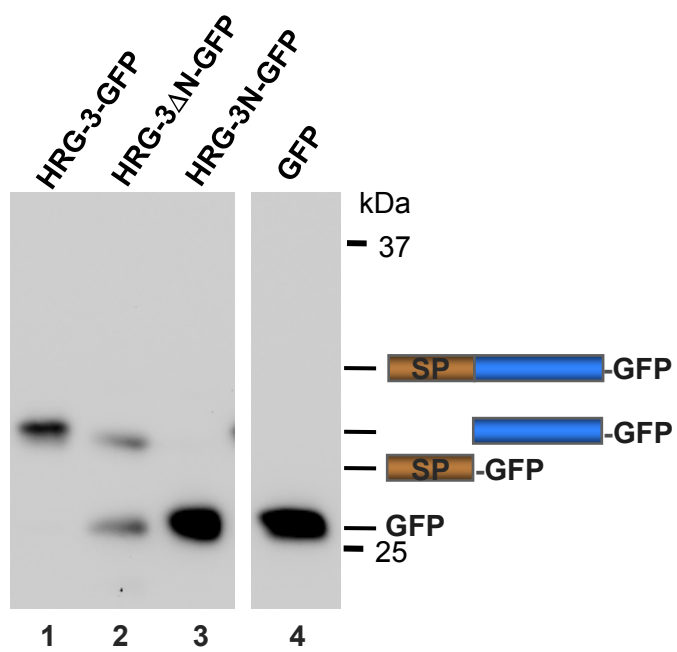
A



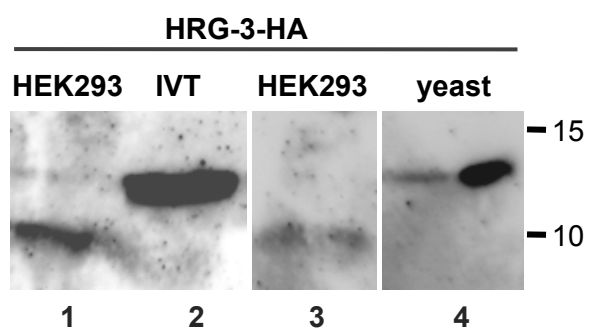
B



C



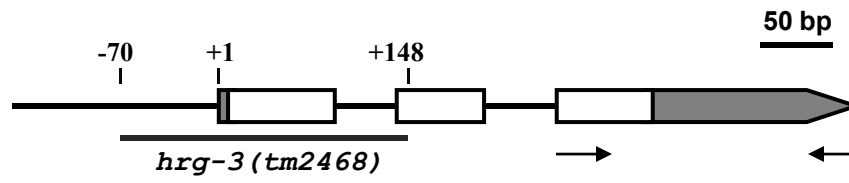
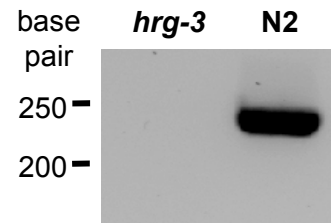
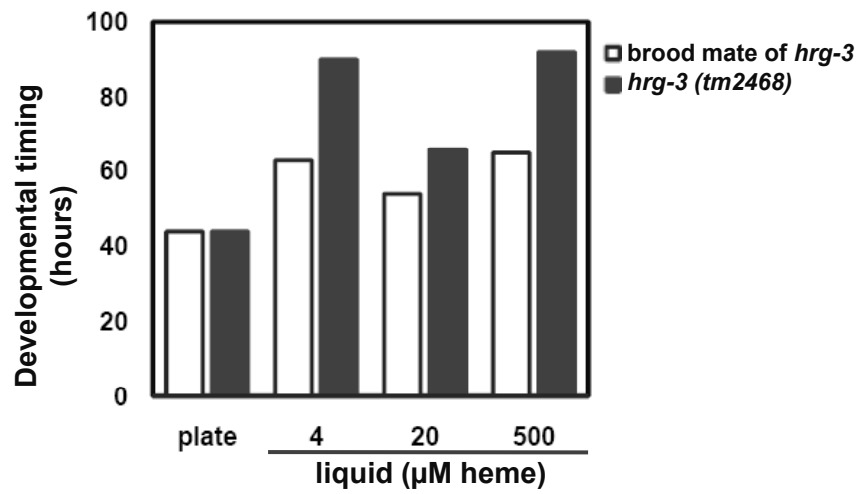
D



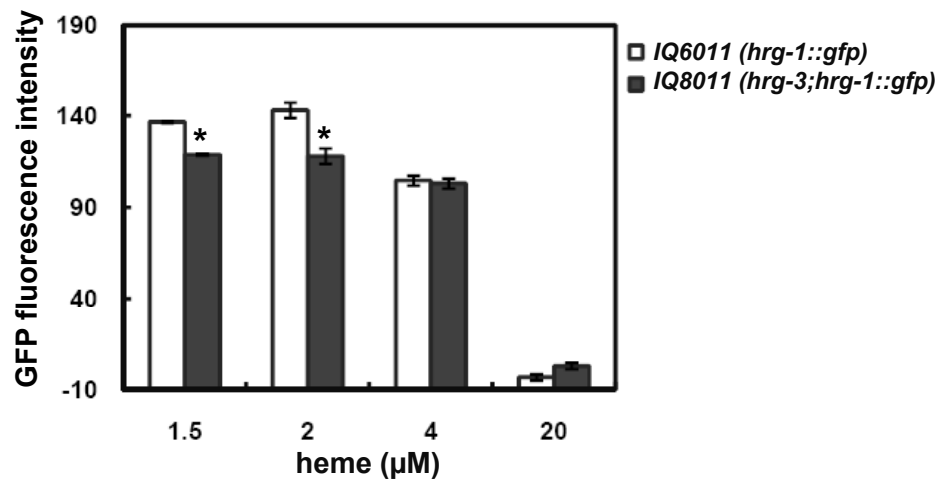
with the wild-type N2 worm. RT-PCR performed using primer sets against the last exon did not yield any product, confirming that *tm2468* is a null mutant (Figure 4.9B). Phenotypic characterization did not reveal any overt defects in morphology, growth rate, and the number of progeny in *tm2468* allele worms compared with N2 wild type strains when the worms were maintained on NGM agar plates (not shown). However, when these worms were grown in axenic mCeHR-2 medium, *hrg-3 (tm2468)* worms exhibited a delayed development that was independent of heme concentrations (Figure 4.9C). Although *hrg-3* expression is highly induced at low heme, there may be some basal expression at higher heme concentrations. The growth delay in *hrg-3* deletion worm could be due to the loss of basal levels of *hrg-3* expression.

To further characterize this allele, we crossed this mutant worm with a well-characterized heme-sensor strain *IQ6011 (hrg-1::gfp)*. In the sensor worm, the intestinal heme status is inversely correlated with the activity of the *hrg-1* promoter and GFP expression (68). Similar to *IQ6011* worms, the *IQ8011 (hrg3;hrg-1::gfp)* worms had reduced GFP intensities in response to higher heme levels. When highly synchronized *IQ8011 (hrg3;hrg-1::gfp)* worms were grown at 1.5 or 2 μ M heme for 3 d, they displayed lower GFP intensities than *IQ6011* (Figure 4.9D). To address whether a loss in *hrg-3* also resulted in altered heme uptake in the intestine, we measured ZnMP, a fluorescent heme analog that has been used to indirectly report heme uptake (68). We found that the steady state levels of ZnMP were not changed in both *hrg-3 (tm2468)* and *IQ8011* worms in comparison to the wild type strains (Figure 4.9E and 4.9F). These results indicated that the altered heme sensing in *IQ8011* worms was not due to changes at the uptake level.

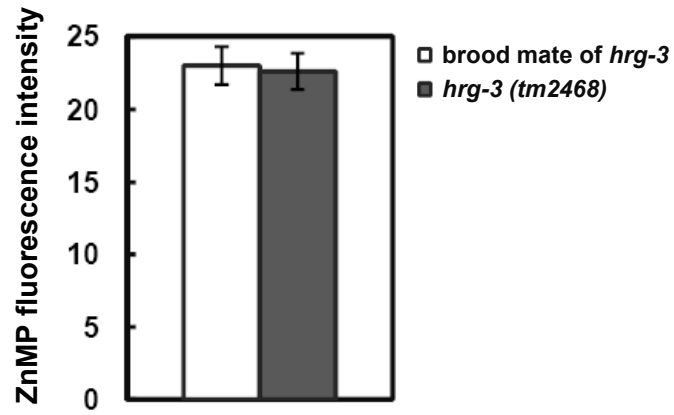
Figure 4.9. Analysis of the *hrg-3* deletion worm. (A) Location of the *tm2468* deletion in *hrg-3* gene. In the *tm2468* allele, part of the promoter region, the first exon, the first intron, and part of the second exon of *hrg-3* gene are deleted. Exons are depicted as empty boxes and untranslated regions are shown as gray boxes. “+1” is the confirmed transcription start site. (B) RT-PCR of *hrg-3* in the deletion worm. Total RNA was extracted from the worms grown at low heme. RT-PCR was performed using the primer set shown as arrows. N2 wild type worms were used as a positive control. (C) The growth rate of the *hrg-3* deletion strain. Developmental timing indicates the number of hours required for the worms to grow from the first larva (L1) stage to the end of the fourth larva (L4) stage. A higher number corresponds to slower growth. Developmental stages were analyzed both on plates and in liquid mCeHR-2 medium supplemented with the indicated amount of heme. (D) Comparison of GFP intensities between *IQ8011* and *IQ6011* worms. Synchronized L1 worms were grown in the indicated heme levels for 3 d. Total worm proteins were extracted and measured for GFP fluorescence. The fluorescence intensities were normalized to protein concentrations. Asterisk indicates $P < 0.05$. (E) and (F) Measurement of ZnMP uptake. Synchronized L1 worms were grown at 2 μ M heme in mCeHR-2 medium for 3 d. The worms were labeled with 10 μ M ZnMP for 16 h. The intensity of ZnMP was measured by epifluorescence microscopy. Brood mate refers to the wild-type worm segregant from the final outcross of the mutant. *IQ6011*: heme sensor strain (*hrg-1::gfp*); *IQ8011*: heme sensor strain with *hrg-3* deletion (*hrg-3; hrg-1::gfp*).

A**B****C**

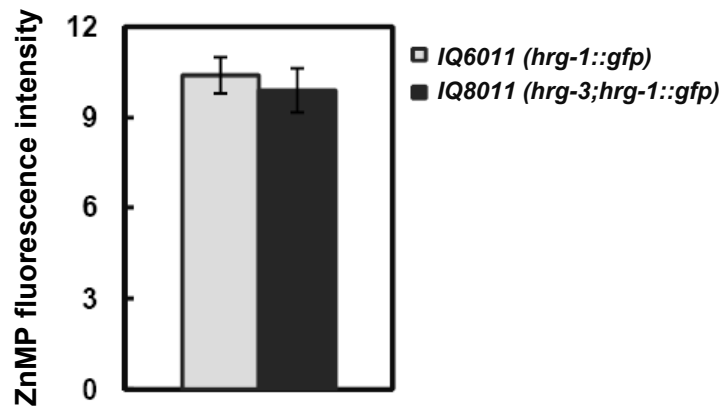
D



E



F



Characterization of HRG-3 in a heme-deficient yeast strain

Yeast provides a comparatively simple genetic system to assay heme homeostasis. To understand the possible functions of HRG-3, we utilized a heme-deficient *S. cerevisiae* strain DY1457 *hem1Δ(6D)* (172). The rate-limiting enzyme in the heme biosynthetic pathway, δ -aminolevulinate synthase (ALAS), is deleted in this *hem1Δ* strain (172). Therefore, this yeast strain completely depends on heme or heme-synthesis intermediates from the environment for its heme-related functions and growth. Untagged or tagged versions of *hrg-3* sequences were cloned into the 2 micron plasmid pYES-DEST52 that contains a GAL1 promoter. All constructs were introduced into the *hem1Δ* yeast and tested for growth. Compared to the control vector, expression of HRG-3-HA resulted in significant reduction in yeast growth when the transformed yeast was grown on plates containing δ -aminolevulinic acid (ALA), the product of ALAS (Figure 4.10A, left panel). A similar effect was observed when the yeast was exposed to 0.25 μ M heme. To test whether excess heme can restore the yeast growth, we also grew the yeast at 10 and 40 μ M heme. However, the yeast transformed with *hrg-3-HA* still exhibited a much slower growth than the control yeast. Furthermore, at all concentrations of ALA and heme, co-expression of a high-affinity heme importer HRG-4 did not restore the growth of the yeast expressing HRG-3-HA to the vector level (Figure 4.10A, right panel).

Interestingly, this toxic effect was abrogated when the N-terminal portion of HRG-3 was deleted (HRG-3 Δ N-HA), indicating that the growth arrest was specifically due to the expression of the full-length HRG-3-HA (Figure 4.10A). In addition, the untagged HRG-3 did not lead to decreased yeast growth, which is different from the tagged construct.

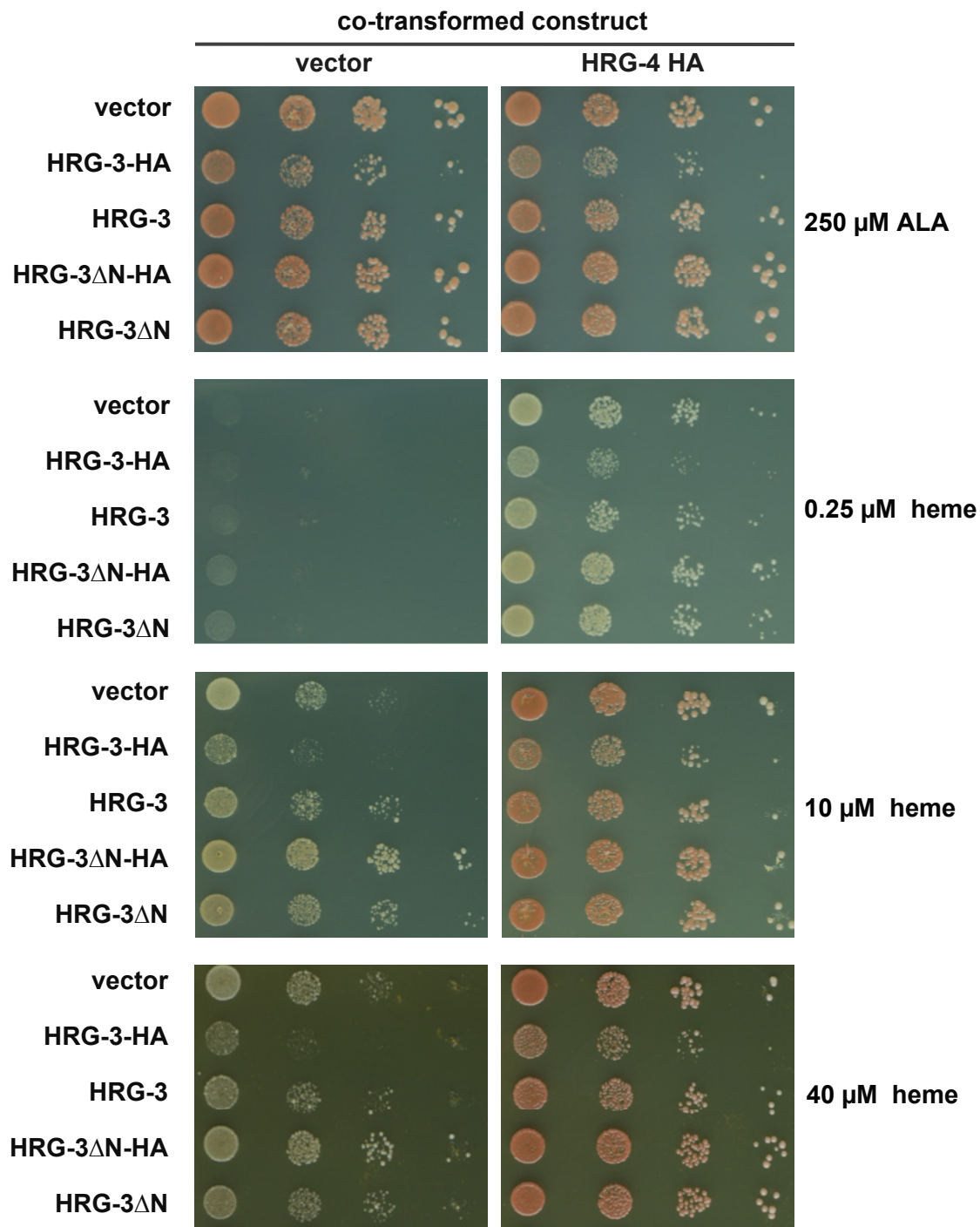
However, we have not been able to confirm whether the untagged protein is actually produced in yeast cells.

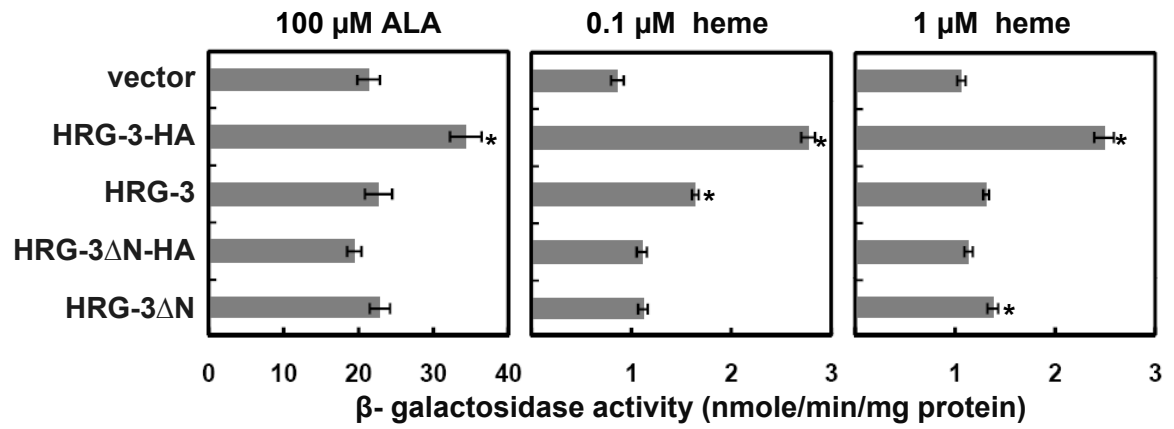
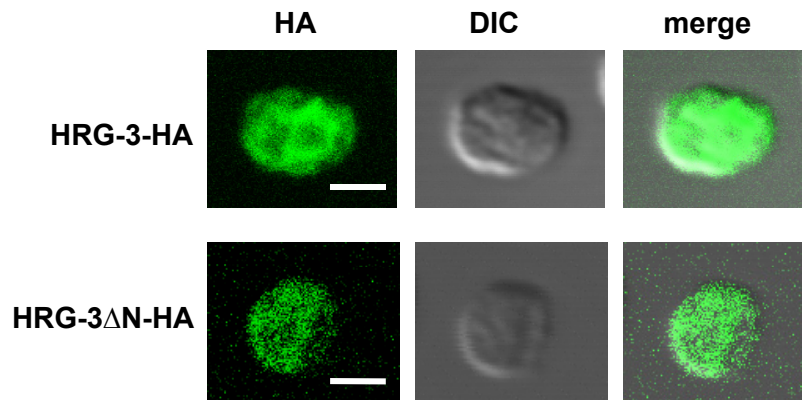
We next transformed HRG-3 constructs together with a CYC1::LacZ construct into *hem1Δ* yeast and measured the β -galactosidase activity. Since heme can induce the activity of CYC1 promoter through the transcriptional activator Hap1, the expression of LacZ positively correlates with intracellular heme levels. In contrast to the results observed on yeast growth, expression of HRG-3-HA increased β -galactosidase activities in the yeast (Figure 4.10B). This suggested that the arrest of yeast growth by the expression of HRG-3-HA is not because of overall heme deficiency, but may be due to perturbed intracellular heme homeostasis or heme-related signaling.

HRG-3-HA expressed in yeast is a full-length protein in which the N-terminal sequence, unlike in mammalian cells, is not processed (Figure 4.9D). Immunofluorescence assays in yeast revealed that the majority of HRG-3-HA displayed intracellular localization, further excluding the possibility that HRG-3 either is excreted from the cells or affects the overall heme levels by regulation uptake at the plasma membrane (Figure 4.10C). In addition, this localization pattern of HRG-3-HA is different from the published punctate signals of Golgi apparatus in yeast (228,229). Similarly, the HRG-3 Δ N-HA construct also exhibited intracellular localization but seemed to have lower protein level than full-length HRG-3.

Figure 4.10. Characterization of HRG-3 in heme deficient *S. cerevisiae*. (A) Expression of HRG-3 reduces yeast growth. *hem1Δ* yeast transformed with the indicated constructs were spotted in 10-fold serial dilutions on synthetic complete medium plates lacking both uracil and histidine. Different concentrations of ALA and heme were added to the assay plates. The yeast growth was analyzed after 3 to 5 d. (B) β -galactosidase activity assays. HRG-3 constructs and the reporter construct CYC1::LacZ were transformed into yeast together. The transformed yeast was grown in different concentrations of ALA and heme for 14 h. Total protein extracts were subjected to a LacZ assay. β -galactosidase activity reflects the activity of the CYC1 promoter which is activated by heme. Asterisk indicates $P < 0.05$ when compared to the vector control. (C) Immunofluorescence assays of HRG-3 proteins in yeast. The transformed yeast was fixed and spheroplasted. Anti-HA and fluorophore-conjugated anti-rabbit IgG antibodies were applied to detect the proteins. Images were acquired with different settings of laser power and detection gain on confocal microscope. (scale bar = 2 μ m)

A



B**C**

Discussion

Identification of *hrg-3* as a heme-regulated gene

Heme regulates the activities of many genes that are involved in erythropoiesis, heme biosynthesis, oxidative stress, oxygen sensing, energy metabolism, and circadian rhythm control (4,118-120). Target genes can be regulated either at the transcriptional level through transcription factors such as Bach1, Rev-erb α , and Hap1 (4,119,123) or post-transcriptionally through regulatory molecules such as the iron regulatory protein IRP2 (230). In this study we have identified a novel *C. elegans* gene, *hrg-3*, that is transcriptionally repressed by heme. Results from microarray, qRT-PCR, Northern blot, and transgenic worms consistently showed that *hrg-3* is highly induced at low heme, and its expression levels inversely correlate with heme concentrations. Neither PPIX nor iron, two structural components of heme, exhibited any regulatory effect on *hrg-3* expression. These results confirmed that *hrg-3* is a heme-responsive gene and the response is specific to heme.

Identification of a 43-bp heme-responsive sequence

Through systematic deletion and bioinformatics analyses, we have located a 43-bp DNA sequence in the *hrg-3* promoter that is responsive to heme. Addition of this sequence to a non-heme regulated basal promoter confers a robust heme response. This sequence does not contain any recognizable binding elements to which known transcription factors Bach1, Rev-erb α , and Hap1 bind.

However, the 43-bp sequence has a conserved GATA site and a SKN-1 binding site. The GATA factor ELT-2 is the predominant transcription factor regulating intestinal gene expression in worms (223,224). In our study, all the *hrg-3* transcriptional reporters

showed GFP expression exclusively in the intestine. When the 20-bp sequence containing the GATA element was deleted, the majority of worms with *hrg-3Δ92::gfp* did not have GFP expression even at low concentration of heme (Figure 4.5). These results support the concept that ELT-2 most likely regulates *hrg-3* intestinal expression. In addition, the conserved AATCATCATCA sequence closely resembles the consensus SKN-1 binding site, which comprises a (G/A)TCAT motif flanked by AT rich sequences (231). Mutating this sequence or knocking down *skn-1* resulted in a dramatic reduction in the *hrg-3* promoter activity at low heme, further confirming the functionality of this SKN-1 binding site. Interestingly, the closest mammalian homolog of SKN-1, the erythroid transcription factor P45 NF-E2, is known to activate the transcription of globin genes in a heme-dependent manner (232-234). In the absence of external heme, Bach1-Maf heterodimers bind to MAREs in the regulatory regions and repress the expression of globin genes (121,122). In response to heme treatment, P45 NF-E2 displaces Bach1 and activates gene expression (233,234). In *C. elegans*, the SKN-1 binding element in the promoter is required for *hrg-3* gene expression at low heme, suggesting that this regulatory mechanism may be different from that of P45 NF-E2.

HRG-3 is a secreted protein

As revealed by all the transcriptional reporters, activity of the *hrg-3* promoter is restricted to the intestine. In the case of translational fusion and ectopic expression constructs, we observed that the HRG-3 localized to the intestinal Golgi apparatus as well as in coelomocytes. In *C. elegans*, coelomocytes are scavenger-like cells that actively endocytose and accumulate a variety of foreign substances such as GFP or its variants from the pseudocoelom (227). Accumulation of GFP fluorescence in coelomocytes has

been used as an indirect way to measure its secretion from other tissues such as the intestine and neurons (227,235). However, this accumulation does not necessarily mean that the untagged endogenous protein is also taken up by coelomocytes. For instance, when the major yolk protein *vit-2* was fused to *gfp*, the protein product accumulated in the pseudocoelom in addition to the oocytes (236). Accordingly, the presence of HRG-3-YFP and HRG-3-mCherry in coelomocytes indicated that HRG-3 traffics to the basal plasma membrane of intestine cells and is secreted into the pseudocoelom.

The amino termini of HRG-3 and its orthologs all meet the criteria for signal peptides (237,238). Within the cell, signal sequences can either undergo cleavage by signal peptidases or present as membrane anchors (239). By expressing HRG-3 in mammalian cells, we found that the N-terminal portion of HRG-3 is sufficient and necessary for Golgi localization of HRG-3. Furthermore, in the case of all HA-tagged and GFP-fused constructs, the mature HRG-3 proteins do not retain this N-terminal region. These results support the possibility that the 25 amino acids at the N-terminus functions as a signal peptide.

Potential biological roles of HRG-3

Following its synthesis in the intestine of worms, HRG-3 is secreted into the pseudocoelom, and presumably taken up by other cell types. Based on the heme response, expression pattern, and trafficking feature, HRG-3 could be involved in intercellular heme transport in *C. elegans* (Figure 4.11). The fact that none of the worm cells have the ability to synthesize heme suggests that other cells have to acquire heme, directly or indirectly, from intestinal cells (160). F₁ progeny from parental worms grown at high concentrations of heme can grow to a later stage in liquid media without any added heme

than those progeny from parental worms grown at low heme, indicating that a proportion of heme is deposited into the developing embryos from somatic cells (Rao *et al.*, unpublished data).

C. elegans has six vitellogenin genes, namely *vit-1* to *vit-6* (240,241). Following synthesis in the intestine of adult hermaphrodites, the proteins are secreted into pseudocoelom and then taken up by the gonad (242,243). In ticks and other insects, vitellogenins have been shown to bind heme and they could be involved in delivering heme to embryos (58,59). Another lipid binding protein *lbp-3* encodes a secreted protein that might function in sequestering or transporting small hydrophobic molecules (244). Interestingly, the expression of *lbp-3* is also upregulated by heme deficiency (Microarray data, Chapter five). HRG-3 might play a similar role in *C. elegans* in cooperation with, or in addition to, vitellogenins or LBPs. Since HRG-3 encodes a secreted protein in response to heme deficiency, it may play a role in intercellular heme trafficking. We have observed that, although *hrg-3* is expressed in male worms (Appendix VI), its expression level in males is much lower than that in hermaphrodites. A microarray analysis showed that *hrg-3* mRNA was 5.4-fold more enriched in hermaphrodites than that in males (245). Moreover, the highest mRNA level of *hrg-3* was detected in young adult, which is the stage when oogenesis and early embryogenesis start. It is possible that HRG-3 may be involved in efficient heme delivery to embryos under the conditions of heme deficiency. However, it remains to be determined whether HRG-3 binds heme.

In *hrg-3* deletion worms, the heme status within the intestine itself is not dramatically altered. This result supports our model that the major function of HRG-3 is not in the intestine, even though it is synthesized in the intestine. The expression of HRG-

3, especially with a C-terminal epitope tag, dramatically arrested yeast growth across all heme concentrations (Figure 4.11). This negative effect on growth is probably not due to overall heme deficiency because high concentration of exogenous heme or co-expression of a high-affinity heme importer HRG-4 does not restore the normal yeast growth. Furthermore, as indicated by the activity of the heme-dependent reporter CYC1::LacZ, the yeast cells expressing HRG-3-HA sense even higher levels of heme in the cytoplasm and nucleus than the control. In yeast, HRG-3-HA accumulates as an unprocessed form within the cells. Therefore, HRG-3-HA may be involved in the sequestration or redistribution of heme within yeast cells such that heme is available for some compartments (e.g. cytoplasm), but not for others (e.g. mitochondria).

We demonstrated that *hrg-3* is regulated by the transcription factor SKN-1. *skn-1* was first identified as a maternal gene required for early embryonic development (246,247). Later studies found that SKN-1 induces the transcription of phase II detoxification genes and contributes to stress resistance and longevity (248,249). It is possible that heme deficiency induces cell stress, which activates *hrg-3* expression through SKN-1. It will be interesting to see whether HRG-3 is involved in any of these pathways.

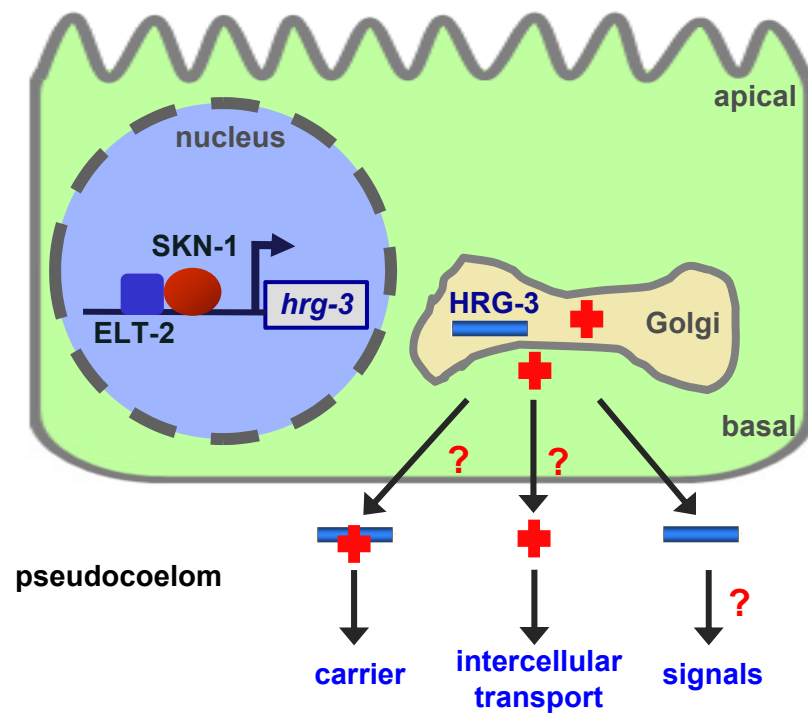
One of the main functions for secreted peptides is signaling, which holds true in the cases of hormones, immune-response molecules and neurotransmitters. For example, in response of iron loading or inflammation, liver secretes a peptide hormone called hepcidin (250). Hepcidin binds the iron exporter ferroportin in enterocytes and macrophages, and leads to decreased uptake or recycling of iron (250). Heme is also a signaling molecule that modulates gene expression and regulates cellular processes (119).

At low concentrations of heme, HRG-3 is synthesized and secreted into the pseudocoelom as a 45-amino acid peptide. Therefore, HRG-3 may be involved in intercellular signaling as a response to heme deficiency.

Figure 4.11. Proposed model of HRG-3 in heme homeostasis. **(A)** In the intestinal cells of *C. elegans*, *hrg-3* is induced by heme deficiency. The transcription factors SKN-1 and ELT-2 are required for *hrg-3* expression. Following its synthesis in the intestine, HRG-3 is secreted into the pseudocoelom. Deletion of *hrg-3* increased the intestinal heme concentration, suggesting that HRG-3 plays a role in mobilizing heme out of the intestine. HRG-3 may function either as an intercellular heme carrier that directly binds heme, or as a signaling molecule that regulates heme transport indirectly. **(B)** When overexpressed in *S. cerevisiae*, HRG-3-HA reduces the growth and division of heme-deficient yeast. This could be due to decreased heme content in certain compartments such as mitochondria. However, the cytoplasm and nucleus of this transformed yeast even sense higher levels of available heme, indicating that expression of HRG-3-HA may be involved in heme sequestration or compartmentalization within yeast cells.

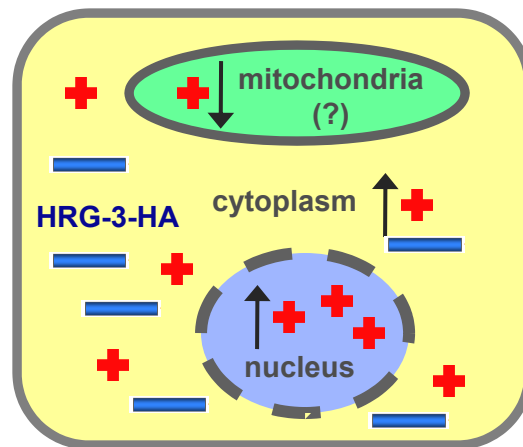
A

worm intestine cells



B

yeast cells



Chapter 5: Global analysis of heme- and oxygen- regulated genes in *C. elegans*

Summary

In biological systems, heme and oxygen are closely intertwined with each other in many respects. Oxygen is required as an electron acceptor in heme biosynthesis, whereas hemoproteins are responsible for the transport and storage of oxygen molecules. In the nematode *C. elegans*, heme-containing proteins such as guanylate cyclases and neural globin GLB-5 are crucial for oxygen sensing. In addition, alterations in either heme or O₂ concentrations affect the metabolic rates of worms. To understand the biological connections and the regulatory network between heme and oxygen, we performed a genome-wide microarray analysis using RNA samples prepared from worms grown at different heme and O₂ concentrations. The results showed that 369 and 94 genes were significantly regulated by heme and oxygen, respectively. Among them, 18 genes were responsive to both factors. Unexpectedly, only four genes were differentially expressed in response to 4% O₂. Quantitative real-time PCR on 20 genes showed consistent results with microarrays. Bioinformatics analysis indicated that the biological processes related to aging and lipid metabolism were highly enriched in heme-regulated genes, whereas many oxygen-responsive genes were associated with transferase activities. Additionally, the molecular function “transporter activity” was over-represented in the genes regulated by low heme, suggesting that heme uptake systems are upregulated in response to heme deficiency. A number of differentially expressed genes encode C-type lectins, UDP-

glucuronosyl transferases, glutathione S-transferases, and cytochrome P450s. Worm interactome analysis indicated that the protein products of 55 heme-regulated genes and 9 oxygen-regulated genes have been shown to interact with other proteins. These molecules may constitute the core heme oxygen regulatory network in *C. elegans*. In summary, these results demonstrate that *C. elegans* can adapt to varying concentrations of heme and O₂ by inducing or repressing gene expression. Genes identified in this microarray could be candidates for the molecules or pathways involved in heme uptake, heme detoxification, and resistance to hyperoxia.

Results

In the previous chapter, we have shown that the expression of *hrg-2* is regulated by heme concentrations. A preliminary microarray experiment with a single biological replicate also indicated that *hrg-2* was regulated by oxygen concentrations (unpublished data, Dr. Wayne Van Voorhies and Dr. Harold Smith). In the experiment, *hrg-2* mRNA showed a 12.5-fold decrease and a 1.8-fold increase in response to 4% and 100% O₂, respectively. Thus, *hrg-2* might be regulated by both heme and oxygen.

Alterations in either heme or oxygen levels can affect the metabolic rates of *C. elegans*. Compared to normoxia, 1% O₂ reduced the metabolic rates of worms by 50% (163). When *C. elegans* were maintained at 1.5 and 500 μ M heme, they exhibited a 40~50% reduction in metabolic rates in comparison to those grown at 20 μ M heme (Appendix VII, unpublished data, in collaboration with Dr. Wayne Van Voorhies,). Interestingly, low concentrations of heme displayed more dramatic effects on the metabolic rates after the worms were exposed to hypoxia (Appendix VII). Little difference in metabolic rates was observed between 4 and 20 μ M heme before hypoxia.

However, after hypoxia treatment for 5 h followed by 15 h recovery, worms from 4 μ M heme had significant lower metabolic rates than those from 20 μ M heme. Additionally, a further decrease of metabolic rate was observed in the worms maintained at 1.5 μ M heme after hypoxia.

Identification of heme- and oxygen- responsive genes

To further understand the regulation of *hrg-2* and the connections between heme and oxygen in *C. elegans*, global changes of gene expression in response to different heme and O₂ concentrations were analyzed by using Affymetrix *C. elegans* Genome Arrays. The experiment design employed a 3 \times 3 full factorial structure. The three concentrations of heme were 1.5 μ M (low), 20 μ M (optimal) and 500 μ M (high), while the concentrations of O₂ were 4% (hypoxic), 21% (normoxic), and 100% (hyperoxic). RNA samples were derived from wild type N2 worms grown under these nine treatments for two successive generations. In this microarray experiment, we found 446 genes that showed ≥ 2.0 fold change and a false discovery rate *q* value < 0.05 in at least one treatment (Figure 5.1A and Appendix VIII). Among these were 351 genes that were transcriptionally regulated by heme and 76 genes that were affected by oxygen. In addition, 18 genes exhibited significant responses to both heme and O₂. Statistically significant interaction between heme and oxygen was observed for only one gene (Figure 5.1A), *cyp-35B2*, which encodes a cytochrome P450 enzyme.

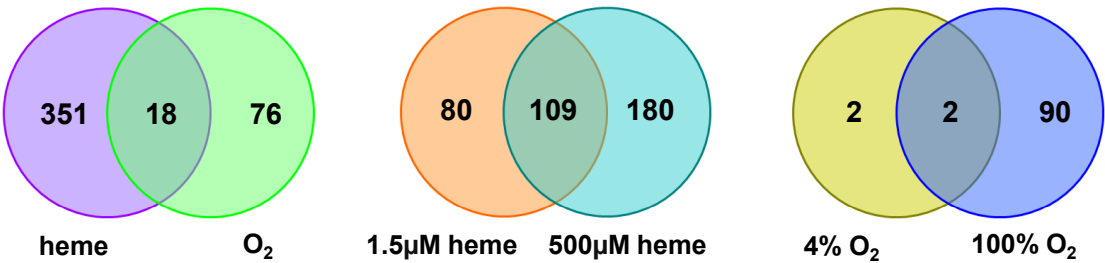
Detailed examination revealed that the mRNA levels of 109 genes were altered at both 1.5 and 500 μ M heme in comparison to 20 μ M heme (Figure 5.1B). In contrast, only two differentially expressed genes overlapped between hypoxic and hyperoxic conditions. We next arbitrarily grouped genes with similar expression profiles together

Figure 5.1. Overview of microarray results. (A) ANOVA models for differentially regulated genes. Based on their transcriptional responses, genes were categorized as regulated by heme, regulated by O₂, regulated by both heme and O₂, and regulated by O₂ in a heme-dependent manner. Cut-off: false discovery rate q value <0.05 and fold change ≥ 2.0 . y_g : the expression value of a gene in a treatment; μ_g : basal expression value of the gene in treatment 20 μ M heme/21% O₂; H: effect of heme; O: effect of O₂; ε : random error. (B) Venn diagram of overlapping genes from different categories. The categories of regulated genes are shown below the Venn diagram. (C) Clustering of regulated genes in the microarray. Differentially expressed genes were grouped into 14 clusters based on their regulations by heme and/or oxygen. Fold changes were converted into heat maps using Multiexperiment Viewer version 4.3.

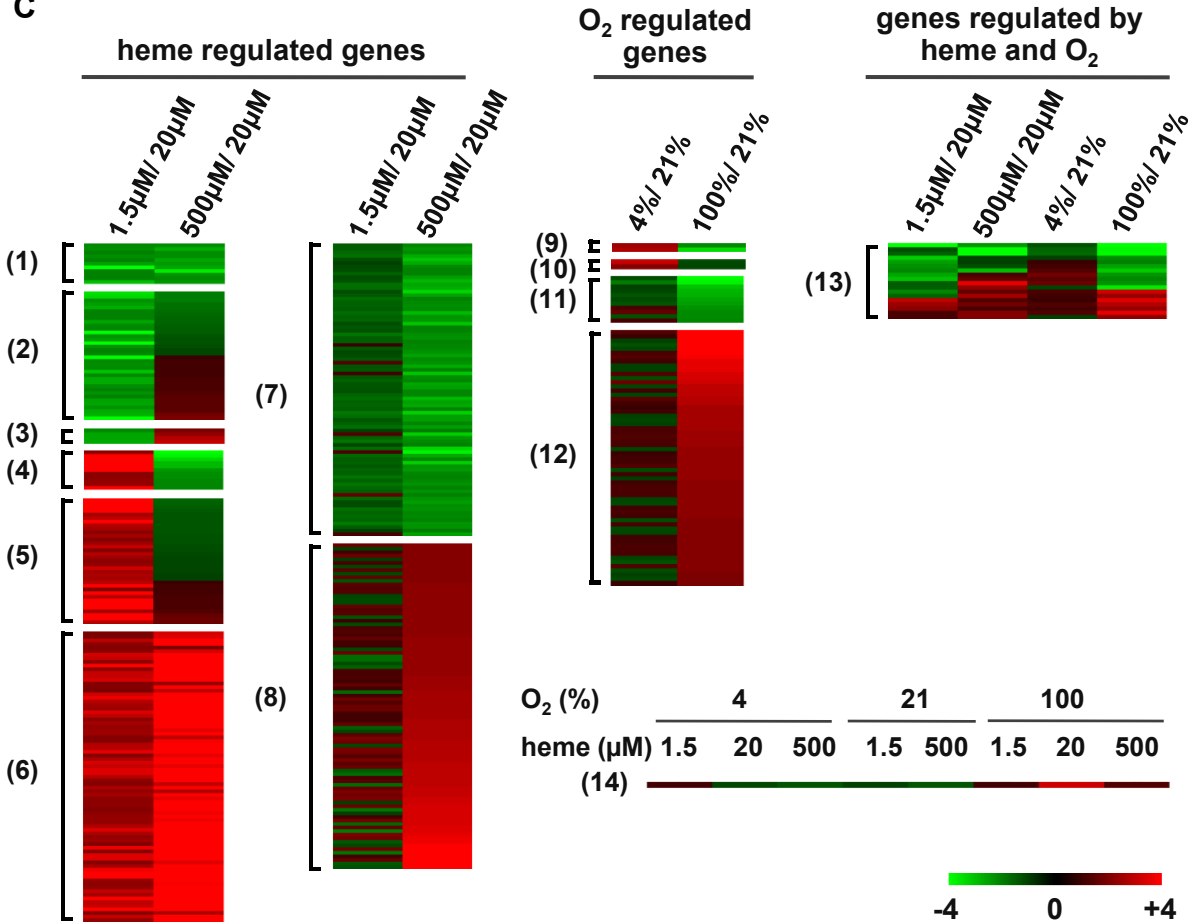
A

Effects	ANOVA model	Changed genes
Heme	$y_g = \mu_g + H + \varepsilon$	351
O ₂	$y_g = \mu_g + O + \varepsilon$	76
Heme + O ₂	$y_g = \mu_g + H + O + \varepsilon$	18
Heme:O ₂	interaction	1

B



C



based on whether the gene was up- or down- regulated at each heme or O₂ concentration compared to the control. The 446 genes were categorized into 14 clusters (Figure 5.1C). Cluster 8 was the largest group comprised of 91 genes that were induced by high heme. In addition, more than 80 genes were present in clusters 6 and 7. Surprisingly, only 4 transcripts (cluster 9 and 10) exhibited increased expression in response to sustained hypoxia, whereas 61 genes (cluster 12) were significantly induced under 100% O₂. One of the two genes in cluster 9, F22B5.4, contains four hypoxia response elements and has been identified as a target for hypoxia-inducible factor (HIF-1) (251,252).

Validation by quantitative real-time PCR

To confirm the microarray results, we performed qRT-PCR on 20 genes utilizing the RNA samples originally used for the microarray analysis (Figure 5.2). The genes tested were selected from each expression cluster. All 160 fold change values (relative to the control group 20 μ M heme/ 21% O₂) for the 20 genes were subjected to correlation analysis between qRT-PCR and Affymetrix microarrays. The microarray results showed that 92 of the 160 data points had fold changes ≥ 2.0 . Out of these 92 data points, 79 were validated by qRT-PCR ($r=0.86$, $P < 0.0001$). An example for the *hrg-2* and the oxygen-responsive gene F22B5.4 is depicted in Figure 5.2B.

Enrichment of biological pathways

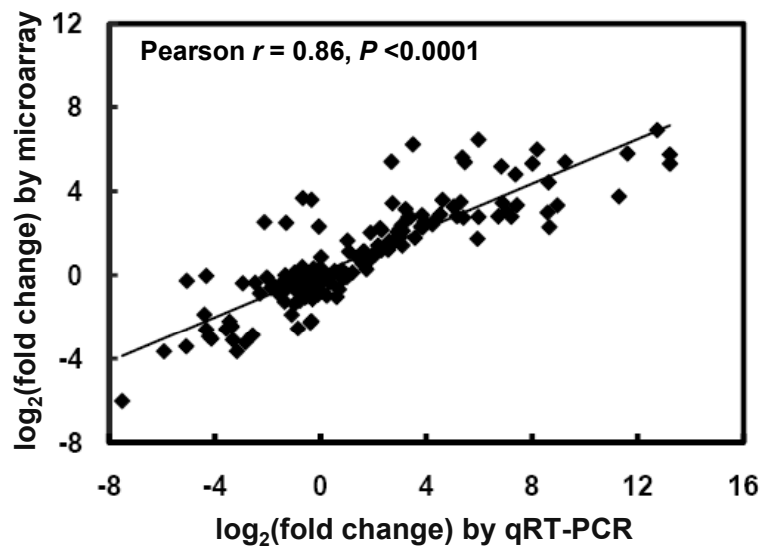
Of the 446 genes regulated by heme and/or O₂, 288 (65%) have been assigned GO terms. Each of the four gene sets, those regulated by 1.5 μ M heme (189), 500 μ M heme (289), 4% O₂ (4), and 100% O₂ (92), was subjected to GO enrichment analyses individually (Table 1). Interestingly, the GO terms “transporter activity” and

Figure 5.2. Validation of gene expression by quantitative real-time PCR. (A)

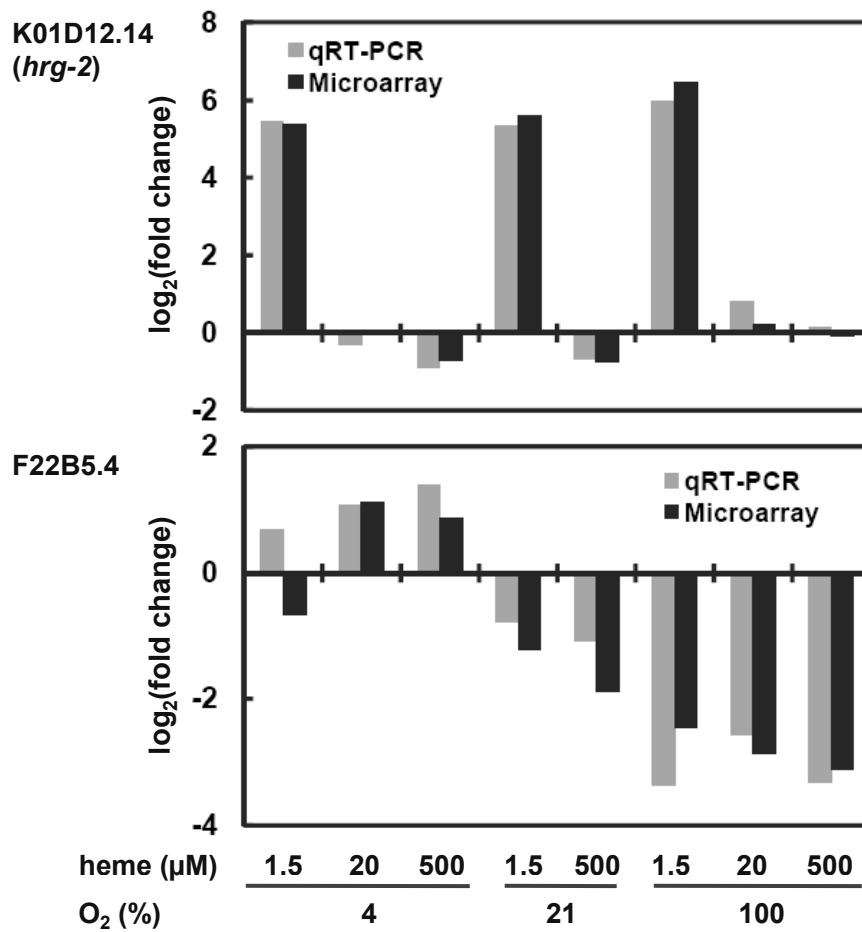
Correlation of gene expression data between microarrays and qRT-PCR. All 160 fold change values (relative to the control group 20 μ M heme/21% O₂) for 20 genes were transformed into log scale. Correlation analysis was performed in GraphPad INSTAT version 3.01 (GraphPad, San Diego). Correlation coefficient (r) was calculated for the comparisons of the 160 data points between the microarray data and qRT-PCR results.

(B) Expression profiles for a *hrg-2* and an oxygen-responsive gene (F22B5.4) in microarray and qRT-PCR.

A



B



“proteolysis” were highly enriched only in the genes regulated by 1.5 μ M heme, whereas GO terms related to carbohydrate metabolism were significantly over-represented in those genes regulated by high heme. In contrast to *hrgs*, many oxygen-responsive genes (*orgs*) were associated with the terms “transferase activity” and “oxidoreductase activity”. In addition, “catalytic activity” was the only GO term that was significantly associated with the genes regulated by 4% O₂.

The processes “lipid transport” and “aging” were significantly enriched in both sets of *hrgs* (Table 1), suggesting that heme may play an important role in regulating lipid homeostasis and life span. In addition, the GO terms “transferase activity, transferring glycosyl groups” and “coenzyme binding” overlapped between *hrgs* and the *orgs*. Due to the large numbers of C-type lectin (*clec*) genes and collagen genes, “carbohydrate binding” and “structural constituent of cuticle” were also observed as significantly enriched GO terms.

We next examined these genes for association with the KEGG pathways (179). Consistent with the GO results, several pathways related to fatty acid metabolism were significantly enriched in the genes regulated by 500 μ M heme (Table 2). In this gene set, the pathway “purine metabolism” was also recognized as a significantly enriched pathway. Three pathways including “metabolism of xenobiotics by cytochrome P450”, “glutathione metabolism”, and “fatty acid metabolism” were over-represented in the genes regulated by 100% O₂. However, no KEGG pathway was significantly enriched in the genes regulated by 1.5 μ M heme or 4% O₂. This probably was because that only few genes in these two categories have been mapped to the KEGG pathways.

Table 1. Gene ontology analysis of *hrgs* and *orgs*.

Gene ontology terms	number of genes	<i>P</i> value	Fold enrichment
Genes regulated by 1.5 μM heme			
transporter activity	19	0.01	2
carbohydrate binding	18	0.00	4.9
sugar binding	14	0.00	4.5
transferase activity, transferring glycosyl groups	11	0.00	4.9
proteolysis	10	0.03	2.2
transferase activity, transferring hexosyl groups	10	0.00	5
peptidase activity	10	0.04	2.1
lipid metabolic process	8	0.02	2.8
cellular lipid metabolic process	6	0.04	3.2
aging	6	0.04	3.2
multicellular organismal aging	6	0.04	3.2
determination of adult life span	6	0.04	3.2
extracellular region	6	0.01	4.8
lipid transport	5	0.00	28
lipid transporter activity	5	0.00	40.4
structural constituent of cuticle	5	0.05	3.6
lipid glycosylation	3	0.03	11.2
lipid modification	3	0.05	8.7
sphingoid biosynthetic process	2	0.03	59.8
ceramide biosynthetic process	2	0.03	59.8
sphingomyelin catabolic process	2	0.04	44.9
phospholipid catabolic process	2	0.04	44.9
sphingomyelin phosphodiesterase activity	2	0.04	44.4
Genes regulated by 500 μM heme			
carbohydrate binding	17	0.00	3
sugar binding	16	0.00	3.4
carboxylic acid metabolic process	13	0.00	3.5
organic acid metabolic process	13	0.00	3.5
multicellular organismal aging	12	0.00	4.3
determination of adult life span	12	0.00	4.3
aging	12	0.00	4.3
amine metabolic process	10	0.00	3.3
nitrogen compound metabolic process	10	0.00	3.1
carbohydrate metabolic process	9	0.04	2.3
phosphate transport	8	0.01	3.3
inorganic anion transport	8	0.02	2.9
anion transport	8	0.03	2.8
amino acid metabolic process	7	0.02	3.1
amino acid and derivative metabolic process	7	0.04	2.8
structural constituent of cuticle	7	0.02	3.3
coenzyme binding	7	0.03	3
lipid transport	6	0.00	22.6
monocarboxylic acid metabolic process	6	0.01	5.2
aromatic compound metabolic process	6	0.01	4.7
lipid transporter activity	6	0.00	31.9
ligase activity, forming carbon-nitrogen bonds	6	0.01	4.3

embryonic pattern specification	5	0.00	14.4
pattern specification process	5	0.00	7.5
purine nucleotide biosynthetic process	5	0.02	4.7
purine nucleotide metabolic process	5	0.02	4.6
cell fate commitment	5	0.04	3.8
glutamine metabolic process	4	0.00	20.1
glutamine family amino acid metabolic process	4	0.00	12.1
amino acid biosynthetic process	4	0.02	7.5
nucleosome assembly	4	0.02	6.9
chromatin assembly	4	0.03	6.2
nitrogen compound biosynthetic process	4	0.03	5.7
amine biosynthetic process	4	0.03	5.7
heterocycle metabolic process	4	0.04	5.2
carbohydrate catabolic process	4	0.04	5.1
fatty acid metabolic process	4	0.04	5.1
P granule	4	0.00	18.2
pole plasm	4	0.00	18.2
nucleosome	4	0.01	8.1
'de novo' IMP biosynthetic process	3	0.00	45.2
IMP biosynthetic process	3	0.00	45.2
IMP metabolic process	3	0.00	45.2
peptidoglycan metabolic process	3	0.00	30.1
purine ribonucleoside monophosphate biosynthetic process	3	0.01	20.1
purine ribonucleoside monophosphate metabolic process	3	0.01	20.1
purine nucleoside monophosphate biosynthetic process	3	0.01	20.1
purine nucleoside monophosphate metabolic process	3	0.01	20.1
fatty acid beta-oxidation	3	0.01	18.1
ribonucleoside monophosphate metabolic process	3	0.01	16.4
ribonucleoside monophosphate biosynthetic process	3	0.01	16.4
fatty acid oxidation	3	0.01	16.4
nucleoside monophosphate biosynthetic process	3	0.02	13.9
nucleoside monophosphate metabolic process	3	0.02	13.9
peroxisome	3	0.04	9.1
microbody	3	0.04	9.1
acyl-CoA oxidase activity	3	0.01	21.9
oxidoreductase activity, acting on the CH-CH group of donors	3	0.01	17.5
Genes regulated by 4% heme			
catalytic activity	2	0.39	2.6
Genes regulated by 100% heme			
transferase activity	16	0.01	2
oxidoreductase activity	12	0.00	3.1
sugar binding	10	0.00	5.4
carbohydrate binding	10	0.00	4.6
cofactor binding	6	0.01	4.6
coenzyme binding	5	0.01	5.5
transferase activity, transferring hexosyl groups	5	0.03	4.3
transferase activity, transferring glycosyl groups	5	0.04	3.8
transferase activity, transferring groups other than amino-acyl groups	4	0.04	5.1
glutathione transferase activity	3	0.00	28.3
transferase activity, transferring alkyl or aryl groups	3	0.02	13.7
peptidoglycan catabolic process	2	0.01	138.1
peptidoglycan metabolic process	2	0.03	69

cell wall catabolic process	2	0.05	41.4
cell wall metabolic process	2	0.05	41.4
lysozyme activity	2	0.02	100.7

Table 2. Enrichment of KEGG pathways in *hrgs* and *orgs*

KEGG pathway	Number of genes	% of genes	<i>P</i> value	Fold enrichment
Genes regulated by 500 μM heme				
Purine metabolism	6	2.1	0.043	2.9
Fatty acid metabolism	5	1.7	0.025	4.1
Polyunsaturated fatty acid biosynthesis	4	1.4	0.003	12.4
alpha-Linolenic acid metabolism	3	1	0.015	14.5
Genes regulated by 100% O₂				
Metabolism of xenobiotics by cytochrome P450	6	6.5	0.000	18.4
Glutathione metabolism	4	4.3	0.003	11.4
Fatty acid metabolism	4	4.3	0.022	5.8

Gene annotation and protein families

In WormBase, 206 out of the 446 regulated genes (46%) have been given gene names based on biological functions, expression patterns, homology to known proteins, or protein-protein interactions (www.wormbase.org, release WS205). Eighteen transcription factors, including 11 zinc finger proteins and 4 F-box A proteins (*fbxa*), were transcriptionally regulated in the microarrays (Table 3). Most of them were upregulated at both low and high heme concentrations, suggesting that these transcription factors may be required for maintaining heme homeostasis through modulating gene expression.

Another interesting protein category regulated by heme was transporters (Table 3). Five out of six vitellogenins were induced at both heme concentrations, indicating that these lipid transport proteins may also play a role in intercellular heme delivery. Two recently identified heme uptake genes, *hrg-1* and *hrg-4*, were induced under heme deficiency (68). In addition, low heme altered the expression levels of three ABC transporters. The multidrug resistance protein 5 (*mrp-5*) was upregulated, while two P-glycoproteins (*pgp-5* and *pgp-6*) were down-regulated. This differential regulation suggests that these transporter genes may play distinct roles in intracellular or intercellular heme transport.

Several other known protein families such as *clecs*, UDP-glucuronosyl transferases (*ugts*), *gsts*, cytochrome P450s, and collagens were also highly enriched in the regulated genes (Table 3). In addition, a total of 57 differentially expressed genes have been identified as the targets of the insulin/IGF-1 receptor DAF-2 or the FOXO family

Table 3. Expression patterns of gene families

Protein families	Number of genes	1.5 μ M		500 μ M		100% oxygen	
		IN [‡]	DE	IN	DE	IN	DE
C-type lectin	33	6	10	13	4	7	5
Transcription factors	18	6		10	5	2	2
Transporters	15	9	3	6	1	2	
UDP–glucuronosyl transferase	15	7	4		3	4	
Glutathione S–transferase	12	2		1	2	8	
Cytochrome P450s	7	2	1		2	2	
Collagen	7	5		7			
Genes regulated by DAF-2 and DAF-16							
Class I genes ^{‡‡}	24	1	7	3	10	8	2
Class II genes	33	10	6	23	1	4	5

[‡]: IN means increase and DE means decrease in gene expression.

^{‡‡}: Class I genes are induced by DAF-2 RNAi and repressed by DAF-16; DAF-2 double RNAi. Class II genes exhibited the opposite expression profiles.

transcription factor DAF-16 (253). Since DAF-2 and DAF-16 play key roles in regulating life span (254), heme and oxygen may be involved in regulating the aging process.

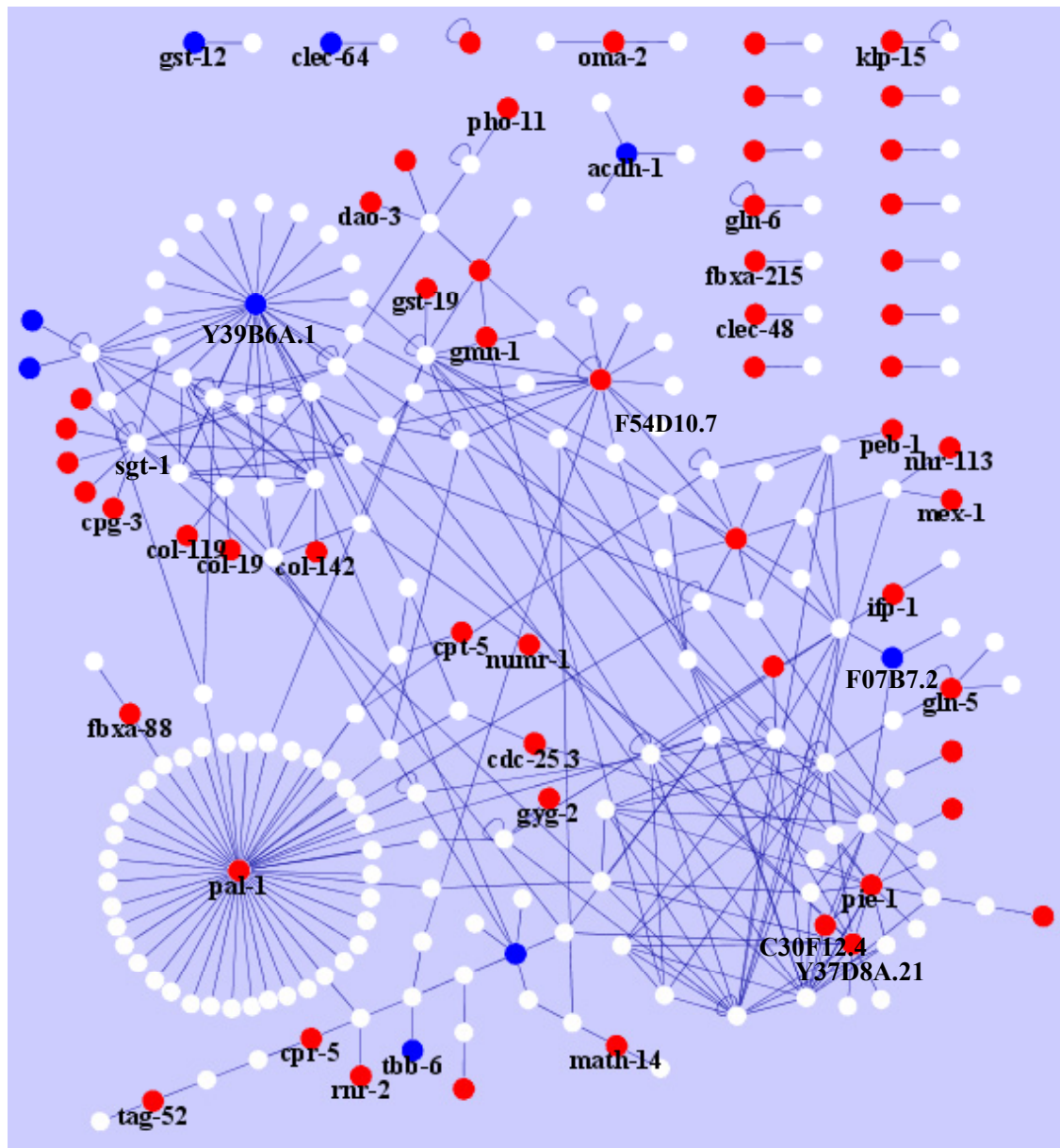
As revealed by GO and KEGG results, many regulated genes are involved in fatty acid metabolism. For example, two fatty acid CoA synthetases, *acs-2* and *acs-7*, were transcriptionally repressed at both altered heme concentrations. Acyl-CoA dehydrogenase (*acdh-1*) and carnitine palmitoyl transferase (*cpt-5*), two genes involved in β -oxidation of fatty acids, also showed decreased expression in at least one heme concentration. Furthermore, heme significantly changed expression of a number of genes that have potential roles in the metabolism and transport of lipids. These results indicate that lipid homeostasis may be perturbed by alteration of heme levels in *C. elegans*.

Worm interactome analysis

In order to understand the regulatory networks of heme and oxygen, all the identified genes were mapped to the worm interactome version 8 (WI8) by using the program Cytoscape (181,182). The WI8 dataset has ~116,000 protein-protein interactions that were derived from testing all the possible interactions among ~10,000 proteins by the yeast two-hybrid system (181,182). Of the 446 regulated genes, 55 *hrgs* and 9 *orgs* were identified in the interaction network (Figure 5.3). These genes included 8 transcription factors. Two transcription factors upregulated at 500 μ M heme, *fbxa-88* and posterior alae in males (*pal-1*), both interacted with the kinase Aurora/Ipl1 related kinase-1. Proteins encoded by several other heme-regulated genes, including geminin-1 (*gmn-1*), dauer or aging adult over-expression (*dao-3*), and intestinal acid phosphatase (*pho-11*), formed a local network with other proteins that may be involved in regulation of the cell

Figure 5.3. Interactome network of heme- and oxygen- regulated genes. Fifty five *hrgs* and 9 *orgs* were mapped to worm interactome version 8 using Cytoscape version 2.6. Blue line indicates interaction. red circles: heme-responsive genes; blue circles: oxygen-responsive genes; white circles: other genes.

A



cycle and proliferation. Additionally, a small glutamine-rich tetratricopeptide repeat protein (*sgt-1*) directly interacted with five *hrgs* and formed another sub-network.

The only possible local interactome network for proteins encoded by *orgs* was identified among Y39B6A.1, F53A9.1, and F53A9.2. They all interacted with the cysteine-rich motor neuron homolog-1 (*crm-1*). In addition, Y39B6.1 had another 25 interacting partners which include four prion-like Q/N-rich (PQN) proteins and three activated in blocked unfolded protein (ABU).

No direct interactions between proteins encoded by *hrgs* and *orgs* were observed by the interactome analysis. However, indirect connections may exist through intermediate proteins. For example, the ORG F07B7.2 may be associated with the HRGs intermediate filament protein (*ifp-1*) and C30F12.4 through T17H7.4 and R02F2.5, respectively. Another *org* encoded protein Y39B6A.1, may have indirect connections with the *hrg* encoded proteins NUMR-1, Y37D8A.21, and F54D10.7.

Identification of genes with similar expression patterns to *hrg-2* and *hrg-3*

Consistent with previous results, *hrg-2* and *hrg-3* were induced by heme deficiency (cluster 5, Figure 5.1C). However, we did not observe significant changes in *hrg-2* expression at different concentrations of oxygen. When all 27 gene chips were considered, the expression patterns exhibited significant correlation between these two genes ($r = 0.88$); 41 and 29 other genes showed similar expression patterns to *hrg-2* and *hrg-3*, respectively ($r > 0.80$, Table 4 and Table 5). Genes with the highest correlation encode such proteins as transporters, UGTs, and GSTs. In mammals, UGT1A1 is involved in the conjugation and clearance of bilirubin, one of the final products from heme degradation (255,256). Some GSTs have been identified as heme binding proteins

(86,87). However, it still needs to be determined whether any of the worm UGTs can conjugate heme and how many of the GSTs we identified interact with heme.

The ABC transporter *mrp-5* had a similar overall expression profile to *hrg-2* ($r = 0.96$), although its induction at 1.5 μM heme was only 2.93 fold. Results from our lab indicated that *mrp-5* is ubiquitously expressed in worm tissues, and it may play an essential role in heme transport (Severance *et al.*, unpublished data). The newly identified heme uptake genes, *hrg-1* and *hrg-4*, also displayed similar expression patterns to *hrg-2*. These similar expression profiles suggested that HRG-2 may be associated with heme transport.

Genes with the highest correlation coefficients to *hrg-3* included *ugt-17*, Na/Ca exchanger-6 (*ncx-6*), and *lbp-3*. Interestingly, *lbp-3* encodes a secreted protein that might function in sequestering or transporting small hydrophobic molecules (244). Since HRG-3 is also a secreted protein, they may have similar functions in heme trafficking pathways.

Discussion

C. elegans tolerates chronic moderate hypoxia

Compared to 21% O₂, 4% O₂ upregulated the expression of only four transcripts in our experiment. This number is in drastic contrast to the 110 genes identified in the microarray analysis by Shen *et al.* (2005). In that experiment, 63 HIF-1 dependent and 47 HIF-1 independent genes showed significant transcriptional responses to hypoxia in *C. elegans* (252). This discrepancy is plausibly due to the differences in the severity of hypoxia. Worms for the published microarray results were exposed to 0.1% O₂ for 4 h,

Table 4. Genes with similar expression profiles to *hrg-2*

WormBase gene ID	Gene name	Function	Correlation coefficient
F14F4.3	<i>mrp-5</i>	Multidrug resistance-associated protein, ABC superfamily	0.961
C29E4.7	<i>gst-1</i>	Thiol oxidoreductase and dehydroascorbate reductase	0.955
C08B6.1	<i>ugt-17</i>	UDP-glucuronosyltransferase	0.95
R02E12.6	<i>hrg-1</i>	Heme transporter	0.949
H23N18.1	<i>ugt-13</i>	UDP-glucuronosyltransferase	0.924
F36H1.5	<i>hrg-4</i>	Heme transporter	0.923
F40F4.4	<i>lbp-3</i>	Lipid binding protein	0.894
C33A12.6	<i>ugt-21</i>	UDP-glucuronosyltransferase	0.888
F58E6.7	<i>hrg-3</i>		0.881
F37B1.6	<i>gst-17</i>	Glutathione S-transferase	0.88
F58G6.2	<i>srm-3</i>	Serpentine receptor, class M	0.871
C07A9.4	<i>ncx-6</i>	Na/Ca exchangers	0.848
F42G9.5	<i>alh-11</i>	Aldehyde dehydrogenase	0.847
ZC443.6	<i>ugt-16</i>	UDP-glucuronosyltransferase	0.839
M02H5.4	<i>nhr-202</i>	Nuclear hormone receptor	0.818
T07C5.1	<i>ugt-50</i>	UDP-glucuronosyltransferase	0.818
C31H5.3	<i>acr-19</i>	Acetylcholine receptor	0.816
C45B2.5	<i>gln-1</i>	Glutamine synthetase	0.802
C02F12.1	<i>tsp-17</i>	Tetraspanin family	0.801

Table 5. Genes with similar expression profiles to *hrg-3*

WormBase gene ID	Gene name	Function	Correlation coefficient
C08B6.1	<i>ugt-17</i>	UDP-glucuronosyltransferase	0.917
K01D12.14	<i>hrg-2</i>		0.881
C07A9.4	<i>ncx-6</i>	Na/Ca exchangers	0.878
F40F4.4	<i>lbp-3</i>	Lipid binding protein	0.869
C29E4.7	<i>gst-1</i>	Thiol oxidoreductase and dehydroascorbate reductase	0.863
F07C4.9	<i>cllec-46</i>	C-type lectin	0.859
R02E12.6	<i>hrg-1</i>	Heme transporter	0.852
ZC443.6	<i>ugt-16</i>	UDP-glucuronosyltransferase	0.847
F37B1.6	<i>gst-17</i>	Glutathione S-transferase	0.844
F14F4.3	<i>mrp-5</i>	Multidrug resistance-associated protein, ABC superfamily	0.843
H23N18.1	<i>ugt-13</i>	UDP-glucuronosyltransferase	0.826
F36H1.5	<i>hrg-4</i>	Heme transporter	0.818
T19H12.9	<i>ugt-12</i>	UDP-glucuronosyltransferase	0.813

which could be classified as severe acute hypoxia. In contrast, the worms for our study were treated with chronic moderate hypoxia (two successive generations at 4% O₂).

HIF-1 is the key regulator of the hypoxia responses in metazoans. Under normal oxygen levels, the HIF-prolyl hydroxylase, an enzyme that requires oxygen and iron, induces the hydroxylation of a proline residue in HIF-1 α (257,258). Hydroxylated HIF-1 α is rapidly degraded through ubiquitylation by the von Hippel-Lindau tumor suppressor E3 ligase (257,258). When oxygen concentration decreases, HIF complexes are stabilized. In *C. elegans*, HIF-1 protein showed only a negligible increase when the O₂ level dropped to 5% for 16 h. Even at 1% O₂ for 16 h, the increase in HIF-1 protein levels was very mild. The maximal induction of HIF-1 was only observed when the worms were grown at $\leq 0.5\%$ O₂ (257,258). Based on the stability of HIF-1 proteins, the 4% O₂ concentration used in our study did not induce a severe hypoxic response.

Although *C. elegans* prefer an optimum concentration of 6% O₂ (118), studies on the metabolic rates suggest that *C. elegans* can tolerate a broad range of oxygen levels. No obvious changes in metabolic rates were observed when worms were maintained at 4% -100% O₂ (163). Surprisingly, even under anoxic condition, worms can survive for >24 h (163). Our observation that only four genes were transcriptionally perturbed at 4% O₂ further confirmed that *C. elegans* can easily adapt to moderate hypoxia. This adaptation could be due to the commonly low oxygen tension in the soil, which is the natural habitat for *C. elegans* (163).

It is worth mentioning that one of the oxygen-regulated genes, F22B5.4, was among the top three HIF-1 targets identified in previous microarray analyses (251,252). In our study, the mRNA level of F22B5.4 was increased by 2.76 fold at 4% O₂ and reduced by

3.44 fold at 100% O₂. Another known HIF target, prolyl 4-hydroxylase α subunit (*phy-2*), showed a 1.62-fold induction at low oxygen and a 2.15-fold down-regulation at 100% O₂. Knock-down of F22B5.4 or deletion of *phy-2* led to higher embryonic lethality under hypoxic conditions, whereas no obvious embryonic phenotype was observed when these worms were maintained under normal O₂ levels (252). These results strongly suggest that F22B5.4 and *phy-2* play critical roles in the tolerance to hypoxic conditions.

Oxygen-regulated genes play important roles in hyperoxia resistance

High concentrations of oxygen are often applied to treat patients with ischemic stroke, brain trauma, neurologic and cardiopulmonary disorders (259). However, hyperoxia inevitably increases the levels of reactive oxygen species (ROS), and therefore leads to oxidative stress and even tissue damage. Cells have evolved multiple mechanisms to defend against hyperoxia. It has been shown in mammals that superoxide dismutases, catalases, heat shock proteins, and metallothioneins are induced under hyperoxic conditions (260-263). In addition, phase II detoxifying enzymes such as GSTs, UGTs, heme oxygenase-1, and NAD(P)H:quinone oxidoreductase-1 have been suggested to play protective roles against oxidative stress (264,265).

We have identified 69 genes (61 in clusters 12, 7 in cluster 13, and 1 in cluster 14) that were induced by hyperoxia in *C. elegans*. Interestingly, eight GSTs and three UGTs were significantly upregulated. All the eight GSTs were recently shown to be induced by oxidative stress in *C. elegans* (266). Knock-down of the bZip transcriptional factor *skn-1* reduced their expression by at least 60%, suggesting that the induction of GSTs by oxidative stress is dependent on this stress-responsive factor (266). These data are consistent with previous results in mice, which showed that the mRNA levels of both

GST-Y α and UGT in lungs were significantly increased after the animals were maintained in pure oxygen for 72 h (264). Another study in mice showed that GST-Pi1 and GST-Mu2 were among the top in a list of genes induced by hyperoxia (267). These results suggested that induction of certain species of GSTs and UGTs under hyperoxic conditions may be important for cellular defense against oxidative stress.

Two cytochrome P450 genes, *cyp-35B2* and *cyp-33C8*, were also induced under hyperoxic conditions. Cytochrome P450 proteins are heme-containing enzymes catalyzing monooxygenase reactions, which are commonly associated with the generation of ROS (268). It has been shown that ROS negatively inhibited the *CYP1A1* gene at the transcriptional level in hepatoma cell lines (269). In contrast to ROS, hyperoxia has been shown to induce the expression of *CYP1A1*. For example, increased levels of CYP1A1 and CYP1A2 proteins have been observed in the livers of rats exposed to >95% O₂ for 24 and 48 h (270). Detailed examination confirmed that these two genes were induced by hyperoxia at the transcriptional level (271). In our microarray study, two cytochrome P450s were also induced by hyperoxia. One of the two genes, *cyp-33C8*, showed the highest fold change (41.9) among the 11 cytochrome P450 genes induced by oxidative stress (266). Furthermore, studies in human lung cell lines and rats showed that activation of CYP1A1/A2 significantly reduced cell death and lung injury caused by hyperoxia (272,273). It will be interesting to test whether CYP-35B2 and CYP-33C8 have protective effects against hyperoxia in *C. elegans*.

Furthermore, two acyl-CoA dehydrogenases and three O-acyltransferase homologs were significantly upregulated by hyperoxia. *acdh-1* showed the highest fold induction (17.74 fold) by 100% O₂ among all the genes tested (Appendix VIII). Thus, alterations in

lipid metabolism may contribute to hyperoxia resistance, possibly by preventing the accumulation of lipid peroxides.

Heme uptake systems induced by heme deficiency

In this study, nineteen genes regulated by low heme were predicted to have transporter activities by GO analysis. Two more proteins in this regulatory category, HRG-1 and HRG-4, have recently been identified as heme importers in *C. elegans* (68). In the worm, HRG-4 transports heme across the apical plasma membrane and HRG-1 is responsible for mobilizing heme out of lysosome-like vesicles (68). Similar to the phenotype of *hrg-4*, knock-down of *mrp-5* significantly increased the resistance to the toxic heme analog gallium protoporphyrin IX (Severance *et al.*, unpublished data). This suggests that *mrp-5* may also play an essential role in heme uptake. In addition, vitellogenin genes were highly induced by alterations in heme concentration. In ticks and other insects, vitellogenins have been shown to bind heme and they are thought to be involved in delivering heme to embryos (58,59). Maternal effects of heme have been observed in *C. elegans*, indicating that some heme is deposited into the developing embryos from somatic cells (Rao *et al.*, unpublished data). Regulated expression of vitellogenins may indicate that they are one of the major players in this transport process.

In addition to heme transporters, genes predicted to encode proteases were also induced by heme deficiency. These putative proteases include two cysteine proteinases cathepsin L (W07B8.1, F32H5.1), two serine carboxypeptidases cathepsin A (K10B2.2, Y40D12A.2), an aspartic protease (C15C8.3), and a metallopeptidase neprilysin (F18A12.4). It has been shown that in blood-feeding parasitic worms, the ingested hemoglobin is digested by a semi-ordered proteolytic pathway that contains aspartic

proteases, cysteine proteases, metalloproteases and exopeptidases (158,274). Knock-down of aspartic protease cathepsin D in *Schistosoma mansoni* resulted in the accumulation of intact hemoglobin in the gut (275). Since the natural food for free-living worms is bacteria, *C. elegans* must have developed an efficient proteolytic system that is responsible for heme acquisition from bacterial hemoproteins. The increased expression of these putative proteases under heme-deficient conditions suggests that they could play important roles in hemoprotein digestion.

Pulse-labeling experiments using zinc mesoporphyrin IX suggested that the heme uptake system was significantly upregulated in response to heme deficiency in *C. elegans* (68). This observation could be explained by the induction of heme transporters and diverse families of proteases.

Biological connections between heme and oxygen in *C. elegans*

In biological systems, heme and oxygen are closely intertwined with each other. On one hand, oxygen is required as an electron acceptor in the heme biosynthetic pathway (138). On the other hand, hemoproteins play critical roles in oxidative stress control as well as the transport and storage of oxygen. Moreover, heme has been shown to regulate the activity of mouse epithelial sodium channels in an oxygen-dependent manner (276). In *C. elegans*, oxygen sensing has been shown to be mediated predominantly by the heme-containing proteins, soluble guanylate cyclases and a neural globin (118,120,277). In a genome-wide RNAi screen, the *org* F22B5.4 was identified as an important modulator of heme sensor *IQ6011* (Severance *et al.*, unpublished data), suggesting it may play a role in both oxygen sensing and heme homeostasis. In addition, we have identified 18 genes that were transcriptionally regulated by both heme and oxygen. Only 50% of

these genes have been named in WormBase. They include four *clecs*, two lysozymes, one *ugt*, one enoyl-CoA hydratase, and one saposin-like protein. Even though, the biological functions of most of these proteins are still unclear. It is likely that further studies of these genes may provide more mechanistic insights into the interplay between heme and oxygen sensing.

Chapter 6: Conclusions and future directions

Conclusions

The long term objective of our lab is to dissect the heme trafficking pathways in eukaryotes. Toward this goal, the free-living worm *C. elegans* was used as a model system because it lacks the whole heme biosynthetic pathway and therefore provides a clean genetic background for studying heme homeostasis (160). An Affymetrix *C. elegans* genome array experiment was performed using RNA extracted from worms that were grown at low (4 μ M), optimal (20 μ M), and high (500 μ M) heme in axenic liquid medium (68). Of the 288 genes that showed significant changes in gene expression, the mRNA levels of two genes, *hrg-2* and *hrg-3*, increased by >70 fold when worms were grown at 4 μ M compared to 20 μ M heme. In the past several years, we performed extensive cell biological and genetic studies on these two novel genes and investigated their possible roles in heme homeostasis in *C. elegans*. The major findings in this study are listed and discussed as follows:

hrg-2

- 1) *hrg-2* is induced by heme deficiency in *C. elegans*. It exhibits strong sequence homology to the family of *cdrs*. However, *hrg-2* is only responsive to heme, whereas the heavy metal cadmium significantly induces *cdr-1* expression.
- 2) *hrg-2* encodes a protein of 279 amino acids, which is a type I membrane protein with a single transmembrane domain at the amino-terminus. In addition, HRG-2 contains a GST-N metaxin-like domain and a GST-C metaxin domain.

- 3) Deletion of *hrg-2* in *C. elegans* resulted in reduced worm growth at low concentrations of heme, indicating the requirement of HRG-2 under these conditions.
- 4) In *C. elegans*, *hrg-2* is expressed in the hypodermal tissues, and the protein localizes to fibrous organelles, the apical plasma membrane, as well as the ER. Possible interactions and heme transfer may exist between HRG-2 and the heme-containing enzymes cytochrome P450s because they have identical topology on the ER. HRG-2 has similarities to Grx3/4 proteins which contain an N-terminal thioredoxin domain and a C-terminal glutaredoxin domain. The thioredoxin domain is essential for hydrophobic interactions with other proteins while the glutaredoxin domain binds and possibly delivers the Fe-S clusters (278,279).
- 5) HRG-2 binds heme and may be involved in heme delivery or trafficking.
- 6) Ectopic expression of HRG-2 rescues the growth of heme-deficient yeast strain *hem1Δ* at low concentrations of heme, possibly through increasing the availability and utilization of heme. The maximum rescuing effect was observed at 0.1 μM, indicating that HRG-2 functions under low heme concentrations, a feature supported by its transcriptional upregulation under low heme in *C. elegans*.

hrg-3

- 1) *hrg-3* is transcriptionally activated in the intestine when *C. elegans* is grown at low concentrations of heme. *hrg-3* specifically responds to heme but not to iron and protoporphyrin IX.
- 2) We have identified a 43-bp region in *hrg-3* promoter that is responsive to heme levels. This region contains a conserved GATA element, which is the binding site for the intestine-specific transcription factor ELT-2. In addition, we have confirmed a

functional element for the stress-responsive transcription factor SKN-1 within this 43-bp region, suggesting that HRG-3 may be involved in responses to environmental stresses.

- 3) The unprocessed full-length HRG-3 protein contains 70 amino acids. Following its synthesis in the intestine, HRG-3 is secreted into the body cavity pseudocoelom possibly as a 45-amino acid mature peptide.
- 4) Deletion of *hrg-3* in *C. elegans* led to an increase in the intestinal heme levels as reported by the heme sensor strain *IQ6011*.
- 5) Ectopic expression of HA-tagged HRG-3 in *hem1Δ* yeast strain dramatically reduced the growth of yeast cells. However, this is not due to overall heme deficiency since we did not observe any decreased activity of the heme-activated CYC1 promoter. Since HRG-3 protein accumulates in the form of unprocessed preprotein inside yeast cells, it is possible that HRG-3 perturbed intracellular homeostasis or compartmentalization of heme within yeast cells.

Heme oxygen microarray

- 1) We identified 369 and 94 genes that are significantly regulated by heme and oxygen, respectively. Among them, 18 genes were responsive to both heme and oxygen.
- 2) Only 4 genes were differentially expressed in response to 4% O₂, confirming that *C. elegans* can tolerate moderate hypoxia.
- 3) Hyperoxia induces the expression of 69 genes, which include 8 GSTs, 3 UGTs, and 2 CYP450s. These genes may play a role in the resistance to hyperoxia.
- 4) Results from the microarray indicate that heme uptake systems are upregulated when *C. elegans* is grown at low heme. More specifically, both the heme transporters and

the putative proteases involved in heme uptake are enriched in the genes regulated by 1.5 μ M heme.

- 5) Based on the results from all 27 *C. elegans* genome arrays, we identified 41 and 29 genes that showed similar expression profiles to *hrg-2* and *hrg-3*, respectively. By knocking down these genes in the deletion background of *hrg-2* or *hrg-3*, we may be able to see more dramatic phenotypes that are dependent on heme concentrations.

Significance and speculations

The free-living roundworm *C. elegans* and related helminths are unable to synthesize heme *de novo*, although they require this tetrapyrrole for diverse biological functions and growth (160). Accordingly, worms must have developed efficient pathways for the uptake and intercellular transport of heme, in order to meet their nutritional requirement. Our lab has previously discovered two heme transporters, HRG-1 and HRG-4, which play an essential role for heme uptake in the worm intestine (68). In this dissertation, we identified two novel heme-responsive genes that are highly induced by heme deficiency in *C. elegans*. Our results support a model in which *hrg-2* is involved in the heme uptake in hypodermal cells, and *hrg-3* plays a role in intercellular heme trafficking. Due to the lack of genomic sequence information from parasitic nematodes, it is unclear whether homologs of *hrg-2* and *hrg-3* exist in helminths which are heme auxotrophs. The discovery of *hrg-2* and *hrg-3* has provided new insights into the heme trafficking pathways in worms. If these pathways are specific to nematodes, they could eventually be used as potential drug targets for helminthic infections. In addition, the findings in this work may help in defining a paradigm for heme homeostasis in other eukaryotes including mammals.

Heme regulates the expression of many genes that are involved in diverse biological processes. Bach1, Rev-erb α , and Hap1 are three heme-regulated transcription factors that have been well characterized. In this study, we identified a 43-bp heme-responsive sequence. This region contains the functional binding sites for ELT-2 and SKN-1. These two transcription factors may work in conjunction with other molecules and specifically regulate a subset of genes in a heme-dependent manner.

To our knowledge, *hrg-3* is the first heme-responsive gene that encodes a secreted protein. Beyond the possible role in intercellular heme trafficking, HRG-3 may be involved in heme-regulated signaling. It could work in a similar way to or in concert with the major yolk protein vitellogenins and thus deliver heme to oocytes and developing embryos. Alternatively, HRG-3 may resemble hepcidin, which is secreted into circulatory system to negatively regulate iron export.

Finally, we have identified 446 genes that are differentially regulated by heme and/or oxygen. In addition to the list of genes with similar expression profiles to *hrg-2* and *hrg-3*, we also found several interesting cellular processes that are associated with heme regulated genes. Further study on the functions associated with heme-responsive genes may lead to deeper insights into the understanding of heme uptake and transport. The molecules upregulated by 100% O₂ may have significance in the resistance to hyperoxia. The 18 genes regulated by both heme and O₂, as well as the sub-interactome map, will provide a large-scale basis for dissecting the regulatory network between heme and O₂.

Future directions

Ectopic expression of HRG-2 in the worm intestine

The functional characterization of HRG-2 in *C. elegans* was limited because there is no direct method to measure the heme content in hypodermal cells. In contrast, our lab has established tools to report the intestinal heme levels, such as *IQ6011* heme sensor strain and the fluorescent heme analog ZnMP.

We have engineered HRG-2-mCherry to be expressed in the intestine by using the intestine-specific *vha-6* promoter. In the *IQ8322* transgenic worm strain, HRG-2-mCherry is predominantly localizes to the apical plasma membrane. It will be very interesting to see whether the intestinal heme levels are changed because of HRG-2 expression. Based on the current results of HRG-2, we expect that the *IQ8322* worms will have an increased ZnMP uptake and a higher sensitivity to gallium protoporphyrin IX (GaPP) toxicity. After crossing into the heme sensor strain, we would expect to see a decreased GFP intensity. These phenotypes may only be observed when the transgenic worms are grown at low heme. However, there are three caveats for this experiment. First, HRG-2-mCherry protein may not be functional due to the interference of the mCherry tag at the C-terminus. Second, heme uptake system in intestinal cells may be different to that in the hypodermal cells. Thus, the function of HRG-2 may require certain auxiliary molecules or interacting proteins that only present in the hypodermal tissues. Third, if HRG-2 is a reductase, ZnMP and GaPP assays will not provide meaningful results because neither heme analogs need to be reduced.

Examination of the possible hemin reductase activity for HRG-2

In the cells, hemin (heme containing an oxidized iron) has to be reduced for its covalent attachment to such hemoproteins as cytochrome c (208,209). HRG-2 may function as a membrane-associated heme reductase thereby increasing the efficiency of cellular heme utilization. An obstacle to directly testing this possibility has been the lack of success in expressing and purifying HRG-2 for biochemical assays. To circumvent this problem, we could express HRG-2 in either yeast or mammalian cells and determine the activity of hemin reductase in crude cell lysates.

Identification of the possible target tissues for HRG-3

When expressed under the intestine-specific promoters, both HRG-3-YFP and HRG-3-mCherry localized to coelomocytes in addition to the intestinal cells. These results suggest that HRG-3 is secreted from the intestinal cells into the pseudocoelom. However, the uptake of HRG-3 proteins by coelomocytes may be an artifact due to the presence of an YFP tag. Identification of HRG-3 target tissues will help in unveiling the biological functions of HRG-3 because we expect the phenotypes to be predominantly associated with the target cells in addition to the cells that synthesize HRG-3. Endogenous HRG-3 could either be located within the pseudocoelom, coelomocytes, or other target tissues. Following its secretion from the intestine, the majority of HRG-3 may stay and function in the pseudocoelom. The fact that we have not yet observed any HRG-3 chimera proteins in pseudocoelom may be due to the quick clearance by coelomocytes. Second, we observed much higher signal of HRG-3-mCherry in coelomocytes than that in intestine cells, supporting the concept that HRG-3 is destined to reside in coelomocytes. Third, HRG-3 is taken up by other tissues such as oocytes and

developing embryos from the pseudocoelom and functions in a similar manner to vitellogenins. We have shown that young adult hermaphrodites have the highest mRNA level of *hrg-3* and the male worms have reduced *hrg-3* expression. We plan to knock down the genes responsible for the endocytosis in coelomocytes in transgenic worms expressing HRG-3-mCherry and examine whether the HRG-3-mCherry appears in other tissues.

Heme binding assays for HRG-3

As previously mentioned, HRG-3 could act as a heme carrier or a signaling molecule. One of the key experiments to differentiate between these two possibilities is to test whether the mature HRG-3 protein interacts with heme. By prediction, the majority of the 45-amino acid HRG-3 peptide is present as random coils. If HRG-3 is a heme carrier, we expect to see a more ordered structure in the presence of its cognate ligand. To examine this possibility, we synthesized a 45-amino acid HRG-3 peptide and plan to determine its secondary structures in the absence or presence of heme using NMR. We will corroborate this result with gel-filtration and reverse phase chromatography.

Detailed understanding of the role SKN-1 plays in *hrg-3* regulation

We have shown that the activation of *hrg-3* requires the transcription factor SKN-1, which is known to induce the expression of phase II detoxification genes (248). Thus, it is possible that heme deficiency results in cellular stress, which in turn induces *hrg-3* expression through SKN-1.

Studies have shown that in response to oxidative stress, SKN-1 protein accumulates in the intestinal nuclei to activate downstream gene expression (280). We have received the transgenic line expressing SKN-1-GFP from Dr. Krause's lab, and plan to grow the

worm in different concentrations of heme to test whether heme deficiency changes the subcellular localization of SKN-1.

To further find out whether *hrg-3* is a phase II detoxification gene, we plan to examine the expression of *hrg-3* in the presence of stress inducers. The *hrg-3::gfp* transgenic worms will be treated with paraquat, which generates intracellular superoxide anions, and GFP intensity and localization will be monitored. To test the effect of thermal stress, which is another inducer of SKN-1 activity (248), we plan to grow these transgenic worms at 29 °C for 20 h and analyze the reporter activity.

Knock-down of other genes in *hrg-2* and *hrg-3* deletion strains

Both *hrg-2* and *hrg-3* deletion worms are viable, and they do not have apparent morphological phenotypes. This suggests that there may exist redundant molecules or parallel pathways. Our microarray results reveal 41 and 29 genes which show similar expression profiles to *hrg-2* and *hrg-3*, respectively. It's highly possible that some of these genes are coordinately regulated with *hrg-2* or *hrg-3* because they may function together. By depleting these genes in *hrg-2/hrg-3* deletion worms, we may be able to observe synthetic phenotypes that are dependent on heme concentrations. Furthermore, RNAi of *cdrs* in *hrg-2* deletion background may also lead to a dramatic phenotype.

Appendices

Appendix I. Deletion worm strains and genotyping primers

Strain	Allele	Deleted region	Sense primer	Anti-sense primer
<i>hrg-2</i>	<i>tm3798</i>	-46 to +456	TTTATGCTCTTCCTGCGAG	TATACCATGCATCCTCTGC
<i>cdr-4</i>	<i>ok863</i>	-432 to +827	CTCAACTACACACGTTCTC	[‡] GAGATTAGATGGAACAAACC
<i>hrg-3</i>	<i>tm2468</i>	-77 to +141	ACCCGTATCTTCATTCTCC	GGATGAGAAATTTAACATTAT CACTTACATC

[‡]: PCR reactions for *cdr-4* genotyping include two primers shown above and a third primer. The sequence of this anti-sense primer is “TCCTTATGAGGTTTGAGATC”.

Appendix II. Worm reporter constructs

Gene	Strain	Vector	Promoter	Gene	3' UTR
<i>hrg-2</i>	<i>IQ8021</i>	pPD95.67	<i>hrg-2</i> , 1.5kb	NLS-GFP	<i>unc-54</i>
	<i>IQ8022</i>	pPD95.67	<i>hrg-2</i> , 1.5 kb	NLS-GFP	<i>hrg-2</i>
	<i>IQ8023</i>	pPD95.67	<i>hrg-2</i> , 0.5 kb	NLS-GFP	<i>unc-54</i>
	<i>IQ8024</i>	pPD95.67	<i>hrg-2</i> , 3 kb	NLS-GFP	<i>unc-54</i>
	<i>IQ8025</i>	pPD95.67	<i>hrg-2</i> , 6 kb	NLS-GFP	<i>unc-54</i>
	<i>IQ8122</i>	pDEST-R4R3	<i>hrg-2</i> , 1.5 kb	<i>hrg-2</i> ::YFP	<i>hrg-2</i>
	<i>IQ8123</i>	pDEST-R4R3	<i>hrg-2</i> , 1.5 kb	<i>hrg-2</i> ::YFP	<i>hrg-2</i>
	(double)	pDEST-R4R3	<i>dpy-7</i>	mCherry::TRAM	<i>unc-54</i>
	<i>IQ8321</i>	pPD49.78	<i>hsp-16</i>	<i>hrg-2</i> ::YFP	<i>hrg-2</i>
	<i>IQ8322</i>	pDEST-R4R3	<i>vha-6</i>	<i>hrg-2</i> ::mCherry	<i>hrg-2</i>
<i>hrg-3</i>	<i>IQ8031</i>	pPD95.67	<i>hrg-3</i> , 3 kb	NLS-GFP	<i>unc-54</i>
	<i>IQ8032/ Δ1</i>	pPD95.67	<i>hrg-3</i> , (-732 to +7)	NLS-GFP	<i>unc-54</i>
	<i>IQ8035/ Δ2</i>	pPD95.67	<i>hrg-3</i> , (-295 to +7)	NLS-GFP	<i>unc-54</i>
	<i>IQ8036/ Δ3</i>	pPD95.67	<i>hrg-3</i> , (-194 to +7)	NLS-GFP	<i>unc-54</i>
	<i>IQ8037/ Δ4</i>	pPD95.67	<i>hrg-3</i> , (-132 to +7)	NLS-GFP	<i>unc-54</i>
	<i>IQ8038/ Δ6</i>	pPD95.67	<i>hrg-3</i> , (-92 to +7)	NLS-GFP	<i>unc-54</i>
	<i>IQ8039/ Δ5</i>	pPD95.67	<i>hrg-3</i> , (-112 to +7)	NLS-GFP	<i>unc-54</i>
	<i>IQ8532/ Δ7</i>	pPD95.67	<i>hrg-3</i> , (-112 to -68; -49 to +7)	NLS-GFP	<i>unc-54</i>
	<i>IQ8133</i>	pDEST-R4R3	<i>hrg-3</i> , 3 kb	<i>hrg-3</i> ::YFP	<i>hrg-3</i>
	<i>IQ8333</i>	pDEST-R4R3	<i>vha-6</i>	<i>hrg-3</i> ::mCherry	<i>hrg-3</i>
	<i>IQ8531/mut1</i>	pPD95.67	<i>hrg-3</i> , mut1 [‡]	NLS-GFP	<i>unc-54</i>
	<i>IQ8631</i>	pPD95.67	<i>Cbrhrg-3</i> , (-300 to 0)	NLS-GFP	<i>unc-54</i>
	<i>IQ8731</i>	pKKMCS	<i>hrg-3</i> , (-132 to +7)	NLS-GFP	<i>unc-54</i>
	<i>IQ8732/con1</i>	pKKMCS	<i>hrg-3</i> , 43bp, 4mer [‡]	NLS-GFP	<i>unc-54</i>
	<i>RT1315[#]</i>		<i>vha-6</i>	MANS-GFP	

[‡]: This construct has the 139 bp *hrg-3* promoter region (-132 to +7 bp) in which the putative SKN-1 binding motif (-92 to -84 bp) was mutated. [‡]: This construct contains four repeats of the conserved region (-112 to -69 bp) from *hrg-3* promoter. [#]: This strain was a gift from Dr. Barth Grant. UTR: untranslated region. NLS: nuclear localization signal. TRAM: translocating chain associated membrane protein.

Appendix III. Primers for Northern blot, qRT-PCR, and RACE

Gene	Experiment	Sense primer	Anti-sense primer
<i>hrg-2</i>	qRT-PCR	GCCTGGCTGATAATCATCTCTTG	ATGGACCTTCTTCATAAATAACT TTCG
	Northern RACE	GCTGAAATGTTATGTCACAAAG GCCACTGCACTTTGTCGCCTGGC	TTATTGCCACAGAGATACAGG GCTTCATCTTCTGTGAAGTTTCCG ATGGC
<i>cdr-1</i>	qRT-PCR	CGTACTTATACGATTTAAAATTG CTGTC	TCTGTGAAGAATCTCGTCGAGC
<i>cdr-2</i>	qRT-PCR	AAGGACACCGTCTACCTATAACC	GGAATTGAACCGTTTCTTGACC
<i>cdr-4</i>	qRT-PCR	CGGAGATTTTGAACCACAAGAA C	CGGTCAGATGAGAACGAATAGG
<i>cdr-7</i>	qRT-PCR	GCTTCTGCTGCTGCTATTTATG	GAGACGGCGGAATTGATAGAG
<i>hrg-3</i>	qRT-PCR	TCTTGTAAGTCTTTTAATCATACT TCTTTTC	ACCTTCTTCTGAATCAGTTTGC
	Northern	ATGGTCAATTTACAAGGTC	TTATCCACCAAAAAACGAGTCAC TC
	RACE	CCAATGTGGAAGTTCGGCCGGT TATG	TCCACCAAAAAACGAGTCACTCG CAGTG

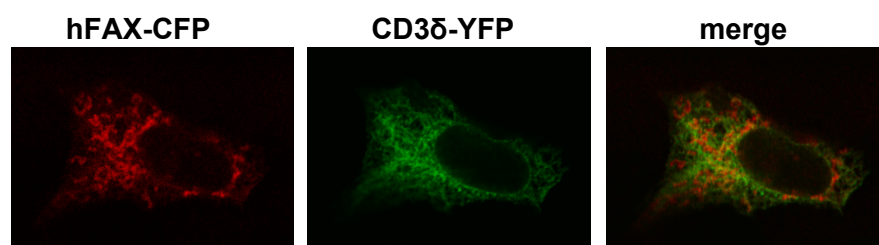
Appendix IV. qRT-PCR primers for microarray experiment

Gene	Sense primer	Anti-sense primer
K10B3.8	TGCTCACGAGGGAGACTAC	CGGTGGACTCAACGACATAG
W03G1.7	CACTTCACTTGACCGACCTTC	CGCACGAACCAACACTTCC
F09G2.3	ATTGCTCCGCTTGTTGCTC	CCTGATGCTGGATTGACTTCG
C15C8.3	TCTCTCCGCTGAAGATGAATC	TTAGACAATTAGGACCAGGAACT C
F15B9.6	AATCATCTTAGCGAAGCCGAAG	CTTGTTCCAGTTGTTGAGAATGC
C10G8.4	GCCGATTTC AACAGTCCTATTTTC	GGTTCACAAGCCGTTCCAC
ZK813.1	CATCGTCCTCCTCGCTCTC	ACTATGTCTTCTTCCATGTCTTCC
F55G11.4	TCTCCAGACGCATTCACTCTC	GCCACTGCTGACCACAAAC
Y62H9A.6	TCTGTCACTTGCTCTTGTATGC	CTCTCTTTCTTCACTGCTGTCTG
K01D12.14	GCCTGGCTGATAATCATCTCTTG	ATGGACCTTCTTCATAAATAACTT TCG
F58E6.7	TCTTGTAAGCTTTTAATCATACTTCTTTT C	ACCTTCTTCTGAATCAGTTTGC
C10C5.5	TTAAATATGCTGACGAACTTGGAATC	GCTCACGGAATGTTGGAACACTAC
K08F4.7	TTGATGCTCGTGCTCTTGC	AATGGAGTCGTTGGCTTCAG
C34H4.1	ACTCTGGTCTTGTTGAATGTTCG	CTGCCTGCTGGTCTCCTG
W06H8.2	AATGGGGAAATGGACAGTTTGG	GAGAGCACCGTCTTGTTTGG
F22A3.6	TGCCTGGAAGAGATGTGCTG	TGGTCCTCCGTTGTGGTTAC
F22B5.4	CGGTACGCTTATGAAGTATATCC	GTCACGAAGTCTCTCCCAGTC
T24B8.5	TATCTCATCGGATTTGTGATTGTG	GGAGTATCGGTAACGCAGAC
F08F8.5	AACTGGAGGATTCGGAAGACC	AAATCTGCGTTCAAATGGATGTTG
F59D8.2	ATTCCACCGCTCTTACCTTCTC	TCATCGTAGTTGCTCTCGTAGTC
F15E11.15	CGAGACGGAAGGAAGTATTGC	CTTGGCGAAATGAACTGAACC

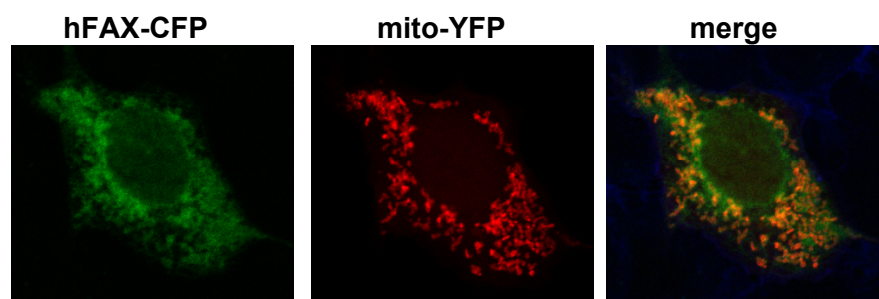
Appendix V. Localization of putative human FAX in HEK293 cells.

(A) Putative hFAX did not co-localize with the ER marker CD3 δ -YFP. **(B)** Putative hFAX shows the same localization pattern as the mitochondrial markers mito-YFP. Putative human FAX: C6orf168 (gene) or NP_115900.1 (protein). Blue color in the merged image on the bottom shows the plasma membrane of the cells.

A

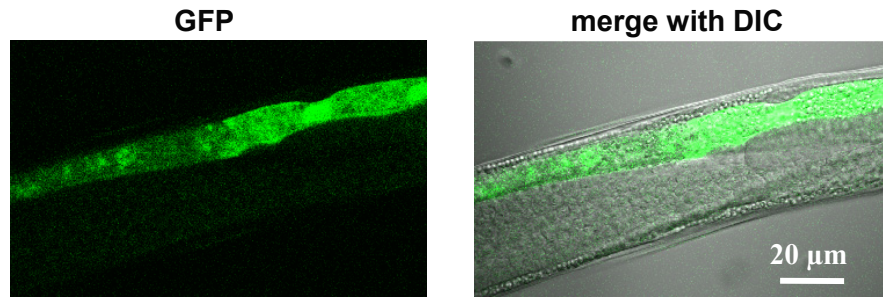


B



Appendix VI. Detection of *hrg-3* expression in male worms.

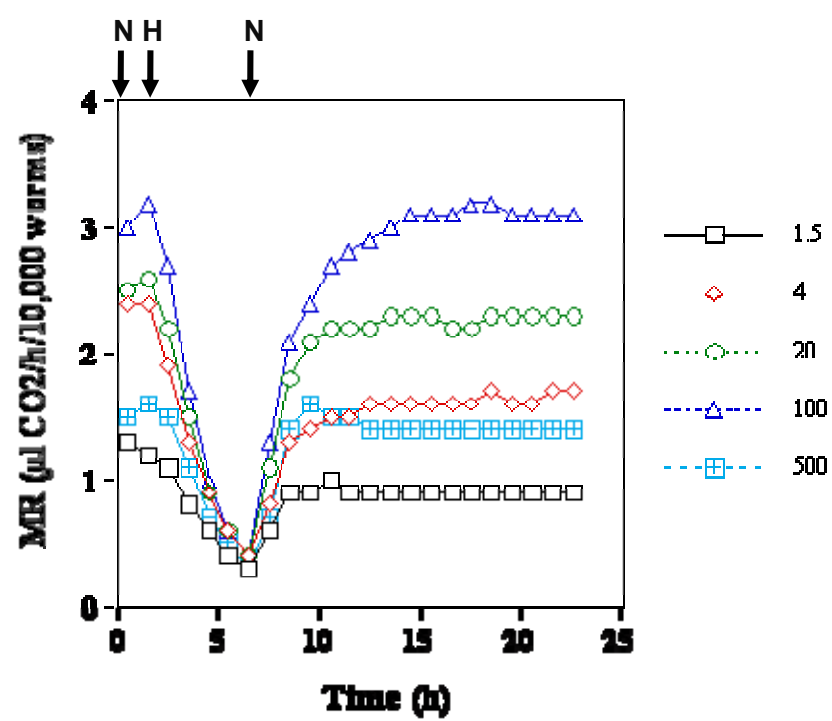
The *IQ8031* worms (rollers) carrying *hrg-3* transcriptional fusion constructs were crossed with N2 males. Progeny male worms with the roller phenotype were moved to mCeHR-2 medium supplemented with 2 μ M heme; GFP expression was analyzed 3 d after growth.



IQ8031 (hrg-3-3kb::gfp), male worm

Appendix VII. Effects of heme on the metabolic rates of *C. elegans*.

Worms grown at five concentrations of heme were moved to 21% O₂ for 2 h, and then exposed to graded hypoxia for 5 h followed by recovery at 21% O₂ for 15 h. The metabolic rate was monitored by measuring CO₂ production. This experiment was performed by Dr. Wayne Van Voorhies at New Mexico State University. N: normoxia. H: hypoxia.



Appendix VIII. The expression profiles of *hrgs* and *orgs*

WormBase gene ID	Gene name	heme (μ M)				Oxygen (%)			
		1.5 vs 20		500 vs 20		4 vs 21		100 vs 21	
		Fold change	<i>q</i> value	Fold change	<i>q</i> value	Fold change	<i>q</i> value	Fold changes	<i>q</i> value
AC3.8	<i>ugt-2</i>	1.77	0.01	-1.15	0.01	1.18	0.01	2.23	0.01
B0024.4		1.24	0.03	2.25	0.03	1.28	0.64	1.06	0.64
B0218.8	<i>cllec-52</i>	-8.64	0.00	2.00	0.00	-1.02	0.74	1.04	0.74
B0286.3		-1.45	0.00	-2.08	0.00	1.06	0.64	1.14	0.64
B0286.6	<i>try-9</i>	-1.50	0.00	-2.35	0.00	-1.13	0.64	-1.07	0.64
B0365.5	<i>cllec-225</i>	-1.66	0.05	-2.15	0.05	-1.05	0.65	1.22	0.65
B0365.6	<i>cllec-41</i>	1.05	0.00	2.33	0.00	1.23	0.44	1.55	0.44
C01F1.3	<i>phi-41</i>	-1.77	0.04	-2.70	0.04	1.09	0.71	1.19	0.71
C01G6.3		3.02	0.04	6.17	0.04	-1.45	0.55	-2.69	0.55
C01G6.7	<i>acs-7</i>	-2.49	0.02	-1.80	0.02	1.27	0.58	-1.12	0.58
C01G8.1		2.17	0.04	4.04	0.04	-1.32	0.57	-1.90	0.57
C02F12.4	<i>tag-52</i>	2.01	0.00	1.05	0.00	-1.02	0.57	1.17	0.57
C03C10.3	<i>rnr-2</i>	2.05	0.01	2.01	0.01	-1.11	0.71	-1.09	0.71
C03D6.6		1.81	0.05	3.69	0.05	-1.46	0.63	-1.58	0.63
C03H5.1	<i>cllec-10</i>	-1.07	0.01	2.16	0.01	1.31	0.35	-1.27	0.35
C04B4.2		2.21	0.05	3.31	0.05	-1.30	0.53	-2.06	0.53
C04F6.1	<i>vit-5</i>	3.34	0.04	14.54	0.04	-1.68	0.70	-1.48	0.70
C04H5.7		3.12	0.03	7.71	0.03	-1.60	0.67	-1.04	0.67
C05A9.1	<i>pgp-5</i>	-2.13	0.01	-1.48	0.01	1.36	0.07	1.94	0.07
C05C10.4	<i>pho-11</i>	-1.22	0.00	-3.02	0.00	-1.00	0.71	1.09	0.71
C05C10.5		2.18	0.05	4.30	0.05	-1.31	0.59	-1.96	0.59
C05E11.4	<i>amt-1</i>	-1.01	0.00	-2.68	0.00	-1.39	0.00	1.91	0.00
C05E4.1	<i>srp-2</i>	1.38	0.02	2.18	0.02	1.39	0.19	-1.34	0.19
C05E4.9	<i>gei-7</i>	-1.19	0.01	-2.15	0.01	-1.14	0.58	1.15	0.58
C06A12.5	<i>lact-6</i>	-1.24	0.01	-2.02	0.01	-1.04	0.53	1.28	0.53
C06B3.7		-2.18	0.02	-2.15	0.02	-1.00	0.29	1.71	0.29
C06C3.4		-1.54	0.04	-2.02	0.04	1.06	0.70	1.15	0.70
C07A9.4	<i>ncx-6</i>	2.75	0.00	-1.06	0.00	1.07	0.68	1.15	0.68
C07A9.8		-1.25	0.03	-2.49	0.03	1.17	0.26	1.99	0.26
C07G1.7		3.00	0.00	1.29	0.00	1.01	0.00	3.47	0.00
C08A9.7	<i>sdz-2</i>	-1.26	0.01	-2.88	0.01	1.15	0.71	1.13	0.71
C08B6.1	<i>ugt-17</i>	6.23	0.00	-1.35	0.00	-1.01	0.51	1.21	0.51
C08E3.1		-2.05	0.05	-1.11	0.05	1.18	0.70	1.11	0.70
C08E3.6	<i>fbxa-163</i>	-1.05	0.00	3.33	0.00	1.18	0.56	1.46	0.56
C08E8.4		1.07	0.26	1.21	0.26	1.20	0.01	2.53	0.01
C09B8.4		-1.21	0.02	-1.91	0.02	-1.11	0.00	2.97	0.00
C09G5.5	<i>col-80</i>	1.46	0.05	2.08	0.05	-1.02	0.68	1.17	0.68
C10C5.5		1.08	0.26	-1.13	0.26	2.48	0.00	-2.18	0.00
C10G8.4		4.44	0.03	13.20	0.03	-1.56	0.70	1.02	0.70
C10H11.6	<i>ugt-26</i>	-2.21	0.00	-2.76	0.00	1.24	0.55	1.39	0.55
C12D5.9		1.09	0.30	-1.07	0.30	-1.14	0.03	-2.58	0.03
C14A6.1	<i>cllec-48</i>	-1.76	0.00	-2.58	0.00	-1.13	0.69	-1.04	0.69
C14C6.5		-1.14	0.00	2.79	0.00	-1.03	0.07	1.66	0.07

C14F5.1	<i>dct-1</i>	2.53	0.00	-1.08	0.00	1.11	0.67	-1.09	0.67
C15A11.4		-1.26	0.17	-1.21	0.17	-1.06	0.00	2.54	0.00
C15C8.3		6.30	0.00	-3.77	0.00	1.04	0.59	1.33	0.59
C16C4.4	<i>math-14</i>	4.62	0.00	1.04	0.00	1.20	0.59	1.16	0.59
C16D9.2	<i>rol-3</i>	-1.75	0.03	-2.73	0.03	1.21	0.69	1.20	0.69
C17C3.12	<i>acdh-2</i>	-1.22	0.01	-1.63	0.01	-1.06	0.00	3.55	0.00
C17C3.18	<i>ins-13</i>	-1.22	0.27	-1.63	0.27	-1.06	0.00	3.55	0.00
C17F4.7		1.05	0.03	3.36	0.03	-1.67	0.39	-2.52	0.39
C17H1.7		1.56	0.00	3.03	0.00	1.22	0.53	1.49	0.53
C17H12.6		-1.32	0.00	2.23	0.00	1.01	0.71	1.08	0.71
C18H9.6		-2.19	0.00	1.13	0.00	-1.17	0.03	1.80	0.03
C24G7.2		-1.21	0.01	-3.36	0.01	1.02	0.62	1.37	0.62
C25A1.8	<i>clcc-87</i>	2.26	0.05	4.60	0.05	-1.43	0.60	-1.90	0.60
C25A8.4		3.03	0.04	8.18	0.04	-1.40	0.71	-1.32	0.71
C26C6.6		1.21	0.03	2.05	0.03	-1.09	0.73	-1.00	0.73
C27A7.6		1.76	0.05	2.94	0.05	-1.23	0.67	-1.36	0.67
C27D9.1		1.95	0.05	2.88	0.05	-1.12	0.58	-1.62	0.58
C28D4.3	<i>gln-6</i>	1.90	0.05	3.53	0.05	-1.25	0.63	-1.52	0.63
C29E4.7	<i>gst-1</i>	9.81	0.00	-2.93	0.00	1.11	0.66	1.22	0.66
C29E6.1	<i>let-653</i>	-1.43	0.05	-2.54	0.05	1.07	0.72	1.17	0.72
C29F3.7		1.12	0.00	2.30	0.00	1.21	0.27	1.54	0.27
C30F12.4		1.58	0.05	2.44	0.05	-1.21	0.55	-1.64	0.55
C31A11.5	<i>oac-6</i>	-1.73	0.00	1.99	0.00	1.11	0.03	2.36	0.03
C31C9.1	<i>tag-10</i>	5.05	0.00	-1.61	0.00	1.08	0.71	0.01	0.71
C31C9.2		-1.73	0.00	-2.04	0.00	1.01	0.75	1.01	0.75
C31H5.3	<i>acr-19</i>	2.58	0.00	-1.32	0.00	1.18	0.39	1.69	0.39
C32E8.4		1.37	0.04	2.61	0.04	-1.22	0.69	1.00	0.69
C32H11.10	<i>dod-21</i>	-1.07	0.00	2.71	0.00	-1.33	0.58	-1.24	0.58
C32H11.12	<i>dod-24</i>	-2.69	0.00	3.07	0.00	1.77	0.51	1.35	0.51
C32H11.4		-2.82	0.00	1.89	0.00	1.42	0.58	1.41	0.58
C33A12.6	<i>ugt-21</i>	2.55	0.00	-1.38	0.00	1.19	0.32	1.57	0.32
C34H4.1		-2.13	0.00	1.56	0.00	1.18	0.00	3.21	0.00
C34H4.2		1.60	0.01	2.11	0.01	1.28	0.03	1.94	0.03
C35A5.3		-1.11	0.05	-1.55	0.05	1.17	0.01	2.07	0.01
C36B1.11		1.61	0.05	2.17	0.05	-1.16	0.59	-1.44	0.59
C37C3.9		1.69	0.05	2.62	0.05	-1.19	0.57	-1.61	0.57
C38D4.6	<i>pal-1</i>	1.67	0.05	2.33	0.05	-1.11	0.62	-1.39	0.62
C43C3.1	<i>ifp-1</i>	-1.51	0.04	-2.17	0.04	1.19	0.67	-1.03	0.67
C44B7.5		3.08	0.05	9.84	0.05	-1.74	0.67	1.09	0.67
C44H9.1	<i>ugt-15</i>	-1.57	0.01	-2.25	0.01	1.18	0.64	1.20	0.64
C45B2.1		3.39	0.03	10.20	0.03	-1.41	0.60	1.69	0.60
C45E5.1		-1.49	0.02	-2.16	0.02	1.08	0.56	1.35	0.56
C45G7.2	<i>ilys-2</i>	2.30	0.01	-1.09	0.01	-1.05	0.27	1.70	0.27
C45G7.5	<i>cdh-10</i>	-1.76	0.04	-2.91	0.04	1.27	0.67	1.30	0.67
C46A5.1		2.04	0.04	2.39	0.04	-1.00	0.68	1.24	0.68
C46C2.5		2.08	0.04	4.17	0.04	-1.43	0.68	-1.34	0.68
C47A10.5		2.79	0.00	-1.35	0.00	1.42	0.03	-1.37	0.03
C49G7.7		-1.47	0.04	1.23	0.04	1.02	0.00	2.37	0.00
C50A2.3		3.06	0.00	-1.24	0.00	1.29	0.26	1.55	0.26
C50E3.11		2.01	0.05	2.96	0.05	-1.21	0.54	-1.86	0.54
C50H11.15	<i>cyp-33C9</i>	2.11	0.00	-1.20	0.00	1.04	0.00	1.90	0.00
C53B4.5	<i>col-119</i>	3.16	0.03	8.84	0.03	-1.30	0.73	-1.06	0.73

C54D1.2	<i>clec-86</i>	-1.80	0.00	1.80	0.00	-1.29	0.04	-2.14	0.04
C54D10.1	<i>cdr-2</i>	1.39	0.12	1.21	0.12	-1.12	0.00	2.91	0.00
C55A6.5	<i>sdz-8</i>	-1.05	0.13	-1.40	0.13	-1.00	0.01	2.29	0.01
C55B7.4	<i>acdh-1</i>	1.12	0.05	-3.51	0.05	1.31	0.00	17.74	0.00
C55F2.1		-1.54	0.00	-2.32	0.00	-1.03	0.51	1.21	0.51
C55F2.2	<i>ilys-4</i>	-1.59	0.00	-2.37	0.00	-1.03	0.52	1.20	0.52
D1054.11		3.75	0.05	11.64	0.05	-1.63	0.68	1.21	0.68
D1086.3		-2.04	0.02	-2.20	0.02	-1.34	0.55	-1.43	0.55
D2089.2		1.39	0.05	2.87	0.05	1.01	0.75	1.03	0.75
E03H4.10	<i>clec-17</i>	1.76	0.08	1.71	0.08	1.11	0.04	2.84	0.04
EEED8.3		2.80	0.04	6.51	0.04	-1.45	0.56	-2.60	0.56
F01D4.1	<i>ugt-43</i>	-2.28	0.00	1.45	0.00	1.13	0.22	1.49	0.22
F01D4.2	<i>ugt-44</i>	-2.68	0.00	1.49	0.00	1.45	0.37	1.20	0.37
F01D5.1		-1.43	0.00	2.97	0.00	1.22	0.41	1.66	0.41
F01D5.2		-1.71	0.00	2.97	0.00	1.27	0.52	1.51	0.52
F01D5.3		-1.40	0.00	3.74	0.00	-1.08	0.51	1.42	0.51
F01G10.3	<i>ech-9</i>	-1.50	0.00	3.60	0.00	1.76	0.00	-2.29	0.00
F02E8.4		2.54	0.05	4.47	0.05	-1.38	0.55	-2.26	0.55
F02H6.5	<i>sqrd-1</i>	-1.19	0.00	-3.09	0.00	-1.34	0.45	1.10	0.45
F07B7.2		1.01	0.19	-1.14	0.19	1.09	0.00	2.18	0.00
F07B7.8		-1.32	0.13	-1.65	0.13	3.03	0.01	-1.19	0.01
F07C4.2	<i>clec-45</i>	10.81	0.00	1.64	0.00	-1.01	0.55	1.67	0.55
F07C4.9	<i>clec-46</i>	11.37	0.00	1.68	0.00	-1.01	0.53	1.73	0.53
F08A8.2		-2.21	0.03	-2.22	0.03	-1.06	0.55	-1.50	0.55
F08A8.3		-1.39	0.00	-2.02	0.00	1.01	0.74	-1.03	0.74
F08F8.5	<i>numr-1</i>	-1.30	0.00	10.52	0.00	1.10	0.59	1.71	0.59
F08G5.6		-2.62	0.00	2.80	0.00	-1.50	0.48	1.20	0.48
F08H9.5	<i>clec-227</i>	-2.03	0.00	-2.58	0.00	-1.03	0.32	-1.53	0.32
F08H9.6	<i>clec-57</i>	-2.05	0.04	-1.61	0.04	1.56	0.03	-1.69	0.03
F09B9.1	<i>oac-14</i>	1.25	0.27	1.14	0.27	1.29	0.01	3.36	0.01
F09C8.1		-1.14	0.00	2.33	0.00	-1.41	0.43	-1.52	0.43
F09E10.3	<i>dhs-25</i>	-1.30	0.00	-2.05	0.00	1.02	0.74	-1.01	0.74
F09F3.9	<i>cpt-5</i>	-2.48	0.00	-2.39	0.00	1.24	0.51	-1.21	0.51
F09G2.3		-1.85	0.00	-2.20	0.00	1.17	0.61	1.19	0.61
F10A3.1		-1.06	0.00	3.25	0.00	1.12	0.56	1.43	0.56
F10A3.2	<i>fbxa-88</i>	-1.21	0.00	2.38	0.00	1.25	0.21	1.54	0.21
F10C2.7		-3.53	0.00	-1.97	0.00	-1.36	0.40	1.34	0.40
F10F2.2		-1.45	0.00	-2.26	0.00	1.13	0.35	1.35	0.35
F11A6.2	<i>scrm-4</i>	-1.50	0.03	1.05	0.03	1.05	0.00	2.63	0.00
F11H8.3	<i>col-8</i>	2.41	0.05	6.98	0.05	-1.25	0.73	1.01	0.73
F12E12.11		-1.05	0.15	-1.17	0.15	-1.11	0.00	2.09	0.00
F13G3.3		-1.48	0.04	-2.06	0.04	1.14	0.71	1.13	0.71
F14B8.3	<i>pes-23</i>	1.96	0.03	3.07	0.03	1.03	0.74	1.10	0.74
F14F4.3	<i>mrp-5</i>	2.93	0.00	-1.37	0.00	1.06	0.09	1.31	0.09
F14H3.6		3.51	0.03	10.32	0.03	-1.49	0.59	-2.50	0.59
F15B9.1	<i>far-3</i>	-1.81	0.05	-2.18	0.05	1.14	0.02	2.96	0.02
F15B9.6		2.42	0.01	1.85	0.01	1.32	0.01	2.82	0.01
F15E11.1		-2.48	0.00	-1.03	0.00	1.01	0.02	-2.02	0.02
F15E11.12		-10.48	0.00	-2.60	0.00	-1.30	0.17	-4.34	0.17
F15E11.15		-10.17	0.00	-2.34	0.00	-1.29	0.04	-4.69	0.04
F17B5.1		1.02	0.03	-2.13	0.03	1.18	0.60	1.40	0.60
F17E9.4		3.01	0.05	9.30	0.05	-1.59	0.65	1.34	0.65

F18A1.7		1.94	0.05	3.45	0.05	-0.54	0.60	-1.72	0.60
F18A12.4		2.84	0.01	1.75	0.01	1.01	0.68	1.20	0.68
F20G2.1		1.39	0.06	1.46	0.06	1.01	0.00	2.64	0.00
F21C10.7		-1.42	0.02	-2.15	0.02	1.06	0.70	-1.07	0.70
F21D5.3		-1.47	0.09	1.03	0.09	2.07	0.03	-1.07	0.03
F21F8.4		-1.47	0.01	2.36	0.01	-1.07	0.00	-3.64	0.00
F21H7.1	<i>gst-22</i>	1.05	0.00	2.42	0.00	1.16	0.41	1.39	0.41
F22A3.6	<i>ilys-5</i>	-1.44	0.21	-1.09	0.21	-1.22	0.00	-8.13	0.00
F22B5.4		-1.82	0.12	-1.73	0.12	2.76	0.00	-3.44	0.00
F22B7.4	<i>fip-1</i>	-1.13	0.04	-2.29	0.04	1.09	0.73	1.03	0.73
F22B7.6	<i>polk-1</i>	1.71	0.03	2.03	0.03	-1.13	0.58	-1.36	0.58
F25A2.1		-1.21	0.00	2.12	0.00	-0.04	0.23	1.59	0.23
F26C11.1		-1.21	0.00	-2.56	0.00	1.31	0.59	1.12	0.59
F26D10.10	<i>gln-5</i>	2.16	0.04	4.51	0.04	-1.36	0.54	-2.30	0.54
F27C8.4	<i>spp-18</i>	-1.75	0.00	3.01	0.00	-1.55	0.12	-1.84	0.12
F27D9.6	<i>dhs-29</i>	-1.40	0.03	-2.15	0.03	1.09	0.72	1.12	0.72
F27E5.1		1.38	0.00	2.16	0.00	-1.00	0.52	-1.14	0.52
F28D1.5	<i>thn-2</i>	1.37	0.01	-2.29	0.01	-1.19	0.49	-1.66	0.49
F28F8.2	<i>acs-2</i>	-1.38	0.03	-2.65	0.03	-1.25	0.55	1.30	0.55
F28G4.1	<i>cyp-37B1</i>	-2.52	0.00	1.41	0.00	-1.97	0.27	-1.21	0.27
F28H7.3		-1.02	0.05	1.64	0.05	-1.32	0.01	-2.50	0.01
F29D11.1	<i>lrp-1</i>	-1.41	0.04	-2.04	0.04	1.13	0.65	1.25	0.65
F32A5.5	<i>aqp-1</i>	-2.03	0.01	-1.74	0.01	-1.01	0.60	-1.21	0.60
F32H5.1		2.80	0.00	-1.19	0.00	1.03	0.72	-1.05	0.72
F35C5.7	<i>clcc-64</i>	1.02	0.29	1.14	0.29	1.12	0.02	2.27	0.02
F35C5.8	<i>clcc-65</i>	-1.35	0.00	1.56	0.00	1.07	0.00	2.15	0.00
F35C5.9	<i>clcc-66</i>	-1.16	0.02	1.95	0.02	1.16	0.00	3.94	0.00
F35E12.8		-1.62	0.00	2.59	0.00	1.03	0.01	2.38	0.01
F35E8.1		-2.63	0.01	-1.57	0.01	-1.48	0.15	1.41	0.15
F35E8.8	<i>gst-38</i>	-1.84	0.00	1.73	0.00	-1.14	0.01	2.31	0.01
F35G2.4	<i>phy-2</i>	-1.50	0.10	-1.86	0.10	1.62	0.03	-2.15	0.03
F35H8.4		1.22	0.04	2.38	0.04	-1.08	0.74	-1.01	0.74
F36A2.3		2.15	0.00	-1.30	0.00	-1.05	0.10	1.35	0.10
F36D3.9	<i>cpr-2</i>	-4.33	0.02	1.01	0.02	1.07	0.14	3.54	0.14
F36H1.5	<i>hrg-4</i>	8.83	0.00	-2.91	0.00	1.14	0.66	1.19	0.66
F37B1.2	<i>gst-12</i>	1.28	0.10	1.14	0.10	-1.20	0.00	3.29	0.00
F37B1.3	<i>gst-14</i>	1.14	0.26	1.11	0.26	1.01	0.00	5.35	0.00
F37B1.5	<i>gst-16</i>	1.18	0.00	1.99	0.00	-1.17	0.00	2.10	0.00
F37B1.6	<i>gst-17</i>	3.22	0.00	-1.08	0.00	-1.05	0.58	1.22	0.58
F37B1.8	<i>gst-19</i>	1.09	0.00	-3.13	0.00	-1.17	0.52	-1.46	0.52
F37B4.7	<i>folt-2</i>	1.15	0.22	-1.08	0.22	-1.07	0.02	2.04	0.02
F38B6.4		-1.34	0.00	-2.21	0.00	1.11	0.67	1.03	0.67
F40F4.4	<i>lbp-3</i>	2.54	0.00	-1.35	0.00	1.05	0.73	1.04	0.73
F41C3.1		1.31	0.12	-1.08	0.12	1.15	0.01	2.41	0.01
F41C3.11		-1.57	0.05	-2.09	0.05	1.20	0.67	1.24	0.67
F41D3.3	<i>nhr-265</i>	-1.34	0.05	-2.61	0.05	1.12	0.73	1.13	0.73
F42A10.7		-2.08	0.00	-1.10	0.00	-1.32	0.16	-1.48	0.16
F42G2.2		2.52	0.00	-1.28	0.00	1.16	0.46	1.32	0.46
F43H9.4		4.41	0.00	1.22	0.00	1.11	0.71	1.18	0.71
F44F4.2	<i>egg-3</i>	1.85	0.05	3.36	0.05	-1.26	0.51	-2.11	0.51
F44G3.10		1.04	0.00	2.67	0.00	-1.01	0.08	1.86	0.08
F45F2.12	<i>his-8</i>	-1.33	0.00	-2.48	0.00	1.12	0.67	1.13	0.67

F45F2.2	<i>his-39</i>	-1.28	0.00	-2.08	0.00	1.07	0.71	1.07	0.71
F46B6.8		-2.17	0.02	1.11	0.02	-1.73	0.30	-1.81	0.30
F47C10.6	<i>ugt-32</i>	-1.01	0.00	-1.80	0.00	-1.27	0.00	2.04	0.00
F47G4.3	<i>gpdh-1</i>	-1.18	0.14	-1.43	0.14	-1.04	0.00	2.59	0.00
F48G7.8		-1.03	0.04	2.03	0.04	-1.11	0.67	1.15	0.67
F49C12.7		-2.31	0.00	-1.20	0.00	1.13	0.00	-2.52	0.00
F49E11.10	<i>scl-2</i>	-2.31	0.02	-1.25	0.02	1.40	0.57	1.17	0.57
F49E12.1		2.65	0.05	5.97	0.05	-1.37	0.71	-1.40	0.71
F49E12.10		-2.22	0.00	1.19	0.00	-1.16	0.17	1.49	0.17
F49E12.2	<i>dod-23</i>	1.61	0.01	4.37	0.01	-1.42	0.62	-1.53	0.62
F49E12.9		-1.81	0.00	1.57	0.00	-1.19	0.00	2.14	0.00
F49F1.6		-1.00	0.00	2.05	0.00	1.10	0.49	1.31	0.49
F52D1.1		-1.63	0.05	-2.10	0.05	1.16	0.66	1.27	0.66
F52E1.1	<i>pos-1</i>	2.36	0.04	4.56	0.04	-1.36	0.60	-1.84	0.60
F52E1.14		1.37	0.00	2.16	0.00	-1.16	0.66	-1.02	0.66
F52F10.4	<i>oac-32</i>	1.13	0.17	1.34	0.17	1.16	0.05	2.10	0.05
F53A9.1		-1.16	0.19	1.02	0.19	-1.10	0.00	2.39	0.00
F53A9.2		1.29	0.06	1.49	0.06	1.20	0.00	2.16	0.00
F53A9.6		-1.20	0.12	-1.21	0.12	1.03	0.00	2.07	0.00
F53B3.6		-1.72	0.05	-2.94	0.05	1.38	0.64	1.44	0.64
F53B6.7		1.22	0.04	2.24	0.04	-1.09	0.73	1.02	0.73
F53C11.1		-1.09	0.00	2.08	0.00	1.09	0.01	1.64	0.01
F53E10.4		-2.67	0.00	1.18	0.00	1.02	0.58	-1.17	0.58
F53F8.3		2.46	0.05	3.57	0.05	-1.30	0.56	-1.99	0.56
F53G12.5	<i>mex-3</i>	1.75	0.05	2.63	0.05	-1.13	0.51	-1.75	0.51
F54B11.10		-1.55	0.04	-2.51	0.04	1.04	0.74	-1.01	0.74
F54B8.4		-1.26	0.06	1.39	0.06	1.28	0.01	2.51	0.01
F54C8.2	<i>cpar-1</i>	1.65	0.05	2.79	0.05	-1.28	0.53	-1.81	0.53
F54C9.8	<i>puf-5</i>	2.44	0.04	5.24	0.04	-1.36	0.60	-1.99	0.60
F54D10.5		1.52	0.04	2.18	0.04	-1.16	0.53	-1.54	0.53
F54D10.7		2.07	0.05	3.01	0.05	-1.26	0.55	-1.84	0.55
F54F3.3		-2.19	0.00	2.00	0.00	-1.41	0.59	-1.11	0.59
F55B11.5		2.15	0.05	3.82	0.05	-1.24	0.71	-1.21	0.71
F55G11.4		-1.16	0.00	3.94	0.00	-1.32	0.49	1.42	0.49
F55G11.5	<i>dod-22</i>	-1.55	0.00	2.38	0.00	1.32	0.43	1.58	0.43
F55G11.8		-1.96	0.00	1.35	0.00	1.48	0.00	2.89	0.00
F56D5.3		1.12	0.13	-1.18	0.13	-1.07	0.00	2.59	0.00
F56D6.15	<i>cllec-69</i>	-1.72	0.00	2.37	0.00	1.20	0.56	1.42	0.56
F56D6.2	<i>cllec-67</i>	-1.74	0.00	2.37	0.00	1.17	0.62	1.34	0.62
F57C2.4		2.87	0.05	6.77	0.05	-1.53	0.68	1.03	0.68
F58B3.2	<i>lys-5</i>	-1.20	0.00	-4.07	0.00	-1.60	0.02	-3.87	0.02
F58B3.3	<i>lys-6</i>	-1.53	0.01	-4.20	0.01	-1.67	0.02	-3.93	0.02
F58E6.7		30.17	0.00	1.06	0.00	1.04	0.57	1.20	0.57
F58E6.8		2.57	0.00	-1.03	0.00	-1.03	0.70	1.07	0.70
F58G6.2	<i>srm-3</i>	2.29	0.00	-2.11	0.00	1.06	0.05	1.71	0.05
F58G6.3		2.22	0.00	-2.22	0.00	-1.06	0.03	1.65	0.03
F58G6.7		2.22	0.00	-2.22	0.00	-1.06	0.03	1.65	0.03
F58G6.9		2.29	0.00	-2.11	0.00	1.06	0.05	1.71	0.05
F59A7.2		-1.04	0.05	-1.66	0.05	1.15	0.01	2.42	0.01
F59D8.1	<i>vit-3</i>	2.81	0.05	9.65	0.05	-1.66	0.50	-1.69	0.50
F59D8.2	<i>vit-4</i>	3.64	0.04	18.07	0.04	-1.80	0.70	-1.28	0.70
H02I12.5		2.11	0.05	3.56	0.05	-1.23	0.59	-1.79	0.59

H13N06.6	<i>tbh-1</i>	2.72	0.04	5.66	0.04	-1.21	0.72	-1.28	0.72
H19M22.3		-1.60	0.04	-2.67	0.04	1.10	0.72	1.17	0.72
H23N18.1	<i>ugt-13</i>	4.94	0.00	-1.50	0.00	1.25	0.53	1.43	0.53
H38K22.5	<i>gly-6</i>	-1.50	0.02	-2.02	0.02	1.07	0.71	-1.03	0.71
K01A2.3		-2.02	0.00	-3.70	0.00	1.04	0.53	-1.47	0.53
K01A2.4		-1.89	0.00	-3.28	0.00	1.14	0.38	-1.44	0.38
K01D12.14	<i>cdr-5</i>	52.78	0.00	-1.51	0.00	-1.05	0.20	1.50	0.20
K02B9.1	<i>meg-1</i>	3.32	0.04	7.22	0.04	-1.42	0.51	-3.09	0.51
K02D7.3	<i>col-101</i>	3.10	0.05	3.61	0.05	-1.23	0.71	-1.25	0.71
K02E10.4		-1.73	0.05	-2.49	0.05	1.07	0.68	1.27	0.68
K02E11.5		-1.17	0.04	-1.77	0.04	1.26	0.00	-2.12	0.00
K05B2.4		-2.47	0.01	-1.32	0.01	1.20	0.51	1.48	0.51
K06C4.4	<i>his-20</i>	-1.36	0.00	-2.50	0.00	1.11	0.67	1.15	0.67
K07A1.6		3.43	0.04	10.34	0.04	-1.47	0.66	1.43	0.66
K07C6.4	<i>cyp-35B1</i>	-1.56	0.02	-2.12	0.02	1.24	0.08	1.96	0.08
K07E3.3	<i>dao-3</i>	-1.79	0.00	-2.48	0.00	1.11	0.60	1.21	0.60
K07G5.5		-1.05	0.02	-2.01	0.02	1.01	0.71	1.10	0.71
K07H8.6	<i>vit-6</i>	3.48	0.05	10.70	0.05	-1.55	0.71	-1.07	0.71
K08B4.3	<i>ugt-19</i>	2.23	0.01	1.18	0.01	1.14	0.01	2.31	0.01
K08F4.7	<i>gst-4</i>	-1.06	0.33	-1.03	0.33	-1.26	0.00	4.38	0.00
K09C4.1		-2.06	0.00	-1.65	0.00	-1.04	0.17	-1.55	0.17
K09F5.2	<i>vit-1</i>	2.78	0.04	7.38	0.04	-1.59	0.66	-1.69	0.66
K10B2.2		8.36	0.00	1.22	0.00	-1.07	0.08	1.33	0.08
K10B2.3	<i>clcc-88</i>	2.24	0.05	4.24	0.05	-1.34	0.58	-2.02	0.58
K10C2.3		-5.82	0.00	-1.29	0.00	-1.43	0.39	1.31	0.39
K10D11.2		1.40	0.09	1.35	0.09	-1.12	0.00	2.22	0.00
K10G4.3		2.19	0.00	-1.10	0.00	1.15	0.54	1.39	0.54
K10H10.2		1.35	0.00	-3.25	0.00	-1.44	0.10	1.28	0.10
K11G9.5		-1.63	0.03	-2.37	0.03	1.18	0.69	1.13	0.69
K11H12.4		-1.56	0.01	2.69	0.01	1.31	0.27	2.45	0.27
M01E11.6	<i>k1p-15</i>	1.64	0.05	2.68	0.05	-1.08	0.51	-1.74	0.51
M02D8.4		-2.02	0.01	-2.26	0.01	1.15	0.38	1.63	0.38
M02D8.5		-1.82	0.00	-2.17	0.00	1.19	0.58	1.16	0.58
M02F4.7	<i>clcc-265</i>	1.20	0.04	2.10	0.04	1.32	0.00	3.64	0.00
M02H5.4	<i>nhr-202</i>	2.27	0.00	-1.33	0.00	1.01	0.10	1.55	0.10
M162.5		-1.09	0.00	-2.02	0.00	1.17	0.15	1.55	0.15
M60.2		-4.22	0.00	-1.48	0.00	-1.08	0.30	-1.88	0.30
M88.1	<i>ugt-62</i>	1.94	0.00	1.03	0.00	1.02	0.00	2.01	0.00
R02E12.6	<i>hrg-1</i>	11.27	0.00	-2.35	0.00	1.13	0.59	1.25	0.59
R03D7.6	<i>gst-5</i>	-1.05	0.01	1.58	0.01	-1.21	0.00	2.03	0.00
R04D3.1	<i>cyp-14A4</i>	3.01	0.01	1.00	0.01	1.15	0.42	1.88	0.42
R04D3.4		2.07	0.05	2.95	0.05	-1.26	0.53	-1.91	0.53
R05H10.6	<i>cdh-7</i>	-1.73	0.04	-3.33	0.04	1.39	0.60	1.64	0.60
R06C7.4	<i>cpg-3</i>	2.69	0.05	6.48	0.05	-1.50	0.63	-1.97	0.63
R08A2.3		1.54	0.05	3.41	0.05	-1.20	0.67	1.20	0.67
R08E5.3		1.17	0.00	-3.77	0.00	-1.68	0.00	1.31	0.00
R08F11.3	<i>cyp-33C8</i>	1.83	0.02	-1.30	0.02	1.12	0.00	3.65	0.00
R08F11.7		-1.23	0.04	-1.90	0.04	1.18	0.00	-2.28	0.00
R09B5.4	<i>fpn-1.2</i>	-2.67	0.00	1.18	0.00	-1.42	0.29	-1.03	0.29
R09B5.8	<i>cnc-3</i>	-1.68	0.04	-2.66	0.04	1.07	0.53	1.65	0.53
R10D12.10		1.10	0.00	2.63	0.00	1.06	0.00	1.83	0.00
R10D12.9		1.10	0.00	2.63	0.00	1.06	0.00	1.83	0.00

R11G11.2	<i>nhr-58</i>	-1.48	0.01	-2.12	0.01	1.30	0.43	1.49	0.43
R186.1		1.71	0.00	-1.28	0.00	1.18	0.00	2.05	0.00
R193.2		4.89	0.00	-2.08	0.00	1.09	0.69	1.13	0.69
R52.8	<i>math-36</i>	2.37	0.00	2.69	0.00	1.26	0.24	1.68	0.24
T01C3.3		2.63	0.04	5.83	0.04	-1.41	0.61	-2.01	0.61
T01C3.4	<i>fil-1</i>	-1.97	0.00	3.48	0.00	-1.36	0.45	-1.06	0.45
T02G5.11		2.26	0.05	3.64	0.05	-1.37	0.53	-2.10	0.53
T04A8.5		-2.02	0.00	-2.16	0.00	-1.24	0.45	-1.32	0.45
T04G9.7		2.22	0.05	4.41	0.05	-1.37	0.68	-1.43	0.68
T04H1.9	<i>tbb-6</i>	-1.18	0.06	1.36	0.06	1.18	0.01	2.25	0.01
T05A10.4		2.20	0.04	6.45	0.04	1.07	0.75	1.02	0.75
T05A10.5	<i>scl-22</i>	2.11	0.05	6.26	0.05	1.15	0.74	1.18	0.74
T05E12.3		2.58	0.03	1.33	0.03	-1.19	0.70	-1.06	0.70
T05E12.6		-1.42	0.06	1.36	0.06	-1.12	0.00	4.18	0.00
T05F1.2		2.27	0.04	3.66	0.04	-1.24	0.59	-1.77	0.59
T05G5.7	<i>rmd-1</i>	2.29	0.04	5.68	0.04	-1.47	0.64	-1.79	0.64
T06D4.1		2.31	0.05	3.72	0.05	-1.33	0.55	-2.11	0.55
T06E6.2	<i>cyb-3</i>	1.75	0.05	2.61	0.05	-1.20	0.58	-1.58	0.58
T08A9.8	<i>spp-4</i>	-1.30	0.14	-1.14	0.14	-1.32	0.00	-2.78	0.00
T09F5.9	<i>clec-47</i>	2.24	0.00	-4.51	0.00	1.70	0.31	1.34	0.31
T11F9.3	<i>nas-20</i>	2.32	0.05	6.25	0.05	-1.14	0.69	1.38	0.69
T12G3.6		2.66	0.03	6.15	0.03	-1.49	0.56	-2.30	0.56
T13F3.6		1.51	0.04	2.93	0.04	-1.30	0.45	-2.11	0.45
T14B4.4	<i>tsp-10</i>	-1.51	0.00	-3.24	0.00	1.10	0.19	-1.55	0.19
T14F9.4	<i>peb-1</i>	-1.43	0.04	-2.30	0.04	1.01	0.61	1.33	0.61
T15B7.3	<i>col-143</i>	3.44	0.04	8.41	0.04	-1.38	0.71	-1.41	0.71
T15B7.4	<i>col-142</i>	1.66	0.02	2.04	0.02	1.04	0.72	1.10	0.72
T16G1.7		-2.72	0.00	-1.79	0.00	1.08	0.70	-1.04	0.70
T19C4.1		-1.61	0.05	-2.41	0.05	1.23	0.67	1.27	0.67
T19D12.4		-1.18	0.00	2.17	0.00	1.34	0.18	1.65	0.18
T19D12.5		-1.18	0.00	2.17	0.00	1.34	0.18	1.65	0.18
T19H12.9	<i>ugt-12</i>	2.49	0.00	-1.10	0.00	1.12	0.43	1.45	0.43
T21C9.13		2.67	0.03	6.25	0.03	-1.40	0.57	-2.22	0.57
T21E8.1	<i>pgp-6</i>	-3.34	0.01	-1.96	0.01	1.43	0.22	2.15	0.22
T22A3.8	<i>lam-3</i>	-1.53	0.04	-2.13	0.04	1.07	0.73	-1.02	0.73
T22B7.3		-1.86	0.03	-2.04	0.03	-1.28	0.34	1.35	0.34
T22B7.7		1.00	0.03	2.24	0.03	1.06	0.29	-1.82	0.29
T22E5.3		-1.52	0.04	-2.16	0.04	1.22	0.65	-1.01	0.65
T22G5.7	<i>spp-12</i>	-2.13	0.04	-3.01	0.04	1.34	0.02	-3.16	0.02
T23F4.1		-1.87	0.00	-2.31	0.00	1.12	0.61	1.23	0.61
T23F4.3		-1.63	0.01	-2.03	0.01	1.05	0.69	1.13	0.69
T24B8.5		-1.87	0.00	4.08	0.00	-1.14	0.28	1.70	0.28
T24E12.5		1.04	0.03	1.99	0.03	1.70	0.00	3.20	0.00
T25E12.5	<i>gyg-2</i>	2.35	0.05	4.46	0.05	-1.32	0.59	-1.93	0.59
T26C5.1	<i>gst-13</i>	-1.33	0.06	1.00	0.06	-1.06	0.00	2.02	0.00
T27B7.4	<i>nhr-115</i>	1.84	0.01	-1.06	0.01	1.15	0.01	2.24	0.01
T28F3.4		1.44	0.03	-1.04	0.03	1.23	0.00	2.05	0.00
T28H10.3		1.06	0.16	1.20	0.16	1.10	0.00	2.08	0.00
W02D9.7	<i>mex-1</i>	2.47	0.04	4.30	0.04	-1.56	0.66	-1.39	0.66
W02F12.3		2.14	0.05	3.93	0.05	-1.38	0.55	-2.16	0.55
W03C9.7		1.93	0.05	3.32	0.05	-1.26	0.52	-1.85	0.52
W03F11.1		3.69	0.04	8.51	0.04	-1.37	0.71	-1.38	0.71

W03G1.7	<i>asm-3</i>	-3.05	0.00	1.12	0.00	-1.79	0.13	-2.23	0.13
W04E12.6	<i>cllec-49</i>	-2.15	0.00	-1.55	0.00	-1.31	0.46	-1.27	0.46
W04E12.8	<i>cllec-50</i>	-2.06	0.00	1.20	0.00	-1.28	0.12	-1.70	0.12
W05F2.3		2.10	0.05	4.39	0.05	-1.39	0.57	-2.11	0.57
W06D11.1		1.52	0.05	2.15	0.05	-1.18	0.61	-1.38	0.61
W06H8.2		1.02	0.15	-1.30	0.15	-1.05	0.00	5.15	0.00
W06H8.8	<i>ttn-1</i>	-1.45	0.02	-2.27	0.02	1.27	0.63	-0.01	0.63
W07B8.1		5.25	0.00	-3.38	0.00	1.15	0.59	1.27	0.59
W07B8.5	<i>cpr-5</i>	1.60	0.00	-2.06	0.00	1.05	0.61	1.18	0.61
W08E12.2		-1.22	0.15	1.23	0.15	-1.15	0.05	2.20	0.05
W10G11.3		1.44	0.04	2.72	0.04	-1.13	0.66	-1.35	0.66
Y105C5B.15		1.04	0.00	2.58	0.00	-1.21	0.00	1.78	0.00
Y19D10A.4		1.15	0.17	1.05	0.17	1.09	0.00	2.36	0.00
Y19D10A.9	<i>cllec-209</i>	-1.84	0.00	3.31	0.00	1.02	0.71	1.15	0.71
Y19D10B.7		-3.23	0.00	-1.04	0.00	-1.02	0.04	-2.23	0.04
Y34D9A.11	<i>spp-23</i>	1.01	0.29	-1.15	0.29	-1.03	0.00	-3.06	0.00
Y37D8A.19		3.46	0.04	9.18	0.04	-1.52	0.68	1.17	0.68
Y37D8A.21		3.46	0.04	9.18	0.04	-1.52	0.68	1.17	0.68
Y37H2A.11		1.03	0.00	4.25	0.00	1.06	0.32	1.76	0.32
Y38E10A.5	<i>cllec-4</i>	1.01	0.24	1.24	0.24	1.38	0.00	3.81	0.00
Y38F1A.6		-1.17	0.02	-1.88	0.02	1.10	0.00	2.29	0.00
Y39A1A.19	<i>fmo-3</i>	-1.65	0.05	-2.26	0.05	1.04	0.56	1.50	0.56
Y39B6A.1		1.44	0.06	0.01	0.06	-1.09	0.00	-2.85	0.00
Y39G10AR.6	<i>ugt-31</i>	-2.27	0.00	-1.96	0.00	1.33	0.51	1.39	0.51
Y39G8B.7		-2.61	0.00	2.30	0.00	-1.02	0.06	2.00	0.06
Y40B10A.6		-1.39	0.00	5.99	0.00	1.23	0.45	1.56	0.45
Y40D12A.2		2.84	0.00	1.15	0.00	1.03	0.25	1.27	0.25
Y41G9A.5		-1.24	0.03	-2.45	0.03	1.22	0.64	1.32	0.64
Y43C5B.3		1.19	0.05	2.97	0.05	-1.17	0.70	1.11	0.70
Y43D4A.3		1.59	0.04	2.28	0.04	-1.17	0.66	-1.28	0.66
Y45F10C.2		1.80	0.04	4.04	0.04	-1.12	0.73	-1.20	0.73
Y45F10C.3	<i>fbxa-215</i>	1.84	0.05	3.13	0.05	-1.27	0.55	-1.87	0.55
Y45G12C.2	<i>gst-10</i>	-1.51	0.08	-1.33	0.08	-1.18	0.01	2.01	0.01
Y46C8AL.2	<i>cllec-174</i>	-1.67	0.00	3.39	0.00	-1.18	0.32	1.28	0.32
Y46C8AL.3	<i>cllec-70</i>	-2.63	0.00	1.16	0.00	1.86	0.00	-2.33	0.00
Y46C8AL.5	<i>cllec-72</i>	-2.24	0.02	1.09	0.02	1.34	0.58	-1.07	0.58
Y46D2A.2		-1.23	0.00	2.24	0.00	-1.02	0.57	1.14	0.57
Y46E12BL.3		1.91	0.05	2.82	0.05	-1.28	0.54	-1.81	0.54
Y49E10.14	<i>pie-1</i>	1.84	0.05	2.83	0.05	-1.22	0.57	-1.65	0.57
Y4C6B.6		-1.33	0.01	1.98	0.01	-1.98	0.00	-3.81	0.00
Y51B9A.8		-1.68	0.00	2.54	0.00	1.15	0.06	2.42	0.06
Y51F10.7		1.14	0.02	2.48	0.02	-1.47	0.55	-1.23	0.55
Y51H7C.3		1.96	0.04	3.22	0.04	-1.29	0.53	-1.95	0.53
Y51H7C.8		1.31	0.05	2.24	0.05	-1.14	0.67	1.12	0.67
Y53H1B.1	<i>cutl-10</i>	-1.25	0.03	-2.25	0.03	1.13	0.60	1.38	0.60
Y54F10AM.11		2.15	0.04	3.43	0.04	-1.25	0.63	-1.56	0.63
Y54G11A.5	<i>ctl-2</i>	-2.26	0.00	-1.33	0.00	-1.04	0.70	1.04	0.70
Y54G11A.7		4.21	0.00	-1.38	0.00	1.24	0.53	1.06	0.53
Y54G2A.8	<i>cllec-82</i>	-2.57	0.00	1.44	0.00	1.10	0.58	-1.14	0.58
Y5H2A.1		-3.00	0.00	-2.33	0.00	-1.15	0.52	1.29	0.52
Y62H9A.3		2.57	0.05	5.11	0.05	-1.43	0.70	-1.18	0.70
Y62H9A.4		3.77	0.04	12.04	0.04	-1.52	0.67	1.27	0.67

Y62H9A.5		3.95	0.05	11.30	0.05	-1.56	0.70	1.02	0.70
Y62H9A.6		4.49	0.04	12.47	0.04	-1.78	0.69	-1.08	0.69
Y66A7A.6	<i>gly-8</i>	-1.77	0.05	-2.28	0.05	1.11	0.67	1.29	0.67
Y69A2AR.13		1.26	0.03	2.42	0.03	-1.07	0.67	1.16	0.67
Y69A2AR.25		1.23	0.03	2.39	0.03	-1.07	0.66	1.20	0.66
Y70C5C.2	<i>cllec-9</i>	1.19	0.04	2.09	0.04	-1.04	0.04	2.21	0.04
Y75B8A.17	<i>gmh-1</i>	1.98	0.03	2.73	0.03	-1.17	0.56	-1.60	0.56
Y75B8A.9	<i>gly-11</i>	-1.60	0.02	-2.07	0.02	1.07	0.70	1.13	0.70
Y80D3A.5	<i>cyp-42A1</i>	-1.66	0.03	-2.13	0.03	1.09	0.73	1.06	0.73
Y82E9BL.10	<i>fbxa-14</i>	-1.34	0.13	-1.01	0.13	1.22	0.00	2.52	0.00
ZC308.4		2.33	0.05	4.45	0.05	-1.33	0.53	-2.33	0.53
ZC410.1	<i>nhr-11</i>	-1.58	0.03	-2.02	0.03	1.02	0.63	1.24	0.63
ZC443.6	<i>ugt-16</i>	5.24	0.00	1.18	0.00	1.24	0.15	2.22	0.15
ZC455.4	<i>ugt-6</i>	-1.96	0.01	-2.33	0.01	1.23	0.65	1.19	0.65
ZC513.6	<i>oma-2</i>	2.26	0.05	3.82	0.05	-1.23	0.52	-2.18	0.52
ZK1025.9	<i>nhr-113</i>	-1.49	0.04	-2.27	0.04	1.13	0.66	1.27	0.66
ZK1037.6		1.47	0.01	2.98	0.01	-1.05	0.74	-1.06	0.74
ZK1127.1	<i>nos-2</i>	2.36	0.05	4.20	0.05	-1.44	0.57	-2.05	0.57
ZK1193.1	<i>col-19</i>	3.11	0.05	9.74	0.05	-1.51	0.65	1.42	0.65
ZK154.1		-1.03	0.05	-2.01	0.05	1.10	0.55	1.51	0.55
ZK228.4		-1.10	0.14	-1.32	0.14	1.27	0.02	2.03	0.02
ZK455.4	<i>asm-2</i>	-2.14	0.00	1.03	0.00	-1.05	0.55	1.15	0.55
ZK550.2		1.08	0.29	-1.07	0.29	1.28	0.04	2.31	0.04
ZK6.10	<i>dod-19</i>	-1.15	0.00	2.10	0.00	1.15	0.12	1.63	0.12
ZK6.11		-2.28	0.00	1.37	0.00	1.10	0.71	1.11	0.71
ZK637.11	<i>cdc-25.3</i>	2.59	0.04	4.70	0.04	-1.42	0.50	-2.56	0.50
ZK666.6	<i>cllec-60</i>	-2.99	0.00	1.55	0.00	1.46	0.01	-2.12	0.01
ZK666.7	<i>cllec-61</i>	-2.04	0.00	1.40	0.00	1.73	0.22	-1.06	0.22
ZK669.3		1.75	0.01	3.28	0.01	1.00	0.62	1.33	0.62
ZK673.9	<i>cllec-143</i>	1.07	0.00	2.04	0.00	1.10	0.05	1.44	0.05
ZK813.1		4.45	0.04	13.82	0.04	-1.55	0.72	-1.12	0.72
ZK813.2		2.97	0.05	4.97	0.05	-1.41	0.65	-1.72	0.65
ZK813.3		3.07	0.04	6.68	0.04	-1.57	0.69	-1.16	0.69
ZK813.7		4.24	0.04	13.37	0.04	-1.58	0.70	1.06	0.70
ZK829.5	<i>tbx-36</i>	2.09	0.05	2.74	0.05	-1.29	0.52	-1.89	0.52
ZK829.9		3.05	0.04	5.73	0.04	-1.43	0.56	-2.40	0.56
ZK858.3	<i>cllec-91</i>	2.37	0.04	5.99	0.04	-1.46	0.56	-2.47	0.56
ZK970.7		1.17	0.02	-2.56	0.02	1.10	0.68	1.29	0.68

20 μ M heme/100% O ₂ vs 20 μ M heme/21% O ₂									
K07C6.3	<i>cyp-35B2</i>	3.09							

Bibliography

1. Uzel, C., and Conrad, M. E. (1998). Absorption of heme iron. *Semin Hematol*, 35: 27-34.
2. Conrad, M. E., and Umbreit, J. N. (2000). Iron absorption and transport-an update. *Am J Hematol*, 64: 287-98.
3. Ponka, P. (1999). Cell biology of heme. *Am J Med Sci*, 318: 241-56.
4. Yin, L., Wu, N., Curtin, J. C., Qatanani, M., Szweggold, N. R., Reid, R. A., Waitt, G. M., Parks, D. J., Pearce, K. H., Wisely, G. B., and Lazar, M. A. (2007). Rev-erb α , a Heme Sensor That Coordinates Metabolic and Circadian Pathways. *Science*, 318: 1786-9.
5. Tsiftoglou, A. S., Tsamadou, A. I., and Papadopoulou, L. C. (2006). Heme as key regulator of major mammalian cellular functions: Molecular, cellular, and pharmacological aspects. *Pharmacol Ther*, 111: 327-45.
6. Faller, M., Matsunaga, M., Yin, S., Loo, J. A., and Guo, F. (2007). Heme is involved in microRNA processing. *Nat Struct Mol Biol*, 14: 23-9.
7. Balla, G., Vercellotti, G. M., Muller-Eberhard, U., Eaton, J., and Jacob, H. S. (1991). Exposure of endothelial cells to free heme potentiates damage mediated by granulocytes and toxic oxygen species. *Lab Invest*, 64: 648-55.
8. Hamza, I. (2006). Intracellular trafficking of porphyrins. *ACS Chem Biol*, 1: 627-9.
9. Bullen, J. J., Rogers, H. J., and Griffiths, E. (1978). Role of iron in bacterial infection. *Curr Top Microbiol Immunol*, 80: 1-35.
10. Wandersman, C., and Stojiljkovic, I. (2000). Bacterial heme sources: the role of heme, hemoprotein receptors and hemophores. *Curr Opin Microbiol*, 3: 215-20.
11. Tong, Y., and Guo, M. (2009). Bacterial heme-transport proteins and their heme-coordination modes. *Arch Biochem Biophys*, 481: 1-15.
12. Létoffé, S., Heuck, G., Delepelaire, P., Lange, N., and Wandersman, C. (2009). Bacteria capture iron from heme by keeping tetrapyrrol skeleton intact. *Proc. Nat. Acad. Sci. U.S.A.*, 106: 11719-24.
13. Idei, A., Kawai, E., Akatsuka, H., and Omori, K. (1999). Cloning and characterization of the *Pseudomonas fluorescens* ATP-binding cassette exporter, HasDEF, for the heme acquisition protein HasA. *J Bacteriol*, 181: 7545-51.
14. Akatsuka, H., Binet, R., Kawai, E., Wandersman, C., and Omori, K. (1997). Lipase secretion by bacterial hybrid ATP-binding cassette exporters: molecular recognition of the LipBCD, PrtDEF, and HasDEF exporters. *J Bacteriol*, 179: 4754-60.
15. Bracken, C. S., Baer, M. T., Abdur-Rashid, A., Helms, W., and Stojiljkovic, I. (1999). Use of heme-protein complexes by the *Yersinia enterocolitica* HemR receptor: histidine residues are essential for receptor function. *J Bacteriol*, 181: 6063-72.
16. Letoffe, S., Delepelaire, P., and Wandersman, C. (2004). Free and hemophore-bound heme acquisitions through the outer membrane receptor HasR have

- different requirements for the TonB-ExbB-ExbD complex. *J Bacteriol*, 186: 4067-74.
17. Izadi-Pruneyre, N., Huche, F., Lukat-Rodgers, G. S., Lecroisey, A., Gilli, R., Rodgers, K. R., Wandersman, C., and Delepelaire, P. (2006). The heme transfer from the soluble HasA hemophore to its membrane-bound receptor HasR is driven by protein-protein interaction from a high to a lower affinity binding site. *J Biol Chem*, 281: 25541-50.
 18. Krieg, S., Huche, F., Diederichs, K., Izadi-Pruneyre, N., Lecroisey, A., Wandersman, C., Delepelaire, P., and Welte, W. (2009). Heme uptake across the outer membrane as revealed by crystal structures of the receptor-hemophore complex. *Proc Natl Acad Sci U S A*, 106: 1045-50.
 19. Lewis, L. A., Sung, M. H., Gipson, M., Hartman, K., and Dyer, D. W. (1998). Transport of intact porphyrin by HpuAB, the hemoglobin-haptoglobin utilization system of *Neisseria meningitidis*. *J Bacteriol*, 180: 6043-7.
 20. Genco, C., and Dixon, DW (2001). Emerging strategies in microbial haem capture. *Mol Microbiol*, 39: 1-11.
 21. Smalley, J. W., Thomas, M. F., Birss, A. J., Withnall, R., and Silver, J. (2004). A combination of both arginine- and lysine-specific gingipain activity of *Porphyromonas gingivalis* is necessary for the generation of the micro-oxo bishaem-containing pigment from haemoglobin. *Biochem J*, 379: 833-40.
 22. DeCarlo, A. A., Paramasvaran, M., Yun, P. L. W., Collyer, C., and Hunter, N. (1999). Porphyrin-Mediated Binding to Hemoglobin by the HA2 Domain of Cysteine Proteinases (Gingipains) and Hemagglutinins from the Periodontal Pathogen *Porphyromonas gingivalis*. *J Bacteriol*, 181: 3784-91.
 23. Smalley, J. W., Birss, A. J., Szmigielski, B., and Potempa, J. (2007). Sequential action of R- and K-specific gingipains of *Porphyromonas gingivalis* in the generation of the haem-containing pigment from oxyhaemoglobin. *Arch Biochem Biophys*, 465: 44-9.
 24. Mazmanian, S. K., Skaar, E. P., Gaspar, A. H., Humayun, M., Gornicki, P., Jelenska, J., Joachmiak, A., Missiakas, D. M., and Schneewind, O. (2003). Passage of heme-iron across the envelope of *Staphylococcus aureus*. *Science*, 299: 906-9.
 25. Torres, V. J., Pishchany, G., Humayun, M., Schneewind, O., and Skaar, E. P. (2006). *Staphylococcus aureus* IsdB is a hemoglobin receptor required for heme iron utilization. *J Bacteriol*, 188: 8421-9.
 26. Dryla, A., Gelbmann, D., von Gabain, A., and Nagy, E. (2003). Identification of a novel iron regulated staphylococcal surface protein with haptoglobin-haemoglobin binding activity. *Mol Microbiol*, 49: 37-53.
 27. Liu, M., Tanaka, W. N., Zhu, H., Xie, G., Dooley, D. M., and Lei, B. (2008). Direct heme transfer from IsdA to IsdC in the iron-regulated surface determinant (Isd) heme acquisition system of *Staphylococcus aureus*. *J Biol Chem*, 283: 6668-76.
 28. Muruyoi, N., Tiedemann, M. T., Pluym, M., Cheung, J., Heinrichs, D. E., and Stillman, M. J. (2008). Demonstration of the iron-regulated surface determinant (Isd) heme transfer pathway in *Staphylococcus aureus*. *J Biol Chem*, 283: 28125-36.

29. Maresso, A. W., Garufi, G., and Schneewind, O. (2008). *Bacillus anthracis* secretes proteins that mediate heme acquisition from hemoglobin. *PLoS Pathog*, 4: e1000132.
30. Zhu, H., Liu, M., and Lei, B. (2008). The surface protein Shr of *Streptococcus pyogenes* binds heme and transfers it to the streptococcal heme-binding protein Shp. *BMC Microbiol*, 8: 15.
31. Liu, M., and Lei, B. (2005). Heme transfer from streptococcal cell surface protein Shp to HtsA of transporter HtsABC. *Infect Immun*, 73: 5086-92.
32. Nygaard, T. K., Blouin, G. C., Liu, M., Fukumura, M., Olson, J. S., Fabian, M., Dooley, D. M., and Lei, B. (2006). The mechanism of direct heme transfer from the streptococcal cell surface protein Shp to HtsA of the HtsABC transporter. *J Biol Chem*, 281: 20761-71.
33. Allen, C. E., and Schmitt, M. P. (2009). HtaA is an iron-regulated hemin binding protein involved in the utilization of heme iron in *Corynebacterium diphtheriae*. *J Bacteriol*, 191: 2638-48.
34. Weissman, Z., Shemer, R., and Kornitzer, D. (2002). Deletion of the copper transporter CaCCC2 reveals two distinct pathways for iron acquisition in *Candida albicans*. *Mol Microbiol*, 44: 1551-60.
35. Santos, R., Buisson, N., Knight, S., Dancis, A., Camadro, J. M., and Lesuisse, E. (2003). Haemin uptake and use as an iron source by *Candida albicans*: role of CaHMX1-encoded haem oxygenase. *Microbiology*, 149: 579-88.
36. Weissman, Z., and Kornitzer, D. (2004). A family of *Candida* cell surface haem-binding proteins involved in haemin and haemoglobin-iron utilization. *Mol Microbiol*, 53: 1209-20.
37. Weissman, Z., Shemer, R., Conibear, E., and Kornitzer, D. (2008). An endocytic mechanism for haemoglobin-iron acquisition in *Candida albicans*. *Mol Microbiol*, 69: 201-17.
38. Kim, D., Yukl, E. T., Moenne-Loccoz, P., and Montellano, P. R. (2006). Fungal heme oxygenases: Functional expression and characterization of Hmx1 from *Saccharomyces cerevisiae* and CaHmx1 from *Candida albicans*. *Biochemistry*, 45: 14772-80.
39. Pendrak, M. L., Chao, M. P., Yan, S. S., and Roberts, D. D. (2004). Heme oxygenase in *Candida albicans* is regulated by hemoglobin and is necessary for metabolism of exogenous heme and hemoglobin to alpha-biliverdin. *J Biol Chem*, 279: 3426-33.
40. Protchenko, O., Rodriguez-Suarez, R., Androphy, R., Bussey, H., and Philpott, C. C. (2006). A screen for genes of heme uptake identifies the FLC family required for import of FAD into the endoplasmic reticulum. *J Biol Chem*, 281: 21445-57.
41. Lara, F. A., Lins, U., Paiva-Silva, G., Almeida, I. C., Braga, C. M., Miguens, F. C., Oliveira, P. L., and Dansa-Petretski, M. (2003). A new intracellular pathway of haem detoxification in the midgut of the cattle tick *Boophilus microplus*: aggregation inside a specialized organelle, the hemosome. *J Exp Biol*, 206: 1707-15.
42. Zhou, G., Kohlhepp, P., Geiser, D., Frasquillo Mdel, C., Vazquez-Moreno, L., and Winzerling, J. J. (2007). Fate of blood meal iron in mosquitoes. *J Insect Physiol*, 53: 1169-78.

43. Egan, T. J. (2008). Recent advances in understanding the mechanism of hemozoin (malaria pigment) formation. *J Inorg Biochem*, 102: 1288-99.
44. Chen, M. M., Shi, L., and Sullivan, D. J., Jr. (2001). Haemoproteus and Schistosoma synthesize heme polymers similar to Plasmodium hemozoin and beta-hematin. *Mol Biochem Parasitol*, 113: 1-8.
45. Oliveira, M. F., Silva, J. R., Dansa-Petretski, M., de Souza, W., Lins, U., Braga, C. M., Masuda, H., and Oliveira, P. L. (1999). Haem detoxification by an insect. *Nature*, 400: 517-8.
46. Oliveira, M. F., Silva, J. R., Dansa-Petretski, M., de Souza, W., Braga, C. M., Masuda, H., and Oliveira, P. L. (2000). Haemozoin formation in the midgut of the blood-sucking insect Rhodnius prolixus. *FEBS Lett*, 477: 95-8.
47. Oliveira, M. F., Timm, B. L., Machado, E. A., Miranda, K., Attias, M., Silva, J. R., Dansa-Petretski, M., de Oliveira, M. A., de Souza, W., Pinhal, N. M., Sousa, J. J., Vugman, N. V., and Oliveira, P. L. (2002). On the pro-oxidant effects of haemozoin. *FEBS Lett*, 512: 139-44.
48. Pascoa, V., Oliveira, P. L., Dansa-Petretski, M., Silva, J. R., Alvarenga, P. H., Jacobs-Lorena, M., and Lemos, F. J. (2002). Aedes aegypti peritrophic matrix and its interaction with heme during blood digestion. *Insect Biochem Mol Biol*, 32: 517-23.
49. Devenport, M., Alvarenga, P. H., Shao, L., Fujioka, H., Bianconi, M. L., Oliveira, P. L., and Jacobs-Lorena, M. (2006). Identification of the Aedes aegypti peritrophic matrix protein AeIMUCI as a heme-binding protein. *Biochemistry*, 45: 9540-9.
50. Braz, G. R., Coelho, H. S., Masuda, H., and Oliveira, P. L. (1999). A missing metabolic pathway in the cattle tick Boophilus microplus. *Curr Biol*, 9: 703-6.
51. Lara, F. A., Lins, U., Bechara, G. H., and Oliveira, P. L. (2005). Tracing heme in a living cell: hemoglobin degradation and heme traffic in digest cells of the cattle tick Boophilus microplus. *J Exp Biol*, 208: 3093-101.
52. Donohue, K. V., Khalil, S. M., Sonenshine, D. E., and Roe, R. M. (2009). Heme-binding storage proteins in the Chelicerata. *J Insect Physiol*, 55: 287-96.
53. Donohue, K. V., Khalil, S. M., Mitchell, R. D., Sonenshine, D. E., and Roe, R. M. (2008). Molecular characterization of the major hemelipoglycoprotein in ixodid ticks. *Insect Mol Biol*, 17: 197-208.
54. Maya-Monteiro, C. M., Daffre, S., Logullo, C., Lara, F. A., Alves, E. W., Capurro, M. L., Zingali, R., Almeida, I. C., and Oliveira, P. L. (2000). HeLp, a Heme Lipoprotein from the Hemolymph of the Cattle Tick, Boophilus microplus. *J Biol Chem*, 275: 36584-9.
55. Gudderra, N. P., Neese, P. A., Sonenshine, D. E., Apperson, C. S., and Roe, R. M. (2001). Developmental profile, isolation, and biochemical characterization of a novel lipoglycoheme-carrier protein from the American dog tick, Dermacentor variabilis (Acari: Ixodidae) and observations on a similar protein in the soft tick, Ornithodoros parkeri (Acari: Argasidae). *Insect Biochem Mol Biol*, 31: 299-311.
56. Gudderra, N. P., Sonenshine, D. E., Apperson, C. S., and Roe, R. M. (2002). Tissue distribution and characterization of predominant hemolymph carrier proteins from Dermacentor variabilis and Ornithodoros parkeri. *J Insect Physiol*, 48: 161-70.

57. Maya-Monteiro, C., Alves, L., Pinhal, N., Abdalla, D., and Oliveira, P. (2004). HeLp, a heme-transporting lipoprotein with an antioxidant role. *Insect Biochem Mol Biol* 34: 81-8.
58. Logullo, C., Moraes, J., Dansa-Petretski, M., Vaz, I. S., Masuda, A., Sorgine, M. H., Braz, G. R., Masuda, H., and Oliveira, P. L. (2002). Binding and storage of heme by vitellin from the cattle tick, *Boophilus microplus*. *Insect Biochem Mol Biol*, 32: 1805-11.
59. Gudderra, N. P., Sonenshine, D. E., Apperson, C. S., and Roe, R. M. (2002). Hemolymph proteins in ticks. *J Insect Physiol*, 48: 269-78.
60. Thompson, D. M., Khalil, S. M. S., Jeffers, L. A., Sonenshine, D. E., Mitchell, R. D., Osgood, C. J., and Michael Roe, R. (2007). Sequence and the developmental and tissue-specific regulation of the first complete vitellogenin messenger RNA from ticks responsible for heme sequestration. *Insect Biochem Mol Biol*, 37: 363-74.
61. Pohl, P. C., Sorgine, M. H., Leal, A. T., Logullo, C., Oliveira, P. L., Vaz Ida, S., Jr., and Masuda, A. (2008). An extraovarian aspartic protease accumulated in tick oocytes with vitellin-degradation activity. *Comp Biochem Physiol B Biochem Mol Biol*, 151: 392-9.
62. Seixas, A., Leal, A. T., Nascimento-Silva, M. C., Masuda, A., Termignoni, C., and da Silva Vaz, I., Jr. (2008). Vaccine potential of a tick vitellin-degrading enzyme (VTDCE). *Vet Immunol Immunopathol*, 124: 332-40.
63. Oliveira, P. L., Kawooya, J. K., Ribeiro, J. M., Meyer, T., Poorman, R., Alves, E. W., Walker, F. A., Machado, E. A., Nussenzveig, R. H., Padovan, G. J., and et al. (1995). A heme-binding protein from hemolymph and oocytes of the blood-sucking insect, *Rhodnius prolixus*. Isolation and characterization. *J Biol Chem*, 270: 10897-901.
64. Machado, E. A., Oliveira, P. L., Moreira, M. F., de Souza, W., and Masuda, H. (1998). Uptake of *Rhodnius* heme-binding protein (RHBP) by the ovary of *Rhodnius prolixus*. *Arch Insect Biochem Physiol*, 39: 133-43.
65. Latunde-Dada, G. O., Simpson, R. J., and McKie, A. T. (2006). Recent advances in mammalian haem transport. *Trends Biochem Sci*, 31: 182-8.
66. Shayeghi, M., Latunde-Dada, G. O., Oakhill, J. S., Laftah, A. H., Takeuchi, K., Halliday, N., Khan, Y., Warley, A., McCann, F. E., Hider, R. C., Frazer, D. M., Anderson, G. J., Vulpe, C. D., Simpson, R. J., and McKie, A. T. (2005). Identification of an intestinal heme transporter. *Cell*, 122: 789-801.
67. Qiu, A., Jansen, M., Sakaris, A., Min, S. H., Chattopadhyay, S., Tsai, E., Sandoval, C., Zhao, R., Akabas, M. H., and Goldman, I. D. (2006). Identification of an intestinal folate transporter and the molecular basis for hereditary folate malabsorption. *Cell*, 127: 917-28.
68. Rajagopal, A., Rao, A. U., Amigo, J., Tian, M., Upadhyay, S. K., Hall, C., Uhm, S., Mathew, M. K., Fleming, M. D., Paw, B. H., Krause, M., and Hamza, I. (2008). Haem homeostasis is regulated by the conserved and concerted functions of HRG-1 proteins. *Nature*, 453: 1127-31.
69. Knutson, M. D., Oukka, M., Koss, L. M., Aydemir, F., and Wessling-Resnick, M. (2005). Iron release from macrophages after erythrophagocytosis is up-regulated

- by ferroportin 1 overexpression and down-regulated by hepcidin. *Proc Natl Acad Sci U S A*, 102: 1324-8.
70. Quigley, J. G., Yang, Z., Worthington, M. T., Phillips, J. D., Sabo, K. M., Sabath, D. E., Berg, C. L., Sassa, S., Wood, B. L., and Abkowitz, J. L. (2004). Identification of a human heme exporter that is essential for erythropoiesis. *Cell*, 118: 757-66.
 71. Quigley, J. G., Burns, C. C., Anderson, M. M., Lynch, E. D., Sabo, K. M., Overbaugh, J., and Abkowitz, J. L. (2000). Cloning of the cellular receptor for feline leukemia virus subgroup C (FeLV-C), a retrovirus that induces red cell aplasia. *Blood*, 95: 1093-9.
 72. Keel, S. B., Doty, R. T., Yang, Z., Quigley, J. G., Chen, J., Knoblaugh, S., Kingsley, P. D., De Domenico, I., Vaughn, M. B., Kaplan, J., Palis, J., and Abkowitz, J. L. (2008). A heme export protein is required for red blood cell differentiation and iron homeostasis. *Science*, 319: 825-8.
 73. Krishnamurthy, P., Ross, D. D., Nakanishi, T., Bailey-Dell, K., Zhou, S., Mercer, K. E., Sarkadi, B., Sorrentino, B. P., and Schuetz, J. D. (2004). The stem cell marker Bcrp/ABCG2 enhances hypoxic cell survival through interactions with heme. *J Biol Chem*, 279: 24218-25.
 74. Jonker, J., Buitelaar, M., Wagenaar, E., van der Valk, M., Scheffer, G., Scheper, R., Plosch, T., Kuipers, F., Elferink, R., Rosing, H., Beijnen, J., and Schinkel, A. (2002). The breast cancer resistance protein protects against a major chlorophyll-derived dietary phototoxin and protoporphyria. *Proc Natl Acad Sci U S A*, 99: 15649-54.
 75. Mitsuhashi, N., Miki, T., Senbongi, H., Yokoi, N., Yano, H., Miyazaki, M., Nakajima, N., Iwanaga, T., Yokoyama, Y., Shibata, T., and Seino, S. (2000). MTABC3, a novel mitochondrial ATP-binding cassette protein involved in iron homeostasis. *J Biol Chem*, 275: 17536-40.
 76. Krishnamurthy, P. C., Du, G., Fukuda, Y., Sun, D., Sampath, J., Mercer, K. E., Wang, J., Sosa-Pineda, B., Murti, K. G., and Schuetz, J. D. (2006). Identification of a mammalian mitochondrial porphyrin transporter. *Nature*, 443: 586-9.
 77. Paterson, J. K., Shukla, S., Black, C. M., Tachiwada, T., Garfield, S., Wincovitch, S., Ernst, D. N., Agadir, A., Li, X., Ambudkar, S. V., Szakacs, G., Akiyama, S. I., and Gottesman, M. M. (2007). Human ABCB6 Localizes to Both the Outer Mitochondrial Membrane and the Plasma Membrane. *Biochemistry*, 46: 9443-52.
 78. Litwack, G., Ketterer, B., and Arias, I. M. (1971). Ligandin: a hepatic protein which binds steroids, bilirubin, carcinogens and a number of exogenous organic anions. *Nature*, 234: 466-7.
 79. Harvey, J. W., and Beutler, E. (1982). Binding of heme by glutathione S-transferase: a possible role of the erythrocyte enzyme. *Blood*, 60: 1227-30.
 80. Tipping, E., Ketterer, B., Christodoulides, L., and Enderby, G. (1976). The interactions of haem with ligandin and aminoazo-dye-binding protein A. *Biochem J*, 157: 461-7.
 81. Tipping, E., Ketterer, B., and Koskelo, P. (1978). The binding of porphyrins by ligandin. *Biochem J*, 169: 509-16.

82. Harwaldt, P., Rahlfs, S., and Becker, K. (2002). Glutathione S-transferase of the malarial parasite *Plasmodium falciparum*: characterization of a potential drug target. *Biol Chem*, 383: 821-30.
83. Hiller, N., Fritz-Wolf, K., Deponte, M., Wende, W., Zimmermann, H., and Becker, K. (2006). *Plasmodium falciparum* glutathione S-transferase--structural and mechanistic studies on ligand binding and enzyme inhibition. *Protein Sci*, 15: 281-9.
84. Srivastava, P., Puri, S. K., Kamboj, K. K., and Pandey, V. C. (1999). Glutathione-S-transferase activity in malarial parasites. *Trop Med Int Health*, 4: 251-4.
85. Platel, D. F., Mangou, F., and Tribouley-Duret, J. (1999). Role of glutathione in the detoxification of ferriprotoporphyrin IX in chloroquine resistant *Plasmodium berghei*. *Mol Biochem Parasitol*, 98: 215-23.
86. van Rossum, A. J., Jefferies, J. R., Rijsewijk, F. A., LaCourse, E. J., Teesdale-Spittle, P., Barrett, J., Tait, A., and Brophy, P. M. (2004). Binding of hematin by a new class of glutathione transferase from the blood-feeding parasitic nematode *Haemonchus contortus*. *Infect Immun*, 72: 2780-90.
87. Zhan, B., Liu, S., Perally, S., Xue, J., Fujiwara, R., Brophy, P., Xiao, S., Liu, Y., Feng, J., Williamson, A., Wang, Y., Bueno, L. L., Mendez, S., Goud, G., Bethony, J. M., Hawdon, J. M., Loukas, A., Jones, K., and Hotez, P. J. (2005). Biochemical characterization and vaccine potential of a heme-binding glutathione transferase from the adult hookworm *Ancylostoma caninum*. *Infect Immun*, 73: 6903-11.
88. Senjo, M., Ishibashi, T., and Imai, Y. (1985). Purification and characterization of cytosolic liver protein facilitating heme transport into apocytochrome b5 from mitochondria. Evidence for identifying the heme transfer protein as belonging to a group of glutathione S-transferases. *J Biol Chem*, 260: 9191-6.
89. Taketani, S., Adachi, Y., Kohno, H., Ikehara, S., Tokunaga, R., and Ishii, T. (1998). Molecular Characterization of a Newly Identified Heme-binding Protein Induced during Differentiation of murine Erythroleukemia Cells. *J Biol Chem*, 273: 31388-94.
90. Dias, J. S., Macedo, A. L., Ferreira, G. C., Peterson, F. C., Volkman, B. F., and Goodfellow, B. J. (2006). The first structure from the SOUL/HBP family of heme-binding proteins, murine P22HBP. *J Biol Chem*, 281: 31553-61.
91. Takahashi, S., Ogawa, T., Inoue, K., and Masuda, T. (2008). Characterization of cytosolic tetrapyrrole-binding proteins in *Arabidopsis thaliana*. *Photochem Photobiol Sci*, 7: 1216-24.
92. Sato, E., Sagami, I., Uchida, T., Sato, A., Kitagawa, T., Igarashi, J., and Shimizu, T. (2004). SOUL in Mouse Eyes Is a New Hexameric Heme-Binding Protein with Characteristic Optical Absorption, Resonance Raman Spectral, and Heme-Binding Properties. *Biochemistry*, 43: 14189-98.
93. Zylka, M. J., and Reppert, S. M. (1999). Discovery of a putative heme-binding protein family (SOUL/HBP) by two-tissue suppression subtractive hybridization and database searches. *Mol Brain Res*, 74: 175-81.
94. Iwahara, S. I., Satoh, H., Song, D. X., Webb, J., Burlingame, A. L., Nagae, Y., and Muller-Eberhard, U. (1995). Purification, characterization, and cloning of a heme-binding protein (23 kDa) in rat liver cytosol. *Biochemistry*, 34: 13398-406.

95. Hirotsu, S., Abe, Y., Okada, K., Nagahara, N., Hori, H., Nishino, T., and Hakoshima, T. (1999). Crystal structure of a multifunctional 2-Cys peroxiredoxin heme-binding protein 23 kDa/proliferation-associated gene product. *Proc Natl Acad Sci U S A*, 96: 12333-8.
96. Immenschuh, S., Nell, C., Iwahara, S.-i., Katz, N., and Muller-Eberhard, U. (1997). Gene Regulation of HBP 23 by Metalloporphyrins and Protoporphyrin IX in Liver and Hepatocyte Cultures. *Biochem Biophys Res Commun*, 231: 667-70.
97. Ishii, T., Kawane, T., Taketani, S., and Bannai, S. (1995). Inhibition of the thiol-specific antioxidant activity of rat liver MSP23 protein by hemin. *Biochem Biophys Res Commun*, 216: 970-5.
98. Vincent, S. H., and Muller-Eberhard, U. (1985). A protein of the Z class of liver cytosolic proteins in the rat that preferentially binds heme. *J Biol Chem*, 260: 14521-8.
99. Stewart, J. M., Slys, G. W., Pritting, M. A., and Muller-Eberhard, U. (1996). Ferriheme and ferroheme are isosteric inhibitors of fatty acid binding to rat liver fatty acid binding protein. *Biochem Cell Biol*, 74: 249-55.
100. Smithies, O., and Walker, N. (1955). Genetic control of some serum proteins in normal humans. *Nature*, 176: 1265-66.
101. Okazaki, T., Yanagisawa, Y., and Nagai, T. (1997). Analysis of the affinity of each haptoglobin polymer for hemoglobin by two-dimensional affinity electrophoresis. *Clin Chim Acta*, 258: 137-44.
102. Wejman, J. C., Hovsepian, D., Wall, J. S., Hainfeld, J. F., and Greer, J. (1984). Structure of haptoglobin and the haptoglobin-hemoglobin complex by electron microscopy. *J Mol Biol*, 174: 319-41.
103. Kristiansen, M., Graversen, J. H., Jacobsen, C., Sonne, O., Hoffman, H.-J., Law, S. K. A., and Moestrup, S. K. (2001). Identification of the haemoglobin scavenger receptor. *Nature* 409: 198-201.
104. Kino, K., Tsunoo, H., Higa, Y., Takami, M., Hamaguchi, H., and Nakajima, H. (1980). Hemoglobin-haptoglobin receptor in rat liver plasma membrane. *J Biol Chem*, 255: 9616-20.
105. Okuda, M., Tokunaga, R., and Taketani, S. (1992). Expression of haptoglobin receptors in human hepatoma cells. *Biochim Biophys Acta*, 1136: 143-9.
106. Bratosin, D., Mazurier, J., Tissier, J. P., Estaquier, J., Huart, J. J., Ameisen, J. C., Aminoff, D., and Montreuil, J. (1998). Cellular and molecular mechanisms of senescent erythrocyte phagocytosis by macrophages. A review. *Biochimie*, 80: 173-95.
107. Delaby, C., Pilard, N., Puy, H., and Canonne-Hergaux, F. (2008). Sequential regulation of ferroportin expression after erythrophagocytosis in murine macrophages: early mRNA induction by haem, followed by iron-dependent protein expression. *Biochem J*, 411: 123-31.
108. Fagoonee, S., Gburek, J., Hirsch, E., Marro, S., Moestrup, S. K., Laurberg, J. M., Christensen, E. I., Silengo, L., Altruda, F., and Tolosano, E. (2005). Plasma protein haptoglobin modulates renal iron loading. *Am J Pathol*, 166: 973-83.
109. Langlois, M. R., and Delanghe, J. R. (1996). Biological and clinical significance of haptoglobin polymorphism in humans. *Clin Chem*, 42: 1589-600.

110. Hrkál, Z., Vodrázka, Z., and Kalousek, I. (1974). Transfer of Heme from Ferrihemoglobin and Ferrihemoglobin Isolated Chains to Hemopexin. *Eur J Biochem*, 43: 73-8.
111. Hvidberg, V., Maniecki, M. B., Jacobsen, C., Hojrup, P., Møller, H. J., and Møestrup, S. K. (2005). Identification of the receptor scavenging hemopexin-heme complexes. *Blood*, 106: 2572-9.
112. Delanghe, J. R., and Langlois, M. R. (2001). Hemopexin: a review of biological aspects and the role in laboratory medicine. *Clin Chim Acta*, 312: 13-23.
113. Vinchi, F., Gastaldi, S., Silengo, L., Altruda, F., and Tolosano, E. (2008). Hemopexin Prevents Endothelial Damage and Liver Congestion in a Mouse Model of Heme Overload. *Am J Pathol*, 173: 289-99.
114. Adams, P., and Berman, M. (1980). Kinetics and mechanism of the interaction between human serum albumin and monomeric haemin. *Biochem J*, 191: 95–102.
115. Dockal, M., Carter, D. C., and Ruker, F. (1999). The three recombinant domains of human serum albumin. Structural characterization and ligand binding properties. *J Biol Chem*, 274: 29303-10.
116. Zunszain, P., Ghuman, J., Komatsu, T., Tsuchida, E., and Curry, S. (2003). Crystal structural analysis of human serum albumin complexed with hemin and fatty acid. *BMC Struct Biol*, 3: 6.
117. Miller, Y. I., and Shaklai, N. (1998). Kinetics of hemin distribution in plasma reveals its role in lipoprotein oxidation. *Biochim Biophys Acta*, 1454: 153-64.
118. Gray, J. M., Karow, D. S., Lu, H., Chang, A. J., Chang, J. S., Ellis, R. E., Marletta, M. A., and Bargmann, C. I. (2004). Oxygen sensation and social feeding mediated by a *C. elegans* guanylate cyclase homologue. *Nature*, 430: 317-22.
119. Mense, S. M., and Zhang, L. (2006). Heme: a versatile signaling molecule controlling the activities of diverse regulators ranging from transcription factors to MAP kinases. *Cell Res*, 16: 681-92.
120. Persson, A., Gross, E., Laurent, P., Busch, K. E., Bretes, H., and de Bono, M. (2009). Natural variation in a neural globin tunes oxygen sensing in wild *Caenorhabditis elegans*. *Nature*, 458: 1030-3.
121. Oyake, T., Itoh, K., Motohashi, H., Hayashi, N., Hoshino, H., Nishizawa, M., Yamamoto, M., and Igarashi, K. (1996). Bach proteins belong to a novel family of BTB-basic leucine zipper transcription factors that interact with MafK and regulate transcription through the NF-E2 site. *Mol Cell Biol*, 16: 6083-95.
122. Kitamuro, T., Takahashi, K., Ogawa, K., Uono-Fujimori, R., Takeda, K., Furuyama, K., Nakayama, M., Sun, J., Fujita, H., Hida, W., Hattori, T., Shirato, K., Igarashi, K., and Shibahara, S. (2003). Bach1 functions as a hypoxia-inducible repressor for the heme oxygenase-1 gene in human cells. *J Biol Chem*, 278: 9125-33.
123. Ogawa, K., Sun, J., Taketani, S., Nakajima, O., Nishitani, C., Sassa, S., Hayashi, N., Yamamoto, M., Shibahara, S., Fujita, H., and Igarashi, K. (2001). Heme mediates derepression of Maf recognition element through direct binding to transcription repressor Bach1. *Embo J*, 20: 2835-43.
124. Graber, S. G., and Woodworth, R. C. (1986). Myoglobin expression in L6 muscle cells. Role of differentiation and heme. *J Biol Chem*, 261: 9150-4.

125. Woessmann, W., and Mivechi, N. F. (2001). Role of ERK activation in growth and erythroid differentiation of K562 cells. *Exp Cell Res*, 264: 193-200.
126. Zhu, Y., Sun, Y., Jin, K., and Greenberg, D. A. (2002). Hemin induces neuroglobin expression in neural cells. *Blood*, 100: 2494-8.
127. Sun, J., Hoshino, H., Takaku, K., Nakajima, O., Muto, A., Suzuki, H., Tashiro, S., Takahashi, S., Shibahara, S., Alam, J., Taketo, M. M., Yamamoto, M., and Igarashi, K. (2002). Hemoprotein Bach1 regulates enhancer availability of heme oxygenase-1 gene. *Embo J*, 21: 5216-24.
128. Suzuki, H., Tashiro, S., Hira, S., Sun, J., Yamazaki, C., Zenke, Y., Ikeda-Saito, M., Yoshida, M., and Igarashi, K. (2004). Heme regulates gene expression by triggering Crm1-dependent nuclear export of Bach1. *EMBO J*, 23: 2544-53.
129. Zenke-Kawasaki, Y., Dohi, Y., Katoh, Y., Ikura, T., Ikura, M., Asahara, T., Tokunaga, F., Iwai, K., and Igarashi, K. (2007). Heme induces ubiquitination and degradation of the transcription factor Bach1. *Mol Cell Biol*, 27: 6962-71.
130. Lazar, M. A., Hodin, R. A., Darling, D. S., and Chin, W. W. (1989). A novel member of the thyroid/steroid hormone receptor family is encoded by the opposite strand of the rat c-erbA alpha transcriptional unit. *Mol Cell Biol*, 9: 1128-36.
131. Miyajima, N., Kadowaki, Y., Fukushige, S., Shimizu, S., Semba, K., Yamanashi, Y., Matsubara, K., Toyoshima, K., and Yamamoto, T. (1988). Identification of two novel members of erbA superfamily by molecular cloning: the gene products of the two are highly related to each other. *Nucleic Acids Res*, 16: 11057-74.
132. Burris, T. P. (2008). Nuclear hormone receptors for heme: REV-ERBalpha and REV-ERBbeta are ligand-regulated components of the mammalian clock. *Mol Endocrinol*, 22: 1509-20.
133. Harding, H. P., and Lazar, M. A. (1995). The monomer-binding orphan receptor Rev-Erb represses transcription as a dimer on a novel direct repeat. *Mol Cell Biol*, 15: 4791-802.
134. Raghuram, S., Stayrook, K. R., Huang, P., Rogers, P. M., Nosie, A. K., McClure, D. B., Burris, L. L., Khorasanizadeh, S., Burris, T. P., and Rastinejad, F. (2007). Identification of heme as the ligand for the orphan nuclear receptors REV-ERBalpha and REV-ERBbeta. *Nat Struct Mol Biol*, 14: 1207-13.
135. Downes, M., Burke, L. J., Bailey, P. J., and Muscat, G. E. (1996). Two receptor interaction domains in the corepressor, N-CoR/RIP13, are required for an efficient interaction with Rev-erbA alpha and RVR: physical association is dependent on the E region of the orphan receptors. *Nucleic Acids Res*, 24: 4379-86.
136. Kaasik, K., and Lee, C. C. (2004). Reciprocal regulation of haem biosynthesis and the circadian clock in mammals. *Nature*, 430: 467-71.
137. Dioum, E. M., Rutter, J., Tuckerman, J. R., Gonzalez, G., Gilles-Gonzalez, M. A., and McKnight, S. L. (2002). NPAS2: a gas-responsive transcription factor. *Science*, 298: 2385-7.
138. Jacobs, N. J., and Jacobs, J. M. (1977). Evidence for involvement of the electron transport system at a late step of anaerobic microbial heme synthesis. *Biochim Biophys Acta*, 459: 141-4.
139. Dagsgaard, C., Taylor, L. E., O'Brien, K. M., and Poyton, R. O. (2001). Effects of anoxia and the mitochondrion on expression of aerobic nuclear COX genes in

- yeast: evidence for a signaling pathway from the mitochondrial genome to the nucleus. *J Biol Chem*, 276: 7593-601.
140. Lee, S. H., and Altenberg, G. A. (2003). Expression of functional multidrug-resistance protein 1 in *Saccharomyces cerevisiae*: effects of N- and C-terminal affinity tags. *Biochem Biophys Res Commun*, 306: 644-9.
 141. Hon, T., Lee, H. C., Hu, Z., Iyer, V. R., and Zhang, L. (2005). The heme activator protein Hap1 represses transcription by a heme-independent mechanism in *Saccharomyces cerevisiae*. *Genetics*, 169: 1343-52.
 142. Lan, C., Lee, H. C., Tang, S., and Zhang, L. (2004). A novel mode of chaperone action: heme activation of Hap1 by enhanced association of Hsp90 with the repressed Hsp70-Hap1 complex. *J Biol Chem*, 279: 27607-12.
 143. Hickman, M. J., and Winston, F. (2007). Heme levels switch the function of Hap1 of *Saccharomyces cerevisiae* between transcriptional activator and transcriptional repressor. *Mol Cell Biol*, 27: 7414-24.
 144. Qi, Z., Hamza, I., and O'Brian, M. R. (1999). Heme is an effector molecule for iron-dependent degradation of the bacterial iron response regulator (Irr) protein. *Proc Natl Acad Sci U S A*, 96: 13056-61.
 145. Marziali, G., Perrotti, E., Ilari, R., Testa, U., Coccia, E. M., and Battistini, A. (1997). Transcriptional regulation of the ferritin heavy-chain gene: the activity of the CCAAT binding factor NF-Y is modulated in heme-treated Friend leukemia cells and during monocyte-to-macrophage differentiation. *Mol Cell Biol*, 17: 1387-95.
 146. Reddy, S. V., Alcantara, O., and Boldt, D. H. (1998). Analysis of DNA binding proteins associated with hemin-induced transcriptional inhibition. The hemin response element binding protein is a heterogeneous complex that includes the Ku protein. *Blood*, 91: 1793-801.
 147. Reddy, S. V., Alcantara, O., Roodman, G. D., and Boldt, D. H. (1996). Inhibition of tartrate-resistant acid phosphatase gene expression by hemin and protoporphyrin IX. Identification of a hemin-responsive inhibitor of transcription. *Blood*, 88: 2288-97.
 148. Zhou, H., Cadigan, K. M., and Thiele, D. J. (2003). A copper-regulated transporter required for copper acquisition, pigmentation, and specific stages of development in *Drosophila melanogaster*. *J Biol Chem*, 278: 48210-8.
 149. Graden, J. A., and Winge, D. R. (1997). Copper-mediated repression of the activation domain in the yeast Mac1p transcription factor. *Proc Natl Acad Sci U S A*, 94: 5550-5.
 150. Gunshin, H., Allerson, C. R., Polycarpou-Schwarz, M., Rofts, A., Rogers, J. T., Kishi, F., Hentze, M. W., Rouault, T. A., Andrews, N. C., and Hediger, M. A. (2001). Iron-dependent regulation of the divalent metal ion transporter. *FEBS Lett*, 509: 309-16.
 151. Chan, M. S., Medley, G. F., Jamison, D., and Bundy, D. A. (1994). The evaluation of potential global morbidity attributable to intestinal nematode infections. *Parasitology*, 109 (Pt 3): 373-87.
 152. Hotez, P. J., Brindley, P. J., Bethony, J. M., King, C. H., Pearce, E. J., and Jacobson, J. (2008). Helminth infections: the great neglected tropical diseases. *J Clin Invest*, 118: 1311-21.

153. Fuller, V., Lilley, C., and Urwin, P. (2008). Nematode resistance. *New Phytol.*, 180: 27-44.
154. Jasmer, D. P., Goverse, A., and Smant, G. (2003). Parasitic nematode interactions with mammals and plants. *Annu Rev Phytopathol*, 41: 245-70.
155. Clemens, L. E., and Basch, P. F. (1989). Schistosoma mansoni: effect of transferrin and growth factors on development of schistosomula in vitro. *J Parasitol*, 75: 417-21.
156. Correa Soares, J. B., Maya-Monteiro, C. M., Bittencourt-Cunha, P. R., Atella, G. C., Lara, F. A., d'Avila, J. C., Menezes, D., Vannier-Santos, M. A., Oliveira, P. L., Egan, T. J., and Oliveira, M. F. (2007). Extracellular lipid droplets promote hemozoin crystallization in the gut of the blood fluke Schistosoma mansoni. *FEBS Lett*, 581: 1742-50.
157. Held, M. R., Bungiro, R. D., Harrison, L. M., Hamza, I., and Cappello, M. (2006). Dietary iron content mediates hookworm pathogenesis in vivo. *Infect Immun*, 74: 289-95.
158. Williamson, A. L., Lecchi, P., Turk, B. E., Choe, Y., Hotez, P. J., McKerrow, J. H., Cantley, L. C., Sajid, M., Craik, C. S., and Loukas, A. (2004). A multi-enzyme cascade of hemoglobin proteolysis in the intestine of blood-feeding hookworms. *J Biol Chem*, 279: 35950-7.
159. Loukas, A., Bethony, J. M., Mendez, S., Fujiwara, R. T., Goud, G. N., Ranjit, N., Zhan, B., Jones, K., Bottazzi, M. E., and Hotez, P. J. (2005). Vaccination with recombinant aspartic hemoglobinase reduces parasite load and blood loss after hookworm infection in dogs. *PLoS Med*, 2: e295.
160. Rao, A. U., Carta, L. K., Lesuisse, E., and Hamza, I. (2005). Lack of heme synthesis in a free-living eukaryote. *Proc Natl Acad Sci U S A*, 102: 4270-5.
161. Epstein, H. F., and Shakes, D. C. (eds) (1995) *Caenorhabditis elegans: Modern Biological Analysis of an Organism Vol. 48. Methods in Cell Biology*. Edited by Wilson, L., and Matsudaira, P., Academic Press, San Diego
162. Nass, R., and Hamza, I. (2007) The nematode *C. elegans* as an animal model to explore toxicology in vivo: solid and axenic growth culture conditions and compound exposure parameters. 1.9.1-1.9.17. *Current Protocols in Toxicology*. Edited by Maines, M. D., Costa, L. G., Hodgson, E., Reed, D. J., and Sipes, I. G., John Wiley & Sons, Inc., New York
163. Van Voorhies, W. A., and Ward, S. (2000). Broad oxygen tolerance in the nematode *Caenorhabditis elegans*. *J Exp Biol*, 203: 2467-78.
164. Gengyo-Ando, K., and Mitani, S. (2000). Characterization of mutations induced by ethyl methanesulfonate, UV, and trimethylpsoralen in the nematode *Caenorhabditis elegans*. *Biochem Biophys Res Commun*, 269: 64-9.
165. Evans, T. C. (2006) (WormBook, ed), The *C. elegans* Research Community, WormBook, doi/10.1895/wormbook.1.108.1, <http://www.wormbook.org>.
166. Praitis, V., Casey, E., Collar, D., and Austin, J. (2001). Creation of low-copy integrated transgenic lines in *Caenorhabditis elegans*. *Genetics*, 157: 1217-26.
167. Livak, K. J., and Schmittgen, T. D. (2001). Analysis of relative gene expression data using real-time quantitative PCR and the 2^{-ΔΔC_T} Method. *Methods*, 25: 402-8.
168. Ahringer, J. (2006) (WormBook, ed), The *C. elegans* Research Community, WormBook, doi/10.1895/wormbook.1.47.1, <http://www.wormbook.org>.

169. Lorenz, H., Hailey, D. W., and Lippincott-Schwartz, J. (2006). Fluorescence protease protection of GFP chimeras to reveal protein topology and subcellular localization. *Nat Methods*, 3: 205-10.
170. Zhu, Y. H., Hon, T., Ye, W. Z., and Zhang, L. (2002). Heme deficiency interferes with the Ras-mitogen-activated protein kinase signaling pathway and expression of a subset of neuronal genes. *Cell Growth Differ*, 13: 431-9.
171. Tsutsui, K. (1986). Affinity chromatography of heme-binding proteins: synthesis of hemin-agarose. *Methods Enzymol*, 123: 331-8.
172. Crisp, R. J., Pollington, A., Galea, C., Jaron, S., Yamaguchi-Iwai, Y., and Kaplan, J. (2003). Inhibition of heme biosynthesis prevents transcription of iron uptake genes in yeast. *J Biol Chem*, 278: 45499-506.
173. Sherman, F. (2002). Getting started with yeast. *Methods Enzymol*, 350: 3-41.
174. Adams, A., D. E. Gottschling, C. A. Kaiser, and T. Stearns. (1997) *Methods in Yeast Genetics: A Laboratory Course Manual.*, Cold Spring Harbor Laboratory Press, Cold Spring Harbor, NY
175. RDevelopmentCoreTeam. (2008) R: A Language and Environment for Statistical Computing, R Foundation for Statistical Computing. <http://www.R-project.org> ISBN 3-900051-07-0., Vienna, Austria
176. Leung, Y. F., Ma, P., Link, B. A., and Dowling, J. E. (2008). Factorial microarray analysis of zebrafish retinal development. *Proc Natl Acad Sci U S A*, 105: 12909-14.
177. Saeed, A. I., Sharov, V., White, J., Li, J., Liang, W., Bhagabati, N., Braisted, J., Klapa, M., Currier, T., Thiagarajan, M., Sturn, A., Snuffin, M., Rezantsev, A., Popov, D., Ryltsov, A., Kostukovich, E., Borisovsky, I., Liu, Z., Vinsavich, A., Trush, V., and Quackenbush, J. (2003). TM4: a free, open-source system for microarray data management and analysis. *Biotechniques*, 34: 374-8.
178. Dennis, G., Jr., Sherman, B. T., Hosack, D. A., Yang, J., Gao, W., Lane, H. C., and Lempicki, R. A. (2003). DAVID: Database for Annotation, Visualization, and Integrated Discovery. *Genome Biol*, 4: P3.
179. Kanehisa, M., Araki, M., Goto, S., Hattori, M., Hirakawa, M., Itoh, M., Katayama, T., Kawashima, S., Okuda, S., Tokimatsu, T., and Yamanishi, Y. (2008). KEGG for linking genomes to life and the environment. *Nucleic Acids Res*, 36: D480-4.
180. Huang da, W., Sherman, B. T., and Lempicki, R. A. (2009). Systematic and integrative analysis of large gene lists using DAVID bioinformatics resources. *Nat Protoc*, 4: 44-57.
181. Simonis, N., Rual, J. F., Carvunis, A. R., Tasan, M., Lemmens, I., Hirozane-Kishikawa, T., Hao, T., Sahalie, J. M., Venkatesan, K., Gebreab, F., Cevik, S., Klitgord, N., Fan, C., Braun, P., Li, N., Ayivi-Guedehoussou, N., Dann, E., Bertin, N., Szeto, D., Dricot, A., Yildirim, M. A., Lin, C., de Smet, A. S., Kao, H. L., Simon, C., Smolyar, A., Ahn, J. S., Tewari, M., Boxem, M., Milstein, S., Yu, H., Dreze, M., Vandenhaute, J., Gunsalus, K. C., Cusick, M. E., Hill, D. E., Tavernier, J., Roth, F. P., and Vidal, M. (2009). Empirically controlled mapping of the *Caenorhabditis elegans* protein-protein interactome network. *Nat Methods*, 6: 47-54.

182. Shannon, P., Markiel, A., Ozier, O., Baliga, N. S., Wang, J. T., Ramage, D., Amin, N., Schwikowski, B., and Ideker, T. (2003). Cytoscape: a software environment for integrated models of biomolecular interaction networks. *Genome Res*, 13: 2498-504.
183. Lomsadze, A., Ter-Hovhannisyan, V., Chernoff, Y. O., and Borodovsky, M. (2005). Gene identification in novel eukaryotic genomes by self-training algorithm. *Nucleic Acids Res*, 33: 6494-506.
184. Bjellqvist, B., Basse, B., Olsen, E., and Celis, J. E. (1994). Reference points for comparisons of two-dimensional maps of proteins from different human cell types defined in a pH scale where isoelectric points correlate with polypeptide compositions. *Electrophoresis*, 15: 529-39.
185. Puntervoll, P., Linding, R., Gemund, C., Chabanis-Davidson, S., Mattingsdal, M., Cameron, S., Martin, D. M., Ausiello, G., Brannetti, B., Costantini, A., Ferre, F., Maselli, V., Via, A., Cesareni, G., Diella, F., Superti-Furga, G., Wyrwicz, L., Ramu, C., McGuigan, C., Gudavalli, R., Letunic, I., Bork, P., Rychlewski, L., Kuster, B., Helmer-Citterich, M., Hunter, W. N., Aasland, R., and Gibson, T. J. (2003). ELM server: A new resource for investigating short functional sites in modular eukaryotic proteins. *Nucleic Acids Res*, 31: 3625-30.
186. Cole, C., Barber, J. D., and Barton, G. J. (2008). The Jpred 3 secondary structure prediction server. *Nucleic Acids Res*, 36: W197-201.
187. Thompson, J. D., Higgins, D. G., and Gibson, T. J. (1994). CLUSTAL W: improving the sensitivity of progressive multiple sequence alignment through sequence weighting, position-specific gap penalties and weight matrix choice. *Nucleic Acids Res*, 22: 4673-80.
188. Saitou, N., and Nei, M. (1987). The neighbor-joining method: a new method for reconstructing phylogenetic trees. *Mol Biol Evol*, 4: 406-25.
189. Tamura, K., Dudley, J., Nei, M., and Kumar, S. (2007). MEGA4: Molecular Evolutionary Genetics Analysis (MEGA) software version 4.0. *Mol Biol Evol*, 24: 1596-9.
190. Blumenthal, T., Evans, D., Link, C. D., Guffanti, A., Lawson, D., Thierry-Mieg, J., Thierry-Mieg, D., Chiu, W. L., Duke, K., Kiraly, M., and Kim, S. K. (2002). A global analysis of *Caenorhabditis elegans* operons. *Nature*, 417: 851-4.
191. Dong, J., Song, M. O., and Freedman, J. H. (2005). Identification and characterization of a family of *Caenorhabditis elegans* genes that is homologous to the cadmium-responsive gene *cdr-1*. *Biochim Biophys Acta*, 1727: 16-26.
192. Cox, E. A., and Hardin, J. (2004). Sticky worms: adhesion complexes in *C. elegans*. *J Cell Sci*, 117: 1885-97.
193. Labouesse, M. (2006) (WormBook, ed), The *C. elegans* Research Community, WormBook, doi/10.1895/wormbook.1.56.1, <http://www.wormbook.org>.
194. Kim, B. E., Wang, F., Dufner-Beattie, J., Andrews, G. K., Eide, D. J., and Petris, M. J. (2004). Zn²⁺-stimulated endocytosis of the mZIP4 zinc transporter regulates its location at the plasma membrane. *J Biol Chem*, 279: 4523-30.
195. Schwartz, M. A., Both, G., and Lechene, C. (1989). Effect of cell spreading on cytoplasmic pH in normal and transformed fibroblasts. *Proc Natl Acad Sci U S A*, 86: 4525-9.

196. Myers, A. M., Pape, L. K., and Tzagoloff, A. (1985). Mitochondrial protein synthesis is required for maintenance of intact mitochondrial genomes in *Saccharomyces cerevisiae*. *EMBO J*, 4: 2087-92.
197. Dorfman, B. Z. (1969). The isolation of adenylosuccinate synthetase mutants in yeast by selection for constitutive behavior in pigmented strains. *Genetics*, 61: 377-89.
198. Shadel, G. S. (1999). Yeast as a model for human mtDNA replication. *Am J Hum Genet*, 65: 1230-7.
199. Liao, V. H., Dong, J., and Freedman, J. H. (2002). Molecular characterization of a novel, cadmium-inducible gene from the nematode *Caenorhabditis elegans*. A new gene that contributes to the resistance to cadmium toxicity. *J Biol Chem*, 277: 42049-59.
200. Dong, J., Boyd, W. A., and Freedman, J. H. (2008). Molecular characterization of two homologs of the *Caenorhabditis elegans* cadmium-responsive gene *cdr-1*: *cdr-4* and *cdr-6*. *J Mol Biol*, 376: 621-33.
201. Ghedin, E., Wang, S., Spiro, D., Caler, E., Zhao, Q., Crabtree, J., Allen, J. E., Delcher, A. L., Guiliano, D. B., Miranda-Saavedra, D., Angiuoli, S. V., Creasy, T., Amedeo, P., Haas, B., El-Sayed, N. M., Wortman, J. R., Feldblyum, T., Tallon, L., Schatz, M., Shumway, M., Koo, H., Salzberg, S. L., Schobel, S., Pertea, M., Pop, M., White, O., Barton, G. J., Carlow, C. K., Crawford, M. J., Daub, J., Dimmic, M. W., Estes, C. F., Foster, J. M., Ganatra, M., Gregory, W. F., Johnson, N. M., Jin, J., Komuniecki, R., Korf, I., Kumar, S., Laney, S., Li, B. W., Li, W., Lindblom, T. H., Lustigman, S., Ma, D., Maina, C. V., Martin, D. M., McCarter, J. P., McReynolds, L., Mitreva, M., Nutman, T. B., Parkinson, J., Peregrin-Alvarez, J. M., Poole, C., Ren, Q., Saunders, L., Sluder, A. E., Smith, K., Stanke, M., Unnasch, T. R., Ware, J., Wei, A. D., Weil, G., Williams, D. J., Zhang, Y., Williams, S. A., Fraser-Liggett, C., Slatko, B., Blaxter, M. L., and Scott, A. L. (2007). Draft genome of the filarial nematode parasite *Brugia malayi*. *Science*, 317: 1756-60.
202. Hill, K. K., Bedian, V., Juang, J. L., and Hoffmann, F. M. (1995). Genetic interactions between the *Drosophila* Abelson (Abl) tyrosine kinase and failed axon connections (fax), a novel protein in axon bundles. *Genetics*, 141: 595-606.
203. Protchenko, O., Shakoury-Elizeh, M., Keane, P., Storey, J., Androphy, R., and Philpott, C. C. (2008). Role of PUG1 in inducible porphyrin and heme transport in *Saccharomyces cerevisiae*. *Eukaryot Cell*, 7: 859-71.
204. McKie, A. T., Marciani, P., Rolfs, A., Brennan, K., Wehr, K., Barrow, D., Miret, S., Bomford, A., Peters, T. J., Farzaneh, F., Hediger, M. A., Hentze, M. W., and Simpson, R. J. (2000). A Novel Duodenal Iron-Regulated Transporter, IREG1, Implicated in the Basolateral Transfer of Iron to the Circulation. *Mol Cell*, 5: 299-309.
205. Ohgami, R. S., Campagna, D. R., Greer, E. L., Antiochos, B., McDonald, A., Chen, J., Sharp, J. J., Fujiwara, Y., Barker, J. E., and Fleming, M. D. (2005). Identification of a ferrireductase required for efficient transferrin-dependent iron uptake in erythroid cells. *Nat Genet*, 37: 1264-9.
206. Ohgami, R. S., Campagna, D. R., McDonald, A., and Fleming, M. D. (2006). The Steap proteins are metalloreductases. *Blood*, 108: 1388-94.

207. Wyman, S., Simpson, R. J., McKie, A. T., and Sharp, P. A. (2008). Dcytb (Cybrd1) functions as both a ferric and a cupric reductase in vitro. *FEBS Lett*, 582: 1901-6.
208. Nicholson, D. W., and Neupert, W. (1989). Import of cytochrome c into mitochondria: reduction of heme, mediated by NADH and flavin nucleotides, is obligatory for its covalent linkage to apocytochrome c. *Proc Natl Acad Sci U S A*, 86: 4340-4.
209. Richard-Fogal, C. L., Frawley, E. R., Bonner, E. R., Zhu, H., San Francisco, B., and Kranz, R. G. (2009). A conserved haem redox and trafficking pathway for cofactor attachment. *EMBO J*, 28: 2349-59.
210. Allhorn, M., Klapyta, A., and Akerstrom, B. (2005). Redox properties of the lipocalin alpha1-microglobulin: reduction of cytochrome c, hemoglobin, and free iron. *Free Radic Biol Med*, 38: 557-67.
211. Hughes, A. L., Powell, D. W., Bard, M., Eckstein, J., Barbuch, R., Link, A. J., and Espenshade, P. J. (2007). Dap1/PGRMC1 binds and regulates cytochrome P450 enzymes. *Cell Metab*, 5: 143-9.
212. Mallory, J. C., Crudden, G., Johnson, B. L., Mo, C., Pierson, C. A., Bard, M., and Craven, R. J. (2005). Dap1p, a heme-binding protein that regulates the cytochrome P450 protein Erg11p/Cyp51p in *Saccharomyces cerevisiae*. *Mol Cell Biol*, 25: 1669-79.
213. Bard, F., Casano, L., Mallabiabarrena, A., Wallace, E., Saito, K., Kitayama, H., Guizzunti, G., Hu, Y., Wendler, F., Dasgupta, R., Perrimon, N., and Malhotra, V. (2006). Functional genomics reveals genes involved in protein secretion and Golgi organization. *Nature*, 439: 604-7.
214. Bornstein, P., McKinney, C. E., LaMarca, M. E., Winfield, S., Shingu, T., Devarayalu, S., Vos, H. L., and Ginns, E. I. (1995). Metaxin, a gene contiguous to both thrombospondin 3 and glucocerebrosidase, is required for embryonic development in the mouse: implications for Gaucher disease. *Proc Natl Acad Sci U S A*, 92: 4547-51.
215. Armstrong, L. C., Komiya, T., Bergman, B. E., Mihara, K., and Bornstein, P. (1997). Metaxin is a component of a preprotein import complex in the outer membrane of the mammalian mitochondrion. *J Biol Chem*, 272: 6510-8.
216. Perally, S., Lacourse, E. J., Campbell, A. M., and Brophy, P. M. (2008). Heme Transport and Detoxification in Nematodes: Subproteomics Evidence of Differential Role of Glutathione Transferases. *J Proteome Res*.
217. Cromer, B. A., Gorman, M. A., Hansen, G., Adams, J. J., Coggan, M., Littler, D. R., Brown, L. J., Mazzanti, M., Breit, S. N., Curmi, P. M., Dulhunty, A. F., Board, P. G., and Parker, M. W. (2007). Structure of the Janus protein human CLIC2. *J Mol Biol*, 374: 719-31.
218. Harrop, S. J., DeMaere, M. Z., Fairlie, W. D., Reztsova, T., Valenzuela, S. M., Mazzanti, M., Tonini, R., Qiu, M. R., Jankova, L., Warton, K., Bauskin, A. R., Wu, W. M., Pankhurst, S., Campbell, T. J., Breit, S. N., and Curmi, P. M. (2001). Crystal structure of a soluble form of the intracellular chloride ion channel CLIC1 (NCC27) at 1.4-A resolution. *J Biol Chem*, 276: 44993-5000.
219. Littler, D. R., Assaad, N. N., Harrop, S. J., Brown, L. J., Pankhurst, G. J., Luciani, P., Aguilar, M. I., Mazzanti, M., Berryman, M. A., Breit, S. N., and Curmi, P. M.

- (2005). Crystal structure of the soluble form of the redox-regulated chloride ion channel protein CLIC4. *FEBS J*, 272: 4996-5007.
220. Tulk, B. M., Kapadia, S., and Edwards, J. C. (2002). CLIC1 inserts from the aqueous phase into phospholipid membranes, where it functions as an anion channel. *Am J Physiol Cell Physiol*, 282: C1103-12.
 221. Berryman, M., Bruno, J., Price, J., and Edwards, J. C. (2004). CLIC-5A functions as a chloride channel in vitro and associates with the cortical actin cytoskeleton in vitro and in vivo. *J Biol Chem*, 279: 34794-801.
 222. Tulk, B. M., Schlesinger, P. H., Kapadia, S. A., and Edwards, J. C. (2000). CLIC-1 functions as a chloride channel when expressed and purified from bacteria. *J Biol Chem*, 275: 26986-93.
 223. Fukushima, T., Hawkins, M. G., and McGhee, J. D. (1998). The GATA-factor elt-2 is essential for formation of the *Caenorhabditis elegans* intestine. *Dev Biol*, 198: 286-302.
 224. McGhee, J. D., Sleumer, M. C., Bilenky, M., Wong, K., McKay, S. J., Goszczynski, B., Tian, H., Krich, N. D., Khattra, J., Holt, R. A., Baillie, D. L., Kohara, Y., Marra, M. A., Jones, S. J., Moerman, D. G., and Robertson, A. G. (2007). The ELT-2 GATA-factor and the global regulation of transcription in the *C. elegans* intestine. *Dev Biol*, 302: 627-45.
 225. Hermann, G. J., Schroeder, L. K., Hieb, C. A., Kershner, A. M., Rabbitts, B. M., Fonarev, P., Grant, B. D., and Priess, J. R. (2005). Genetic analysis of lysosomal trafficking in *Caenorhabditis elegans*. *Mol Biol Cell*, 16: 3273-88.
 226. Shi, A., Sun, L., Banerjee, R., Tobin, M., Zhang, Y., and Grant, B. D. (2009). Regulation of endosomal clathrin and retromer-mediated endosome to Golgi retrograde transport by the J-domain protein RME-8. *EMBO J*, 28: 3290-302.
 227. Fares, H., and Greenwald, I. (2001). Genetic analysis of endocytosis in *Caenorhabditis elegans*: coelomocyte uptake defective mutants. *Genetics*, 159: 133-45.
 228. Gaynor, E. C., Chen, C. Y., Emr, S. D., and Graham, T. R. (1998). ARF is required for maintenance of yeast Golgi and endosome structure and function. *Mol Biol Cell*, 9: 653-70.
 229. Hashimoto, H., Abe, M., Hirata, A., Noda, Y., Adachi, H., and Yoda, K. (2002). Progression of the stacked Golgi compartments in the yeast *Saccharomyces cerevisiae* by overproduction of GDP-mannose transporter. *Yeast*, 19: 1413-24.
 230. Goessling, L. S., Mascotti, D. P., and Thach, R. E. (1998). Involvement of heme in the degradation of iron-regulatory protein 2. *J Biol Chem*, 273: 12555-7.
 231. Blackwell, T. K., Bowerman, B., Priess, J. R., and Weintraub, H. (1994). Formation of a monomeric DNA binding domain by Skn-1 bZIP and homeodomain elements. *Science*, 266: 621-8.
 232. Sawado, T., Igarashi, K., and Groudine, M. (2001). Activation of beta-major globin gene transcription is associated with recruitment of NF-E2 to the beta-globin LCR and gene promoter. *Proc Natl Acad Sci U S A*, 98: 10226-31.
 233. Sun, J., Brand, M., Zenke, Y., Tashiro, S., Groudine, M., and Igarashi, K. (2004). Heme regulates the dynamic exchange of Bach1 and NF-E2-related factors in the Maf transcription factor network. *Proc Natl Acad Sci U S A*, 101: 1461-6.

234. Tahara, T., Sun, J., Igarashi, K., and Taketani, S. (2004). Heme-dependent up-regulation of the alpha-globin gene expression by transcriptional repressor Bach1 in erythroid cells. *Biochem Biophys Res Commun*, 324: 77-85.
235. Sieburth, D., Madison, J. M., and Kaplan, J. M. (2007). PKC-1 regulates secretion of neuropeptides. *Nat Neurosci*, 10: 49-57.
236. Paupard, M. C., Miller, A., Grant, B., Hirsh, D., and Hall, D. H. (2001). Immunocytochemical localization of GFP-tagged yolk proteins in *C. elegans* using microwave fixation. *J Histochem Cytochem*, 49: 949-56.
237. Inouye, S., Soberon, X., Franceschini, T., Nakamura, K., Itakura, K., and Inouye, M. (1982). Role of positive charge on the amino-terminal region of the signal peptide in protein secretion across the membrane. *Proc Natl Acad Sci U S A*, 79: 3438-41.
238. von Heijne, G., and Abrahmsen, L. (1989). Species-specific variation in signal peptide design. Implications for protein secretion in foreign hosts. *FEBS Lett*, 244: 439-46.
239. Martoglio, B., and Dobberstein, B. (1998). Signal sequences: more than just greasy peptides. *Trends Cell Biol*, 8: 410-5.
240. Spieth, J., Denison, K., Kirtland, S., Cane, J., and Blumenthal, T. (1985). The *C. elegans* vitellogenin genes: short sequence repeats in the promoter regions and homology to the vertebrate genes. *Nucleic Acids Res*, 13: 5283-95.
241. Spieth, J., and Blumenthal, T. (1985). The *Caenorhabditis elegans* vitellogenin gene family includes a gene encoding a distantly related protein. *Mol Cell Biol*, 5: 2495-501.
242. Blumenthal, T., Squire, M., Kirtland, S., Cane, J., Donegan, M., Spieth, J., and Sharrock, W. (1984). Cloning of a yolk protein gene family from *Caenorhabditis elegans*. *J Mol Biol*, 174: 1-18.
243. Kimble, J., and Sharrock, W. J. (1983). Tissue-specific synthesis of yolk proteins in *Caenorhabditis elegans*. *Dev Biol*, 96: 189-96.
244. Plenefisch, J., Xiao, H., Mei, B., Geng, J., Komuniecki, P. R., and Komuniecki, R. (2000). Secretion of a novel class of iFABPs in nematodes: coordinate use of the *Ascaris*/*Caenorhabditis* model systems. *Mol Biochem Parasitol*, 105: 223-36.
245. Jiang, M., Ryu, J., Kiraly, M., Duke, K., Reinke, V., and Kim, S. K. (2001). Genome-wide analysis of developmental and sex-regulated gene expression profiles in *Caenorhabditis elegans*. *Proc Natl Acad Sci U S A*, 98: 218-23.
246. Bowerman, B., Draper, B. W., Mello, C. C., and Priess, J. R. (1993). The maternal gene *skn-1* encodes a protein that is distributed unequally in early *C. elegans* embryos. *Cell*, 74: 443-52.
247. Bowerman, B., Eaton, B. A., and Priess, J. R. (1992). *skn-1*, a maternally expressed gene required to specify the fate of ventral blastomeres in the early *C. elegans* embryo. *Cell*, 68: 1061-75.
248. An, J. H., and Blackwell, T. K. (2003). SKN-1 links *C. elegans* mesendodermal specification to a conserved oxidative stress response. *Genes Dev*, 17: 1882-93.
249. Tullet, J. M., Hertweck, M., An, J. H., Baker, J., Hwang, J. Y., Liu, S., Oliveira, R. P., Baumeister, R., and Blackwell, T. K. (2008). Direct inhibition of the longevity-promoting factor SKN-1 by insulin-like signaling in *C. elegans*. *Cell*, 132: 1025-38.

250. Nemeth, E., Tuttle, M. S., Powelson, J., Vaughn, M. B., Donovan, A., Ward, D. M., Ganz, T., and Kaplan, J. (2004). Hepcidin regulates cellular iron efflux by binding to ferroportin and inducing its internalization. *Science*, 306: 2090-3.
251. Bishop, T., Lau, K. W., Epstein, A. C., Kim, S. K., Jiang, M., O'Rourke, D., Pugh, C. W., Gleadle, J. M., Taylor, M. S., Hodgkin, J., and Ratcliffe, P. J. (2004). Genetic analysis of pathways regulated by the von Hippel-Lindau tumor suppressor in *Caenorhabditis elegans*. *PLoS Biol*, 2: e289.
252. Shen, C., Nettleton, D., Jiang, M., Kim, S. K., and Powell-Coffman, J. A. (2005). Roles of the HIF-1 hypoxia-inducible factor during hypoxia response in *Caenorhabditis elegans*. *J Biol Chem*, 280: 20580-8.
253. Murphy, C. T., McCarroll, S. A., Bargmann, C. I., Fraser, A., Kamath, R. S., Ahringer, J., Li, H., and Kenyon, C. (2003). Genes that act downstream of DAF-16 to influence the lifespan of *Caenorhabditis elegans*. *Nature*, 424: 277-83.
254. Larsen, P. L., Albert, P. S., and Riddle, D. L. (1995). Genes that regulate both development and longevity in *Caenorhabditis elegans*. *Genetics*, 139: 1567-83.
255. Nowell, S. A., Leakey, J. E., Warren, J. F., Lang, N. P., and Frame, L. T. (1998). Identification of enzymes responsible for the metabolism of heme in human platelets. *J Biol Chem*, 273: 33342-6.
256. Xie, W., Yeuh, M. F., Radominska-Pandya, A., Saini, S. P., Negishi, Y., Bottroff, B. S., Cabrera, G. Y., Tukey, R. H., and Evans, R. M. (2003). Control of steroid, heme, and carcinogen metabolism by nuclear pregnane X receptor and constitutive androstane receptor. *Proc Natl Acad Sci U S A*, 100: 4150-5.
257. Epstein, A. C., Gleadle, J. M., McNeill, L. A., Hewitson, K. S., O'Rourke, J., Mole, D. R., Mukherji, M., Metzen, E., Wilson, M. I., Dhanda, A., Tian, Y. M., Masson, N., Hamilton, D. L., Jaakkola, P., Barstead, R., Hodgkin, J., Maxwell, P. H., Pugh, C. W., Schofield, C. J., and Ratcliffe, P. J. (2001). *C. elegans* EGL-9 and mammalian homologs define a family of dioxygenases that regulate HIF by prolyl hydroxylation. *Cell*, 107: 43-54.
258. Jaakkola, P., Mole, D. R., Tian, Y. M., Wilson, M. I., Gielbert, J., Gaskell, S. J., Kriegsheim, A., Hebestreit, H. F., Mukherji, M., Schofield, C. J., Maxwell, P. H., Pugh, C. W., and Ratcliffe, P. J. (2001). Targeting of HIF- α to the von Hippel-Lindau ubiquitylation complex by O₂-regulated prolyl hydroxylation. *Science*, 292: 468-72.
259. Al-Waili, N. S., Butler, G. J., Beale, J., Abdullah, M. S., Hamilton, R. W., Lee, B. Y., Lucas, P., Allen, M. W., Petrillo, R. L., Carrey, Z., and Finkelstein, M. (2005). Hyperbaric oxygen in the treatment of patients with cerebral stroke, brain trauma, and neurologic disease. *Adv Ther*, 22: 659-78.
260. Chen, Z., Chintagari, N. R., Guo, Y., Bhaskaran, M., Chen, J., Gao, L., Jin, N., Weng, T., and Liu, L. (2007). Gene expression of rat alveolar type II cells during hyperoxia exposure and early recovery. *Free Radic Biol Med*, 43: 628-42.
261. Clerch, L. B. (2000). Post-transcriptional regulation of lung antioxidant enzyme gene expression. *Ann N Y Acad Sci*, 899: 103-11.
262. Ho, Y. S., Dey, M. S., and Crapo, J. D. (1996). Antioxidant enzyme expression in rat lungs during hyperoxia. *Am J Physiol*, 270: L810-8.
263. Lee, P. J., and Choi, A. M. (2003). Pathways of cell signaling in hyperoxia. *Free Radic Biol Med*, 35: 341-50.

264. Cho, H. Y., Jedlicka, A. E., Reddy, S. P., Kensler, T. W., Yamamoto, M., Zhang, L. Y., and Kleeberger, S. R. (2002). Role of NRF2 in protection against hyperoxic lung injury in mice. *Am J Respir Cell Mol Biol*, 26: 175-82.
265. Zhu, H., Jia, Z., Zhang, L., Yamamoto, M., Misra, H. P., Trush, M. A., and Li, Y. (2008). Antioxidants and phase 2 enzymes in macrophages: regulation by Nrf2 signaling and protection against oxidative and electrophilic stress. *Exp Biol Med (Maywood)*, 233: 463-74.
266. Park, S. K., Tedesco, P. M., and Johnson, T. E. (2009). Oxidative stress and longevity in *Caenorhabditis elegans* as mediated by SKN-1. *Aging Cell*, 8: 258-69.
267. Perkowski, S., Sun, J., Singhal, S., Santiago, J., Leikauf, G. D., and Albelda, S. M. (2003). Gene expression profiling of the early pulmonary response to hyperoxia in mice. *Am J Respir Cell Mol Biol*, 28: 682-96.
268. Zangar, R. C., Davydov, D. R., and Verma, S. (2004). Mechanisms that regulate production of reactive oxygen species by cytochrome P450. *Toxicol Appl Pharmacol*, 199: 316-31.
269. Morel, Y., and Barouki, R. (1998). Down-regulation of cytochrome P450 1A1 gene promoter by oxidative stress. Critical contribution of nuclear factor 1. *J Biol Chem*, 273: 26969-76.
270. Moorthy, B., Nguyen, U. T., Gupta, S., Stewart, K. D., Welty, S. E., and Smith, C. V. (1997). Induction and decline of hepatic cytochromes P4501A1 and 1A2 in rats exposed to hyperoxia are not paralleled by changes in glutathione S-transferase-alpha. *Toxicol Lett*, 90: 67-75.
271. Couroucli, X. I., Welty, S. E., Geske, R. S., and Moorthy, B. (2002). Regulation of pulmonary and hepatic cytochrome P4501A expression in the rat by hyperoxia: implications for hyperoxic lung injury. *Mol Pharmacol*, 61: 507-15.
272. Bhakta, K. Y., Jiang, W., Couroucli, X. I., Fazili, I. S., Muthiah, K., and Moorthy, B. (2008). Regulation of cytochrome P4501A1 expression by hyperoxia in human lung cell lines: Implications for hyperoxic lung injury. *Toxicol Appl Pharmacol*, 233: 169-78.
273. Sinha, A., Muthiah, K., Jiang, W., Couroucli, X., Barrios, R., and Moorthy, B. (2005). Attenuation of hyperoxic lung injury by the CYP1A inducer beta-naphthoflavone. *Toxicol Sci*, 87: 204-12.
274. Williamson, A. L., Brindley, P. J., Knox, D. P., Hotez, P. J., and Loukas, A. (2003). Digestive proteases of blood-feeding nematodes. *Trends Parasitol*, 19: 417-23.
275. Morales, M. E., Rinaldi, G., Gobert, G. N., Kines, K. J., Tort, J. F., and Brindley, P. J. (2008). RNA interference of *Schistosoma mansoni* cathepsin D, the apical enzyme of the hemoglobin proteolysis cascade. *Mol Biochem Parasitol*, 157: 160-8.
276. Wang, S., Publicover, S., and Gu, Y. (2009). An oxygen-sensitive mechanism in regulation of epithelial sodium channel. *Proc Natl Acad Sci U S A*, 106: 2957-62.
277. Cheung, B. H., Arellano-Carbajal, F., Rybicki, I., and de Bono, M. (2004). Soluble guanylate cyclases act in neurons exposed to the body fluid to promote *C. elegans* aggregation behavior. *Curr Biol*, 14: 1105-11.

- 278. Bandyopadhyay, S., Gama, F., Molina-Navarro, M. M., Gualberto, J. M., Claxton, R., Naik, S. G., Huynh, B. H., Herrero, E., Jacquot, J. P., Johnson, M. K., and Rouhier, N. (2008). Chloroplast monothiol glutaredoxins as scaffold proteins for the assembly and delivery of [2Fe-2S] clusters. *EMBO J*, 27: 1122-33.
- 279. Lillig, C. H., Berndt, C., and Holmgren, A. (2008). Glutaredoxin systems. *Biochim Biophys Acta*, 1780: 1304-17.
- 280. Inoue, H., Hisamoto, N., An, J. H., Oliveira, R. P., Nishida, E., Blackwell, T. K., and Matsumoto, K. (2005). The *C. elegans* p38 MAPK pathway regulates nuclear localization of the transcription factor SKN-1 in oxidative stress response. *Genes Dev*, 19: 2278-83.